Nanomaterial Strategies to Enhance Antiretroviral Efficacy for Vaginal Drug Delivery

Emily Anne Krogstad

A dissertation
submitted in partial fulfillment of the
requirements for the degree of

Doctor of Philosophy

University of Washington

2015

Reading Committee:

Kim Woodrow, Chair

Daniel Ratner

Jeanne Marrazzo

Program Authorized to Offer Degree:
Bioengineering

University of Washington

Abstract

Nanomaterial Strategies to Enhance Antiretroviral Efficacy for Vaginal Drug Delivery

Emily Anne Krogstad

Chair of the Supervisory Committee:
Professor Kim Woodrow
Bioengineering

HIV continues to infect millions of people worldwide, and without an effective vaccine or cure available, there is need for new methods to prevent infection. Women are disproportionately impacted by HIV due to biologic vulnerabilities and social inequalities, and are especially at risk in places with high HIV incidence like sub-Saharan Africa. Topical microbicides are products in development that can be vaginally administered to prevent HIV infection. Since microbicides are a female-initiated product, they would fill an important gap in the array of currently available prevention options that are targeted toward men such as circumcision and condoms. Unfortunately, only one topical microbicide to date has demonstrated modest efficacy in clinical trials, with an overall 39% reduction in HIV acquisition. New strategies are needed to improve the effectiveness of topical microbicides.

In this work, we explored several nanomaterials including nanoparticles, nanofibers, and nanoparticle/nanofiber composites as novel drug delivery platforms for topical microbicides. We hypothesized that by engineering nanocarriers to deliver multiple drugs in combination, provide

sustained release, and have tailored interactions with cervicovaginal mucus, nanomaterials would allow for more effective delivery of antiretroviral drugs to vaginal tissue. We also explored nanofibers as a delivery vehicle for both drugs and nanoparticles and evaluated their ability to enhance vaginal retention relative to liquid-based dosage forms.

We found that both nanoparticles and nanofibers offer much potential for enhancing drug delivery to vaginal tissue. Nanoparticles were developed to load several different antiretroviral drugs and show enhanced efficacy against HIV-1 *in vitro* compared to free drug alone. Nanofibers were demonstrated to be able to load many agents relevant to vaginal drug delivery at remarkably high levels (up to 60% by mass), provide both quick and sustained drug release, release active drug with action against HIV-1, and act as a physical and chemical barrier to sperm. Finally, nanoparticle/nanofiber composites were found to dramatically enhance nanoparticle and drug retention in the reproductive tract of mice, providing proof-of-concept for a new platform for the vaginal administration of nanoparticles that is both solid-state and practical to administer. We expect that results from this work will be impactful not only for the microbicide field, but also for other applications, including the prevention and treatment of other sexually transmitted infections, mucosal vaccination, and topical drug delivery to mucosal sites.

TABLE OF CONTENTS

List of Figures.

List of Tables.

SUMMARY OF RESEARCH AIMS

Developing an effective topical microbicide for the prevention of sexually transmitted HIV-1 has been a significant but elusive research goal for the past two decades. Despite dozens of microbicides entering clinical trials, there has been only a singular clinical success, which resulted in a 39% reduction in HIV-1 infection in women. While these results were important in establishing proof-of-concept that microbicides can prevent HIV-1 infection, efficacy remains a limiting factor. Current microbicide formulations, which deliver free drugs such as tenofovir or dapivirine, depend on the drug half-life to determine the frequency of dosing required. Frequent repeated application of these products is necessary to establish drug concentrations required for efficacy, making the product dependent on high levels of adherence not achievable in low-resource settings. Thus, there is need for a microbicide formulation that provides long-acting, sustained protection against HIV. In this dissertation, we aim to enhance microbicidal efficacy by developing nanomaterial platforms for vaginal drug delivery that can simultaneously deliver multiple agents with different physicochemical properties and extend the length of drug release and retention in the vaginal tract. In Aims 1 and 2, we explore nanoparticles and nanofibers for their potential as antiretroviral drug delivery platforms. In Aim 3, we combine nanoparticles and nanofibers into a single composite platform that we hypothesized would provide enhanced vaginal retention of nanoparticles.

AIM 1: Explore ARV-loaded nanoparticle-mediated delivery as a strategy to enhance drug efficacy against HIV-1. We selected drugs based on previous studies demonstrating their potency and synergy with other agents (e.g., tenofovir and efavirenz). ARVs suitable for intracellular delivery were encapsulated in poly(lactic-co-glycolic acid) nanoparticles using emulsion or precipitation techniques. Particles were characterized for size, surface charge, drug loading, toxicity, and release kinetics, as well as HIV-1 inhibitory activity using a TZM-bl reporter assay.

AIM 2: Demonstrate versatility of nanofibers for quick release vaginal drug delivery and scalability. Polymers of interest for vaginal drug delivery including poly(vinyl alcohol) (PVA), poly(L-lactic acid), and poly(ethylene oxide) were electrospun into fiber meshes and characterized for physical properties. Antiretroviral agents of differing classes and aqueous solubilities were electrospun into fibers as proof-of-concept of the amenability of electrospinning to vaginal drug delivery. Fibers were characterized for size, drug crystallinity, dissolution time, drug release kinetics, toxicity, and bioactivity. Manufacturing scale-up potential was evaluated

by comparing properties of tenofovir-loaded PVA fibers electrospun using small scale versus production scale instruments.

AIM 3: Evaluate nanoparticle/nanofiber composite materials as platform for enhancing vaginal retention of nanoparticles *in vivo*. Composite fiber meshes were synthesized using PEG-coated mucus-penetrating PLGA nanoparticles and two different mucoadhesive polymers for fibers. Composite materials were characterized for their ability to encapsulate and release intact nanoparticles that maintain their size and surface charge after dissolution *in vitro*. Fiber composites were then evaluated as a practical method for the vaginal delivery of nanoparticles using a murine model. Equivalent doses of fluorescent nanoparticles were administered intravaginally to mice in either aqueous suspensions or composite fibers. Tissue retention and biodistribution of fluorescent nanoparticles from 1h – 7d were evaluated using Xenogen imaging and tissue homogenization methods. Similar studies were repeated with etravirine-loaded nanoparticles to evaluate the pharmacokinetics after administration in either aqueous suspensions or composite fibers.

ACKNOWLEDGEMENTS

I express my deepest thanks to Dr. Kim Woodrow for her exceptional advising and support over the last five years. It had been a dream of mine to work in a lab focused on translational research for global health applications, and I am incredibly thankful for Kim's willingness to trust me as a first-year grad student and provide an opportunity to do exactly that. I appreciate how she has shaped the way I think about scientific research to be from a hypothesis-driven, question-based framework. It has been a privilege to learn from Kim's creative and rational approaches to exploring new ideas for HIV prevention and treatment, and from her enthusiasm for understanding the science underlying the work. I am thankful for how she as advocated for me as a student: for her open door to meet and discuss challenges, for all of the opportunities to present at conferences and publish research, and for seeing me through the PhD.

I also thank my Supervisory Committee for their advice and valuable feedback on my research design and direction: Dr. Suzie Pun, Dr. Dan Ratner, Dr. Jeanne Marrazzo, and Dr. Carey Farquhar. I have appreciated their time, constructive feedback, and encouragement to aim high.

To my many colleagues in the Woodrow Lab, thank you for making the lab such an encouraging and team-based environment for doing research! Particular thanks to Renuka Ramanathan, who has been with me for the whole journey. I am thankful for her constant friendship and for her collaboration through all of the mouse studies. I thank Dr. Thanyanan Chaowanachan for her big smile from my first day in lab that continues through today, and for her thorough and careful training of me in BSL-2/3 lab techniques. Thank you to Dr. Cameron Ball for being not only an outstanding collaborator scientifically, but also for being a compassionate friend, and for turning me into a fellow bicycling enthusiast. I thank Joe Phan for his friendship, awesome baking skills, and his calm, relaxed attitude that has made lab a positive working environment. I thank Shijie Cao for his help with the scale-up *in vivo* studies, and Dr. Jaehyung Park for his mentorship and sense of humor. I thank Anna Blakney for her willingness to help out with LC-MS/MS, and for her example of simultaneously working efficiently and enjoying life. Thank you to the undergraduates who have worked with me, Andrew Johnson and Christina Nhan, for their many hours of hard work, cheerfulness, and patience. I also thank Rick Edmark for his dedication to the behind-the-scenes logistics that make the Woodrow Lab run smoothly, and for his humility and positivity. Thank you to Dr. Sharon Golan-Paz, Arielle Steger, Dr. Yonghou Jiang, Hannah Frizzell, and Karl Thoreson and for valuable conversations and support.

I acknowledge the many teachers and professors I have had over the years who have impacted the world by dedicating their lives to helping students learn well. I especially thank Dr. Chun Wang, who advised me as an undergraduate in his lab and encouraged me to pursue graduate studies, and Dr. Sunny Choh, who taught me the very basics of working in a lab.

Finally, thanks to the many people in my life who have been my support network through this process, providing invaluable encouragement and friendship. I thank my parents for their unconditional love and for the opportunities they have provided. I appreciate my sister and brother for their Skype teas, phone calls, and visits to empathize about the joys and challenges of graduate school. Thank you to several friends who have helped immensely in this process: Shefali Oza for sharing her global perspective, Dr. Carly Holstein for being my writing buddy through many exams, and Rochelle Nguyen for her example of perseverance and courage. Thank you to Heidi Schuler, Mary Smith, Leah Gross, Lisa Echert, and Meagan Wright for being such good friends and housemates. Thank you to my "second family" in Seattle for all of your love: Peter and Megumi Morrill (and Koko, Joh, and Keita), Sarah Gerdts, Mcklyn Valenciano, Lori Tang, Julie Boiroux, Audrey Na, Eiji Ono, Steve and Ann Moll, Nikki and Ben Murphy, Beth Thielen, and John Secord. Thank you to my dear friends Ken and Francie Knutzen, who have provided mentorship and opened up their peaceful home to me. I am also thankful for friends in Minnesota for their care and long-distance support along the journey: Jeanne and Chris Adams, Nikki Fraser, Lisa Bergh, Melissa Boecher, and Tracy Marko.

DEDICATION

This dissertation is dedicated to all of those affected by HIV/AIDS globally.

1 Introduction: Nanomaterial strategies for vaginal drug delivery.

Portions adapted from: Krogstad E, Rathbone MJ, Woodrow KA (2014) Vaginal Drug Delivery. In: Domb AJ, Khan W, editors. Focal Controlled Drug Delivery. Advances in Delivery Science and Technology. Springer US. pp. 607–651.

1.1 SIGNIFICANCE. Highlighting the need for female-initiated HIV prevention methods.

HIV has infected nearly 70 million people and caused an estimated 35 million deaths since the beginning of the epidemic in 1981[1]. Sub-Saharan Africa has been disproportionately impacted by this pandemic, accounting for 69% of the 34 million people currently living with HIV worldwide[1]. Even though the HIV pandemic continues to be a clear global health priority, it remains without a cure. The best available treatment, highly active antiretroviral therapy (HAART), does not completely eradicate the virus from the body[2], and an effective vaccine against HIV remains to be developed. Furthermore, while HAART has dramatically improved outcomes for many of those infected with HIV, it is an expensive and lifelong therapy, rendering it unfeasible for the majority of HIV-infected persons who live in low-income settings. With the lack of a vaccine or effective cure for HIV, practical strategies are needed to prevent more people from becoming infected with HIV.

Importantly, women bear a disproportionate burden of those infected with HIV in sub-Saharan Africa, accounting for 58% of those infected in 2011[3]. Because the majority of HIV infections are sexually transmitted, early prevention efforts have focused on condom use and behavioral modifications, termed the "ABC" approach (Abstain, Be faithful, use Condoms). Unfortunately, women in these areas often lack power to negotiate condom use or their partner's faithfulness, and this approach has had limited success[4]. With three times more women than men ages 15-24 in sub-Saharan Africa infected with HIV, there is particular need for female-controlled methods for prevention of sexual HIV transmission[5].

Microbicides are agents that can be applied topically to the vaginal mucosa or rectum to prevent sexual transmission of HIV. There has been extensive research to develop topical microbicides, resulting in over 73 preclinical trials and 45 clinical trials[6]. Some of the first microbicides contained drugs with nonspecific mechanisms of action such as surfactants, polyanions, dendrimers, and buffering gels[7]. These microbicides interfered with binding of HIV to CD4 cells by interfering with envelope glycoproteins, or were aimed at keeping the pH of the vagina low to reduce the infectivity of pathogens[8]. One of these early microbicides that reached clinical trials contained the surfactant nonoxynol-9. Disappointingly, after testing in Africa and Thailand, it was shown to cause an increase in susceptibility to HIV infections[9]. Polyanion-based microbicides included Carraguard, cellulose sulfate, and PRO 2000. These products showed

better *in vitro* inflammatory and toxicity profiles compared to nonoxynol-9, but did not show any improvement over placebo in reducing HIV infection in clinical trials[10]. Vaginal milieu protectors such as BufferGel were designed to maintain vaginal pH and subsequently inactivate virus, but also failed to be effective in clinical trials[11].

Despite over a decade of research and dozens of products reaching clinical trials, there has been only a singular success in the HIV microbicide field to date. The CAPRISA 004 trial provided the first proof of concept that topical microbicides can prevent HIV-1 infection in humans[12]. In this trial, vaginal gel containing a reverse transcriptase inhibitor (1% tenofovir) was shown to reduce HIV-1 infection in women by 39% compared to placebo gel. This trial shifted the paradigm for designing microbicides from acting nonspecifically against HIV toward acting specifically through use of antiviral drugs. Ongoing microbicides in clinical trials include vaginal gels that delivering ARVs including dapivirine and UC781[10], and continuing trials testing tenofovir gel. Vaginal rings have also emerged as a promising dosage form for providing sustained microbicide release, and may be a more acceptable option for some populations. Dapivirine and maraviroc vaginal rings are in ongoing clinical trials[8]. Recently, the 1% tenofovir vaginal gel arm of the VOICE trial was halted early due to lack of efficacy[13]. Lack of adherence to daily gel use, different dosing regimens (daily vs. before and after sex), and different study populations may have contributed to differences between the VOICE and CAPRISA 004 trials. These conflicting results highlight the need for a more effective microbicide that provides longer lasting protection. Dosage forms are needed that result in greater user adherence to meet diverse preferences of women.

In this work, we study the potential of nanomaterials to provide sustained drug release and enhance antiviral efficacy for next-generation microbicides. Three nanomaterial platforms are presented: (1) nanoparticles, (2) nanofibers, and (3) nanoparticle/nanofiber composites. By facilitating intracellular delivery and sustaining release of drug, we hypothesize that a single vaginal administration of drug-loaded nanoparticles can result in more effective protection against HIV-1 than free drug. Nanofibers are explored as a novel dosage form for vaginal drug delivery that provides versatility for combination drug delivery, flexibility in product geometry, and potential for manufacturing scale-up. Finally, nanoparticle/nanofiber composites are explored as a single material that can provide both a method for practical vaginal administration enhanced retention of nanoparticles for pericoital and sustained release HIV prevention applications.

1.2 BACKGROUND. Engineering nanomaterials for vaginal drug delivery.

1.2.1 Vaginal anatomy and physiology

While the human vagina has great potential as an administration route for drug delivery, several challenges remain due to its variable nature and innate barriers. Of primary importance, the conditions of the vaginal environment vary greatly among women and change with age, menstrual cycle, and sexual activity. Besides HIV prevention, overcoming barriers in vaginal drug delivery would have implications for sexually transmitted infection (STI) prevention and treatment, bacteriovaginosis, yeast infections, delivery of mucosal vaccines, contraception, and other reproductive health applications.

Anatomy

The vagina is a fibromuscular, expandable S-shaped tube approximately 6-10 cm in length[14,15]**.** It can be divided into four major areas: the posterior fornix, anterior fornix, and two lateral fornices. The vaginal wall is comprised of four layers, the outer epithelial layer, lamina propria (or tunica), muscle layer, and areolar connective tissue[16]. The epithelial layer contains nonsecretory stratified squamous epithelial cells and is generally 200-300 μm thick (25 layers), depending on the menstrual cycle[16,17]. The lamina propria contains collagen and elastin and rich supply of vascular and lymphatic channels[16]. The muscle layer is made of smooth, elastic fibers in both circular and longitudinal directions. The vagina has a large surface area available for drug delivery that is provided by microridges and rugae, or traverse muscular folds, at its surface[18].

Physiology

Besides the anatomical advantage of a large surface area for vaginal drug delivery, the vagina also has the physiologic advantage of an abundant network of vasculature. The blood supply enters from uterine and pudental arteries and leaves via the internal iliac veins[14,20]— bypassing liver metabolism and the "first pass effect" encountered through oral administration[18]. Normal microflora of the vagina include a mix of anaerobic microbes, mainly different strains of *Lactobacillus* that can vary with ethnicity (*L. crispatus, L. iners, L. gasseri*, and *L. jensenii* are among the most common)[21]. Lactobacilli help to maintain normal vaginal pH, and some strains produce hydrogen peroxide to regulate bacterial growth[16]. Without population of the vagina by commensal bacteria, the vagina is at increased risk of colonization by opportunistic pathogens. A variety of vaginal enzymes are also present that pose a barrier to peptide delivery[18,22].

Though the vagina itself does not possess secretory glands, it is typically coated in a thin film of secretions present from cervical secretions, cervical mucus, and transudation from blood vessels[16]. Vaginal fluid is composed of carbohydrates, enzymes, enzyme inhibitors, alcohols, hydroxyl ketones, amino acids, aliphatic acids, immunoglobulins, and aromatic compounds[18,23]. Cervical mucus varies in its rheological properties and can provide a barrier for drug diffusion into vaginal epithelium. It can be characterized by viscoelasticity, spinnbarkeit (stretchability), hydration, and pH[24]. Vaginal pH varies with the menstrual cycle and physical location in the vagina, with the pH being lowest near the anterior fornix and highest near the cervix[14,25]. The normal pH range is 4-5 for vaginal fluid and 7-9 for cervical mucus[20,21]. The commensal bacteria *Lactobacillus* helps maintain vaginal pH by converting glycogen from sloughed epithelial cells into lactic acid[20] The volume of vaginal secretions is variable, with women of reproductive age documented to discharge 3-4 g per 4 h, while menopausal women produced 1.5-2 g per 4 h[20]. The variability in volume and composition of vaginal secretions will affect the dissolution of various dosage forms, absorption of drugs, and rate of flow out of the vagina.

1.2.2 Early stages of HIV-1 infection

Human immunodeficiency virus (HIV-1) is a retrovirus of subclass lentivirinae and is responsible for causing acquired immunodeficiency syndrome (AIDS)[26]. Heterosexual transmission of HIV infection occurs primarily through the female genital tract[27]. HIV-1 infection is established through semen or other biologic fluids that penetrate the vaginal epithelium or cervical tissue to reach immune target cells including CD4+ T cells, dendritic cells, and macrophages[26]. While the exact mechanism of HIV-1 infection is unknown, several proposed mechanisms include transcytosis through epithelial cells, transmigration of epithelial cells, uptake by Langerhans cells or CD4+ cells, and virus transport through physical abrasions of the epithelium[26,28]. Besides free virus, there is also potential for HIV to be transmitted through cell-associated virus from HIV-infected donor cells[29]. SIV has been shown to penetrate the cervicovaginal epithelium within 30-60 minutes in macaque models[30]. The challenge of developing a microbicide to prevent HIV-1 infection is to ensure protective levels of antiviral drug in all of these potential targets over time scale of HIV persistence.

1.2.3 Drug targets in the HIV lifecycle

HIV-1 first enters cells through interactions with the viral membrane glycoproteins gp41 and gp120 and the cell membrane receptor CD4 and CXC chemokine receptor type 4 (CXCR4) or CC chemokine receptor type 5 (CCR5)[31]. Next, the HIV enzyme reverse transcriptase converts single stranded viral RNA to double stranded cDNA, which is then transported into the nucleus.

During integration, the HIV enzyme integrase incorporates viral DNA into the cellular genome, at which point the virus is designated a "provirus". Upon cellular activation, viral DNA is transcribed into mRNA along with human DNA, and translated to protein in the cytoplasm. Finally, new viral assembly, budding, and maturation occur via the organization of viral mRNA and proteins with the assistance of the HIV enzyme protease. New virus particles are then able to bud off the cell and infect new cells[31].

1.2.4 Selecting antiretroviral drugs for HIV prevention

Antiretroviral (ARV) drugs have been designed to interfere at each stage in the virus lifecycle and have been classified according to their mechanism of action. The main classes of ARVs include entry or fusion inhibitors, reverse transcriptase inhibitors, integrase inhibitors, and protease inhibitors. Most of the ARVs available were designed for therapy for those already infected with HIV, but many may also have application for HIV prevention. The physicochemical properties and pharmacokinetics must be carefully considered in selecting drug candidates for

topical application and choosing an appropriate dosage form. Parameters including solubility, ionization state, molecular weight, partition coefficient, and permeability greatly influence drug distribution both locally and systemically. Properties and structures of several ARVs of interest to our research are listed in Appendix A and B. The biopharmaceutics classification system (BCS) is used to classify therapeutic agents as Class I (high solubility, high permeability), Class II (low solubility, high permeability), Class III (high solubility and low permeability), and Class IV (low solubility and low permeability)[8]. Solubility is a thermodynamic parameter that refers to the concentration of a molecule presented to solution, whereas permeability is a kinetic parameter describing the rate that molecules can cross membrane barriers[32]. ARVs from all BCS classes have been considered, but many drugs fall under class II and therefore are limited by solubility[8]. Dosage forms including nanoparticles as proposed here may facilitate greater intracellular concentrations for such drugs with low aqueous solubility.

Pharmacokinetic properties must be also considered individually for each drug, as effective concentrations must be maintained at the site of HIV transmission in the presence of virus. These include absorption (affected by diffusion, pKa, logP), distribution (Vd, protein binding), metabolism (drug half life), and excretion. ARVs will transport differently based on these properties, route of administration, and varying conditions within the vagina. For example, tenofovir (TFV) is a BCS Class I nucleoside reverse transcriptase inhibitor (NRTI) with high aqueous solubility. It achieves 100-fold greater concentrations in cervicovaginal fluid and genital tissue when administered vaginally compared to orally[33,34]. In contrast, tenofovir disoproxil

fumarate (TDF) is a prodrug version of TFV with greater lipophilicity and permeability that can achieve 1000-fold higher intracellular concentration of tenofovir diphosphate than the TFV parent drug[35]. Drug diffusion across the vaginal epithelium occurs primarily by three pathways: (1) diffusion through transcellular route by the presence of a concentration gradient, (2) diffusion between cells via paracellular transport, and (3) vesicular or receptor-mediated transport[18]. Pharmacodynamic properties such as toxicity and potency (IC50) are also key considerations. An ideal ARV for HIV prevention will have high solubility at vaginal pH (4-5), high potency (IC50 in micro or nanomolar range), and long half-life (>24h). Delivery platforms that utilize nanomaterials to alter drug pharmacokinetics and solubility may allow for enhanced activity of some drugs.

1.2.5 Current products for vaginal drug delivery

Vaginal drug delivery systems can be categorized into three groups based on physical state: liquids, semi-solids, and solids (tablets, rings, films). Each dosage form has unique constraints in terms of shape, volume, excipients, manufacturability, storage requirements, and acceptability. See Table 1-1 for comparison and examples of these categories.

Table 1-1 Comparison of current dosage forms for vaginal drug delivery

STRATEGY	EXAMPLES	ADVANTAGES	DISADVANTAGES
Solid	Vaginal ring Film Sponge Tablet Capsule Suppository Diaphragm	• Ease of application • Capacity for sustained release • Long shelf life • Minimal packaging • Controllable geometry	• Mechanical requirements of vaginal rings limit drug selection • Must be hydrated for drug release
Semi-Solid	Gel Cream Ointment	• Can be designed for bioadhesive and rheological properties • Large area of initial coverage • High user acceptability in sub-Saharan Africa	• Limited retention time • Messiness, leakage • Limited chemical compatibility with drugs with poor aqueous solubility
Liquid	Foam Spray Douche	• Can be designed for bioadhesive and rheological properties • Large area of initial coverage	• Very limited retention time • Messiness, leakage • Limited chemical compatibility with drugs with poor aqueous solubility

Liquids

Examples of liquid dosage forms are foams and douches. Liquids have the advantage of superior coverage and control over rheological properties. However, they are limited by leakage, messiness, and inadequate retention. For these reasons, the microbicide field has moved away from liquid dosage forms as vaginal microbicides.

Semi-solids

Semi-solid intravaginal delivery systems include vaginal gels and ointments. Similar to liquid dosage forms, semi-solid dosage forms can also be designed to have specific osmolarity, rheological properties, and bioadhesive properties. Appropriate osmolarity is critical in maintaining microbicide safety, since a hyperosmotic gel can cause irritation and an inflammatory response. Vaginal gels should be targeted to be less than 1000 mOsm/kg[36]. Typical specific viscosity values for gels and films have been reported as 80 Pa•s and 0.01 Pa•s, respectively, and can inform designing future products for maximum spreading and retention[37,38]. Although semi-solids provide better retention than liquids, they are still limited by short residence times in the vagina. Natural polymers such as chitosan and carrageenan and high molecular weight poly(ethylene glycol) have been investigated as materials that promote bioadhesion[39]. Concerns have been raised about the ability of semi-solids to maintain API bioactivity for long-term storage and packaging costs[36].

Solids

The most common solid dosage forms currently available for vaginal delivery include vaginal tablets, intravaginal rings (IVRs), drug-eluting diaphragms, suppositories, and vaginal films. Solid dosage forms have been prioritized in the field due to their stability, controllable geometries, and potential for sustained release.

Drug-eluting diaphragms and IVRs are both dosage forms that can provide sustained drug release and potentially overcome barriers with adherence. Major *et al* recently reported on a dapivirine-eluting SILCS diaphragm that would provide protection against both HIV and unwanted pregnancy[40]. They found that mechanical properties were maintained with 10% drug loading and controlled drug release for 6 months. IVRs have received growing interest in the last decade, with at least five IVRs already on the market for contraception and estrogen replacement therapy and several in clinical trials as microbicides[41]. IVRs have been formulated to deliver dapivirine, maraviroc, acyclovir, and tenofovir either alone or in combination[41–43]. One of the main advantages of IVRs is their ability to provide sustained release on the order of

months with zero order release kinetics. Rings can be designed as matrix rings, with drug incorporated throughout the ring polymer, or as reservoir rings with rate-controlling membranes. Challenges facing translation of IVRs are limitations on types of drugs that can be formulated due to manufacturing requirements, and potential safety issues with long-term drug exposure[44].

Films and tablets represent dosage forms that may be more appropriate for pericoital applications, where quick drug release is desirable. Examples of microbicide films in development include dapivirine[45], IQP-0528[46], and polystyrene sulfonate[47]. Advantages of vaginal films include minimal packaging, discreetness, and limited product leakage. However, films have a limited maximum capacity for drug loading (up to 40 mg)[36] and can be messy and sticky during insertion[44]. Vaginal tablets can be scaled up easily and inexpensively and are simple to insert. For both films and tablets, more research is required to understand how such dosage forms will dissolve and distribute in the vagina in limited (and variable) volumes of fluid.

1.2.6 Design considerations for the ideal microbicide

Safety considerations

Of primary importance in designing a microbicide is that it is safe to tissue. Given the history of microbicide clinical trials outlined earlier where some products were actually found to *increase* the risk for HIV-acquisition[9], it is imperative that safety be rigorously studied as part of preclinical development. A microbicide should not interfere with normal vaginal microflora and should cause minimal irritation and inflammation[29]. Finally, a microbicide should be non-abrasive and have no sharp edges to prevent the creation of breaches in the epithelium.

Reaching target cells and tissue

For an effective microbicide, it must provide sufficient concentrations of ARV in target cells and tissue for the duration of risk for HIV. Nonhuman primate studies with high dose challenges of simian immunodeficiency virus (SIV) or simian-human immunodeficiency virus (SHIV) show that cellular targets of HIV are distributed throughout the epithelium and stroma of vagina, ectocervix, and endocervix[48–50]. Thus, a drug delivery system or ARV drug must be able to penetrate both the mucus and tissue barriers of the vagina to reach target cells. Cervicovaginal mucus is produced at the rate of 2-8 mL/day and cleared every 6-17 hours[51]. Strategies to penetrate this barrier will be discussed in more detail later in this chapter. As HIV-1 has potential to be transmitted through infected cells that may be present in semen[29], a microbicide must be able to target both free virions and cell-associated virions. Finally, it must be effective in highly

variable vaginal conditions, particularly changes in vaginal pH and fluid volume due to intercourse, menstrual cycle, or infection.

Providing complete coverage of the cervicovaginal tract

Another feature of an ideal microbicide is that it provides protective concentrations of drug along the entire cervicovaginal tract. Inadequate coating of vaginal rugae has been associated with incomplete protection against STIs[52]. Protecting the cervix is also desirable, as first cellular targets for HIV have been observed in endocervial epithelium[53]. Thus, dosage forms that can coat the entire cervicovaginal surface area will be crucial for establishing protection. Microbicides are also prone to dilution from vaginal and seminal secretions, and forces during coitus can reduce retention of product[54]. Therefore, one important consideration in designing next-generation microbicides is to provide high retention and complete coverage of the cervicovaginal tract.

Delivery of multiple agents in combination

HIV-1 is known to mutate rapidly and develop into strains that are resistant to ARVs. There has been concern that the benefits of preventing new HIV cases with PrEP may be offset by increase in resistant strains of HIV and loss of principle treatment options[55]. Preventing HIV at several stages in its life cycle by delivering a combination of agents with different mechanisms of action will have the greatest likelihood of increasing efficacy and reducing development of resistant strains[56–58]. However, delivering multiple agents with diverse physicochemical properties simultaneously is a challenge for many currently available dosage forms. Vaginal gels are best suited for delivering hydrophilic compounds and stability of some APIs is a major concern[36]. Vaginal rings are also limited by the manufacturing process and mechanical properties required for insertion[41].

Practical for use in low-resource settings

Finally, it is important to recognize that many people currently infected with HIV-1 live in low-resource settings, with two-thirds of those infected living in sub-Saharan Africa[1]. A microbicide meant for translation to these settings must be inexpensive and easily scaled up for manufacturing. Solid dosage forms may be best for tropical climates in Africa and Asia, as they offer longer shelf lives and greater stability at high humidity and temperature.

Designing products for high user adherence

Clinical trials for both oral and vaginal pre-exposure prophylaxis (PrEP) have shown that high user adherence is key in achieving high efficacy. Unfortunately, adherence to different dosage forms has been widely variable across different trials and study demographics. In the CAPRISA-004 trial, the 1% TFV gel arm resulted in an overall reduction of HIV-acquisition of 39%[12]. Further analyses showed that those who reported use of gel in 80% or more of sex acts had a 54% lower risk of HIV acquisition, and those who had more than 1000 ng/mL of tenofovir in cervicovaginal secretions had a 74% lower risk of HIV[59]. Although the overall reduction of 39% was modest, a clear adherence-efficacy relationship is seen from the results. Three randomized controlled trials tested the efficacy of daily oral emtricitabine/TFV among different study populations and also found increasing efficacy with increasing adherence (iPrEX, TDF2, Partners PReP)[60–62]. The results of these clinical trials provide convincing scientific evidence that biologically, the use of ARVs for prevention reduces risk for HIV infection if the ARVs actually used.

However, adherence remains a significant challenge for oral and vaginal PrEP in sub-Saharan Africa. To date there has only been one clinical trial for vaginal microbicides that has shown a protective effect. The CAPRISA-004 trial showed 39% efficacy in preventing HIV-1 infection for women assigned to use a 1% TFV vaginal gel relative to placebo gel[12]. The subsequent FemPREP (oral ARV tablets) and VOICE clinical trials (oral TFV tablets and 1% TFV vaginal gel arms) were halted early due to inefficacy, with low adherence cited as a primary reason[13,63]. FACTS-001 was a follow-up trial to CAPRISA-004 using the same pericoital dosing regimen, but it also failed to show efficacy, likely attributable to low adherence[64].

Reasons for poor adherence in these trials are complex. Product use has been found to depend not only on desirable or undesirable characteristics of the specific vaginal product itself (which vary from woman to woman), but also factors that may apply to all vaginal dosage forms in general. These factors include fears of safety or product harm, stigma of using ARV-containing products, preferences of the male partner, societal pressures, and interactions with the research study team[65,66]. Many of these reasons given for product use or non-use apply to all vaginal dosage forms and cannot be addressed by making changes in product design. It is important to recognize that addressing the social or educational reasons for non-use may not be possible through an engineered solution. Instead, it highlights the need for increased collaboration between scientists, product developers, and behavioral scientists, clinicians, and educators in the development and introduction of a new microbicide product.

The lack of adherence in recent clinical trials also demonstrates the need for a variety of dosage forms for women with diverse ranges of needs and preferences. Some of the key considerations in designing a vaginal dosage form for increased adherence include ease of insertion, the degree of lubrication, and external leakage/messiness[67]. Organoleptic properties including color, taste, odor, and texture are also important factors that impact acceptability. Many women prefer to be able to use a product discreetly without their partner's knowledge, so a microbicide that is colorless, odorless, and tasteless would be preferred. Time for product dissolution or spreading and the use of applicators or type of packaging can also contribute to a woman's ability to use a product discreetly. Cultural and personal preferences also vary widely[68], so preferences of women in relevant populations should be taken into consideration during the design of a microbicide.

Another factor that will likely affect user adherence is the dosing frequency and regimen that is required (e.g., 1x/day, pericoital, sustained release). For example, vaginal films have been designed to hydrate and dissolve in 4-20 minutes and release drug quickly during that time[45,46]. Such a product could be applied shortly before intercourse to provide protective levels of drug and used pericoitally as needed. In contrast, vaginal rings have been designed to provide sustained release over the course of weeks to months. Zero-order release kinetics have been reported up to 90 days for vaginal rings delivering TFV and levonorgestrel[69]. Due to variable needs and preferences of women, there is need for both pericoital and sustained release microbicides. However, given the challenges of low user adherence observed with once-daily or pericoital dosage forms in clinical trials, the microbicide field has shifted toward prioritizing sustained release dosage forms, primarily intravaginal rings[70,71].

The decision of whether to use a product or not is affected by more than the preclinical safety and efficacy data. End user perspectives and cultural context are crucial to consider during early stages in the development of a new microbicide platform. Woodsong and Holt have reviewed the acceptability and preferences for vaginal dosage forms intended for prevention of HIV and define important concepts related to end users[67]. *Acceptability* refers to a person's willingness to try or use a product, while *adherence* refers to a person's compliance with all product requirements and product use regimens[67]. *User preferences* are the product characteristics that are most desired out of a range of options. A *conceptual framework* describes broader involvement of multiple spheres of influence, including culture, economics, politics, family, and partner support[67]. In Table 1-2 below, three vaginal dosage forms that have been studied in clinical trials (gels, films, rings) are compared in terms of user preferences, actual acceptability and adherence in clinical trials, and feasibility based on technical constraints.

Table 1-2 Comparison of user preferences, feasibility, and acceptability of vaginal dosage forms in microbicide clinical trials.

	Vaginal gel	**Vaginal film**	**Intravaginal ring**
Dose and Duration	1-4.5 mL gel, inserted once daily or pericoitally (BAT-24 regimen)	1x2 cm or 1x1 - 2x2 inch film; inserted pericoitally	1 ring that provides continuous drug levels for 28d, 3 months, or 1 year
User preferences: positive attributes	-Increased lubrication (reported as both positive and negative) -Increased "wetness" / leakage (reported as both positive and negative, depending on study)	-Product discreetness -Minimal leakage -Quick absorption -Amount of lubrication provided (reported as both positive and negative) -No applicator required -Easy to insert (reported as both positive and negative) -Minimal waste disposal required, other than packaging	-Hypothesized increased user adherence due to less frequent user action (ongoing clinical trials) -Less frequent insertion required (less privacy needed) -Continuous drug levels provide protection for those at risk for unplanned or unwanted sex
User preferences: negative attributes	-Increased lubrication -Leakage/discharge -Visual appearance when discharged -Messiness due to leakage, clumping -Ability to use without partner's knowledge ("discreet use" depends on partner) -Frequent privacy required for daily or BAT-24 insertion -How/where to dispose of used single-use applicators	-Sharp edges -Minimal lubrication -Difficult to insert due to stickiness (reported as both positive and negative)	-Many users initially skeptical of size, shape, but uncertainty usually dissipates after first use -Discreetness? 25% of male partners can feel rings in US and African studies -Ring expulsions: rate of ~8% (in US and African studies) -Removal of ring for menses or for cleaning (potentially before indicated removal) -How to dispose of used rings; need to return to clinic?
Technical constraints (feasibility of addressing user preferences)	-Limited capacity to provide continuous sustained release -Formulating agents with diverse physicochemical properties in aqueous dosage form -Need for applicators -Shelf-stability of aqueous dosage form	-Limited capacity to provide continuous sustained release -Low reported drug loading capacity (<2 %w/w) -Excipients needed to achieve desired mechanical properties for insertion	-Need mechanical design optimization to prevent ring expulsions -Modifications in product design or regimen to allow for removal / cleaning
Acceptability and adherence in clinical trials	-Overall mixed results -DUET cervical barrier/gel study showed high acceptability (Montgomery *et al* 2010) -HTPN035 showed high acceptability (Karim *et al* 2011) -CAPRISA 004 showed high acceptability (97.4%) but variable adherence; increasing efficacy with increasing adherence (Karim *et al* 2010, Kashuba *et al* 2015) - VOICE trial showed low adherence overall (<40% of users had detectable TFV in plasma (Dai *et al* 2015) -FACTS 003 showed low adherence (Rees *et al* 2015)	-Overall high acceptability - 89% of film users in 3-country African study liked it, 87% would use again (Nel *et al* 2011) ->80% liked N-9 film (Cameroon) (Visness *et al* 1998)	-Overall very high acceptability, especially once women try them (initial reactions negative) -100% of users in one study reported they would use IVR if found effective (Van der *et al* Straten 2012) -Very high adherence in another study (82-95%) (Montgomery *et al* 2012)

Male partner feedback (*not as widely studied, small sample sizes)	-85% of male partners who knew about product use were supportive (Minnis *et al* 2013) -Overall high support for Carraguard gel in South African study (Kelly 2015 *et al*)	High acceptability by male partners; only 7% reported disliking film (Nel *et al* 2011)	High acceptability by male partners (Van der Straten *et al* 2012)
References	Woodsong and Holt 2015, Karim 2010, Kashuba 2015, Karim 2011 Dai 2015, Rees 2015, Minnis 2013, Kelly 2015, Montgomery 2010	Woodsong and Holt 2015, Visness 1998, Nel 2011, Garg 2010, Morrow 2014, Akil 2011	Woodsong and Holt 2015, Van der Straten 2012, Montgomery 2012

References for table: vaginal gels [11,12,64,67,72–76]; vaginal films [36,45,67,68,77,78]; intravaginal rings [67,79,80]

1.2.7 Literature Review: nanomaterials for vaginal drug delivery

Here we present a review of literature pertaining to nanoparticles and nanofibers for vaginal drug delivery, the focus of the completed and proposed work presented in this document. Figure 1-1 highlights rationale for why nanomaterials are of interest for HIV prevention and other vaginal drug delivery applications.

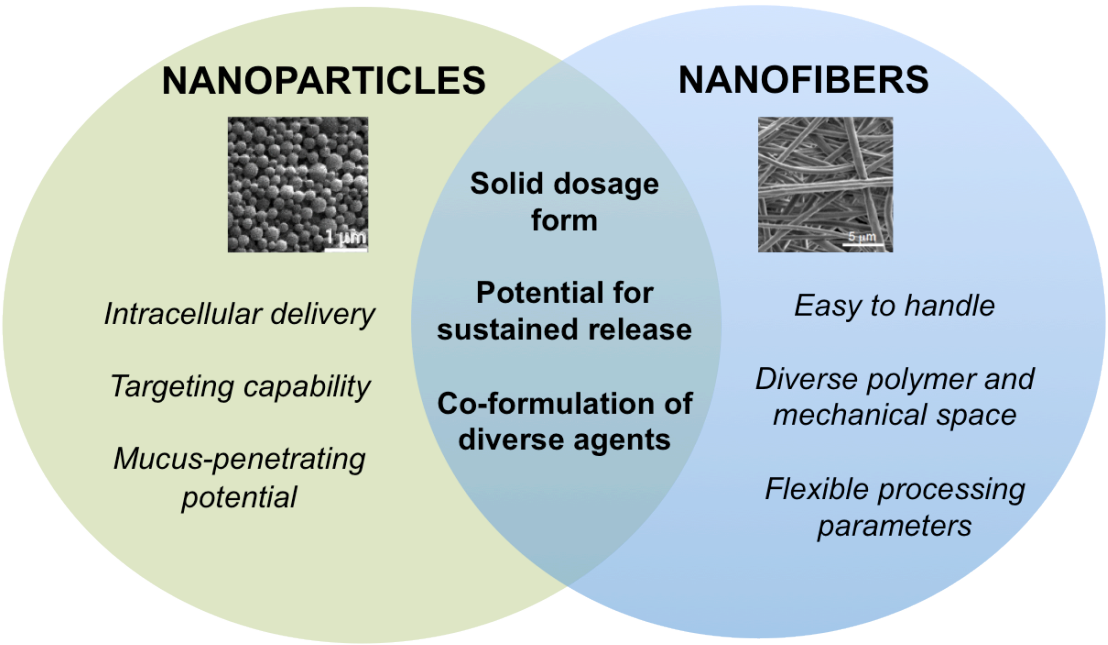

Figure 1-1. Rationale for novel nanomaterial strategies for vaginal drug delivery.

1.2.8 Nanoparticles for vaginal drug delivery

1.2.8.1 Nanocarriers for drug delivery: overview

Nanocarriers have been widely investigated for many drug delivery applications due to their potential for intracellular delivery, sustained release, formulating a diverse range of agents, and targeting capabilities. Nanocarriers are identified by their size of 10-1000 nm and include

carriers such as nanoparticles, liposomes, micelles, dendrimers, nanotubes, and nanolipogels. They have been studied as delivery vehicles to the cardiovascular, pulmonary, and central nervous systems for applications such as cancer therapy, hormone delivery, and vaccination, and many have advanced to clinical trials[81]. Many extensive reviews on nanocarriers for drug delivery have been published[82–84].

One advantage that nanocarriers facilitate compared to other delivery systems is their ability to deliver contents intracellularly, which may allow for greater concentrations of drug to reach their targets. Submicron-sized particles have been shown to have greater cell uptake and better submucosal penetration than microparticles[83]. Nanocarriers have been documented to enter cells via endocytic pathways, pinocytosis, receptor-mediated transport, and facilitated transport[85]. The small size of nanocarriers that enables intracellular delivery is an attractive feature of this system, particularly for agents with intracellular sites of action.

Nanocarriers also provide a strategy to sustain the release of agents over time, decreasing the need for frequent administration. Poly(lactic-co-glycolic acid) (PLGA) particles have been show to escape the endosomal compartment and remain in the cytoplasm for extended periods of time[86]. Animal studies using PLGA nanoparticles for gene delivery have shown sustained levels of tissue gene expression for at least four weeks after administration[87]. Additional studies have shown that nanoparticles can extend the period of drug delivery from 3 days to 2 weeks or longer compared with free drug in solution[86,88].

Besides providing intracellular delivery and sustained release of agents, nanocarriers enable versatility in the types of agents that can be delivered. Nanocarriers can be made from polymers with varying rates of degradation, chemical and physical properties. They have been used to deliver a diverse range of agents including hydrophilic drugs[89], hydrophobic drugs[88], DNA[87], siRNA[90,91], and proteins[92]. For many of these agents, encapsulation within nanocarriers provides protection from degradation due to surrounding environment. This is particularly true for drugs and proteins that are susceptible to enzymatic or hydrolytic degradation[93].

Both synthetic and natural materials have been used to create nanocarriers[94]. PLGA has been one of the most widely used synthetic polymers for nanoparticles, due to its controllable degradation rate and biocompatibility, and it is already being used in humans for sutures, bone screws, and contraceptive implants[83]. Other synthetic materials such as poly(lactic acid) (PLA)[95], poly(caprolactone) (PCL)[96], and poly(acrylates)[97] have also been used as materials for nanoparticles. Synthetic materials offer the advantage of providing greater control over the molecular weight distribution and side chain identity compared to natural materials. Some natural polymers that have been used for fabricating nanocarriers include chitosan, alginate,

collagen, and gelatin[98]. Natural polymers often possess reactive sites that can be crosslinked or modified with ligands, and they are generally cytocompatible, although some concerns have been raised about their immunogenicity[94].

Several fabrication methods have been used to synthesize nanoparticles, including single and double emulsion techniques[99], nanoprecipitation[100], spray drying, and electrospraying[101]. Concerns have been raised with the ability to scale-up emulsion and nanoprecipitation techniques, and spray-drying can result in reduced product yields[99]. After fabrication, particles are generally characterized for their size and zeta potential using dynamic light scattering, morphology with scanning electron microscopy, and drug loading and release using chromatographic methods. Various assays are used to confirm that agents retain their activity after encapsulation into particles and are biocompatible, depending on the application.

Despite all the potential advantages that nanocarriers offer for enhanced delivery, several barriers exist that have prevented nanocarriers from advancing towards clinical application. First, a trade-off exists between enhanced uptake and controlled release. While the small size of nanocarriers enhances tissue penetration and intracellular uptake, this comes at a cost of a less controllable release profile due to their large surface area. Smaller nanoparticles generally display significant burst release, while larger particles display more controlled release but have reduced uptake[85]. Second, depending on surface properties, nanoparticles can have poor colloidal stability and problems with aggregation[102,103]. Third, low drug encapsulation efficiencies have been observed for some agents[104], likely due to drug partitioning into the aqueous phase during formulation. Finally, nanocarriers have been shown to either stimulate or suppress immune responses, and methods to characterize potential adverse immunologic responses are not yet well established[105]. Immunoglobulins and complement proteins C3, C4, and C5 are capable of binding to the surface of some nanoparticles, making them detectable by the mononuclear phagocytic system and preventing them from reaching their targets [106]. New approaches are needed to address these concerns and more extensively evaluate the immune response to nanoparticles. For instance, modifying particle surface chemistry to prevent aggregation may enhance colloidal stability and reduce interactions with the immune system, and higher encapsulation efficiencies may be obtained using electrospraying technology for particle synthesis

1.2.8.2 Nanocarriers that overcome barriers vaginal drug delivery

Due to their ability to be rationally designed for specific environments, nanocarriers are a promising platform to overcome barriers associated with mucosal delivery routes including to

the vaginal and cervical epithelium. Nanocarriers are being developed that can penetrate the mucus layer[107,108] and respond to pH changes within the vagina[109,110] for optimal delivery. Local administration of nanocarriers to the vagina also allows for the bypass hepatic first pass metabolism, higher local drug concentrations at the site of infection, and reduced side effects compared to systemic delivery. This is especially beneficial for diseases that are transmitted sexually like HIV, in which the initial cellular targets of viral infection are the immune cells of the vagina and cervix. Additionally, the cervicovaginal tract offers a large area for nanocarrier delivery because the surface is comprised of numerous folds called rugae. Several helpful reviews on nanoparticles for mucosal drug delivery have been published[85,111–113]. Here we will focus on nanomaterials engineering strategies that have been used to overcome specific barriers related to vaginal drug delivery (Figure 1-2).

1.2.8.3 Overcoming the mucus barrier

Although local delivery offers many advantages, one particularly challenging aspect of vaginal delivery is that of the mucus barrier produced by mucus-secreting cervical cells. Cervicovaginal mucus is a crosslinked viscoelastic hydrogel composed primarily of water with approximately 2-5% mucin by weight[113]. The composition, pH, and rheological properties are highly variable, depending on the menstrual cycle and health and reproductive status of the woman. The presence of semen (pH 7-8) also influences mucus properties[114]. The pore size of cervicovaginal mucus has been estimated to be 340 nm on average, with a range of 50-1800 nm[115]. Notably, cervicovaginal fluid is a discontinuous layer, with some areas along the cervicovaginal tract having no mucus and some areas having a mucus layer that is several millimeters thick[116]. Because mucus is shear-thinning, it is able to maintain an unstirred layer of mucus called the adherent layer that lies directly underneath the more rapidly cleared luminal layer[24,113]. The mucus barrier must be crossed in order for nanoparticles to reach the underlying target cells, but its variable properties make it challenging to characterize.

Nanoparticles are being designed to overcome this barrier by controlling the surface properties and size of particles to modulate their interaction with the mucus layer[85,113,114,117]. Particle size in the range of 200-500 nm has been found to be optimal for diffusion through mucus[113]. Large particles (>1000 nm) are too large to penetrate porous mucus network, but small particles (100 nm) can become physically entrapped within the tortuous polymer network[116]. The hydrophobicity of the particle surface also appears to greatly impact particle diffusivity. PEGylation of particles has been shown to increase transport in mucus[113,118,119]

Further, surface charge has been shown to greatly influence particle diffusion through mucus. Negatively charged particles are able to move more quickly through mucus than positively charged particles, likely due to electrostatic repulsion between particles and negatively charged functional groups on mucin[116]. The effect of electrostatics on transport through mucus has been demonstrated with HIV virions themselves. The production of lactic acid in cervical mucus has been shown to neutralize the negative surface charge of the HIV virion and significantly slow its

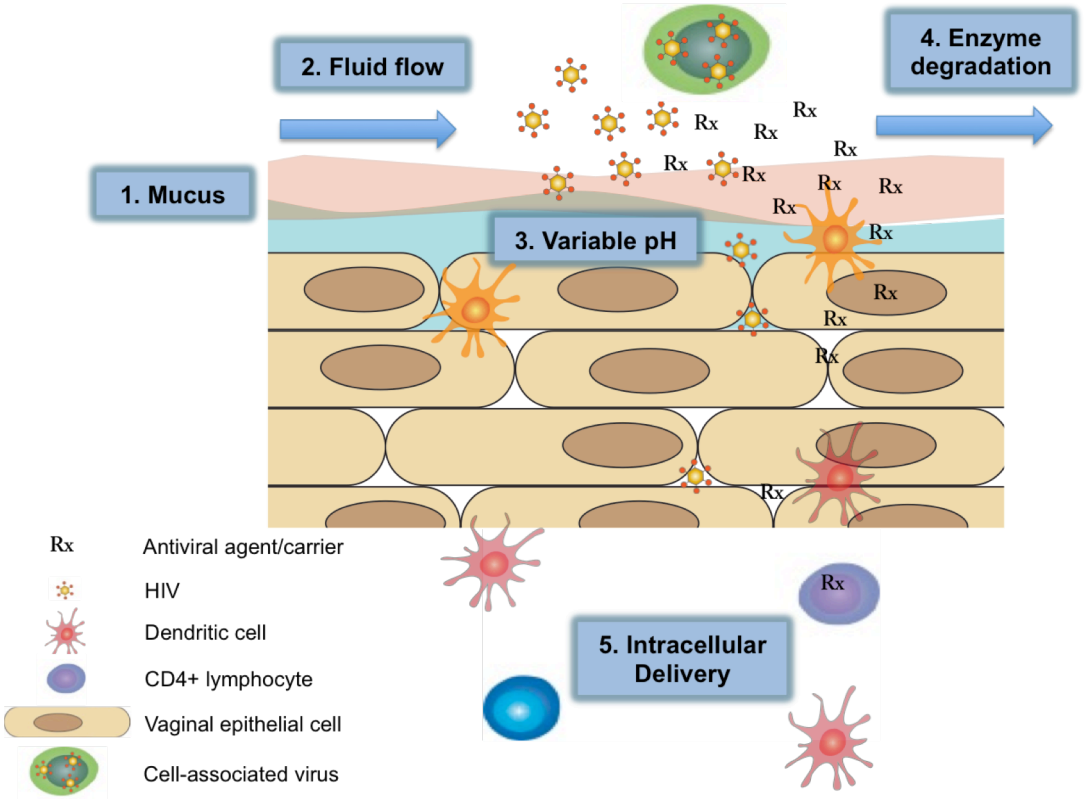

Barrier	1. Mucus	2. Fluid flow	3. Variable pH	4. Enzyme degradation	5. Intracellular delivery
Strategy	Mucus penetrating particles	Nanoparticles that interact with mucus Delivery systems for sustained release	pH-responsive drug delivery	Protection of contents within particles	Targeted nanoparticles Engineering particle size, shape, surface charge for intracellular uptake
References	107, 113, 114, 117	104, 107, 113, 114, 117	109, 110, 156	91, 92	96, 137, 140, 144

Figure 1-2. Strategies to overcome barriers in vaginal drug delivery.

diffusion compared to cervicovaginal mucus at pH 6-7, in which HIV can maintain its negative charge[120].

Mucoadhesive particles and mucoevasive particles have proposed as two strategies to overcome the mucosal barrier. Mucoadhesive particles are typically fabricated with a positively charged surface that will electrostatically bind to the negatively charged carboxyl and sulfate groups on mucin[85]. These particles are designed to remain in the mucus, slowly releasing their contents that can then diffuse through the mucus layer into underlying cells. Chitosan has been used as a material for mucoadhesive particles for nasal siRNA delivery[90] and vaginal drug delivery[104] because of its cationic nature resulting from protonated amine groups. In addition to surface charge, another determinant of mucoadhesion is size. Meng *et al* studied the effect of particle size on mucoadhesion and encapsulation efficiency of the microbicidal drug candidate tenofovir[104]. They found that 188 nm particles demonstrated a 2-fold increase in mucoadhesion to porcine vaginal tissue compared with 900 nm particles. However, the smaller particles only resulted in 5% encapsulation efficiency compared with 20% for the larger particles, so the authors concluded that the larovger-sized particles were most optimal for delivery of tenofovir. One must consider the balance between size and diffusivity in designing mucoadhesive particles. While smaller particles have increased surface area that leads to greater mucoadhesion, they may also have increased diffusivity in mucus compared to larger particles.

A contrasting approach to mucoadhesive particles is to create mucus-penetrating particles that are able to reach the underlying cells in the submucosa by penetrating the mucus layer. Since particle retention is also limited by the periodic sloughing of the mucus layer, particles that are trapped within this layer may be expelled before reaching their cellular targets[85]. As such, several groups have designed the surface properties of nanoparticles so that they can better penetrate the negatively charged mucus layer[107,113,116,118]. One of the more successful strategies has been to mimic viral strategies for mucus penetration by creating hydrophilic, net neutrally charged surface to minimize adhesion-causing hydrophobic and electrostatic interactions[85,113].

The density of poly(ethylene glycol) (PEG) surface coating and molecular weight of PEG were found to greatly influence transport, as demonstrated by Wang *et al* [119]. A highly dense surface coating of PEG was found to result in faster transport due to minimized hydrophobic interactions with mucin. Low molecular weight PEG was also found to enhance transport, with 2 kDa and 5 kDa PEG resulting in much faster transport than 10 kDa PEG. The authors suggested that high molecular weight PEG may result in entanglements with mucin polymer chains, preventing diffusion[119]. Using this strategy, Lai *et al* modified the surface of polystyrene nanoparticles with a high density of low molecular weight (2 kDa) PEG to create a net-neutrally

charged, hydrophilic surface[113]. They found transport rates in human mucus were enhanced by three orders of magnitude for 200 and 500 nm particles. Mert *et al* have also shown that a dense coating of low molecular weight PEG is optimal for mucus penetration[118]. They report that Vitamin E / 5kDa PEG (VP5k)–coated PLGA nanoparticles better penetrate human cervicovaginal mucus than poly(vinyl alcohol) or 1kDa PEG–coated particles, and that VP5k allowed for controlled release of paclitaxel over 4 days. They attributed this difference to the denser PEG coating and more neutral surface charge for 5kDa PEG-coated particles compared with the 1kDA PEG particles.

Conferring a negative surface charge to nanoparticles also appears to enhance their ability to penetrate mucus. Das Neves *et al* have studied the influence of surface charge on rate of transport in simulated vaginal fluid containing mucin adjusted to pH 4.2 and 7.0[116]. They evaluated dapivirine-loaded PCL particles with three different surface coatings: poloxamer 338 NF (PEO), sodium lauryl sulfate (SLS), and cetyltrimethylammonium bromide (CTAB). They found that all PCL particles were mildly mucoadhesive on their own, likely due to hydrophobic interactions between the PCL polymer and mucin. However, they reported that nanoparticles with negatively charged surfaces (modified with PEO or SLS) were able to move through mucus simulant by subdiffusive transport at rates that may be appropriate for microbicide delivery. In contrast, transport of nanoparticles with positively charged surfaces (CTAB-modified) was impaired, likely from electrostatic interactions with mucin. This work highlights the importance of considering surface charge in engineering nanoparticles with mucoevasive properties.

There is emerging evidence that conventional (i.e., uncoated) polymeric nanoparticles may be unable to penetrate cervicovaginal mucus to reach the underlying target cells. For example, Yu *et al* report that PLGA particles were slowed by 12,000-fold in human cervicovaginal mucus compared to water, whereas particles made from the diblock copolymer PLGA-PEG were slowed only 8-fold in human cervicovaginal mucus compared to water [108]. Cu *et al* have studied the distribution of PEG-modified (mucus-penetrating), avidin-modified (mucoadhesive), and unmodified PLGA nanoparticles following intravaginal administration in mice[117]. They found that that surface properties significantly impact their ability to penetrate tissue. Approximately five times greater vaginal retention was observed for both the mucus-penetrating PEG particles and the mucoadhesive avidin-modified particles over 24 h compared to unmodified PLGA particles. However, significantly more PEG-modified PLGA particles remained in tissue extracts up at to 6 hours following administration, leading the authors to conclude that the mucus-penetrating modification was most effective for intravaginal delivery. Ensign *et al* developed mucus-penetrating 5 kDa PEG-conjugated polystyrene particles loaded with acyclovir that were able to

prevent herpes simplex virus 2 (HSV-2) in mice[107]. The acyclovir mucus-penetrating particles protected 53% of mice against HSV-2 challenge compared to 16% of mice receiving soluble drug. In addition, they found over a nearly three-fold improvement in tissue coverage (from 30 to 87%) and longer tissue retention provided by mucus-penetrating particles compared with conventional (carboxyl-modified polystyrene) particles.

While the improved mucus penetration and tissue retention attained by mucus-penetrating particles represents an important advance in vaginal drug delivery, some challenges remain. Particularly, the effect of modifying surface properties for mucus penetration on intracellular uptake has yet to be determined. Particles with a net neutral charge may be optimal for penetrating mucus, but there may be a trade-off with lower levels of intracellular uptake. Size, material composition, and surface chemistry have been shown to affect cell uptake[121–123]. Specifically, PEG modification has been shown to reduce phagocytosis in macrophages[121,124]. Studies that pair mucus penetration capabilities of nanoparticles with their intracellular uptake, such as those performed by das Neves *et al*, would provide valuable insight into this potential setback[96,116]. Balance between ability of nanoparticles to penetrate the mucus layer and deliver their payload intracellularly may best be achieved by evaluating particle transport, intracellular uptake, and cytotoxicity in parallel for all formulations.

1.2.8.4 Overcoming variations in vaginal pH

Another challenge unique to vaginal drug delivery is the varying pH present in the reproductive tract. Normal physiologic pH in the vagina ranges from 4-6, but can change with the presence of bacterial infections, changes in the menstrual cycle, or presence of semen[21,85]. Lactobacilli convert glycogen to lactic acid and are the primary microbe responsible for maintaining vaginal pH in premenopausal women[85]. Once particles penetrate the vaginal epithelium, they would be subject to increasing pH in the subepithelial layer and intracellularly.

Instead of seeing vaginal pH fluctuation as a barrier, several groups have used this variation as a stimulus for “smart” drug delivery from nanoparticles. The normally acidic pH of the vagina is altered during sexual intercourse, since the pH of semen is known to be basic (7-8) with a high buffering capacity[125]. Polymers that are soluble in alkaline solutions but insoluble in acidic solutions could serve as stimuli-responsive materials to release drug contents upon an increase in pH. Such polymers could be used to trigger release of agents that block HIV action when the virus enters the body in semen. Zhang *et al* have created Eudragrit® S-100/PLGA pH-reponsive particles for semen-triggered vaginal delivery of tenofovir[109]. Eudragrit S-100® is a pH-responsive copolymer made from methacrylic acid-methyl methacrylate (1:2) that is soluble in

an alkaline environment. They show a 4-fold increase in drug release rate from these particles over 72 hours in the presence of a semen fluid simulant (pH 7.6) compared with vaginal fluid simulant (pH 4.2). Yoo *et al* also investigated Eudragrit® S-100 as a material to create pH-responsive particles for mucosal delivery[110]. They show that particles loaded with hydrophilic or hydrophobic model drugs release <40% of contents *in vitro* at pH 4.0 over six hours, compared to nearly 100% of contents at pH 7.4 within one hour. While this system has yet to be evaluated *in vivo*, initial results suggest that pH-triggered release from Eudragit® particles may be a feasible method for stimuli-responsive drug delivery to the vagina.

1.2.8.5 Vaginal delivery of antiretroviral agents, proteins, and nucleic acids

First generation microbicides for HIV chemoprophylaxis were based on materials with nonspecific action against HIV and included surfactants, polyanions, and dendrimers[7]. Disappointingly, these products failed to show efficacy in clinical trials, with some even increasing susceptibility to HIV. The first microbicide to show clinical efficacy was a microbicide gel containing 1% TFV, resulting in an overall 39% reduction in HIV infections among South African women[12]. The current paradigm for designing microbicides has shifted to focus on agents with specific mechanisms of actions against HIV[126]. While delivering agents with specific against HIV may prove to be more effective than nonspecific methods, formulating them into vaginal products so that they are active and bioavailable has been challenging.

Nanoparticles offer several advantages for the development of HIV microbicides in particular, including overcoming challenges of drug stability and solubility, co-delivery of diverse agents, and providing sustained release. First, many ARVs have low aqueous solubility, making them hard to administer in their free forms. Nanoparticles have been used to encapsulate and release dozens of hydrophobic drugs, including many ARVs[85,127]. They also offer a means to protect their contents from premature degradation by vaginal pH and enzymes. Nanoparticles have been made that encapsulate ARVs including zidovudine[124,128], efavirenz[88], saquinavir[129], lopinavir[88], ritonavir[88], tenofovir[104,109], tenofovir disoproxil fumarate[109], dapivirine[96], and indinavir[130]. Some of these particles were designed for systemic delivery for HIV therapy, and some were proposed for topical application for HIV prevention. Several helpful reviews have previously been published on ARV-loaded nanoparticles[127,131,132].

One paradigm for engineering next-generation microbicides is that of highly active antiretroviral therapy (HAART). HAART has been used successfully to treat people infected by HIV through the co-administration of multiple antiretroviral drugs, surmounting the drug-resistant strains that come from a rapidly mutating virus. However, co-formulating antiviral drugs of

diverse physicochemical properties into a single product has posed a challenge for topical microbicide development. Polymeric nanoparticles are a platform that allows for individual formulation of ARVs that can subsequently be delivered simultaneously.

Chaowanachan *et al* have investigated the potential for ARV nanoparticles to provide drug synergy[133]. They formulated PLGA nanoparticles loaded with efavirenz (EFV) or saquinavir (SQV) and evaluated their antiviral activity and synergy with free TFV in TZM-bl cells. EFV nanoparticles resulted an approximately 50-fold decrease in IC50 value compared to free EFV, in addition to strong synergism when delivered with TFV. SQV nanoparticles resulted in a ~2-fold reduction in IC50 and also showed synergistic activity in combination with TFV. Even though intracellular delivery was not measured in this study, the authors expect this is the mechanism by which nanoparticles produced increased activity compared to free drug. This work not only demonstrates the potential for nanoparticles to facilitate greater delivery than unformulated ARVs, but also to allow for drug-drug interactions that may not be possible just by delivering free drug combinations.

In addition to the delivery of hydrophobic ARV drugs, nanocarriers have also been used as a vehicle for the vaginal delivery of biologic agents, including peptides and nucleic acids. These agents would likely be quickly degraded by the acidic vaginal pH or enzymes in their free form, so nanocarriers may prove especially helpful for their delivery.

PSC-RANTES, a chemokine analogue that blocks CCR5 expression, is of particular interest for vaginal drug delivery due to its picomolar potency and its demonstrated *in vivo* protection against HIV-1 when topically applied in rhesus macaques[134]. However, for *in vivo* efficacy, doses were required which were orders of magnitude higher than concentrations necessary for *in vitro* efficacy. Hypothesizing that nanoparticles could overcome problems with free protein delivery such as poor submucosal tissue penetration or premature protein degradation, Ham *et al* have created PLGA nanoparticles loaded with PSC-RANTES[92]. Indeed, they found a five-fold increase in tissue uptake over four hours for PSC-RANTES encapsulated in nanoparticles versus unformulated PSC-RANTES in an *ex vivo* cervical tissue model. Nanoparticles also provided enhanced tissue penetration of the peptide and localization at basal layers of epithelium. They also report that encapsulation into nanoparticles did not affect the *in vitro* anti-HIV activity of PSC-RANTES. Approximately 70% of the peptide was released *in vitro* over 30 days, with release being affected by the pH of release media and the L (lactide):G (glycolide) ratio of PLGA used for nanoparticle formulation. Decreased PSC-RANTES release was observed with increased pH (4.6 to 7.4) and with increasing L:G ratio (50:50 to 85:15). These results provide evidence that PLGA nanoparticles can be used to encapsulate and sustain

release of a peptide relevant to vaginal drug delivery, and further, that the L:G ratio of PLGA may be used to control release kinetics.

PLGA nanoparticles have also been investigated as a strategy for the vaginal delivery of nucleic acids. Woodrow *et al* loaded PLGA nanoparticles with siRNA targeted against the gene encoding enhanced green fluorescent protein and studied gene expression after topical intravaginal application to transgenic mice[91]. *In vitro* release studies showed that particles were able to provide sustained, linear release of siRNA over 30 days, with about 50% of total encapsulated siRNA released. Sustained gene silencing was observed throughout the mouse reproductive tract for at least 14 days after a single topical application of nanoparticles, and histological analysis revealed that particles were able to penetrate deeply into the epithelial tissue. The authors concluded that PLGA nanoparticles provide effective and sustained release of siRNA and are less inflammatory that siRNA lipoplexes, and thus demonstrate an expanded application of PLGA nanoparticles to mucosal surfaces. This work has been expanded on by Eszterhas *et al*, who hypothesized that by lowering expression of CD4 and CCR5 receptors in tissue, infection could be reduced because HIV would be less able to enter cells[135]. They delivered CD4- and CCR5-specific siRNA in INTERFERin® (Genesee Scientific) nanoparticles to human cervical explants and monitored gene expression and HIV-1 infection over five days. Explants exposed to nanoparticles were found to have lower levels of CD4 and CCR5 transcripts, as well as reduced HIV-1 reverse transcripts. They also observed increased production of IFN-alpha, a potent antiviral cytokine, which may strengthen antiviral activity. These examples demonstrate that nanoparticles can be used to effectively deliver siRNA intravaginally, which may have applications for topical microbicides for HIV prevention.

1.2.8.6 Drug targeting and intracellular vaginal delivery

Besides the challenge of formulating multiple drugs for simultaneous delivery, user adherence has been a substantial challenge in clinical trials of vaginal microbicides for HIV-prevention. Low adherence to vaginal gels requiring daily administration has been suggested as a primary reason for the lack of efficacy observed in FEM-PREP and VOICE trials[63,136]. The development of a long-acting microbicide that requires less frequent administration provides a means to increase adherence. As discussed previously, nanoparticles have been shown to provide sustained release of agents for 2-4 weeks after a single administration. As such, nanoparticles may offer a means to create a long-acting microbicide by allowing for sustained intracellular delivery and targeting of agents with activity against HIV. A comparison of intracellular drug levels after *in vitro* delivery of ARV nanoparticles is shown in Appendix F.

Research done by Destache *et al* has provided insight into the persistence time and intracellular release profiles of ARV-loaded PLGA nanoparticles in peripheral blood mononuclear cells (PBMCs)[88]. They synthesized efavirenz, lopinavir, and ritonavir-loaded nanoparticles and measured intracellular drug levels over 28 days. Free drugs administered to PBMCs reached a peak concentration at 8 hours and were eliminated within 48 hours. In contrast, ARV-loaded nanoparticles reached peak drug concentrations at 24-96 hours, and drug levels persisted at >0.9 μg for the full 28 days of the study. This study provides strong evidence for the ability of PLGA nanoparticles to provide sustained release of ARVs and potential application for a long-acting microbicide.

Das Neves *et al* have done work to investigate the relationships between surface modification of nanoparticles, cellular uptake, and antiviral activity using six cell types relevant to vaginal HIV transmission[96]. They formulated dapivirine-loaded PCL nanoparticles with three different surface modifiers (CTAB, PEO, or SLS) to create particles with either positively or negatively charged surfaces. Nanoparticles with a positive surface charge (CTAB) resulted in higher drug concentrations in VK2/E6E7 vaginal epithelia cells and HeLa cervical cells compared to negatively charged particles (SLS, PEO). They found that all nanoparticles resulted in enhanced intracellular drug levels in phagocytic cells and similar or improved activity against HIV compared to free drug, indicating a passive targeting mechanism of nanoparticles. Due to the relatively high levels of cytotoxicity observed with CTAB-modified particles, they concluded that particles with a negative surface charge (PEO or SLS-modified) were better candidates for vaginal delivery of dapivirine. This study is consistent with other research that has shown that for some drugs, ARV-nanoparticles result in enhanced antiviral activity when compared to free ARVs[133].

Another strategy for the delivery of antiretrovirals has been termed “nanoART” (nano-antiretroviral therapy), which refers to crystalline drug broken into nano-sized pieces using techniques like wet-milling. NanoART has been proposed as a strategy to overcome pharmacokinetic limitations of ARVs by providing a more long-acting formulation with better biodistribution. Nowacek *et al* have investigated several wet-milled ARVs for their physicochemical properties, intracellular delivery, and ability to prevent HIV-1 replication in monocyte-derived macrophages[137]. They found that properties such as particle size, surface charge, and shape influence cell uptake and antiretroviral efficacy. Specifically, a strong correlation of 0.92 was found between intracellular drug levels and protection against HIV for efavirenz and atazanavir. These results suggest that intracellular drug delivery is a key component of establishing high levels of efficacy. Roy *et al* evaluated nanoART in HIV-1

infected human peripheral blood lymphocyte-reconstituted mice for the combination delivery of ARVs as a long-acting formulation[138]. They found decreased viral replication and higher CD4+ T-cell populations for mice receiving weekly subcutaneous injections of nanoART compared to orally administered conventional ARVs. While nanoART has shown promise as a strategy for systemic delivery of ARVs for HIV therapy, little work has been done yet to evaluate nanoART for topical application for HIV prevention.

A distinctive feature of nanoparticles compared with other delivery systems is their ability to be targeted to specific cell types through passive or active targeting. Passive targeting is based on physicochemical properties like hydrophobicity and size that lead to preferential uptake, whereas active targeting involves the use of targeting ligands or molecules. Targeted nanoparticles have been widely investigated as a strategy for cancer therapy, as many types of tumors are known to overexpress specific receptors[139]. Nanoparticles have been targeted to tumor surfaces using molecules such as monoclonal antibodies, aptamers, oligopeptides, and folic acid[140]. Targeted nanoparticles may also have valuable applications in vaginal drug delivery, particularly for HIV treatment and prevention. However, unlike in some types of tumor targeting, a surface marker that is unique to all cells infected with HIV has not been identified[141]. HIV is known to infect only certain cell types, including CD4+ T cells, CD4+ monocytes/macrophages, dendritic cells, follicular dendritic cells, some fibroblasts, and microglial cells[141]. Consequently, the HIV receptor CD4, coreceptors CCR5 and CXCR4, and macrophage or dendritic cell receptors may serve as potential targets. Gunaseelan *et al* have published an informative review on targeting strategies for HIV infection[141].

Much research on HIV targeting has been aimed at developing a drug delivery system to eradicate virus from already infected persons through targeting reservoir cell populations that are latently infected with HIV. In particular, many strategies have focused on targeting the CD4+ lymphocyte[142] or macrophage reservoirs[143,144]. Macrophages constitute a major HIV reservoir that harbor the virus in its latent form and are resistant to the cytotoxic effects of HIV, preventing its complete eradication from the body. Though CD4+ lymphocytes represent the largest HIV reservoir by number, the dynamics of HIV replication in macrophages indicate that this reservoir may be of even greater importance. Unlike CD4+ lymphocytes, which are rapidly killed by HIV, macrophages have been shown to continually produce high levels of HIV for at least 60 days after virus challenge[143].

Tuftsin is a tetrapeptide (Thr-Lys-Pro-Arg) that has been shown to naturally activate macrophages[144]. It binds specifically to macrophages, monocytes, and polymorphonuclear leukocytes. Dutta *et al* have designed poly(propylenimine) (PPI) nanoparticle dendrimers

conjugated with tuftsin to deliver efavirenz to macrophages[144]. They showed a 34.5-fold increased cellular uptake for the dendrimers conjugated with tuftsin compared with free drug, as well as significantly higher cellular uptake of tuftsin-conjugated PPI nanoparticles versus PPI nanoparticles. Interestingly, they also observed increased uptake of tuftsin-conjugated PPI nanoparticles in HIV-infected macrophages versus uninfected macrophages, which they attribute to an increased activation state of macrophages infected with HIV. Other strategies for targeting macrophages include molecules that target the formyl peptide receptor 1, mannose receptor, or the Fc receptor[141].

While macrophages may represent a primary target for targeting HIV reservoirs for therapy, other cell types may more appropriate targets for HIV prevention strategies that are intravaginally administered. Perhaps the most relevant targets for prevention are the cells considered to be the initial sites of HIV infection, including CD4+ T cells and Langerhans cells. HIV infection is thought be established through the transport of free HIV virions or cell-associated virus (primarily in macrophages) through the vaginal or cervical epithelium to underlying CD4+ cells[145]. Targeting strategies that would prevent this transport of free or cell-associated virus are potential approaches for designing novel microbicides.

In addition to cells expressing CXCR4 or CCR5, dendritic cells also play an important role in establishing productive HIV infection. Dendritic cells can uniquely bind to HIV without the use of these receptors by means of interactions between DC-SIGN and viral gp120[146]. Langerhans cells can mediate transinfection by transporting virions across the cervicovaginal epithelium to susceptible cells and migrating to T-cell-rich lymph nodes[146]. Targeting dendritic cells may therefore be a useful strategy for creating a more effective HIV microbicide. For example, Penadés *et al* have developed mannosylated gold nanoparticles that interfere with DC-SIGN as a potential microbicide[147]. They report that these gold particles are able to inhibit DC-SIGN-mediated trans-infection of human T cells. By mimicking the HIV virus in its cluster presentation of oligomannosides, this group was able to utilize the high surface area of nanoparticles allows for maximal interaction with gp120. Other targeting strategies specific to dendritic cells include targeting the C-type lectins present on dendritic cells, the CD205 receptor, or Langerin found on intraepithelial Langerhans cells[148].

Given the variety of cell types that can be infected by HIV, nanoparticles targeted to just one cell type may not be sufficient to prevent infection or completely eradicate virus from all reservoir sites. However, as the biology of HIV transmission becomes better understood, nanoparticles offer a strategy to specifically target early stage viral-host interactions. It is also conceivable that multiple types of nanoparticles that target different cell populations could be

delivered simultaneously. Nanoparticles have also been made that directly target the HIV virus itself instead of indirectly targeting cells that could be infected by HIV. Examples include silver nanoparticles that have been found to specifically interfere with HIV entry[149] and polystyrene particles with concanavalin-A on their surface that can capture viral gp120[150].

1.2.8.7 Future challenges and directions for nanoparticles for vaginal delivery

Beyond the advances made in overcoming mucus barrier and variations in vaginal pH, several challenges remain for successful nanoparticle-mediated vaginal drug delivery. First, there is a need for studies that investigate how long nanoparticles can sustain the delivery of drugs to the vagina and surrounding tissue. As discussed previously, much work has demonstrated the potential of nanoparticles to sustain drug release when delivered via other routes of administration. Cellular uptake of dapivirine-loaded nanoparticles and intracellular dapivirine levels have been monitored over 6-10 hours in six cell types relevant to vaginal drug delivery[96]. Similar studies are needed that compare differences in intracellular drug concentrations from delivering nanoparticle-formulated drug versus free drug, evaluated in vaginal cell lines but over time scales extending to several days or weeks. Discerning whether these drug levels actually correspond to protective concentrations that could prevent diseases such as HIV-1 would be of great relevance to this field.

Even if nanoparticles are shown to sustain intracellular drug levels and provide a long-acting dosage form, a practical method of administration of nanoparticles to the vaginal mucosa is still lacking. Several *in vivo* studies have administered nanoparticles intravaginally to mice in aqueous suspensions[107,117], but it is unclear how this would translate to human use. A method of vaginal delivery for nanoparticles is needed that allows for a long product shelf life and enhanced retention time to provide better coverage of the vaginal tissue. One potential solution may be combination dosage forms, such as nanoparticles that release from a solid-state dosage form such as a vaginal ring, diaphragm, or electrospun nanofiber mesh. Further work that evaluates shelf stability, vaginal retention, and biodistribution that result from various dosage forms would serve to more quickly advance this work to clinical applications. Although there are many complex barriers that have prevented effective vaginal drug delivery in the past, nanocarriers represent a versatile delivery vector that may be able to overcome them.

1.2.9 Nanofibers for vaginal drug delivery

1.2.9.1 Nanofibers for drug delivery: overview

Electrospinning technology has been an area of tremendous growth in the last decade[151], as it offers great flexibility to engineer platforms that can be tailored to specific applications. Electrospinning is a simple process in which a polymer solution is pumped through a needle and an electric field is applied across the positively charged needle and grounded collector. Static electrical charges are induced on the molecules of the polymer solution, which then repel each other[152]. The polymer liquid is stretched into fibers upon the force of the electric field overcoming the surface tension of the solution. As the fibers stretch toward the collector and the solvent evaporates, they undergo whipping instability and form a mat of fibers on the collector. We refer the reader to several reviews on the topic of electrospun fibers for a more detailed explanation[151,153,154].

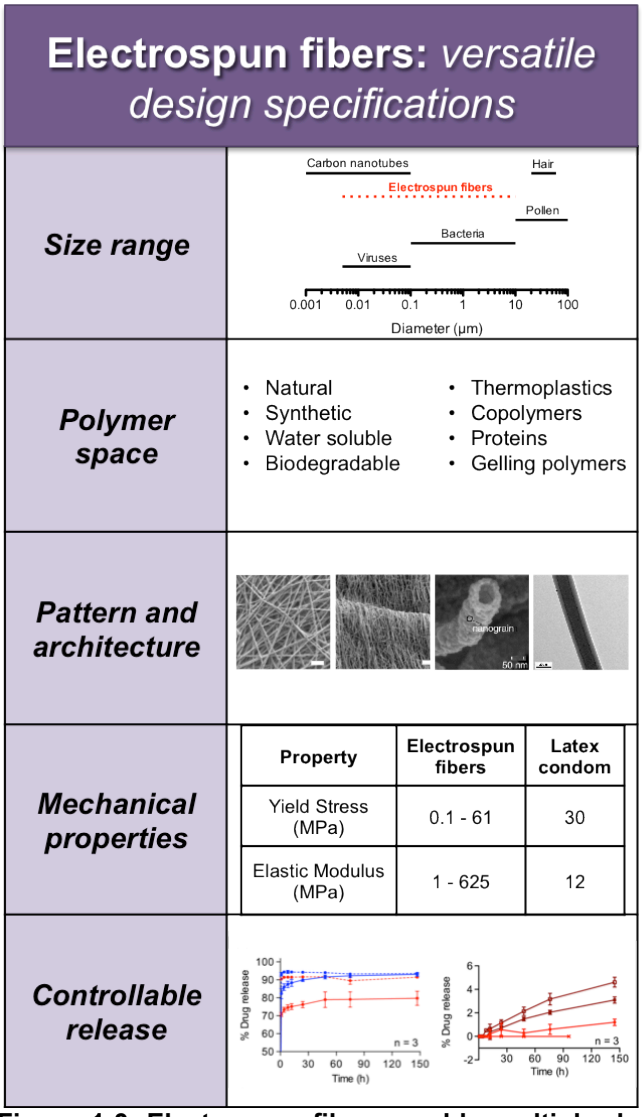

Figure 1-3. Electrospun fibers enable multiple design specifications within a single device.

One of the attractive features of electrospinning is its versatility in terms of material selection, control over processing parameters, and product geometries (Figure 1-3). Over 100 polymers of both hydrophilic and hydrophobic nature have been electrospun as of 2007[154]. Polymers can be blended prior to electrospinning to adjust properties like degradation rate and mechanical behavior[155]. Properties including fiber diameter, pore size, spatial deposition, and alignment can be controlled through modifying parameters like flow rate, applied voltage, and polymer concentration[151,153,156,157]. Electrospun fibers can also be

engineered to mimic the structure of the native extracellular matrix, a crosslinked porous network of glycosanimoglycans with collagen fibers ranging from 500 nm to 15 μm in diameter[158]. As such, they have been investigated for applications including 3D tissue engineering scaffolds[152,159,160] and medical device coatings to reduce the foreign body reaction[161]. Geometries of the fiber mat (e.g., aligned mats, hollow tubes, yarn) and the degree of fiber alignment can be controlled by changing the nozzle configuration or type of collector[153]. Another advantage of electrospinning is that it is economical, allowing for high encapsulation efficiencies and relatively easy scale-up[152].

Electrospun fibers have recently been investigated for their potential as drug delivery systems. Fibers offer a large surface area-to-volume ratio that is amenable to quick drug delivery and have the capacity for high drug loading[162]. In addition, fibers can be engineered to achieve desired release properties by selecting materials with appropriate degradation rates, controlling electrospinning process parameters, and varying the drug binding mechanism. Fibers have been electrospun to deliver drugs such as antibiotics, anticancer drugs, proteins, and DNA[153]. Methods for incorporating drugs into fibers include adding drug to the polymer solution prior to electrospinning, or coating fibers with drug after electrospinning. Some have also utilized hydrogen bonding, hydrophobic, or electrostatic interactions between drug and polymer to complex drugs with fibers[151,163]. Drug release from fibers is governed by three mechanisms: (1) desorption of drugs from fibers surface, (2) solid-state diffusion of drug through fibers, (3) polymer degradation of fibers in vivo[151]. Several strategies have been employed to control drug release from fibers, including embedding drug within fibers versus coating drugs on the outside of fibers, modulating polymer crystallinity, changing fiber diameter, and creating a rate-controlling outer fiber shell using coaxial or emulsion spinning[151]. One of the key strategies has been using coaxial electrospinning to create “core-shell” fibers. Coaxial spinning allows for two different polymers to be electrospun into a single fiber, with one material forming an outer shell and another forming an inner core. This technique can protect biologic agents, nucleic acids, and even cells from organic solvents and the effects of the electric field, in addition to providing another way to modulate release[164,165].

1.2.9.2 Considerations in engineering nanofibers for vaginal drug delivery

Although electrospun fibers have been widely investigated for many drug delivery applications including transdermal[166], oral[167,168], ocular[169], and abdominal delivery[170], they are just beginning to be explored for vaginal drug delivery. Two publications demonstrate proof-of-concept for electrospun fibers as a drug delivery platform to the vaginal mucosa[171,172].

Huang *et al* have electrospun cellulose acetate phthalate (CAP) fibers that dissolve quickly upon increase in pH as potential semen-triggered microbicides[171]. CAP is an especially interesting material for HIV prevention given its ability to induce conformational changes in HIV glycoproteins and interfere with entry. To enhance the inherent antiviral activity of the CAP fibers, the fibers were loaded with two reverse transcriptase inhibitors (TMC 125 or tenofovir disproxil fumarate). Unloaded CAP fibers were found to neutralize 50% of HIV virus at 0.05 mg/mL CAP, and drug-loaded CAP fibers were found to achieve complete neutralization at 0.5 µg tenofovir disproxil fumarate /mL. Electrospun fibers displayed low toxicity toward vaginal epithelial cells (<1.8 mg/mL CAP) as well as three strains of Lactobacillus (<0.1 mg/mL CAP). Fibers were observed to completely dissolve in less than 20 s when added to mixtures of semen and vaginal fluid simulant (VFS), in contrast to their insolubility in VFS alone. The authors expect that these fibers would remain intact upon vaginal insertion, and then locally dissolve and release ARVs upon exposure to semen.

As described in more depth in Chapter 3, we report electrospinning fiber meshes from blends of PLLA and PEO loaded with ARV and contraceptive agents for the prevention of HIV-1 infection and unwanted pregnancy[172]. Electrospun fibers incorporating inhibitors of viral reverse transcriptase and CCR5 binding that potently inhibited HIV infection *in vitro*. The PLLA and PEO blends demonstrated rapid burst release of >70% of ARV payload within one hour in vaginal fluid simulant. By blending the amorphous isomer poly(D,L)-lactic acid (PDLLA) with semi-crystalline PLLA, burst release was prevented and a small degree of sustained release (5%) was observed for maraviroc over 144 h. Fiber meshes were also shown to act as a both a chemical and physical barrier to sperm. The fibers could act to chemically inhibit sperm by releasing glycerol monolaurate to impair sperm motility and physically blocked sperm from penetrating the tortuous fibrous mesh. Fiber meshes were electrospun into a cylindrical geometry intended to provide physical coverage of both the vaginal epithelium and cervix. Nanofibers were shown to provide enhanced coverage of the mucosal tissue when were applied to mice. We envision that fiber meshes could be inserted simply with a tampon applicator, rendering this platform as discreet, female-controlled, and reversible. We project that the application of drug-eluting fibers for vaginal delivery can extend beyond use as a microbicide and contraceptive to other applications such as mucosal vaccine delivery, STI treatment, and rectal microbicides. Figure 1-4 summarizes potential applications of nanofibers for vaginal drug delivery.

Since these two reports have been published, there have been several other reports of electrospun fibers investigated for vaginal drug delivery[173–179]. More extensive literature exists

for applications of electrospun fibers in transdermal drug delivery, wound dressings, and tissue engineering. We will now discuss aspects of electrospinning fibers for drug delivery using examples from literature and comment on their implications for vaginal drug delivery.

1.2.9.3 Engineering nanofibers with controllable release profiles

Electrospun fibers have been engineered to provide long-term sustained release of drugs over several months, ultrafast burst release within seconds, and asynchronous release of multiple agents. All three of these release profiles may be desirable for various applications for delivery to the lower female reproductive tract. For example, a quick-dissolving fiber platform may be most appropriate for a pericoitally administered microbicide so that the drug is able to reach target cell populations to provide protection before the virus. However, for a fiber-incorporating vaginal ring or diaphragm intended to remain in place for weeks to months, fibers that can provide long-term, sustained drug release with zero order kinetics would be preferable. One can envision many types of products being created from electrospun fibers for vaginal delivery that facilitate release on time scales of less than five minutes to several months.

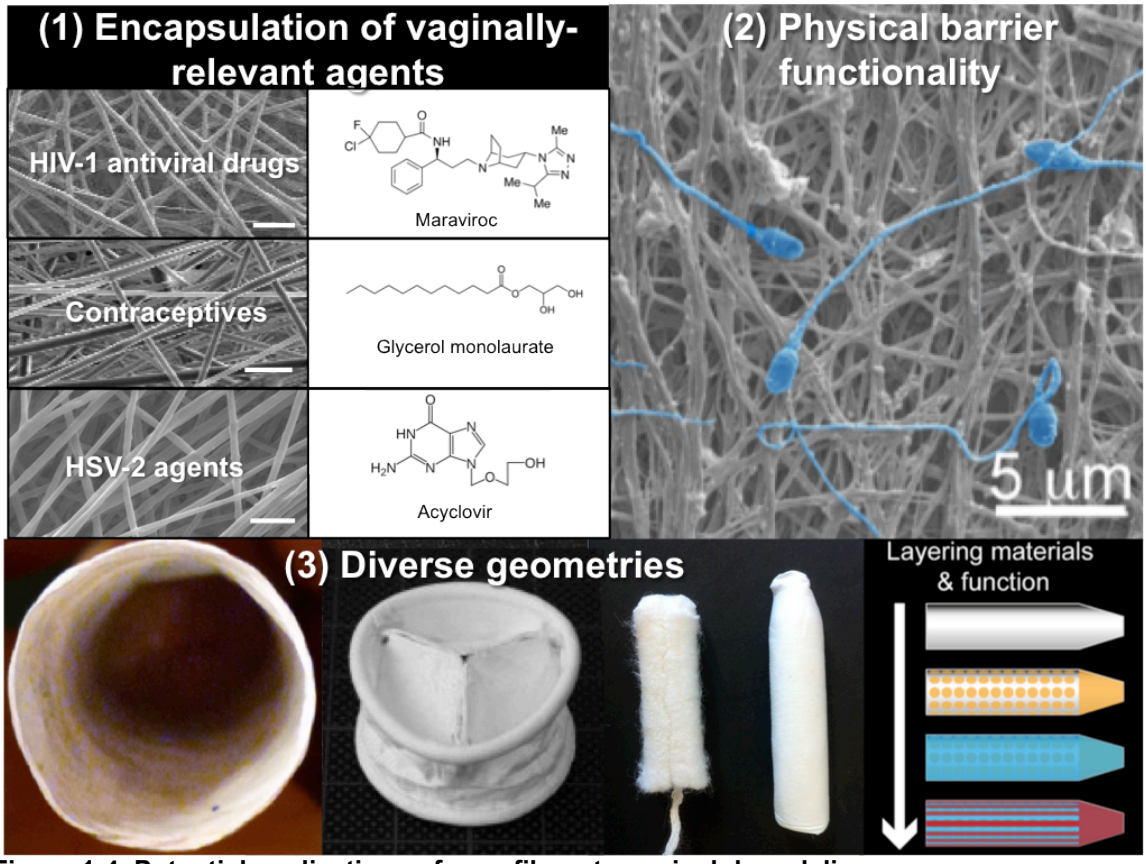

Figure 1-4. Potential applications of nanofibers to vaginal drug delivery.

Many studies have been done showing that controlled release is possible from nanofibers[180–183]. Strategies to control drug release from fibers include coating them after electrospinning to prevent burst release[184,185], creating a core-shell fiber structure using emulsion or coaxial electrospinning[186–188], crosslinking the polymer to slow release[189], and introducing air into fibers with an air displacement technique[181]. Simply modifying the choice or ratio of the polymer/drug combination can also be used as a means to control release. Jannesari *et al* demonstrated that by lowering ciprofloxacin HCl drug loading from 10% to 5% in poly(vinyl alcohol)/poly(vinyl acetate) fibers, the burst release effect was reduced from ~75% to ~25% of total drug content, with sustained release observed for 80 days[190]. Xie *et al* developed PLGA nanofibers as chemotherapy implants, and demonstrated in vitro release of drug for 60 days[191]. In settings where adherence to a product that must be frequently administered is a challenge, such as sub-Saharan Africa, a vaginal product that provides predictable, sustained release of active agents over a longer time is desirable. Furthermore, given the high rate of clearance in the vagina and presence of enzymes and reactive oxygen species that can degrade drugs[18,192], the potential of fibers to slowly release drug while protecting unreleased contents from the vaginal microenvironment is promising.

Besides their ability to provide controlled release over weeks to months, electrospun fibers can also be designed to provide ultrafast release of drugs. Such a release profile may be desirable for vaginal delivery applications such as for pericoital HIV prevention or contraception in which the product is applied just prior to or after intercourse. Polymers that degrade quickly (e.g., poly(vinyl alcohol) (PVA), PEO, alginate, chitosan) may be good candidates for quick release vaginal drug delivery. Examples of fibers designed for sublingual or oral delivery are especially insightful for engineering fibers with a quick release profile. Li *et al* created PVA nanofibers for the quick release of caffeine and riboflavin that dissolved in less than 5 seconds and displayed burst release of 100% of caffeine and 40% of riboflavin within 60 seconds[167]. Marci *et al* created fibers for the topical delivery of a hydrophilic peptide with controllable release kinetics[193]. By changing polymer composition, they were able to change the dominate release mechanism from polymer erosion to diffusion, and thus obtain release over 9 hours to 4 days Similar strategies may be useful for engineering fibers as quick-dissolving platforms for vaginal drug delivery.

Another attractive feature of electrospun fibers is the ability to obtain asynchronous release profiles, in which the timing, order, and duration of the release of multiple drugs can be controlled. By layering or simultaneously electrospinning different fiber types, customized release profiles for multiple agents can be obtained within a single device. Okuda *et al* show

time-programmed release of two model dyes from tetra-layered poly(L-lactide-co-ε-caprolactone) fibers incorporating "barrier" and "basement" fiber layers to modulate release[194]. By changing the thickness and fiber diameters of the mesh layers, they were able to extend the release suppressing-period for one dye from 30 minutes to 1 hour. Combination therapies have improved clinical outcomes for many diseases, including the advent of HAART for the treatment of HIV[195]. Applying the paradigm of HAART to HIV prevention has been considered as a promising strategy in the microbicide development field, but strategies to deliver multiple drugs simultaneously from one product are lacking. Electrospun fibers may offer a drug delivery platform that not only allows for the coformulation of multiple drugs, but also for asynchronous release of those drugs. Few existing drug delivery platforms can offer the same versatility in release profiles as electrospun fibers.

1.2.9.4 Fibers enable encapsulation and simultaneous delivery of diverse agents including drugs, biologics, and cells.

Many diverse agents have been proposed for vaginal drug delivery, including drugs with a wide range of physicochemical properties, peptides, nucleic acids, antibodies, and nanocarriers. These agents are often difficult to co-formulate into a single device, and sometimes even challenging to individually formulate into carriers by themselves. Additionally, due to the acidic environment and degrading enzymes present in the vagina[18], many of these agents degrade before reaching their targets. Since some polymers can be electrospun in water instead of organic solvents, fibers offer a platform to protect biologic agents from harsh formulation conditions, as well as from conditions present in the vagina. The versatility of materials that can be used in electrospinning can allow for individual fiber types that can be customized to encapsulate specific agents. Multiple fiber types could then be layered or simultaneously electrospun using multi-jet configurations, enabling the creation of a single product capable of simultaneously delivering multiple diverse agents. This would have profound implications for multipurpose prevention technologies, which are products that act against multiple indications, such as preventing HIV-1 infection and unwanted pregnancy. In addition, fibers may be a suitable platform for the delivery of nanoparticles, which are of great relevance for vaginal delivery but lack a practical method for uniform intravaginal distribution.

The materials selection and processing requirements for vaginal rings impose constraints on what pharmaceutical agents can be loaded[41], and hydrophobic drugs are have limited solubility in vaginal gels[196]. In contrast, numerous studies show that electrospun fibers can incorporate drugs with a wide range of solubility[166,172,197,198]. Electrospun fibers have been used as a means

to increase bioavailability of poorly water-soluble drugs by solid dispersion. Verreck *et al* created fibers loaded with a poorly water-soluble drug, itraconazole, and confimed with differential scanning calorimetry the lack of a melting endotherm for the drug, suggesting a solid drug dispersion within fibers[199]. Yu *et al* have shown similar improvement of delivery of ketoprofen from drug-loaded fibers via solid dispersion[200]. This strategy is of particular interest for vaginal drug delivery, since many ARVs of interest for topical HIV prevention have low aqueous solubility that limits their formulation in products like vaginal gels[46]. Fibers offer potential to increase bioavailability of such drugs for intravaginal administration.

Biologic agents including peptides, antibodies, enzymes, bacteria, and nucleic acids have been proposed for vaginal delivery. However, designing vehicles that can both encapsulate and deliver biologics to the vaginal mucosa without altering their activity remains a challenge. Electrospinning has been used to encapsulate a wide range of biologics, including proteins[201,202], viruses[203], DNA[204], siRNA[205], bacteria[206,207], and cells[208]. Maretschek *et al* demonstrated tunable release of cytochrome C, a hydrophilic protein, from PLLA nanofibers by blending in a more hydrophilic polymer (PEG) to increase release[209]. Growth factors including human β-nerve growth hormone and basic fibroblast growth factor have also been embedded within[202,210] or immobilized onto the surface of nanofibers[211] for tissue engineering applications. Two groups utilized coaxial spinning to protect adenovirus for gene delivery or plasmid DNA within the core of fibers during electrospinning[203,204]. They demonstrated that these agents retained bioactivity when released from fibers in vitro. Another group reported on the controlled release of siRNA from PCL fibers for 28 days, with a silencing efficiency of 61-81% similar to conventional siRNA transfection[205]. Although many of the examples discussed here has been targeted toward cancer therapy or tissue engineering applications, nanofibers may serve as useful drug delivery systems for antibodies against HIV-1 or sperm, bacteria such as Lactobacilli for the treatment of bacterial vaginosis, antigens for mucosal vaccines, or siRNA or DNA for vaginally administered gene therapy.

1.2.9.5 Nanoparticle/nanofiber composites for vaginal drug delivery

One aspect of nanofibers that may prove especially valuable for vaginal drug delivery is their potential to deliver intact nanoparticles, as methods suitable for the vaginal delivery of nanoparticles are currently limited. Delivering nanoparticles in a conventional vaginal gel raises concerns about suboptimal retention, high external leakage that could decrease user acceptability, and poor stability of nanoparticles in an aqueous environment for long-term storage. Given the breadth of work being done in designing nanoparticles for vaginal drug

delivery as discussed previously, a platform that provides enhanced nanoparticle retention and reduced leakage is greatly needed.

As discussed in the previous section, nanofibers provide many potential advantages for vaginal drug delivery. Perhaps most importantly, they are a solid-state dosage form that we hypothesized to provide enhanced retention and less leakage than aqueous or semisolid dosage forms. Fibers also have a large surface area-to-volume ratio for quick dissolution, can be fabricated in to multiple geometries for practical administration, and offer great diversity in the types of polymers that can be electrospun and agents that can be delivered. Several groups have shown that nanoparticles can be successfully incorporated into and used to control release from nanofibers[101,212–214]. Release profiles can be tuned based on the drug/material combination. Composites made from coumarin-6 PLGA nanoparticles and PVA/PEO fibers showed 100% dye release within 24 hours[212]. In contrast, a zero-order release of fibroblast growth factor from heparin-based nanoparticle / chitosan fiber composites was observed over 30 days[213]. Besides a wide range in release profiles, nanofibers can also serve to protect agents from the surrounding environment. Chen *et al* observed sustained release of intact siRNA for 50 days from chitosan nanoparticles embedded within PLGA fibers[214]. Nanoparticle/nanofiber composites may offer not only a suitable platform for the vaginal delivery of nanoparticles, but also another method for controlling release profiles and enabling intracellular delivery from a single product.

Methods for fabricating nanoparticle/nanofiber composites

Several methods have been used to create micro or nanoparticle/nanofiber composites, including emulsion electrospinning, direct addition of nanoparticles to electrospinning solution, and co-electrospinning with a "sacrificial" polymer. Emulsion electrospinning involves the addition of an aqueous solution containing the active pharmaceutical ingredient (API) to an organic polymer solution, and then electrospinning into fibers. Dong *et al* have utilized this method to create polyurethane fiber meshes with PVA nanoparticles containing bovine serum albumin (BSA) or epidermal growth factor (EGF)[215]. While they presented images of distinct nanoparticles within fibers, they do not measure release rates or loading efficiency. Similarly, Qi *et al* made PLLA nanofibers with BSA-loaded calcium alginate microspheres using the emulsion electrospinning method[216]. Emulsion electrospinning has most commonly been used to encapsulate hydrophilic agents. In contrast, the method of direct addition has been used for both hydrophilic and hydrophobic agents, as employed by Wang *et al* [217] and Beck-Broichsetter

et al [212]. In this method, preformed particles (either lyophilized or concentrated via centrifugation) are simply resuspended in a polymer solution for electrospinning.

A third method to form composites involves co-spinning a sacrificial polymer containing preformed particles with another polymer. After electrospinning, the sacrificial layer is then dissolved away, leaving the particles entrapped within the nanofiber mesh. Ionescu *et al* used this technique to create polystyrene microspheres embedded in a PCL mesh, with PEO acting as the sacrificial polymer[218]. The authors used this method to avoid altering mechanical properties of the PCL scaffold, which they had previously observed when directly electrospinning microparticles into PCL fibers. They found similar release kinetics for fibers containing microsphere-encapsulated BSA and chondroitin sulfate compared to microspheres alone over 4 weeks. These studies demonstrate that these methods are viable methods for fabricating particle/nanofiber composite materials. However, there are likely additional methods for fabricating composite nanoparticle/nanofiber materials remaining to be explored.

Previous work evaluating composite nanoparticle/nanofiber meshes

As shown in a compiled table in Appendix G, nanoparticle/nanofiber composites have previously been investigated for a variety of applications, including achieving sustained release of dyes[212,217], biologics[213,215,216,219], small molecule drugs[217,220–225], siRNA[214], and metal ions[226]. Some of the first work evaluating nanoparticle/nanofiber composites for small molecule delivery was done using fluorescent dyes. Wang *et al* showed that composite nanoparticle/electrospun fiber meshes could be used to modulate release of the hydrophilic dye Rhodamine B over 72 h[217]. They loaded Rhodamine B and naproxen into chitosan nanoparticles, and then electrospun PCL nanofibers containing these particles. By loading Rhodamine B in the nanoparticles instead of directly into the fibers, they were able to greatly reduce burst release of drug from 90% to 15% over 72 h. Similarly, Beck-Broichsitter *et al* loaded a hydrophobic dye (coumarin-6) into PLGA nanoparticles, and then added these particles to PVA or PEO solutions to obtain electrospun composite meshes[212]. They found that drug release was slightly slowed from glutaraldehyde-crosslinked PVA meshes compared with PEO meshes or bare nanoparticles. Crosslinked PVA/nanoparticle meshes had ~75% cumulative release in 2 h, compared with ~100% release for PEO/nanoparticle meshes or from nanoparticles alone. This work established important proof-of-concept that nanoparticle/nanofiber composites can be fabricated to sustain drug release.

Recent work in the nanoparticle/nanofiber composite field has expanded from sustaining delivery of small molecule drugs and dyes toward sustaining release of proteins and growth

factors for tissue engineering applications[213,215,216,219]. Many groups have demonstrated that the burst release of drug or protein from nanoparticles can be reduced by electrospinning them within nanofibers to slow diffusion. This strategy for sustaining release has also been applied to creating platforms for locally delivered, sustained cancer therapy[221,222,227] and antibiotic treatment for improved wound healing[219,224,226]. Other groups have designed nanoparticles for pH- or enzyme-triggered drug release within composite fibers[227,228], or creating pH- or heat-sensitive composite fibers for stimuli-responsive delivery[229]. While these strategies certainly may have useful applications in HIV prevention, few groups have looked at using nanofibers as a vehicle to deliver intact *nanoparticles* themselves as opposed to sustaining the release of biologic agent or drug. Determining whether fibers can release intact particles that are capable of intracellular uptake and subsequent drug release remains an important gap for the field to investigate. This is our aim in the work presented in Chapter 5 and will be discussed in further detail there.

1.2.9.6 Versatility in engineering bulk properties of fibers: functionalized surfaces, mechanical properties, stimuli-responsive.

Along with versatility in the types of agents that can be encapsulated in electrospun fibers, they offer versatility in bulk properties that can be engineered, including modifying surface chemistry, mechanical properties, and stimuli-responsive drug release. Such features are attractive for vaginal drug delivery, potentially allowing for products to be engineered with mucoadhesive coatings to confer greater retention, mechanical properties appropriate for vaginal insertion, and “smart” drug release mechanisms that are triggered by vaginal physiologic cues.

The surfaces of electrospun fibers have been chemically functionalized with drugs, enzymes, cytokines, bioactive ligands, and polysaccharides to produce desired functions[230]. Strategies that have been used for surface modification are well described in the reviews by Yoo *et al* [230] and Agarwal *et al* [231] and include plasma treatment, surface grafting, co-electrospinning, and a wet chemical method. Of particular interest to vaginal drug delivery would be engineering the surface of fibers to be mucoadhesive. Poor vaginal retention has been cited as a problem for vaginal gel and other microbicide formulations, which can wash out with vaginal fluid flow or can leak from normal movement or due to gravity[111,146,232]. Thus, engineering the surface of a nanofiber-based drug delivery system to be mucoadhesive may alleviate some of these problems. Puttipaiboon *et al* electrospun gastro-mucoadhesive fibers out of a blend of chitosan, PEO, and the corn-derived biopolymer zein[233]. They selected chitosan for its mucoadhesive

properties and zein for its resistance to gastric fluid degradation, and found that electrospun fiber films had adhesive strength similar to other gastro-mucoadhesive materials. By selecting materials for specific surface properties or modifying the fiber mesh surface post-electrospinning, fibers offer potential for a more efficient, longer-lasting formulation for vaginal drug delivery.

Depending on the method of insertion and the desired time scale of release, vaginal products have differing mechanical requirements. Vaginal rings must be flexible enough to be inserted without damaging tissue, but stiff enough so they do not slip or become expelled during normal use[42]. Diaphragms require a low compression relaxation value so they can form-fit closely around the cervix[40]. A relatively high tensile strength of vaginal films has been found to be important for optimal insertion and handling[234]. Nanofibers have previously been engineered to have a wide range in mechanical properties. Baji *et al* have published an informative review on the effects of electrospinning parameters on fiber morphology, microstructure, and tensile properties[235]. For example, mechanical properties such as elastic modulus and strength have been found to increase with decreasing fiber diameter[235]. Additives like carbon nanotubes have been used to increase polymer chain orientation within fibers, and thus strengthen their mechanical properties[236]. Another way to modulate mechanical properties is by increasing fiber alignment with a rotating mandrel collector[237,238]. The ability to tune mechanical properties may offer a unique advantage for electrospun fibers to be tailored to the mechanical requirements of a variety of vaginal devices.

With the advances in "smart" polymers for drug delivery, there are opportunities to create nanofibers with stimuli-triggered release. Huang *et al* has published a review on stimuli-responsive fibers, documenting reports of different types of fibers that change in response to pH, temperature, photo/optical, magnetic field, humidity, ethanol, glucose, or proteins[156]. One potential physiologic cue relevant to vaginal delivery is change in pH, as the presence of semen (pH 7-8) during intercourse raises the normal vaginal pH (pH 4-6)[171]. Other potential stimuli for vaginal delivery are the presence of reactive oxygen species, response to a vaginal enzyme, or an increase in temperature upon fiber insertion that would cause a transition in material properties and subsequent release of active agents.

1.2.9.7 Diverse geometries in three-dimensional nanofiber structure can be obtained.

Another unique feature of nanofibers is their ability to be fabricated into a variety of geometries. Not only can the intrinsic geometry of individual fibers be controlled (i.e. fiber morphology, porosity, diameter), but also the structural geometry of the bulk fiber mesh. Much

work has been done in designing three-dimensional scaffolds from nanofibers for tissue engineering[239–242]. Using techniques such as mixed electrospinning or multilayered electrospinning, one can obtain spatial control over the material composition of three dimensional fiber structures[240]. McLure *et al* have created a three-layered blood vessel scaffold from PCL, elastin, and collagen blends with appropriate mechanical properties for each layer[242]. Teo *et al* created tubular electrospun scaffolds with fibers aligned to a 54.7° angle (optimal for blood vessel engineering) by using a collector with angled sharp metal blades[243]. Layering or co-electrospinning drug-loaded fibers would allow for the creation of composite materials that could serve as multipurpose prevention technologies to simultaneously address needs for HIV prevention and contraception.

Even more complex geometries of electrospun fibers have been obtained, such as a three-dimensional heart valve scaffold[244,245]. These groups used convex or mildly concave collectors to obtain scaffolds, but more concave surfaces could be coated using air-blowing assisted electrospinning[246]. Given preliminary results showing that electrospun fibers serve as an effective barrier to sperm[172], their ability to be configured into complex geometries may allow for their application to contraceptive devices such as vaginal diaphragms, rings, or sponges.

1.2.9.8 Considerations in creating products for global settings.

Since an estimated 95% of the 36 million people infected with HIV live in developing countries[247], it is important to consider what types of products would be most realistic for low-resource settings. Microbicides or contraceptive products that are available in a solid-state dosage form, have a long shelf life, and can be scaled-up in a cost-effective manner are highly desirable. Scale-up of electrospinning is discussed in more depth in Chapter 4. Electrospun fibers represent a solid-state dosage form that may provide enhanced stability compared with semi-solid dosage forms like vaginal gels. Kayaci *et al* encapsulated vanillin within cyclodextrin inclusion complexes in PVA nanofibers and found prolonged shelf-life and high temperature stability of the meshes[248]. Additionally, PVA nanofibers were found to enhance the shelf-life of lipase enzyme, even at elevated temperature and humidity[201]. Similar enhancements in stability for ARVs or contraceptive agents would be valuable for vaginal drug delivery applications. Several manufacturers have also established cost-effective methods for large-scale productions of electrospun fibers[152]. Electrospun fibers represent a solid-state dosage form that would be easy to store and transport, result in minimal waste, and be scaled-up for mass production. Thus, fibers may offer advantages for creating economic products for low-resource settings.

1.2.9.9 Feasibility and acceptability of electrospun fibers for vaginal drug delivery.

While no clinical data is available for evaluating the acceptability and user preferences for electrospun fibers as a vaginal delivery platform, inferences can be drawn from clinical trials for vaginal films (Table 1-2). One of the conceptual dosage forms for fibers is similar to a vaginal film. Like films, fibers are a solid-state dosage form, can be formed into flexible fabrics with similar geometry and thickness to a vaginal film, and be inserted digitally without the use of an applicator. There are multiple other potential dosage forms for fibers (e.g., cervical cap, capped tube, use of tampon applicator for insertion, diaphragm), but one of the current leading candidates for moving forward is most similar to a vaginal film.

One clinical trial is especially insightful for understanding user preferences based on properties of the vaginal dosage form itself (i.e., technical design constraints). Nel *et al* conducted a trial among 526 participants in Burkina Faso, Tanzania, and Zambia where each woman was given three placebo vaginal products (vaginal film, vaginal soft gel-capsule, and vaginal tablet) to use for 7d each and provide feedback[68]. Overall, women preferred the vaginal film over the other two dosage forms, but preferences varied by country. Factors that contributed to the women's preferences included ease of insertion, time for product dissolution, and amount of lubrication they felt that the product provided[68]. Similar factors will be important to evaluate for fiber dosage forms, in addition to product geometry, texture, and viscosity upon dissolution. While fibers will likely need to be optimized to meet the same user preferences as films including dissolution time and ease of insertion, fibers offer some advantages over films in terms of technical constraints. Fibers have been shown to provide controllable drug release[176,249] and have a high drug loading capacity of at least 60 wt%[175], whereas current film formulations have limited abilities to provide sustained release or load high amounts of drug. Similar clinical studies will be needed to define user preferences and acceptability for fibers as a novel vaginal drug delivery platform.

Studies that connect user perceptibility and user preferences of vaginally administered fibers will be important to evaluate for the fiber platform. Morrow *et al* have studied user perceptions of vaginal gels and films with varying design characteristics like viscosity, spread, and dissolution[78,250]. Such studies have provided useful data that connects user sensory perceptions with vaginal product design qualities, and may prove valuable for the fiber platform as well. Finally, collaborating with behavioral and social scientists to consider the cultural and societal context for microbicide use will be imperative in evaluating the clinical efficacy and acceptability of a new microbicide platform.

1.2.9.10 Future challenges and directions in nanofibers for vaginal drug delivery

While the versatility of nanofibers offers many potential benefits for vaginal drug delivery, several challenges remain. One important limitation of nanofibers for vaginal drug delivery is that of limited penetration depth. Unlike nanoparticles, which are able to diffuse through tissue and be targeted for intracellular delivery, nanofibers do not offer opportunities for such targeting. Nanofibers are better suited to deliver agents that at locally within the penetration depth of the unformulated drug. On a basic science level, the fundamental physics of electrospinning are still not fully understood[153]. Continued research in this area may allow for even more control over fiber morphology and drug distribution, which will be key for reproducible and predictable pharmacokinetics. Release profiles that occur through both diffusion and degradation mechanisms can be difficult to predict, so fibers made from biodegradable materials must be carefully engineered so that the drug contents do not burst release at toxic levels.

Further, limited *in vivo* testing of nanofibers for drug delivery has been completed, especially for vaginal delivery. Biocompatibility, inflammatory, and immune responses of nanofibers administered intravaginally must be well characterized before fiber-based vaginal products advance to clinical trials. Additionally, although conceptually fibers could be formed into diverse geometries, work remains to be done to evaluate what forms are practical for vaginal administration. Characterization of the mechanics, retention, and dissolution of various configurations will be necessary for advancing fibers for use in vaginal delivery. Safety and efficacy of fibers for vaginal delivery will need to be thoroughly evaluated before preclinical research can be translated to clinical applications. Despite these challenges, electrospun fibers offer much potential as a vaginal delivery platform for products beyond HIV microbicides and contraception to other reproductive health applications like STI treatment, yeast infections, surgical meshes, and mucosal vaccines.

1.3 REFERENCES

1. World Health Organization. HIV/AIDS. *WHO Global Health Observatory* at <http://www.who.int/gho/hiv/en/>
2. Davey, R. T. *et al.* HIV-1 and T cell dynamics after interruption of highly active antiretroviral therapy (HAART) in patients with a history of sustained viral suppression. *Proc. Natl. Acad. Sci.* **96,** 15109–15114 (1999).
3. Joint United Nations Programme on HIV/AIDS. *Regional Fact Sheet 2012: Sub-Saharan Africa*. 1–3 (UNAIDS, 2012).
4. Morris, G. C. & Lacey, C. J. Microbicides and HIV prevention: lessons from the past, looking to the future: *Curr. Opin. Infect. Dis.* **23,** 57–63 (2010).
5. Joint United Nations Programme on HIV/AIDS. *UNAIDS World AIDS Day Report, 2011*. 1–52 (UNAIDS, 2011).
6. Cutler, B. & Justman, J. Vaginal microbicides and the prevention of HIV transmission. *Lancet Infect. Dis.* **8,** 685–697 (2008).
7. Nuttall, J. Microbicides in the prevention of HIV infection: current status and future directions. *Drugs* **70,** 1231–1243 (2010).
8. Date, A. A. & Destache, C. J. A review of nanotechnological approaches for the prophylaxis of HIV/AIDS. *Biomaterials* **34,** 6202–6228 (2013).
9. Van Damme, L. *et al.* Effectiveness of COL-1492, a nonoxynol-9 vaginal gel, on HIV-1 transmission in female sex workers: a randomised controlled trial. *The Lancet* **360,** 971–977 (2002).
10. Ramjee, G., Kamali, A. & McCormack, S. The last decade of microbicide clinical trials in Africa: from hypothesis to facts: *AIDS* **24,** S40–S49 (2010).
11. Abdool Karim, S. S. *et al.* Safety and effectiveness of BufferGel and 0.5% PRO2000 gel for the prevention of HIV infection in women: *AIDS* **25,** 957–966 (2011).
12. Karim, Q. *et al.* Effectiveness and Safety of Tenofovir Gel, an Antiretroviral Microbicide, for the Prevention of HIV Infection in Women. *Science* **329,** 1168 (2010).
13. Microbicide Trials Network. *MTN statement on decision to discontinue use of tenofovir gel in VOICE, major HIV prevention study in women*. (Microbicide Trials Network, 2011). at <http://www.mtnstopshiv.org/node/3909>
14. Brannon-Peppas, L. Novel vaginal drug release applications. *Adv. Drug Deliv. Rev.* **11,** 169–177 (1993).
15. Hussain, A. & Ahsan, F. The vagina as a route for systemic drug delivery. *J. Controlled Release* **103,** 301–313 (2005).
16. Alexander, N. J. *et al.* Why consider vaginal drug administration? *Fertil. Steril.* **82,** 1–12 (2004).
17. Platzner, W. & Poisel, S. in *Human Reproductive Medicine: The Human Vagina* (eds. Hafez, E. S. . & Evans, T. N.) **2,** 39–54 (North Holland Publishing, 1978).
18. Richardson, J. L. & Illum, L. (D) Routes of delivery: Case studies: (8) The vaginal route of peptide and protein drug delivery. *Adv. Drug Deliv. Rev.* **8,** 341–366 (1992).
19. Pearson Education, Inc. Ch 27 Vaginal Anatomy. at <http://apbrwww5.apsu.edu/thompsonj/Anatomy%20&%20Physiology/2020/2020%20Exam%20Reviews/Exam%205/CH27%20Vaginal%20Anatomy.htm>
20. Knuth, K., Amiji, M. & Robinson, J. R. Hydrogel delivery systems for vaginal and oral applications: Formulation and biological considerations. *Adv. Drug Deliv. Rev.* **11,** 137–167 (1993).
21. Ravel, J. *et al.* Vaginal microbiome of reproductive-age women. *Proc. Natl. Acad. Sci.* **108,** 4680–4687 (2010).
22. Lee, V. H. L. & Yamamoto, A. Penetration and enzymatic barriers to peptide and protein absorption. *Adv. Drug Deliv. Rev.* **4,** 171–207 (1989).
23. Wagner, G. & Levin, R. J. in *Human Reproductive Medicine: The Human Vagina* (eds. Hafez, E. S. . & Evans, T. N.) **2,** 121–137 (North Holland Publishing, 1978).
24. Cone, R. A. Barrier properties of mucus. *Adv. Drug Deliv. Rev.* **61,** 75–85 (2009).
25. Kistner, R. W. in *Human Reproductive Medicine: The Human Vagina* (eds. Hafez, E. S. . & Evans, T. N.) **2,** 109–120 (North Holland Publishing, 1978).
26. Rohan, L. & Mallipeddi. Progress in antiretroviral drug delivery using nanotechnology. *Int. J. Nanomedicine* 533 (2010). doi:10.2147/IJN.S7681

27. Stein, Z. A. HIV prevention: the need for methods women can use. *Am. J. Public Health* **80,** 460–462 (1990).
28. Hladik, F. & McElrath, M. J. Setting the stage: host invasion by HIV. *Nat. Rev. Immunol.* **8,** 447–457 (2008).
29. Hladik, F. & Doncel, G. F. Preventing mucosal HIV transmission with topical microbicides: Challenges and opportunities. *Antiviral Res.* **88, Supplement,** S3–S9 (2010).
30. Hu, J., Gardner, M. B. & Miller, C. J. Simian immunodeficiency virus rapidly penetrates the cervicovaginal mucosa after intravaginal inoculation and infects intraepithelial dendritic cells. *J. Virol.* **74,** 6087–6095 (2000).
31. Coiras, M., López-Huertas, M. R., Pérez-Olmeda, M. & Alcamí, J. Understanding HIV-1 latency provides clues for the eradication of long-term reservoirs. *Nat. Rev. Microbiol.* **7,** 798–812 (2009).
32. Avdeef, A. *Absorption and Drug Development: Solubility, Permeability, and Charge State*. (John Wiley & Sons, 2012).
33. Schwartz, J. L. *et al.* A Multi-Compartment, Single and Multiple Dose Pharmacokinetic Study of the Vaginal Candidate Microbicide 1% Tenofovir Gel. *PLoS ONE* **6,** e25974 (2011).
34. Patterson, K. B. *et al.* Penetration of Tenofovir and Emtricitabine in Mucosal Tissues: Implications for Prevention of HIV-1 Transmission. *Sci. Transl. Med.* **3,** 112re4–112re4 (2011).
35. Durand-Gasselin, L. *et al.* Nucleotide analogue prodrug tenofovir disoproxil enhances lymphoid cell loading following oral administration in monkeys. *Mol. Pharm.* **6,** 1145–1151 (2009).
36. Garg, S. *et al.* Advances in development, scale-up and manufacturing of microbicide gels, films, and tablets. *Antiviral Res.* **88,** S19–S29 (2010).
37. Andrews, G. P. *et al.* Characterization of the Rheological, Mucoadhesive, and Drug Release Properties of Highly Structured Gel Platforms for Intravaginal Drug Delivery. *Biomacromolecules* **10,** 2427–2435 (2009).
38. Dobaria, N., Badhan, A. & Mashru, R. A Novel Itraconazole Bioadhesive Film for Vaginal Delivery: Design, Optimization, and Physicodynamic Characterization. *AAPS PharmSciTech* **10,** 951–959 (2009).
39. Asane, G. S. *et al.* Polymers for Mucoadhesive Drug Delivery System: A Current Status. *Drug Dev. Ind. Pharm.* **34,** 1246–1266 (2008).
40. Major, I. *et al.* A modified SILCS contraceptive diaphragm for long-term controlled release of the HIV microbicide dapivirine. *Contraception* **88,** 58–66 (2013).
41. Malcolm, R. K., Edwards, K.-L., Kiser, P., Romano, J. & Smith, T. J. Advances in microbicide vaginal rings. *Antiviral Res.* **88, Supplement,** S30–S39 (2010).
42. Johnson, T. J., Gupta, K. M., Fabian, J., Albright, T. H. & Kiser, P. F. Segmented polyurethane intravaginal rings for the sustained combined delivery of antiretroviral agents dapivirine and tenofovir. *Eur. J. Pharm. Sci.* **39,** 203–212 (2010).
43. Moss, J. A. *et al.* Simultaneous Delivery of Tenofovir and Acyclovir via an Intravaginal Ring. *Antimicrob. Agents Chemother.* **56,** 875–882 (2011).
44. CAMI Multipurpose Prevention Technologies for Reproductive Health: 2011 Think Tank. in 1–34 (2011).
45. Akil, A. *et al.* Development and characterization of a vaginal film containing dapivirine, a non-nucleoside reverse transcriptase inhibitor (NNRTI), for prevention of HIV-1 sexual transmission. *Drug Deliv. Transl. Res.* **1,** 209–222 (2011).
46. Ham, A. S. *et al.* Vaginal Film Drug Delivery of the Pyrimidinedione IQP-0528 for the Prevention of HIV Infection. *Pharm. Res.* **29,** 1897–1907 (2012).
47. Garg, S. *et al.* Development and Characterization of Bioadhesive Vaginal Films of Sodium Polystyrene Sulfonate (PSS), a Novel Contraceptive Antimicrobial Agent. *Pharm. Res.* **22,** 584–595 (2005).
48. Ma, Z., Lü, F. X., Torten, M. & Miller, C. J. The Number and Distribution of Immune Cells in the Cervicovaginal Mucosa Remain Constant throughout the Menstrual Cycle of Rhesus Macaques. *Clin. Immunol.* **100,** 240–249 (2001).
49. Zhang, Z.-Q. *et al.* Roles of substrate availability and infection of resting and activated CD4+ T cells in transmission and acute simian immunodeficiency virus infection. *Proc. Natl. Acad. Sci. U. S. A.* **101,** 5640–5645 (2004).

50. Pudney, J., Quayle, A. J. & Anderson, D. J. Immunological Microenvironments in the Human Vagina and Cervix: Mediators of Cellular Immunity Are Concentrated in the Cervical Transformation Zone1. *Biol. Reprod.* **73,** 1253–1263 (2005).
51. Saltzman, W. M. *Drug Delivery : Engineering Principles for Drug Therapy: Engineering Principles for Drug Therapy*. (Oxford University Press, 2001).
52. Achilles, S. L., Shete, P. B., Whaley, K. J., Moench, T. R. & Cone, R. A. Microbicide efficacy and toxicity tests in a mouse model for vaginal transmission of Chlamydia trachomatis. *Sex. Transm. Dis.* **29,** 655–664 (2002).
53. Zhang, Z.-Q. *et al.* Sexual Transmission and Propagation of SIV and HIV in Resting and Activated CD4+ T Cells. *Science* **286,** 1353–1357 (1999).
54. Geonnotti, A. R., Peters, J. J. & Katz, D. F. Erosion of microbicide formulation coating layers: effects of contact and shearing with vaginal fluid or semen. *J. Pharm. Sci.* **94,** 1705–1712 (2005).
55. Hurt, C. B., Eron, J. J. & Cohen, M. S. Pre-Exposure Prophylaxis and Antiretroviral Resistance: HIV Prevention at a Cost? *Clin. Infect. Dis.* **53,** 1265–1270 (2011).
56. Doncel, G. F. Exploiting common targets in human fertilization and HIV infection: development of novel contraceptive microbicides. *Hum. Reprod. Update* **12,** 103–117 (2006).
57. Klasse, P. J., Shattock, R. & Moore, J. P. Antiretroviral drug-based microbicides to prevent HIV-1 sexual transmission. *Annu. Rev. Med.* **59,** 455–471 (2008).
58. Friend, D. R. & Doncel, G. F. Combining prevention of HIV-1, other sexually transmitted infections and unintended pregnancies: Development of dual-protection technologies. *Antiviral Res.* **88, Supplement,** S47–S54 (2010).
59. Karim, S. S. A., Kashuba, A. D., Werner, L. & Karim, Q. A. Drug concentrations after topical and oral antiretroviral pre-exposure prophylaxis: implications for HIV prevention in women. *The Lancet* **378,** 279–281 (2011).
60. Grant, R. M. *et al.* Preexposure Chemoprophylaxis for HIV Prevention in Men Who Have Sex with Men. *N. Engl. J. Med.* **363,** 2587–2599 (2010).
61. Thigpen, M. C. *et al.* Antiretroviral Preexposure Prophylaxis for Heterosexual HIV Transmission in Botswana. *N. Engl. J. Med.* **367,** 423–434 (2012).
62. Baeten, J. M. *et al.* Antiretroviral Prophylaxis for HIV Prevention in Heterosexual Men and Women. *N. Engl. J. Med.* **367,** 399–410 (2012).
63. Van Damme, L. *et al.* Preexposure Prophylaxis for HIV Infection among African Women. *N. Engl. J. Med.* **367,** 411–422 (2012).
64. Rees, H. FACTS 001 Phase III Trial of Pericoital Tenofovir 1% Gel for HIV Prevention in Women. (2015).
65. van der Straten, A. *et al.* Perspectives on use of oral and vaginal antiretrovirals for HIV prevention: the VOICE-C qualitative study in Johannesburg, South Africa. *J. Int. AIDS Soc.* **17,** (2014).
66. van der Straten, A. *et al.* Disclosure of pharmacokinetic drug results to understand nonadherence: *AIDS* **29,** 2161–2171 (2015).
67. Woodsong, C. & Holt, J. D. S. Acceptability and preferences for vaginal dosage forms intended for prevention of HIV or HIV and pregnancy. *Adv. Drug Deliv. Rev.* **92,** 146–154 (2015).
68. Nel, A. M., Mitchnick, L. B., Risha, P., Muungo, L. T. M. & Norick, P. M. Acceptability of Vaginal Film, Soft-Gel Capsule, and Tablet as Potential Microbicide Delivery Methods Among African Women. *J. Womens Health* **20,** 1207–1214 (2011).
69. Clark, J. Vaginal ring for tenofovir and levonorgestrel delivery for 90 days. (2013).
70. Microbicide Trials Network. A Multi-Center, Randomized, Double-Blind, Placebo-Controlled Phase 3 Safety and Effectiveness Trial of a Vaginal Matrix Ring Containing Dapivirine for the Prevention of HIV-1 Infection in Women. at <http://www.mtnstopshiv.org/studies/3614>
71. International Partnership for Microbicides. IPM 027 (The Ring Study). at <http://www.ipmglobal.org/our-work/research/ipm-027-ring-study-0>
72. Kashuba, A. D. M. *et al.* Genital Tenofovir Concentrations Correlate With Protection Against HIV Infection in the CAPRISA 004 Trial: Importance of Adherence for Microbicide Effectiveness. *JAIDS J. Acquir. Immune Defic. Syndr.* **69,** 264–269 (2015).
73. Dai, J. Y. *et al.* Pharmacological Measures of Treatment Adherence and Risk of HIV Infection in the VOICE Study. *J. Infect. Dis.* jiv333 (2015). doi:10.1093/infdis/jiv333
74. Minnis, A. M. *et al.* Adherence and Acceptability in MTN 001: A Randomized Cross-Over Trial of Daily Oral and Topical Tenofovir for HIV Prevention in Women. *AIDS Behav.* **17,** 737–747 (2013).

75. Kelly, C. A. *et al.* To tell or not to tell: male partner engagement in a Phase 3 microbicide efficacy trial in South Africa. *Cult. Health Sex.* **17,** 1004–1020 (2015).
76. Montgomery, E. *et al.* An acceptability and safety study of the Duet cervical barrier and gel delivery system in Zimbabwe. *J. Int. AIDS Soc.* **13,** 1–13 (2010).
77. Visness, C. M., Ulin, P., Pfannenschmidt, S. & Zekeng, L. Views of Cameroonian sex workers on a woman-controlled method of contraception and disease protection. *Int. J. STD AIDS* **9,** 695–699 (1998).
78. Morrow, K. M. & Rohan, L. Vaginal Film User Evaluations: Developer Considerations from Initial Impressions and User Sensory Perceptions and Experiences during Vaginal Sex. (2014).
79. van der Straten, A. *et al.* High Acceptability of a Vaginal Ring Intended as a Microbicide Delivery Method for HIV Prevention in African Women. *AIDS Behav.* **16,** 1775–1786 (2012).
80. Montgomery, E. T. *et al.* Vaginal Ring Adherence in Sub-Saharan Africa: Expulsion, Removal, and Perfect Use. *AIDS Behav.* **16,** 1787–1798 (2012).
81. Zhang, L. *et al.* Nanoparticles in Medicine: Therapeutic Applications and Developments. *Clin. Pharmacol. 38 Ther.* **83,** 761–769 (2007).
82. Rawat, M., Singh, D., Saraf, S. & Saraf, S. Nanocarriers: Promising Vehicle for Bioactive Drugs. *Biol. Pharm. Bull.* **29,** 1790–1798 (2006).
83. Panyam, J. & Labhasetwar, V. Biodegradable nanoparticles for drug and gene delivery to cells and tissue. *Adv. Drug Deliv. Rev.* **55,** 329–347 (2003).
84. Ganta, S., Devalapally, H., Shahiwala, A. & Amiji, M. A review of stimuli-responsive nanocarriers for drug and gene delivery. *J. Controlled Release* **126,** 187–204 (2008).
85. Mallipeddi, R. & Rohan, L. C. Nanoparticle-based vaginal drug delivery systems for HIV prevention. *Expert Opin. Drug Deliv.* **7,** 37–48 (2010).
86. Panyam, J., Zhou, W.-Z., Prabha, S., Sahoo, S. K. & Labhasetwar, V. Rapid endo-lysosomal escape of poly(dl-lactide-co-glycolide) nanoparticles: implications for drug and gene delivery. *FASEB J.* **16,** 1217–1226 (2002).
87. Cohen, H. *et al.* Sustained delivery and expression of DNA encapsulated in polymeric nanoparticles. *Gene Ther.* **7,** 1896–1905 (2000).
88. Destache, C. J. *et al.* Combination antiretroviral drugs in PLGA nanoparticle for HIV-1. *BMC Infect. Dis.* **9,** 198 (2009).
89. Alukda, D., Sturgis, T. & Youan, B.-B. C. Formulation of tenofovir-loaded functionalized solid lipid nanoparticles intended for HIV prevention. *J. Pharm. Sci.* **100,** 3345–3356 (2011).
90. Liu, X. *et al.* The influence of polymeric properties on chitosan/siRNA nanoparticle formulation and gene silencing. *Biomaterials* **28,** 1280–1288 (2007).
91. Woodrow, K. A. *et al.* Intravaginal gene silencing using biodegradable polymer nanoparticles densely loaded with small-interfering RNA. *Nat. Mater.* **8,** 526–533 (2009).
92. Ham, A., Cost, M., Sassi, A., Dezzutti, C. & Rohan, L. Targeted Delivery of PSC-RANTES for HIV-1 Prevention using Biodegradable Nanoparticles. *Pharm. Res.* **26,** 502–511 (2009).
93. Perera, G., Greindl, M., Palmberger, T. F. & Bernkop-Schnürch, A. Insulin-loaded poly(acrylic acid)-cysteine nanoparticles: Stability studies towards digestive enzymes of the intestine. *Drug Deliv.* **16,** 254–260 (2009).
94. Chakravarthi, S., Robinson, D. & De, S. in *Nanoparticulate Drug Delivery Systems* (ed. Thassu, D.) **20075963,** 51–60 (Informa Healthcare, 2007).
95. Xiong, X. Y., Tam, K. C. & Gan, L. H. Release kinetics of hydrophobic and hydrophilic model drugs from pluronic F127/poly(lactic acid) nanoparticles. *J. Controlled Release* **103,** 73–82 (2005).
96. das Neves, J. *et al.* Polymeric Nanoparticles Affect the Intracellular Delivery, Antiretroviral Activity and Cytotoxicity of the Microbicide Drug Candidate Dapivirine. *Pharm. Res.* **29,** 1468–1484 (2012).
97. Turos, E. *et al.* Penicillin-bound polyacrylate nanoparticles: Restoring the activity of β-lactam antibiotics against MRSA. *Bioorg. Med. Chem. Lett.* **17,** 3468–3472 (2007).
98. Dang, J. M. & Leong, K. W. Natural polymers for gene delivery and tissue engineering. *Adv. Drug Deliv. Rev.* **58,** 487–499 (2006).
99. Jain, R. A. The manufacturing techniques of various drug loaded biodegradable poly(lactide-co-glycolide) (PLGA) devices. *Biomaterials* **21,** 2475–2490 (2000).
100. Bilati, U., Allémann, E. & Doelker, E. Development of a nanoprecipitation method intended for the entrapment of hydrophilic drugs into nanoparticles. *Eur. J. Pharm. Sci.* **24,** 67–75 (2005).

101. Bock, N., Dargaville, T. R. & Woodruff, M. A. Electrospraying of polymers with therapeutic molecules: State of the art. *Prog. Polym. Sci.* **37,** 1510–1551 (2012).
102. Avgoustakis, K. *et al.* Effect of copolymer composition on the physicochemical characteristics, in vitro stability, and biodistribution of PLGA–mPEG nanoparticles. *Int. J. Pharm.* **259,** 115–127 (2003).
103. Santander-Ortega, M. J., Csaba, N., Alonso, M. J., Ortega-Vinuesa, J. L. & Bastos-González, D. Stability and physicochemical characteristics of PLGA, PLGA:poloxamer and PLGA:poloxamine blend nanoparticles: A comparative study. *Colloids Surf. Physicochem. Eng. Asp.* **296,** 132–140 (2007).
104. Meng, J., Sturgis, T. F. & Youan, B.-B. C. Engineering tenofovir loaded chitosan nanoparticles to maximize microbicide mucoadhesion. *Eur. J. Pharm. Sci.* **44,** 57–67 (2011).
105. Dobrovolskaia, M. A. & McNeil, S. E. Immunological properties of engineered nanomaterials. *Nat. Nanotechnol.* **2,** 469–478 (2007).
106. Owens III, D. E. & Peppas, N. A. Opsonization, biodistribution, and pharmacokinetics of polymeric nanoparticles. *Int. J. Pharm.* **307,** 93–102 (2006).
107. Ensign, L. M. *et al.* Mucus-Penetrating Nanoparticles for Vaginal Drug Delivery Protect Against Herpes Simplex Virus. *Sci. Transl. Med.* **4,** 138ra79–138ra79 (2012).
108. Yu, T. *et al.* Biodegradable mucus-penetrating nanoparticles composed of diblock copolymers of polyethylene glycol and poly(lactic-co-glycolic acid). *Drug Deliv. Transl. Res.* **2,** 124–128 (2012).
109. Zhang, T., Sturgis, T. F. & Youan, B.-B. C. pH-responsive nanoparticles releasing tenofovir intended for the prevention of HIV transmission. *Eur. J. Pharm. Biopharm.* **79,** 526–536 (2011).
110. Yoo, J.-W., Giri, N. & Lee, C. H. pH-sensitive Eudragit nanoparticles for mucosal drug delivery. *Int. J. Pharm.* **403,** 262–267 (2011).
111. Rohan, L. C. & Sassi, A. B. Vaginal Drug Delivery Systems for HIV Prevention. *AAPS J.* **11,** 78–87 (2009).
112. Takeuchi, H., Yamamoto, H. & Kawashima, Y. Mucoadhesive nanoparticulate systems for peptide drug delivery. *Adv. Drug Deliv. Rev.* **47,** 39–54 (2001).
113. Lai, S. K., Wang, Y.-Y. & Hanes, J. Mucus-penetrating nanoparticles for drug and gene delivery to mucosal tissues. *Adv. Drug Deliv. Rev.* **61,** 158–171 (2009).
114. das Neves, J., Amiji, M. & Sarmento, B. Mucoadhesive nanosystems for vaginal microbicide development: friend or foe? *Wiley Interdiscip. Rev. Nanomed. Nanobiotechnol.* **3,** 389–399 (2011).
115. Lai, S. K., Wang, Y.-Y., Hida, K., Cone, R. & Hanes, J. Nanoparticles reveal that human cervicovaginal mucus is riddled with pores larger than viruses. *Proc. Natl. Acad. Sci.* **107,** 598–603 (2009).
116. das Neves, J. *et al.* Interactions of Microbicide Nanoparticles with a Simulated Vaginal Fluid. *Mol. Pharm.* **9,** 3347–3356 (2012).
117. Cu, Y., Booth, C. J. & Saltzman, W. M. In vivo distribution of surface-modified PLGA nanoparticles following intravaginal delivery. *J. Controlled Release* **156,** 258–264 (2011).
118. Mert, O. *et al.* A poly(ethylene glycol)-based surfactant for formulation of drug-loaded mucus penetrating particles. *J. Controlled Release* **157,** 455–460 (2012).
119. Wang, Y.-Y. *et al.* Addressing the PEG Mucoadhesivity Paradox to Engineer Nanoparticles that 'Slip' through the Human Mucus Barrier. *Angew. Chem. Int. Ed.* **47,** 9726–9729 (2008).
120. Lai, S. K. *et al.* Human Immunodeficiency Virus Type 1 Is Trapped by Acidic but Not by Neutralized Human Cervicovaginal Mucus. *J. Virol.* **83,** 11196–11200 (2009).
121. Alexis, F., Pridgen, E., Molnar, L. K. & Farokhzad, O. C. Factors Affecting the Clearance and Biodistribution of Polymeric Nanoparticles. *Mol. Pharm.* **5,** 505–515 (2008).
122. Zahr, A. S., Davis, C. A. & Pishko, M. V. Macrophage Uptake of Core−Shell Nanoparticles Surface Modified with Poly(ethylene glycol). *Langmuir* **22,** 8178–8185 (2006).
123. Schäfer, V. *et al.* Phagocytosis of Nanoparticles by Human Immunodeficiency Virus (HIV)-Infected Macrophages: A Possibility for Antiviral Drug Targeting. *Pharm. Res.* **9,** 541–546 (1992).
124. Mainardes, R. M., Gremião, M. P. D., Brunetti, I. L., da Fonseca, L. M. & Khalil, N. M. Zidovudine-loaded PLA and PLA–PEG blend nanoparticles: Influence of polymer type on phagocytic uptake by polymorphonuclear cells. *J. Pharm. Sci.* **98,** 257–267 (2009).
125. Owen, D. H. & Katz, D. F. A Review of the Physical and Chemical Properties of Human Semen and the Formulation of a Semen Simulant. *J. Androl.* **26,** 459–469 (2005).
126. Whaley, K. J., Hanes, J., Shattock, R., Cone, R. A. & Friend, D. R. Novel Approaches to Vaginal Delivery and Safety of Microbicides: Biopharmaceuticals, Nanoparticles, and Vaccines. *Antiviral Res.* **88, Supplement,** S55–S66 (2010).

127. Lembo, D. & Cavalli, R. Nanoparticulate delivery systems for antiviral drugs. *Antivir. Chem. Chemother.* **21,** 53–70 (2010).
128. Bender, A. *et al.* Inhibition of HIV in vitro by antiviral drug-targeting using nanoparticles. *Res. Virol.* **145,** 215–220 (1994).
129. Shah, L. K. & Amiji, M. M. Intracellular Delivery of Saquinavir in Biodegradable Polymeric Nanoparticles for HIV/AIDS. *Pharm. Res.* **23,** 2638–2645 (2006).
130. Dou, H. *et al.* Laboratory investigations for the morphologic, pharmacokinetic, and anti-retroviral properties of indinavir nanoparticles in human monocyte-derived macrophages. *Virology* **358,** 148–158 (2007).
131. Hillaireau, H., Le Doan, T. & Couvreur, P. Polymer-Based Nanoparticles for the Delivery of Nucleoside Analogues. *J. Nanosci. Nanotechnol.* **6,** 2608–2617 (2006).
132. Sharma, P. & Garg, S. Pure drug and polymer based nanotechnologies for the improved solubility, stability, bioavailability and targeting of anti-HIV drugs. *Adv. Drug Deliv. Rev.* **62,** 491–502 (2010).
133. Chaowanachan, T., Krogstad, E., Ball, C. & Woodrow, K. A. Drug Synergy of Tenofovir and Nanoparticle-Based Antiretrovirals for HIV Prophylaxis. *PLoS ONE* (Forthcoming).
134. Lederman, M. M. *et al.* Prevention of Vaginal SHIV Transmission in Rhesus Macaques Through Inhibition of CCR5. *Science* **306,** 485–487 (2004).
135. Eszterhas, S. K., Ilonzo, N. O., Crozier, J. E., Celaj, S. & Howell, A. L. Nanoparticles containing siRNA to silence CD4 and CCR5 reduce expression of these receptors and inhibit HIV-1 infection in human female reproductive tract tissue explants. *Infect. Dis. Rep.* **3,** (2011).
136. Microbicide Trials Network. *Daily HIV Prevention Approaches Didn't Work for African Women in the VOICE Study*. (2013). at <http://www.mtnstopshiv.org/node/4877>
137. Nowacek, A. S. *et al.* Analyses of nanoformulated antiretroviral drug charge, size, shape and content for uptake, drug release and antiviral activities in human monocyte-derived macrophages. *J. Controlled Release* **150,** 204–211 (2011).
138. Roy, U. *et al.* Pharmacodynamic and Antiretroviral Activities of Combination Nanoformulated Antiretrovirals in HIV-1-Infected Human Peripheral Blood Lymphocyte-Reconstituted Mice. *J. Infect. Dis.* (2012). doi:10.1093/infdis/jis395
139. Brannon-Peppas, L. & Blanchette, J. O. Nanoparticle and targeted systems for cancer therapy. *Adv. Drug Deliv. Rev.* **64, Supplement,** 206–212 (2012).
140. Gu, F. X. *et al.* Targeted nanoparticles for cancer therapy. *Nano Today* **2,** 14–21 (2007).
141. Gunaseelan, S., Gunaseelan, K., Deshmukh, M., Zhang, X. & Sinko, P. J. Surface modifications of nanocarriers for effective intracellular delivery of anti-HIV drugs. *Adv. Drug Deliv. Rev.* **62,** 518–531 (2010).
142. Dahl, V., Josefsson, L. & Palmer, S. HIV reservoirs, latency, and reactivation: Prospects for eradication. *Antiviral Res.* **85,** 286–294 (2010).
143. Aquaro, S. *et al.* Macrophages and HIV infection: therapeutical approaches toward this strategic virus reservoir. *Antiviral Res.* **55,** 209–225 (2002).
144. Dutta, T., Garg, M. & Jain, N. K. Targeting of efavirenz loaded tuftsin conjugated poly(propyleneimine) dendrimers to HIV infected macrophages in vitro. *Eur. J. Pharm. Sci.* **34,** 181–189 (2008).
145. Collins, K. B., Patterson, B. K., Naus, G. J., Landers, D. V. & Gupta, P. Development of an in vitro organ culture model to study transmission of HIV-1 in the female genital tract. *Nat. Med.* **6,** 475 (2000).
146. das Neves, J., Amiji, M. M., Bahia, M. F. & Sarmento, B. Nanotechnology-based systems for the treatment and prevention of HIV/AIDS. *Adv. Drug Deliv. Rev.* **62,** 458–477 (2010).
147. Arnáiz, B., Martínez-Ávila, O., Falcon-Perez, J. M. & Penadés, S. Cellular uptake of gold nanoparticles bearing HIV gp120 oligomannosides. *Bioconjug. Chem.* **23,** 814–825 (2012).
148. Woodrow, K. A., Bennett, K. M. & Lo, D. D. Mucosal Vaccine Design and Delivery. *Annu. Rev. Biomed. Eng.* **14,** 17–46 (2012).
149. Lara, H. H., Ayala-Nuñez, N. V., Ixtepan-Turrent, L. & Rodriguez-Padilla, C. Mode of antiviral action of silver nanoparticles against HIV-1. *J. Nanobiotechnology* **8,** 1 (2010).
150. Hayakawa T *et al.* Concanavalin A-immobilized polystyrene nanospheres capture HIV-1 virions and gp120: potential approach towards prevention of viral transmission. *J. Med. Virol.* **56,** 327–31 (1998).
151. Leung, V. & Ko, F. Biomedical applications of nanofibers. *Polym. Adv. Technol.* **22,** 350–365 (2011).

152. Teo, W.-E., Inai, R. & Ramakrishna, S. Technological advances in electrospinning of nanofibers. *Sci. Technol. Adv. Mater.* **12,** 013002 (2011).
153. Sill, T. J. & von Recum, H. A. Electrospinning: Applications in drug delivery and tissue engineering. *Biomaterials* **29,** 1989–2006 (2008).
154. Liang, D., Hsiao, B. S. & Chu, B. Functional electrospun nanofibrous scaffolds for biomedical applications. *Adv. Drug Deliv. Rev.* **59,** 1392–1412 (2007).
155. Gunn, J. & Zhang, M. Polyblend nanofibers for biomedical applications: perspectives and challenges. *Trends Biotechnol.* **28,** 189–197 (2010).
156. Huang, C. *et al.* Stimuli-responsive electrospun fibers and their applications. *Chem. Soc. Rev.* **40,** 2417 (2011).
157. Fridrikh, S., Yu, J., Brenner, M. & Rutledge, G. Controlling the Fiber Diameter during Electrospinning. *Phys. Rev. Lett.* **90,** (2003).
158. Zhang, K. *et al.* Genipin-crosslinked silk fibroin/hydroxybutyl chitosan nanofibrous scaffolds for tissue-engineering application. *J. Biomed. Mater. Res. A* **95A,** 870–881 (2010).
159. Teo, W.-E., He, W. & Ramakrishna, S. Electrospun scaffold tailored for tissue-specific extracellular matrix. *Biotechnol. J.* **1,** 918–929 (2006).
160. Venugopal, J. & Ramakrishna, S. Applications of Polymer Nanofibers in Biomedicine and Biotechnology. *Appl. Biochem. Biotechnol.* **125,** 147–158 (2005).
161. Cao, H., Mchugh, K., Chew, S. Y. & Anderson, J. M. The topographical effect of electrospun nanofibrous scaffolds on the in vivo and in vitro foreign body reaction. *J. Biomed. Mater. Res. A* **93A,** 1151–1159 (2009).
162. Yu, D.-G. Electrospun nanofiber-based drug delivery systems. *Health (N. Y.)* **01,** 67–75 (2009).
163. Patel, S. K., Lavasanifar, A. & Choi, P. Roles of Nonpolar and Polar Intermolecular Interactions in the Improvement of the Drug Loading Capacity of PEO-b-PCL with Increasing PCL Content for Two Hydrophobic Cucurbitacin Drugs. *Biomacromolecules* **10,** 2584–2591 (2009).
164. Heunis, T. D. J. & Dicks, L. M. T. Nanofibers Offer Alternative Ways to the Treatment of Skin Infections. *J. Biomed. Biotechnol.* **2010,** 1–11 (2010).
165. Tiwari, S. K., Tzezana, R., Zussman, E. & Venkatraman, S. S. Optimizing partition-controlled drug release from electrospun core–shell fibers. *Int. J. Pharm.* **392,** 209–217 (2010).
166. Taepaiboon, P., Rungsardthong, U. & Supaphol, P. Vitamin-loaded electrospun cellulose acetate nanofiber mats as transdermal and dermal therapeutic agents of vitamin A acid and vitamin E. *Eur. J. Pharm. Biopharm.* **67,** 387–397 (2007).
167. Li, X., Kanjwal, M. A., Lin, L. & Chronakis, I. S. Electrospun polyvinyl-alcohol nanofibers as oral fast-dissolving delivery system of caffeine and riboflavin. *Colloids Surf. B Biointerfaces* **103,** 182–188 (2013).
168. Ignatious, F., Sun, L., Lee, C.-P. & Baldoni, J. Electrospun Nanofibers in Oral Drug Delivery. *Pharm. Res.* **27,** 576–588 (2010).
169. Bernards, D. A. *et al.* Ocular Biocompatibility and Structural Integrity of Micro- and Nanostructured Poly(caprolactone) Films. *J. Ocul. Pharmacol. Ther.* 130207065900009 (2013). doi:10.1089/jop.2012.0152
170. Meinel, A. J., Germershaus, O., Luhmann, T., Merkle, H. P. & Meinel, L. Electrospun matrices for localized drug delivery: Current technologies and selected biomedical applications. *Eur. J. Pharm. Biopharm.* **81,** 1–13 (2012).
171. Huang, C. *et al.* Electrospun cellulose acetate phthalate fibers for semen induced anti-HIV vaginal drug delivery. *Biomaterials* **33,** 962–969 (2012).
172. Ball, C., Krogstad, E., Chaowanachan, T. & Woodrow, K. A. Drug-Eluting Fibers for HIV-1 Inhibition and Contraception. *PLoS ONE* **7,** e49792 (2012).
173. Blakney, A. K., Krogstad, E. A., Jiang, Y. H. & Woodrow, K. A. Delivery of multipurpose prevention drug combinations from electrospun nanofibers using composite microarchitectures. *Int. J. Nanomedicine* **9,** 2967–2978 (2014).
174. Ball, C. & Woodrow, K. A. Electrospun Solid Dispersions of Maraviroc for Rapid Intravaginal Preexposure Prophylaxis of HIV. *Antimicrob. Agents Chemother.* **58,** 4855–4865 (2014).
175. Krogstad, E. A. & Woodrow, K. A. Manufacturing scale-up of electrospun poly(vinyl alcohol) fibers containing tenofovir for vaginal drug delivery. *Int. J. Pharm.* **475,** 282–291 (2014).

176. Carson, D., Jiang, Y. & Woodrow, K. A. Tunable Release of Multiclass Anti-HIV Drugs that are Water-Soluble and Loaded at High Drug Content in Polyester Blended Electrospun Fibers. *Pharm. Res.* (2015). doi:10.1007/s11095-015-1769-0
177. Nagy, Z. K. *et al.* Nanofibrous solid dosage form of living bacteria prepared by electrospinning. *Express Polym. Lett.* **8,** 352–361 (2014).
178. Brako, F., Raimi-Abraham, B., Mahalingam, S., Craig, D. Q. M. & Edirisinghe, M. Making nanofibres of mucoadhesive polymer blends for vaginal therapies. *Eur. Polym. J.* **70,** 186–196 (2015).
179. Sharma, R., Garg, T., Goyal, A. K. & Rath, G. Development, optimization and evaluation of polymeric electrospun nanofiber: A tool for local delivery of fluconazole for management of vaginal candidiasis. *Artif. Cells Nanomedicine Biotechnol.* 1–8 (2015). doi:10.3109/21691401.2014.966194
180. Cui, W. *et al.* Investigation of Drug Release and Matrix Degradation of Electrospun Poly(dl-lactide) Fibers with Paracetanol Inoculation. *Biomacromolecules* **7,** 1623–1629 (2006).
181. Yohe, S. T., Colson, Y. L. & Grinstaff, M. W. Superhydrophobic Materials for Tunable Drug Release: Using Displacement of Air To Control Delivery Rates. *J. Am. Chem. Soc.* **134,** 2016–2019 (2012).
182. Zhang, Y. Z. *et al.* Coaxial Electrospinning of (Fluorescein Isothiocyanate-Conjugated Bovine Serum Albumin)-Encapsulated Poly(ε-caprolactone) Nanofibers for Sustained Release. *Biomacromolecules* **7,** 1049–1057 (2006).
183. Zamani, M., Morshed, M., Varshosaz, J. & Jannesari, M. Controlled release of metronidazole benzoate from poly ε-caprolactone electrospun nanofibers for periodontal diseases. *Eur. J. Pharm. Biopharm.* **75,** 179–185 (2010).
184. Chunder, A., Sarkar, S., Yu, Y. & Zhai, L. Fabrication of ultrathin polyelectrolyte fibers and their controlled release properties. *Colloids Surf. B Biointerfaces* **58,** 172–179 (2007).
185. Zeng, J. *et al.* Poly(vinyl alcohol) Nanofibers by Electrospinning as a Protein Delivery System and the Retardation of Enzyme Release by Additional Polymer Coatings. *Biomacromolecules* **6,** 1484–1488 (2005).
186. Yang, Y., Li, X., Qi, M., Zhou, S. & Weng, J. Release pattern and structural integrity of lysozyme encapsulated in core–sheath structured poly(dl-lactide) ultrafine fibers prepared by emulsion electrospinning. *Eur. J. Pharm. Biopharm.* **69,** 106–116 (2008).
187. Yu, D.-G. *et al.* Solid dispersions in the form of electrospun core-sheath nanofibers. *Int. J. Nanomedicine* **6,** 3271–3280 (2011).
188. Yarin, A. L. Coaxial electrospinning and emulsion electrospinning of core-shell fibers. *Polym. Adv. Technol.* **22,** 310–317 (2011).
189. Kenawy, E.-R., Abdel-Hay, F. I., El-Newehy, M. H. & Wnek, G. E. Controlled release of ketoprofen from electrospun poly(vinyl alcohol) nanofibers. *Mater. Sci. Eng. A* **459,** 390–396 (2007).
190. Jannesari, M., Varshosaz, J., Morshed, M. & Zamani, M. Composite poly(vinyl alcohol)/poly(vinyl acetate) electrospun nanofibrous mats as a novel wound dressing matrix for controlled release of drugs. *Int. J. Nanomedicine* 993 (2011). doi:10.2147/IJN.S17595
191. Xie, J. & Wang, C.-H. Electrospun Micro- and Nanofibers for Sustained Delivery of Paclitaxel to Treat C6 Glioma in Vitro. *Pharm. Res.* **23,** 1817–1826 (2006).
192. Mehta, S. *et al.* Vaginal distribution and retention of a multiparticulate drug delivery system, assessed by gamma scintigraphy and magnetic resonance imaging. *Int. J. Pharm.* **426,** 44–53 (2012).
193. Macri, L. K., Sheihet, L., Singer, A. J., Kohn, J. & Clark, R. A. F. Ultrafast and fast bioerodible electrospun fiber mats for topical delivery of a hydrophilic peptide. *J. Controlled Release* **161,** 813–820 (2012).
194. Okuda, T., Tominaga, K. & Kidoaki, S. Time-programmed dual release formulation by multilayered drug-loaded nanofiber meshes. *J. Controlled Release* **143,** 258–264 (2010).
195. Palella, F. J. *et al.* Declining Morbidity and Mortality among Patients with Advanced Human Immunodeficiency Virus Infection. *N. Engl. J. Med.* **338,** 853–860 (1998).
196. Veazey, R. S. *et al.* Protection of rhesus macaques from vaginal infection by vaginally delivered maraviroc, an inhibitor of HIV-1 entry via the CCR5 co-receptor. *J. Infect. Dis.* **202,** 739–744 (2010).
197. Prabaharan, M., Jayakumar, R. & Nair, S. V. in *Biomedical Applications of Polymeric Nanofibers* (eds. Jayakumar, R. & Nair, S.) **246,** 241–262 (Springer Berlin Heidelberg, 2011).
198. Xu, X., Chen, X., Wang, Z. & Jing, X. Ultrafine PEG–PLA fibers loaded with both paclitaxel and doxorubicin hydrochloride and their in vitro cytotoxicity. *Eur. J. Pharm. Biopharm.* **72,** 18–25 (2009).

199. Verreck, G., Chun, I., Peeters, J., Rosenblatt, J. & Brewster, M. E. Preparation and Characterization of Nanofibers Containing Amorphous Drug Dispersions Generated by Electrostatic Spinning. *Pharm. Res.* **20,** 810–817 (2003).
200. Yu, D.-G., Branford-White, C., Shen, X.-X., Zhang, X.-F. & Zhu, L.-M. Solid Dispersions of Ketoprofen in Drug-Loaded Electrospun Nanofibers. *J. Dispers. Sci. Technol.* **31,** 902–908 (2010).
201. Wang, Y. & Hsieh, Y.-L. Immobilization of lipase enzyme in polyvinyl alcohol (PVA) nanofibrous membranes. *J. Membr. Sci.* **309,** 73–81 (2008).
202. Choi, J. S., Choi, S. H. & Yoo, H. S. Coaxial electrospun nanofibers for treatment of diabetic ulcers with binary release of multiple growth factors. *J. Mater. Chem.* **21,** 5258 (2011).
203. Liao, I. ., Chen, S., Liu, J. . & Leong, K. . Sustained viral gene delivery through core-shell fibers. *J. Controlled Release* **139,** 48–55 (2009).
204. Saraf, A., Baggett, L. S., Raphael, R. M., Kasper, F. K. & Mikos, A. G. Regulated non-viral gene delivery from coaxial electrospun fiber mesh scaffolds. *J. Controlled Release* **143,** 95–103 (2010).
205. Cao, H., Jiang, X., Chai, C. & Chew, S. Y. RNA interference by nanofiber-based siRNA delivery system. *J. Controlled Release* **144,** 203–212 (2010).
206. Salalha, W., Kuhn, J., Dror, Y. & Zussman, E. Encapsulation of bacteria and viruses in electrospun nanofibres. *Nanotechnology* **17,** 4675–4681 (2006).
207. Gensheimer, M. *et al.* Novel Biohybrid Materials by Electrospinning: Nanofibers of Poly(ethylene oxide) and Living Bacteria. *Adv. Mater.* **19,** 2480–2482 (2007).
208. Townsend-Nicholson, A. & Jayasinghe, S. N. Cell Electrospinning: a Unique Biotechnique for Encapsulating Living Organisms for Generating Active Biological Microthreads/Scaffolds. *Biomacromolecules* **7,** 3364–3369 (2006).
209. Maretschek S, Greiner A & Kissel T. Electrospun biodegradable nanofiber nonwovens for controlled release of proteins. *J. Control. Release Off. J. Control. Release Soc.* **127,** 180–7 (2008).
210. Chew SY, Wen J, Yim EK & Leong KW. Sustained release of proteins from electrospun biodegradable fibers. *Biomacromolecules* **6,** (2005).
211. Patel, S. *et al.* Bioactive Nanofibers: Synergistic Effects of Nanotopography and Chemical Signaling on Cell Guidance. *Nano Lett.* **7,** 2122–2128 (2007).
212. Beck-Broichsitter, M. *et al.* Novel 'Nano in Nano' Composites for Sustained Drug Delivery: Biodegradable Nanoparticles Encapsulated into Nanofiber Non-Wovens. *Macromol. Biosci.* **10,** 1527–1535 (2010).
213. Zomer Volpato, F. *et al.* Preservation of FGF-2 bioactivity using heparin-based nanoparticles, and their delivery from electrospun chitosan fibers. *Acta Biomater.* **8,** 1551–1559 (2012).
214. Chen, M. *et al.* Chitosan/siRNA Nanoparticles Encapsulated in PLGA Nanofibers for siRNA Delivery. *ACS Nano* **6,** 4835–4844 (2012).
215. Dong, B., Smith, M. E. & Wnek, G. E. Encapsulation of Multiple Biological Compounds Within a Single Electrospun Fiber. *Small* **5,** 1508–1512 (2009).
216. Qi, Hu, P., Xu, J. & Wang. Encapsulation of Drug Reservoirs in Fibers by Emulsion Electrospinning: Morphology Characterization and Preliminary Release Assessment. *Biomacromolecules* **7,** 2327–2330 (2006).
217. Wang, Y. *et al.* Electrospun composite nanofibers containing nanoparticles for the programmable release of dual drugs. *Polym. J.* **43,** 478–483 (2011).
218. Ionescu, L. C., Lee, G. C., Sennett, B. J., Burdick, J. A. & Mauck, R. L. An anisotropic nanofiber/microsphere composite with controlled release of biomolecules for fibrous tissue engineering. *Biomaterials* **31,** 4113–4120 (2010).
219. Xie, Z. *et al.* Dual growth factor releasing multi-functional nanofibers for wound healing. *Acta Biomater.* **9,** 9351–9359 (2013).
220. Song, B., Wu, C. & Chang, J. Controllable delivery of hydrophilic and hydrophobic drugs from electrospun poly(lactic-co-glycolic acid)/mesoporous silica nanoparticles composite mats. *J. Biomed. Mater. Res. B Appl. Biomater.* **100B,** 2178–2186 (2012).
221. Qiu, K. *et al.* Doxorubicin-loaded electrospun poly(L-lactic acid)/mesoporous silica nanoparticles composite nanofibers for potential postsurgical cancer treatment. *J. Mater. Chem. B* (2013). doi:10.1039/C3TB20636J
222. Zheng, F., Wang, S., Shen, M., Zhu, M. & Shi, X. Antitumor efficacy of doxorubicin-loaded electrospun nano-hydroxyapatite–poly(lactic-co-glycolic acid) composite nanofibers. *Polym Chem* **4,** 933–941 (2013).

223. Kouhi, M., Morshed, M., Varshosaz, J. & Fathi, M. H. Poly (ε-caprolactone) incorporated bioactive glass nanoparticles and simvastatin nanocomposite nanofibers: Preparation, characterization and in vitro drug release for bone regeneration applications. *Chem. Eng. J.* **228,** 1057–1065 (2013).
224. Hou, Z. *et al.* Electrospun Upconversion Composite Fibers as Dual Drugs Delivery System with Individual Release Properties. *Langmuir* **29,** 9473–9482 (2013).
225. Yan, E. *et al.* Electrospun polyvinyl alcohol/chitosan composite nanofibers involving Au nanoparticles and their in vitro release properties. *Mater. Sci. Eng. C* **33,** 461–465 (2013).
226. Lee, S. J. *et al.* Electrospun chitosan nanofibers with controlled levels of silver nanoparticles. Preparation, characterization and antibacterial activity. *Carbohydr. Polym.* **111,** 530–537 (2014).
227. Yuan, Z. *et al.* Synergistic mediation of tumor signaling pathways in hepatocellular carcinoma therapy via dual-drug-loaded pH-responsive electrospun fibrous scaffolds. *J Mater Chem B* **3,** 3436–3446 (2015).
228. Acosta, C. *et al.* Polymer Composites Containing Gated Mesoporous Materials for On-Command Controlled Release. *ACS Appl. Mater. Interfaces* **6,** 6453–6460 (2014).
229. Huang, C.-H. *et al.* Preparation of a thermo- and pH-sensitive nanofibrous scaffold with embedded chitosan-based nanoparticles and its evaluation as a drug carrier. *Cellulose* **21,** 2497–2509 (2014).
230. Yoo, H. S., Kim, T. G. & Park, T. G. Surface-functionalized electrospun nanofibers for tissue engineering and drug delivery. *Adv. Drug Deliv. Rev.* **61,** 1033–1042 (2009).
231. Agarwal, S., Wendorff, J. H. & Greiner, A. Chemistry on Electrospun Polymeric Nanofibers: Merely Routine Chemistry or a Real Challenge? *Macromol. Rapid Commun.* **31,** 1317–1331 (2010).
232. El-Sadr WM *et al.* Safety and acceptability of cellulose sulfate as a vaginal microbicide in HIV-infected women. *AIDS Lond. Engl.* **20,** 1109–16 (2006).
233. Puttipaiboon, N., Yoovidhya, T. & Wongsasulak, S. Fabrication and Gastro-Mucoadhesive Property of Zein-PEO-Chitosan Blend Ultrafine Fibrous Films. *Proc. NanoThailand 2012* 13–16 (2012).
234. Yoo, J.-W., Dharmala, K. & Lee, C. H. The physicodynamic properties of mucoadhesive polymeric films developed as female controlled drug delivery system. *Int. J. Pharm.* **309,** 139–145 (2006).
235. Baji, A., Mai, Y.-W., Wong, S.-C., Abtahi, M. & Chen, P. Electrospinning of polymer nanofibers: Effects on oriented morphology, structures and tensile properties. *Compos. Sci. Technol.* **70,** 703–718 (2010).
236. Ayutsede, J. *et al.* Carbon Nanotube Reinforced Bombyx mori Silk Nanofibers by the Electrospinning Process. *Biomacromolecules* **7,** 208–214 (2006).
237. Katta, P., Alessandro, M., Ramsier, R. D. & Chase, G. G. Continuous Electrospinning of Aligned Polymer Nanofibers onto a Wire Drum Collector. *Nano Lett.* **4,** 2215–2218 (2004).
238. Li, W.-J., Mauck, R. L., Cooper, J. A., Yuan, X. & Tuan, R. S. Engineering controllable anisotropy in electrospun biodegradable nanofibrous scaffolds for musculoskeletal tissue engineering. *J. Biomech.* **40,** 1686–1693 (2007).
239. Wang, S., Zhang, Y., Yin, G., Wang, H. & Dong, Z. Electrospun polylactide/silk fibroin–gelatin composite tubular scaffolds for small-diameter tissue engineering blood vessels. *J. Appl. Polym. Sci.* **113,** 2675–2682 (2009).
240. Kidoaki, S., Kwon, I. K. & Matsuda, T. Mesoscopic spatial designs of nano- and microfiber meshes for tissue-engineering matrix and scaffold based on newly devised multilayering and mixing electrospinning techniques. *Biomaterials* **26,** 37–46 (2005).
241. Pham, Q. P., Sharma, U. & Mikos, A. G. Electrospun Poly(ε-caprolactone) Microfiber and Multilayer Nanofiber/Microfiber Scaffolds: Characterization of Scaffolds and Measurement of Cellular Infiltration. *Biomacromolecules* **7,** 2796–2805 (2006).
242. McClure, M. J., Sell, S. A., Simpson, D. G., Walpoth, B. H. & Bowlin, G. L. A three-layered electrospun matrix to mimic native arterial architecture using polycaprolactone, elastin, and collagen: A preliminary study. *Acta Biomater.* **6,** 2422–2433 (2010).
243. Teo, W. E., Kotaki, M., Mo, X. M. & Ramakrishna, S. Porous tubular structures with controlled fibre orientation using a modified electrospinning method. *Nanotechnology* **16,** 918–924 (2005).
244. van Lieshout, M. I., Vaz, C. M., Rutten, M. C. M., Peters, G. W. M. & Baaijens, F. P. T. Electrospinning versus knitting: two scaffolds for tissue engineering of the aortic valve. *J. Biomater. Sci. Polym. Ed.* **17,** 77–89 (2006).
245. Del Gaudio, C., Grigioni, M., Bianco, A. & De Angelis, G. Electrospun bioresorbable heart valve scaffold for tissue engineering. *Int. J. Artif. Organs* **31,** 68–75 (2008).

246. Szentivanyi, A., Chakradeo, T., Zernetsch, H. & Glasmacher, B. Electrospun cellular microenvironments: Understanding controlled release and scaffold structure. *Adv. Drug Deliv. Rev.* **63,** 209–220 (2011).
247. Food and Agricultural Organization of the United Nations. AIDS - a threat to rural Africa. at <http://www.fao.org/FOCUS/E/aids/aids1-e.htm>
248. Kayaci, F. & Uyar, T. Encapsulation of vanillin/cyclodextrin inclusion complex in electrospun polyvinyl alcohol (PVA) nanowebs: Prolonged shelf-life and high temperature stability of vanillin. *Food Chem.* **133,** 641–649 (2012).
249. Chou, S.-F., Carson, D. & Woodrow, K. A. Current strategies for sustaining drug release from electrospun nanofibers. *J. Controlled Release* (2015). doi:10.1016/j.jconrel.2015.09.008
250. Morrow, K. M. *et al.* Designing Preclinical Perceptibility Measures to Evaluate Topical Vaginal Gel Formulations: Relating User Sensory Perceptions and Experiences to Formulation Properties. *AIDS Res. Hum. Retroviruses* **30,** 78–91 (2014).

2 Antiretroviral drug-loaded nanoparticles to enhance drug efficacy against HIV-1.

Portions adapted from: Chaowanachan, T., Krogstad, E., Ball, C. & Woodrow, K. A. Drug Synergy of Tenofovir and Nanoparticle-Based Antiretrovirals for HIV Prophylaxis. *PLoS ONE* **8,** e61416 (2013).

2.1 ABSTRACT

The use of drug combinations has revolutionized the treatment of HIV, but there is no equivalent combination product that exists for prevention, particularly for topical HIV prevention. We hypothesized that encapsulating antiretroviral (ARV) drugs into polymeric nanoparticles would enhance drug bioavailability and improve anti-HIV-1 efficacy compared to unformulated drug. We fabricated two types of nanoparticles, each loaded with a single antiretroviral that acts on a specific step of the viral replication cycle. Here we describe the production and characterization of PLGA nanoparticles loaded with efavirenz (EFV) or saquinavir (SQV) and their ability to prevent HIV-1 *in vitro*. Biodegradable poly(lactide-*co*-glycolide) nanoparticles loaded with efavirenz (NP-EFV) or saquinavir (NP-SQV) were individually prepared by emulsion or nanoprecipitation techniques. Nanoparticles had reproducible size (d ~200 nm) and zeta potential (-25 mV). The drug loading of the nanoparticles was approximately 7% (w/w). NP-EFV and NP-SQV were nontoxic to TZM-bl cells and ectocervical explants. Both NP-EFV and NP-SQV exhibited potent protection against HIV-1 BaL infection *in vitro*. The HIV inhibitory effect of nanoparticle-formulated ARVs showed up to a 50-fold reduction in the 50% inhibitory concentration (IC_{50}) compared to free drug. ARVs with different physicochemical properties can be encapsulated individually into nanoparticles to potently inhibit HIV. Our findings demonstrate encapsulating EFV into nanoparticles greatly enhances activity against HIV while maintaining safety for topical application.

2.2 INTRODUCTION

Sexual transmission is the primary cause of new HIV-1 infections worldwide, which today exceed 6,000 infections daily[1,2]. Sub-Saharan Africa bears the burden of the global HIV/AIDS epidemic, and women in this region are disproportionately affected by the pandemic[3,4]. Women account for three-quarters of Africans between the ages of 15 and 24 who are HIV-positive, and HIV/AIDS is the leading cause of death among women of reproductive age[4]. In the absence of an effective vaccine, and as long as new infections continue to outpace advances made in

treatment with antiretroviral (ARV) drugs[5], biomedical prevention strategies are critical for stemming the spread of HIV. Oral pre-exposure prophylaxis (PrEP) and topical microbicides are the lead strategies for preventing HIV infection, but there is still a critical need for methods with greater efficacy to protect women[6]. Long-acting ARV drug combinations have the potential to enhance the efficacy of current ARV-based prevention strategies by overcoming low user adherence, and harnessing drug combinations with synergistic activity and breadth of coverage against the global diversity of HIV variants. However, the physicochemical diversity of ARV drugs precludes their co-formulation and limits access to all possible combinations of the >20 ARV drugs approved for clinical use[7–9]. Strategies that enable ARV drugs to be easily combined and provide sustained antiretroviral activity have the greatest potential to impact the efficacy of future biomedical prevention methods.

Nanocarrier systems provide an innovative approach for developing long-acting ARV drug combinations and have already been explored for use in HIV treatment and prevention[10–13]. The availability of different carrier systems, combined with the versatility of drugs that can be encapsulated for controlled release, motivate the use of nanocarrier systems for ARV drug delivery in different applications. In addition, nanocarriers have been shown in a number of examples to increase the activity and reduce cytotoxicity of several ARV drugs [14–16]. The selection of a nanocarrier system for drug delivery depends on the properties of the drug but also on the physical and chemical attributes of the final nanoformulation. The ability to control these attributes is important because the pharmacokinetics of the resulting nanoformulated drug can differ significantly from the parent compound. Properties of the delivery system such as carrier size, architecture and surface chemistry can also affect the activity of nanoformulated drugs. For example, Nowacek et al. demonstrated that physical characteristics of nanoparticles formed by wet-milling water-insoluble ARV drugs, i.e., particle size, surface charge, and shape, were correlated with macrophage uptake and resulted in greater antiretroviral efficacy[17]. The potential for rational design of drug carriers to enhance drug potency and efficacy may have important applications for prophylaxis.

Nanocarrier systems also have the capacity to address challenges associated with delivering drug combinations. The success of highly active antiretroviral therapy (HAART) provides a paradigm for developing the next generation ARV-based prevention strategies, giving rise to the possibility that a combination of potent and broadly active inhibitors will provide superior protection against HIV transmission and reduce the likelihood of emerging drug resistance. Drug combinations can also markedly expand the antiretroviral activity of single agents used alone by facilitating unique mechanisms of drug–drug activity when used in

combination. For example, inhibition of drug metabolizing enzymes or efflux transporter systems has been implicated in the improved virological response to ARV drug combinations such as ritonavir in combination with saquinavir (SQV), and tenofovir (TFV) in combination with emtricitabine (FTC) or efavirenz (EFV) [18–21]. However, due to physicochemical incompatibilities, not all ARV drugs are amenable to combinations that may lead to beneficial combination drug activity. As such, nanocarrier mediated ARV delivery may allow for the exploration of unique drug-drug interactions of otherwise incompatible ARV compounds or modulate drug delivery profiles necessary to achieve drug synergy using specific drug combinations.

Here we describe the formulation of NP-ARVs and their *in vitro* anti-HIV activity and *ex vivo* safety. To overcome challenges associated with formulating multiple ARV compounds that are chemically incompatible, we fabricated polymeric nanoparticles encapsulating individual ARV drugs. The non-nucleoside reverse transcriptase inhibitor (NNRTI) EFV and the protease inhibitor (PI) SQV were chosen for nanoparticle formulations. These drugs have complementary mechanisms of action and different resistance profiles against HIV-1, but are challenging to co-formulate into a single vaginal gel due to their low aqueous solubilities. We show that EFV and SQV could be individually fabricated into biodegradable poly(lactide-*co*-glycolide) (PLGA) nanoparticles with high loading and encapsulation efficiency. NP-ARVs were nontoxic in cell culture and in mucosal tissue explants. In comparison to free ARVs, ARVs formulated in nanoparticles showed up to a 50-fold increase in antiviral activity. Collectively, our data show that PLGA-based nanoparticle formulations are a promising platform for vaginal delivery of ARVs with low aqueous solubility. The implications of our results may support a new paradigm for delivery of combination ARVs for HIV-1 prevention.

2.3 MATERIALS AND METHODS

2.3.1 Materials

Poly(DL-lactide-*co*-glycolide) (PLGA) with molar ratios of 50:50 was purchased from DURECT Corporation (Lactel - B6010-2P, MW ~30 KD) and Sigma-Aldrich (Resomer - 502H, MW ~30 KD). Chemical reagents for nanoparticle preparation were purchased from Fisher Scientific. Cell culture reagents (GIBCO, Invitrogen by Life Sciences Inc.) were used for the TZM-bl infectivity and cytotoxicity assays. The Promega™ Luciferase Assay System (Promega Co., Madison, WI) was used to determine luciferase protein expression. Tenofovir (TFV), efavirenz (EFV), and saquinavir (SQV) were obtained through the NIH AIDS Research and Reference Reagent Program (http://www.aidsreagent.org/).

2.3.2 Fabrication of ARV loaded nanoparticles

Blank nanoparticles (vehicle control) and nanoparticles loaded with EFV or SQV were formulated individually. EFV loaded nanoparticles (NP-EFV) were formulated using a single emulsion technique as previously described[22,23]. All concentrations described below are expressed in % w/v unless noted otherwise. In each preparation, EFV was dissolved in dichloromethane (DCM) containing 1.5% PLGA (w/v, Lactel - B6010-2P). Mass percentage of drug initially dissolved in PLGA (theoretical drug loading) was 15% (w/w). This mixture was then added drop-wise to an aqueous phase containing an emulsifier (5% aqueous solution of polyvinyl alcohol, PVA) to form an oil-in-water emulsion (o/w). A probe sonicator (3 mm diameter, Sonicator XL, Misonix, Farmingdale, NY) was used to homogenize the emulsion for 60 sec at 65 W. After solvent evaporation in an aqueous solution of 0.25% PVA for 3 h, nanoparticles were washed with deionized water three times by centrifugation at 14,000×g for 10 min (Sorvall Ultra 80, Waltham, MA). To formulate SQV loaded nanoparticles (NP-SQV), we used a nanoprecipitation technique[24]. SQV were dissolved in acetone containing 0.33% PLGA (w/v, Resomer - 502H) with 15% (w/w) theoretical drug loading. Then SQV-PLGA solution was added by syringe pump at a 1 mL/min flow rate to an aqueous solution containing 0.1% phosphate-buffered saline (0.01 M PBS, pH 7.4) and 0.1% dioctyl sulfosuccinate sodium (DSS) surfactant while it was stirring. Nanoparticles were formed instantly upon mixing due to the immiscibility of the polymer and non-solvent. After solvent evaporation, nanoparticles were washed as described above. The nanoparticles were suspended in deionized water and were lyophilized for 24 h under vacuum at 0.120 mbarr at −86°C (FreeZone 2.5 Plus, Labcono, Kansas City, MO). The dried nanoparticles were stored at −86°C until use.

2.3.3 Characterization of nanoparticles

Size and zeta potential of the fabricated nanoparticles were determined using a Zetasizer Nano ZS90 (Malvern Instruments, AR). Size and morphology of nanoparticles were confirmed by scanning electron microscopy (SEM) visualized with a JEOL-7000 (JEOL Ltd, Sheboygan, WI) scanning electron microscope. Samples of nanoparticles were dusted onto carbon tape, coated with gold, and imaged using a 10 kV electron beam.

2.3.4 Drug loading

Verification of drug-polymer association in nanoparticles was performed using Fourier transform infrared spectroscopy (FTIR). Briefly, 3-5 mg of nanoparticles were mixed with

potassium bromide (KBr) using a mortar and pestle and analyzed in FTIR. Infrared spectra over a range of wavenumber 500 to 4000 cm^{-1} were monitored for the presence of the functional groups corresponding to the characteristic peaks of EFV or SQV. The amount of EFV and SQV actually loaded in nanoparticles was determined using a Shimadzu Prominence LC20AD high performance liquid chromatography (HPLC) system and LC Solutions software. A C18 column (Phenomenex, Torrance, CA), 5 µm, 250 x 4.6 mm i.d., was used for analysis with isocratic mode at a flow rate of 1.0 mL/min. Methods used to analyze EFV and SQV were based on those described previously for detecting SQV[25]. The mobile phase consisted of a mixture of 10 mM ammonium acetate buffer in HPLC grade water and acetonitrile at a 35:65 ratio (v/v). SQV was detected at 238 nm and EFV was detected at 246 nm with retention times of 7.5 min and 8.6 min, respectively. Standard solutions of EFV and SQV were prepared at 1 mg/mL in dimethyl sulfoxide (DMSO) and diluted to generate the calibration curves. Analysis methods were validated with standard solutions and spiked samples. Linearity was established from 50 ng/mL to 10 µg/mL for EFV and 250 ng/mL to 50 µg/mL for SQV using a 10 µL injection volume. Nanoparticles were dissolved in DMSO to assess drug loading and encapsulation efficiency. For all *in vitro* assays, the delivered dose of the formulated ARV drug is defined and calculated based on the total drug loaded in the polymeric nanoparticle. Therefore, we delivered a mass concentration of the drug-loaded polymer to achieve the desired molar concentration of the drug given the volume requirements for the particular assay.

2.3.5 In vitro release

To determine the release profiles of NP-ARVs in a physiological condition relevant to the vagina, an *in vitro* release study was conducted over 144 h using a vaginal fluid simulant (VFS) as the release medium[26]. Triplicate samples of approximately 2 mg of either NP-EFV or NP-SQV were suspended in 500 µL of VFS and added into individual dialysis tubes (1kDa cut-off, GE Healthcare Bio-Sciences Corp., NJ). The dialysis tubes were placed in individual 50-mL tubes containing 5 or 15 mL of VFS for SQV and EFV, respectively, and incubated at 37°C on an orbital shaker at 100 rpm. At set time points (0.5, 1, 4, 8, 24, 48, 72, 144 h), 200 µL of samples were collected and replaced with fresh VFS. UV-HPLC methods were used to quantify the amount of drug in samples as described above.

2.3.6 Cells, tissues and viruses

TZM-bl cells, PM1 cells, and HIV-1 BaL isolate were obtained through the NIH AIDS Research and Reference Reagent Program (http://www.aidsreagent.org/). TZM-bl cells are an engineered HeLa cells that express CD4, CCR5 and CXCR4 as previously described were used

as reporter cells in the infectivity assay as described previously[27–30]. Cells were maintained at 37°C, 5% CO_2 in Dulbecco's Modified Eagle Medium (DMEM) with 10% fetal bovine serum, 1% 100X penicillin/streptomycin, and 1% 200 mM L-glutamine. PM1 cells were maintained at 37°C, 5% CO_2 in RPMI 1640 with 10% fetal bovine serum, 1% 100X penicillin/streptomycin, and 1% 200 mM L-glutamine and were used for preparing HIV-1 viral stock[31].

2.3.7 Cellular viability assay

TZM-bl cells were seeded in a 96-well plate at 5,000 cells/well and incubated overnight to allow the cells to adhere to the well. Dilutions of drugs (free and nanoparticle forms) were added to triplicate wells of TZM-bl cells. Wells containing cells alone served as controls. Cell cultures in the absence and presence of drugs were incubated for 48 h. To determine cell culture viability, metabolic capacity of cells was measured using the Promega CellTiter-Blue™ assay according to the manufacturer's instructions. The ability of cells to reduce a resazurin indicator dye to fluorescent resorufin was measured using a plate reader at 560/590 nm (excitation/emission) and normalized to media only-treated cells (100% viability). DMSO served as positive control.

2.3.8 Antiviral activity

The inhibitory activity of free and nanoparticle ARVs against HIV-1 BaL was determined in TZM-bl cells by luciferase quantification of cell lysates[32,33]. Cells were seeded at 5,000 cells/well and grown to approximately 50-60% confluence overnight prior to infection. Dilutions of each drug were added to triplicate wells. After 1 h, HIV-1 BaL at an approximate $TCID_{50}$ (50% tissue culture infectious dose) of 300 per well was added to each pre-treated well. Media controls (wells containing cells alone) were included in every run for luminescent background subtraction. Cells grown in the absence of virus served as the negative infectivity control (100% inhibition), while cells infected with virus in the absence of drug served as the positive infectivity control (0% inhibition). After 48 h, cells were lysed and luciferase expression was determined in relative light units (RLUs) using a luminometer. The percent inhibition was calculated for all test and control cultures to determine the 50% inhibition concentration (IC_{50}) value of each drug. The IC_{50} values of NP-ARVs were calculated using drug concentrations that corresponded to the actual drug loading determined by HPLC.

2.3.9 Ex vivo *toxicity assay*

Ectocervical tissues from two macaques (Tissue Banking and Distribution Program, the Washington National Primate Research Center) were processed for polarized explant cultures as previously described[34–36]. The explant cultures were set up on the day of surgery. Briefly, the

macaque ectocervical explant cultures were established in duplicate by inserting a circular tissue punch through a hole in a transwell with the luminal epithelium side up. The edges around the explant were sealed with Matrigel™ (BD Biosciences, San Jose, CA). A 0.1 mg/mL suspension of either NP-EFV or NP-SQV in 200 μL of culture media (DMEM with 10% fetal bovine serum, 1% 100X penicillin/streptomycin, and 1% 200 mM L-glutamine) was added on the apical side of the tissue. Untreated explants (culture media) and explants treated with 0.4% nonoxynol-9 (N-9) gel served as controls. All explant cultures were maintained at 37°C in a 5% CO_2 atmosphere. After 18-24 h, the explants were washed and one of each duplicate was incubated in RPMI containing 250 μg/mL MTT [1-(4,5-dimethylthiazol- 2-yl)-3,5-diphenylformazan] for 4 h. The explants were removed and placed in 1 mL of methanol overnight to extract the formazan dye produced by live tissue. The next day, the explants were removed from methanol and placed on a paper towel to dry and be weighed. The color extracted in methanol was read for optical density at 595 nm. Percent viability of the treated explants was determined by correcting the optical density (OD) with the weight of the corresponding explant. The other explant was frozen in an embedding medium (Tissue-Tek, Sakura Finetek USA Inc., CA) and processed for histology by cryosectioning and hematoxylin-eosin staining by Comparative Pathology Program/Histology and Imaging Core Research Laboratory, University of Washington School of Medicine at South Lake Union, Seattle, WA.

2.3.10 Statistical and mathematical analyses

The IC_{50} values were calculated using a four-parameter sigmoid regression and bootstrapping (MATLAB R2010b software, MathWorks, Natick, Massachusetts) as previously described [37]. Briefly, confidence intervals were determined using a sampling procedure that created data sets by random sampling with replacement for curve fits 1000 times. The IC_{50} values for each drug alone and in combination are presented as median IC_{50}, 95% confidence interval (C.I.) based on percentiles from a histogram of IC_{50} values, and the coefficient of variation (Cv).

2.4 RESULTS

2.4.1 ARVs are effectively formulated into polymeric nanoparticles

We demonstrate that ARV compounds with low aqueous solubility can be formulated into PLGA nanoparticles with reproducible size, shape, and high drug loading content. We chose EFV and SQV as model drugs with low aqueous solubility (<0.1 mg/mL) that may be

challenging to combine with TFV, especially for topical microbicide applications. The calculated value of the partition coefficient (logP) and aqueous solubility are useful parameters to determine the physicochemical properties of the ARVs[38]. The logP values of EFV and SQV are 3.8 – 4.5, and their aqueous solubility at 25°C are 8.55 μg/mL and 2.47 μg/mL, respectively[39]. Despite the similar logP and aqueous solubility, EFV and SQV required different methods for encapsulation into PLGA nanoparticles. For NP-EFV, a single emulsion-solvent evaporation technique was employed wherein the EFV and polymer were combined in DCM and aqueous PVA was used as a surfactant. NP-SQV formulated by the same technique resulted in low loading (<1% w/w) (data not shown). Therefore, NP-SQV were fabricated by a nanoprecipitation method in which two miscible solvents are employed to induce the precipitation of the drug and polymer mixture. Nanoprecipitation allows for instantaneous particle formation due to the miscibility of the polymer solvent and non-solvent, compared to the slower particle hardening process that occurs with the single emulsion process[22,24]. We also modified the formulation process by using acetone and adjusting the solvent/non-solvent ratio to prevent partition of SQV to the aqueous phase.

Table 2-1. Physicochemical properties of nanoparticles loaded with anti-HIV agents.

Drug[a]	Theoretical Drug Loading (% w/w)	Size[b] (d.nm. ± SD)	PDI[b]	Zeta Potential[b] (mV ± SD)	Actual Drug Loading (% w/w, ± SD)	Encapsulation Efficiency (%, ± SD)
EFV	15	227 ± 1.8	0.05	-24.4 + 7.3	6.7 ± 0.4	44.5 ± 2.7
SQV	15	189 ± 96.3[c]	0.486	-24.2 ± 1.5	7.2 ± 2.2	48.3 ± 15.2

[a]Efavirenz (EFV) and Saquinavir (SQV) nanoparticles were synthesized using single emulsion and nanoprecipitation techniques, respectively.
[b]The particle size, polydispersity indices (PDI) and zeta potential were determined using dynamic light scattering (DLS); data are the average of three batches.
[c]Particles showed two peak sizes. This number represents the average peak intensity size for three batches of SQV nanoparticles. Two of the three batches displayed bimodal size distribution with one peak ~100-200 nm and another peak at ~600-2500 nm. Since the large peaks are likely indicative of aggregated clumps of particles and not individual particles, these large peaks were not included in the average size shown here but still affect the PDI value.

Table 2-1 lists properties of NP-EFV and NP-SQV fabricated with emulsion and nanoprecipitation techniques, respectively. Both NP-EFV and NP-SQV showed a large negative zeta-potential of approximately -25 mV, a value predictive of high colloidal stability due to large repulsive charges[40]. NP-EFV had a particle size of approximately 200 nm with low polydispersity (<0.08). However, in some cases, NP-SQV showed two distinctly sized populations, indicating bimodal distribution. One population had a mean diameter of ~100 - 200 nm, and we detected a second population with a mean diameter of ~600 - 2500 nm. We used scanning electron microscopy (SEM) to confirm the size and morphology of nanoparticles. SEM micrographs

revealed that both NP-EFV and NP-SQV were spherical with an average particle diameter of ~200 nm (Figure 2-1). Owing to the SEM results, we expect the bimodal distribution observed with DLS can be attributed to a population of nanoparticle aggregates in aqueous suspension. Our findings are similar to those describing manufacturing of PLGA nanoparticles via emulsion and nanoprecipitation techniques[23,24,32,41,42]. Our results suggest that these two techniques are suitable for encapsulating hydrophobic drugs.

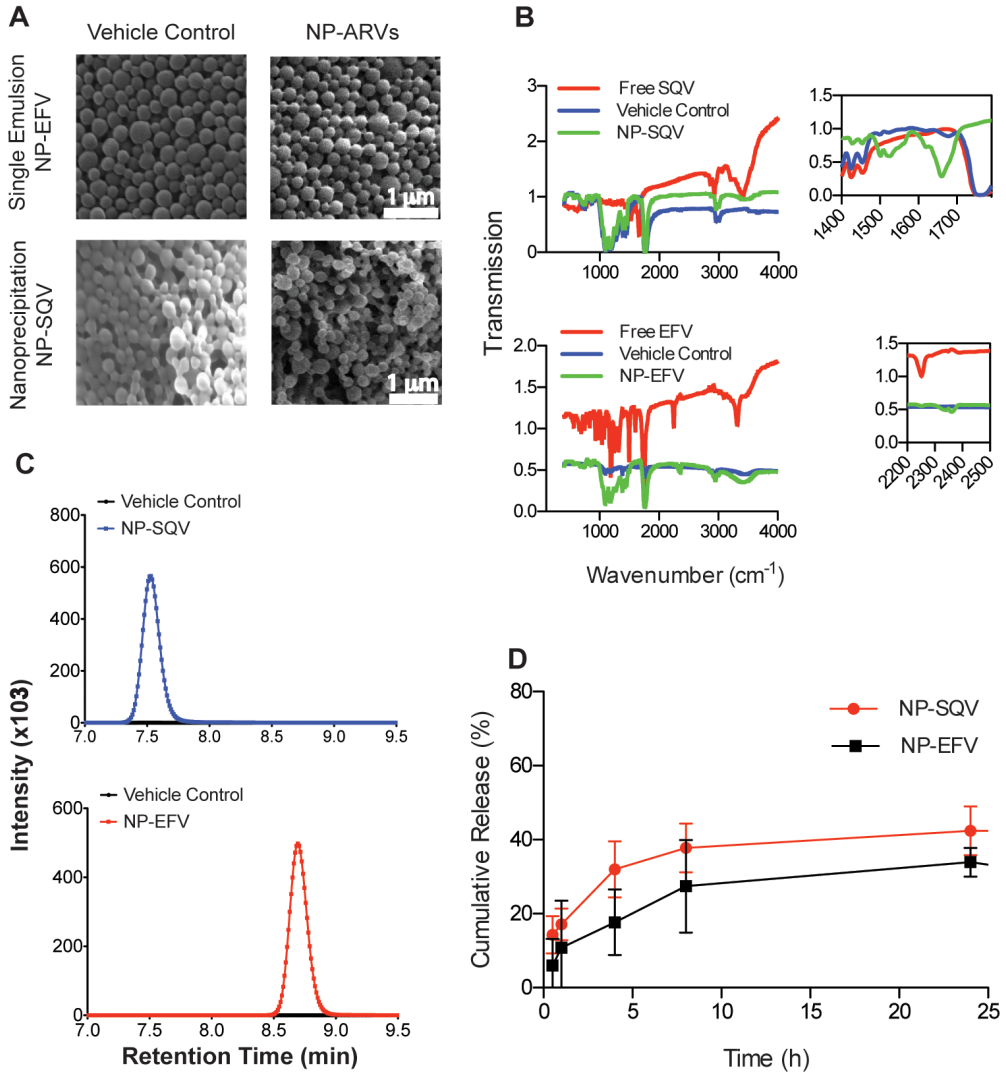

Figure 2-1. Properties of PLGA nanoparticles loaded with efavirenz or saquinavir. (A) Scanning electron photomicrographs (magnification, 15,000×) of nanoparticles encapsulated with antiretroviral drugs efavirenz (NP-EFV) or saquinavir (NP-SQV). (B) Fourier transform infrared spectroscopy (FTIR) confirmation of the antiretroviral drugs loaded into PLGA nanoparticles. Insets show characteristic frequencies of SQV and EFV and the PLGA polymer (Vehicle Control). (C) HPLC chromatograms of vehicle control (black), SQV (blue) and EFV (red) nanoparticles showing the detection of SQV and EFV only in ARV loaded nanoparticles. No drug peak was detected in the vehicle control nanoparticles. (D) Cumulative release of EFV and SQV from nanoparticles in a vaginal fluid simulant (VFS) showing the release of SQV and EFV over 24h.

FTIR spectroscopy and UV-HPLC was used to confirm drug loading into polymer nanoparticles. FTIR absorption spectra for NP-ARVs detected characteristic bond vibrational frequencies for both the drug compound and the PLGA polymer. Infrared absorbance spectra of NP-SQV demonstrated characteristic frequencies of the phenyl (1500 cm^{-1}) and amide carbonyl (1695 cm^{-1}) present in the drug, as well as the ester stretching frequency (1750 cm^{-1}) indicative of the polymer (Figure 2-1). FTIR spectra of NP-EFV showed absorption bands at 2300 cm^{-1} from the alkyne and at 600 - 800 cm^{-1} from the C-Cl alkyl halide stretching, in addition to the ester band from the PLGA polymer. These FTIR results strongly indicate drug loading within the polymer nanoparticles.

To quantify actual drug loading and encapsulation efficiency, we employed established methods for detection and separation of EFV and SQV from excipients of the nanoparticle formulation process using UV-HPLC. We demonstrate that nanoparticles prepared with a theoretical drug loading of 15% (weight of ARV to weight of polymer, w/w) achieved average actual drug loading of approximately 7% (w/w) and encapsulation efficiency of approximately 50% (Table 2-1). We validated our method for dissolution of the polymer matrix to release the drug for detection using vehicle control nanoparticles (no drug) spiked with known quantities of drug. These validation experiments indicated a high recovery (97-99%) and demonstrated the accuracy of our methods to quantify drug loading. As shown in Figure 2-1, SQV and EFV were detected only in ARV loaded nanoparticles, whereas no compounds of similar retention time were detected in the vehicle control nanoparticles. NP-EFV had a comparatively high drug loading of 6.7 ± 0.4% (w/w) sufficient for use in our *in vitro* efficacy studies[43–45]. Using the nanoprecipitation technique, we obtained NP-SQV that had 24 times higher drug loading and encapsulation efficiency of ~50% compared to NP-SQV formulated using a single emulsion technique.

To determine if we could achieve higher encapsulation efficiencies, we also prepared nanoparticles with a lower initial drug loading of 5 – 7.5% (w/w). For NP-EFV, we observed that decreasing the theoretical drug loading decreased the actual loading of EFV, but had no effect on the encapsulation efficiency. NP-EFV with 15% (w/w) theoretical drug loading improved the actual drug loading by 2-fold compared to preparing particles with 5% (w/w) theoretical drug loading (actual drug loading = 3.0 $\pm$ 0.45 % w/w). In contrast to NP-EFV, we observed that reducing the initial amount of SQV used in the nanoprecipitation process doubled the encapsulation efficiency without reducing the drug loading. The actual drug loading of NP-SQV was independent of the initial loading in the range tested. NP-SQV with a

theoretical drug loading of 7.5% (w/w) or 15% (w/w) had similar actual drug loading of 6-7% (w/w).

2.4.2 Nanoparticles modulate ARV release

We investigated the drug release profile of NP-ARVs using a vaginal fluid simulant (VFS) that mimics the composition and viscoelastic properties of cervico-vaginal secretions produced by healthy, non-pregnant, premenopausal women[26]. UV-HPLC was used to measure drug release from nanoparticles into VFS over 144h. The *in vitro* release of both EFV and SQV from nanoparticles followed a biphasic release profile, where an initial burst release of 10-20% of drug was observed within 1h followed by sustained drug release over 24h. During the first 24h, we observed a total cumulative release of 33.9 $\pm$ 3.9% and 42.4 $\pm$ 6.6% for EFV and SQV, respectively (Figure 2-1). Although we measured drug release out to 144h, we did not detect a significant accumulation of drug release after 24h. The percent cumulative release at 24h corresponds to a mass ratio of 0.022 mg EFV/mg PLGA and 0.025 mg SQV/mg PLGA released at 24h. Based on drug loading and release results, as well as the reported IC_{50} values for free ARVs, we estimated that delivering approximately 10^{-3} mg/mL of NP-SQV or 10^{-6} mg/mL of NP-EFV would be sufficient to observe *in vitro* protection using the TZM-bl assay.

2.4.3 NP-ARVs are nontoxic to in vitro *cell line and* ex vivo *ectocervical explants*

PLGA nanoparticles loaded with EFV or SQV were neither cytotoxic to cells nor tissue explants over the range of concentrations evaluated. We evaluated cytotoxicity of our NP-ARVs in TZM-bl cell culture before testing their bioactivities to exclude effects of nanoparticles on the viability of TZM-bl cells. Cytotoxicity of our NP-ARVs was measured over a range of polymer concentrations from 1 to 10,000 μg/mL after 48 h of exposure. Compared with the negative control (media only), vehicle control nanoparticles at concentrations $\leq$ 5 mg polymer/mL showed no reduction of viability (100% $\pm$ 8%), suggesting that PLGA nanoparticles alone are not cytotoxic below these concentrations. We observed >80% viability of TZM-bl cells for NP-EFV and NP-SQV tested at $\leq$1,000 μg of polymer/mL ($\leq$48 μM EFV and $\leq$26 μM SQV) (Figure 2-2). Both NP-EFV and NP-SQV showed cytotoxicity at concentrations >5 mg polymer/mL (>240 μM EFV and >130 μM SQV). Since anti-HIV bioactivity was measured at doses well below polymer concentrations that were cytotoxic, we did not expect toxicity to confound the outcome of the antiviral activity assays.

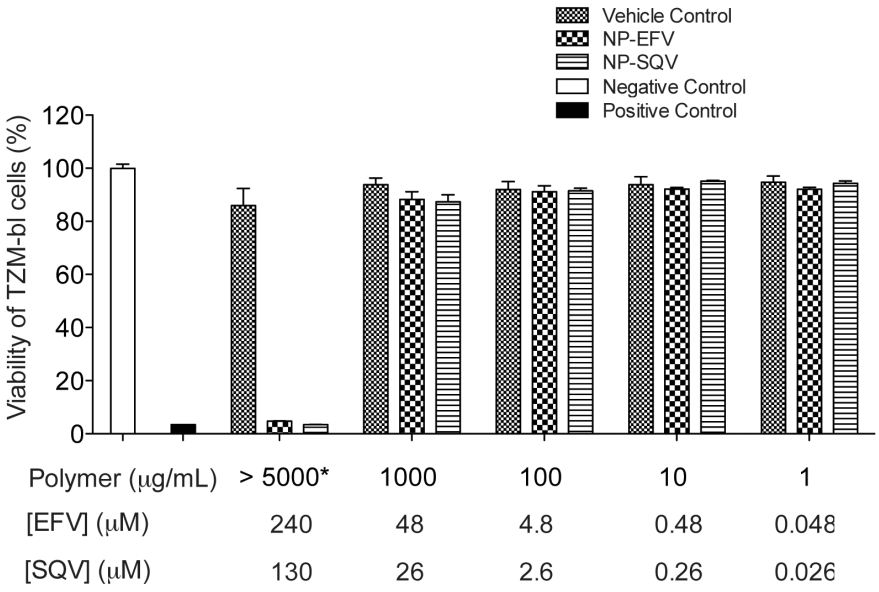

Figure 2-2. PLGA nanoparticles loaded with EFV or SQV show low cytotoxicity. Viability of TZM-bl cells measured by the CellTiter-Blue™ (Promega) viability assay demonstrating non-toxic concentrations (>80% viability) of efavirenz nanoparticles (NP-EFV) and saquinavir nanoparticles (NP-SQV) at ≤1,000 μg of polymer/mL (≤48 μM EFV and ≤26 μM SQV). Vehicle control nanoparticles at the concentrations tested showed no reduction of viability (100% ± 8%), indicating non-cytotoxicity of PLGA polymer. Negative control = media only, Positive control = DMSO. *Vehicle control for NP-SQV was measured at 10,000 μg of polymer/mL.

To confirm the results obtained with *in vitro* cytotoxicity in TZM-bl cells, we evaluated the safety of our NP-ARVs using polarized explant cultures. We chose to test nanoparticles (NP-ARVs or vehicle control) at a 0.1 mg/mL dose. This dose was shown to be nontoxic to TZM-bl cells and is several-fold higher than doses required for efficacy *in vitro*. We used two explant tissues per treatment – one for the MTT assay and the other for histology. For controls, explants were treated with either 0.4% nonoxynol-9 (N-9) or media (untreated). We evaluated explants for viability and tissue morphology at 18-24 h after application. The N-9-treated explants showed significant reduction in tissue viability, as measured by the MTT assay (n = 1), and destruction of the epithelial layer was observed by histology (n = 1) (Figure 2-3). The toxicity of N-9 found in our study was consistent with previous studies performed using human explant tissues[34,35]. Viability of explants determined by the MTT assay showed that neither NP-EFV (n = 1) nor NP-SQV (n = 1) altered tissue viability compared to the media control (untreated explants, n = 3). Histological analysis of the ectocervical explants after 24 h of exposure to NP-ARV produced no visual changes to the integrity of epithelial layer. The results with ectocervical tissue explants confirmed the findings obtained using the TZM-bl cytotoxicity model, suggesting that our NP-ARV are nontoxic to the cells and are a

biocompatible vehicle for drug delivery to the mucosal tissue, particularly the ectocervical tissue of the lower female reproductive tract.

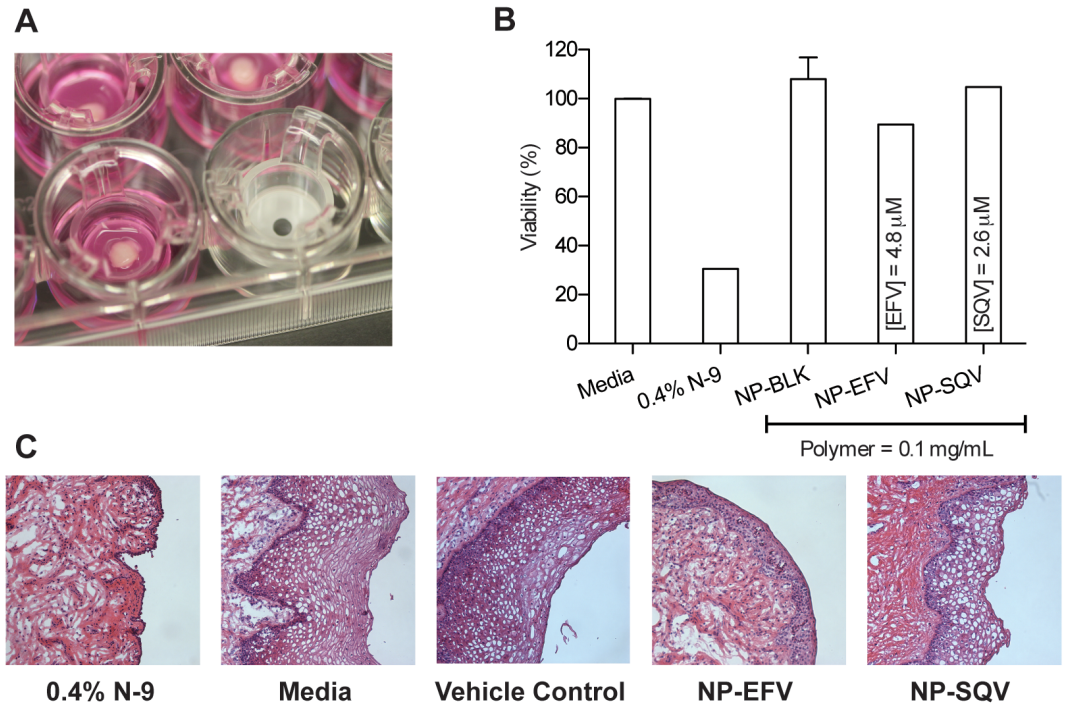

Figure 2-3. Ectocervical explants confirm the safety of NP-ARVs. Viability of explants from two macaques was assessed at 18-24h after application using an MTT assay and histology. (A) A circular tissue punch of macaque ectocervical explants was inserted through a transwell membrane and placed to assure exposure to products (luminal epithelium up). (B) Viability of explants measured by the MTT assay demonstrating viability of explant tissue exposed to nanoparticles loaded with efavirenz (NP-EFV, n = 1) or saquinavir (NP-SQV, n = 1). Tissue viability was similar to media control (untreated explants, n = 3) while the toxicity control (nonoxynol-9 (N-9) treated explant, n = 1) showed significant reduction in tissue viability. (C) Histological photographs of macaque ectocervical explants (hematoxylin and eosin stain; magnification, x100) show no visual changes following exposure to both NP-EFV and NP-SQV treated explants, and the destruction of the epithelial layer of an N-9-treated explant.

2.4.4 NP-ARVs potently inhibit HIV-1 BaL infection

To ensure ARVs loaded into nanoparticles retained reproducible bioactivity against HIV-1, we tested three batches of NP-EFV using the TZM-bl assay. As described in the methods, a mass concentration of the drug-loaded polymer was delivered to achieve the desired molar drug concentration in the assay volume irrespective of the observed drug release kinetics. We observed consistent activity between three independent batches of NP-EFV to inhibit HIV-1 BaL at nanomolar levels, with an average IC_{50} value of 0.52 $\pm$ 0.17 nM (mean $\pm$ SD, n = 3).

This value is lower than previously reported IC_{50} values of unformulated (free) EFV, indicating no loss in drug activity due to the formulation processes[46].

We further evaluated antiviral activities of NP-ARVs in comparison with their free forms. After exposure of TZM-bl cells to NP-ARVs or free ARVs, we observed potent antiviral activity against HIV-1 BaL with estimated IC_{50} values in the nanomolar and micromolar ranges for EFV and SQV, respectively (Table 2-2). Compared with free EFV, NP-EFV showed higher HIV inhibitory activity, with a 50-fold reduction in IC_{50} (Figure 2-4). NP-SQV also showed higher HIV inhibitory activity when compared with free SQV, with a nearly 2-fold reduction of the IC_{50} . We observed that blank nanoparticles (vehicle control) tested at the same ranges of polymer concentrations showed no HIV inhibition and were comparable to the negative media control (<5%). This indicates that PLGA nanoparticles alone do not provide inhibition against HIV-1 infection. Together, our results suggest that ARVs loaded into nanoparticles possess potent bioactivity that is superior to that of

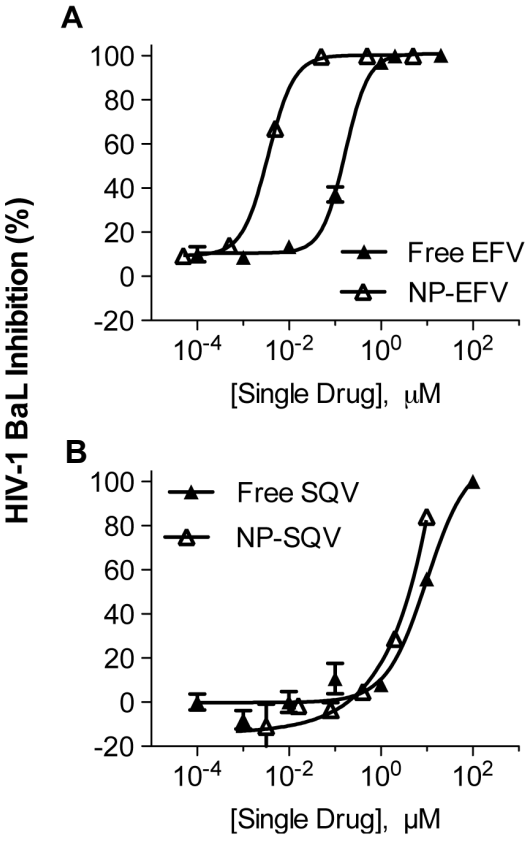

Figure 2-4. NP-ARVs show potent antiviral activity. The dose-response curves show antiviral activity of free EFV, free SQV, and EFV and SQV loaded nanoparticles (NP-EFV and NP-SQV). Data represent mean values obtained from triplicate infections in TZM-bl cells.

Table 2-2. Summary of 50% inhibitory concentrations (IC_{50}) determined by infecting TZM-bl cells with HIV-1 BaL.

Free ARV vs. NP-ARV			
Drug(s)	**IC_{50} (median)**	**95% C.I.[a]**	**C_V[a]**
Free EFV	0.164 μM	[0.001, 0.204] μM	0.320
Free SQV	9.79 μM	[9.25, 11.3] μM	0.047
NP-EFV	0.003 μM	[0.00197, 0.00481] μM	0.301
NP-SQV	6.08 μM	[5.84, 6.21] μM	0.016

[a] Data show the confidence interval (C.I.) based on the 2.5 and 97.5 percentiles of bootstrapped IC_{50} estimates, and the coefficient of variation (Cv) of the IC_{50} of each drug alone.

unformulated ARVs. Since PLGA nanoparticles are known to enhance internalization and intracellular uptake[43,47–49], we hypothesize that the enhanced potency of our NP-ARVs formulated with PLGA may be due to higher intracellular ARV drug concentration.

2.5 DISCUSSION

Combination drug approaches are an emerging paradigm for the prevention of HIV-1 infection. However, chemical incompatibilities prevent the combination of many existing drugs in a manner that could enhance potency by realizing unique combination drug activities. We hypothesized that polymeric nanocarriers could facilitate the discovery of unexplored drug-drug activities by enabling the combination of chemically incompatible agents. We demonstrate that ARVs can be encapsulated within polymeric nanoparticles to provide enhanced protection against HIV *in vitro*. Our findings reveal a relevant strategy for delivering multiple ARVs in combination to enhance drug potency, lower cytotoxicity and reduce the likelihood for developing drug resistance. We expect that the versatility of nanoparticle delivery platforms will result in broad applications for HIV chemoprophylaxis and treatment. ARV-encapsulating nanoparticles may overcome barriers in the delivery of agents with diverse physicochemical properties, particularly via administration routes with limited dosage forms for combination drug delivery such as topically to the genital and rectal mucosa.

Our NP-ARVs demonstrate enhanced antiviral activity against HIV-1 BaL compared to unformulated ARVs. Using an *in vitro* TZM-bl indicator cell model previously used to evaluate drug candidates for topical microbicides[32,33], we observed higher inhibitory activity of NP-EFV than free EFV with a 50-fold reduction in IC_{50}. Similarly, NP-SQV showed greater anti-HIV activity when compared to the free drug. SQV is the first HIV-protease inhibitor marketed for the treatment of HIV and is currently recommended in combination therapy regimen with nucleoside inhibitors of HIV reverse transcriptase[9,13]. Nevertheless, its poor absorption is a prominent pharmacologic characteristic of SQV[18,50–52]. Previous studies have shown that administration of polymeric nanoparticles significantly increases the intracellular concentration and permeability of SQV[53,54]. We expect that the improved bioactivity of our NP-SQV is due to similarly increased bioavailability provided by the nanoparticle formulation.

NP-ARVs formulated with PLGA have previously been demonstrated to facilitate drug uptake resulting in higher intracellular drug concentrations and greater inhibitory activity[43,49]. Destache et al. showed that monocyte-derived macrophage (MDM) cells incubated with ARV loaded PLGA nanoparticles exhibited higher intracellular drug concentrations than those

incubated with free ARVs. Although we did not measure intracellular uptake of particles in this study, the 50-fold reduction in IC_{50} values between NP-ARVs and free drugs suggests that the particulate nature of our delivery platform plays a major role in improving bioactivity. As Destache et al. observed, it is likely that the PLGA nanoparticles facilitate increased drug uptake and intracellular retention of our ARV drug candidates.

The *in vitro* drug release profile of our NP-ARVs showed an initial burst release within 1h followed by a small degree of sustained release of drug over 24h (Figure 2-1). We expected that this biphasic release profile would provide a sufficient amount of rapid release of ARVs to prevent HIV-1 infection soon after application and then sustain the release of drugs for prolonged protection. The *in vitro* release studies from EFV nanoparticles may have been limited by poor aqueous solubility of EFV and small release buffer volumes needed to maintain a concentration detectable by HPLC, resulting in sink conditions not being met. Future release experiments using a cosolvent such as polysorbate 80 or PEG 400 may prove useful in establishing sink conditions[55,56]. *In vitro* release profiles can be affected by the environmental conditions. As reported by Ham et al., the percent drug release from nanoparticles at pH 7.4 was lower compared to the release profiles obtained at pH 4.6[32]. While we have not yet investigated *in vitro* release profiles at different pH conditions, further *in vitro* release studies are planned to determine the impact of pH on drug release in addition to intracellular drug concentrations.

Currently, nanoparticle encapsulation as a drug delivery system is being investigated in numerous therapeutic fields[16]; however, it is still emerging within the microbicide field[15]. In this study, we provide evidence for the efficacy of a PLGA nanocarrier system to achieve HIV-1 inhibition. Our results suggest that PLGA nanoparticles are a safe delivery platform for encapsulating and delivering ARVs.

2.6 ACKNOWLEDGEMENTS

We thank F. Hladik and R. Astronomo for assistance with the cervical tissue explant models, and S.E. Holte for assistance with estimating confidence intervals by bootstrapping. The research was supported by funding to K.A.W. from NIH grant AI094412 and partial support from the University of Washington and the Creative and Novel Ideas in HIV Research award (AI027767). C.B. and E.K. are partially supported by NSF Graduate Research Fellowships. The funders had no role in study design, data collection and analysis, decision to publish, or preparation of the manuscript.

2.7 REFERENCES

1. McMichael, A. J. & Haynes, B. F. Lessons learned from HIV-1 vaccine trials: new priorities and directions. *Nat. Immunol.* **13,** 423–427 (2012).
2. Hladik, F. & Doncel, G. F. Preventing mucosal HIV transmission with topical microbicides: Challenges and opportunities. *Antiviral Res.* **88, Supplement,** S3–S9 (2010).
3. Quinn, T. C. & Overbaugh, J. HIV/AIDS in Women: An Expanding Epidemic. *Science* **308,** 1582–1583 (2005).
4. Joint United Nations Programme on HIV/AIDS. *UNAIDS World AIDS Day Report, 2011*. 1–52 (UNAIDS, 2011).
5. Fauci, A. S. *et al.* HIV Vaccine Research: The Way Forward. *Science* **321,** 530–532 (2008).
6. Karim, S. S. A., Kashuba, A. D., Werner, L. & Karim, Q. A. Drug concentrations after topical and oral antiretroviral pre-exposure prophylaxis: implications for HIV prevention in women. *The Lancet* **378,** 279–281 (2011).
7. Kim, P. S. & Read, S. W. Nanotechnology and HIV: potential applications for treatment and prevention. *Wiley Interdiscip. Rev. Nanomed. Nanobiotechnol.* **2,** 693–702 (2010).
8. Whaley, K. J., Hanes, J., Shattock, R., Cone, R. A. & Friend, D. R. Novel Approaches to Vaginal Delivery and Safety of Microbicides: Biopharmaceuticals, Nanoparticles, and Vaccines. *Antiviral Res.* **88, Supplement,** S55–S66 (2010).
9. Carpenter CJ, Cooper DA, Fischl MA & et al. Antiretroviral therapy in adults: updated recommendations of the international aids society–usa panel. *JAMA* **283,** 381–390 (2000).
10. Dou, H. *et al.* Development of a macrophage-based nanoparticle platform for antiretroviral drug delivery. *Blood* **108,** 2827–2835 (2006).
11. Nowacek, A. S. *et al.* Nanoformulated Antiretroviral Drug Combinations Extend Drug Release and Antiretroviral Responses in HIV-1-Infected Macrophages: Implications for NeuroAIDS Therapeutics. *J. Neuroimmune Pharmacol.* **5,** 592–601 (2010).
12. Nowacek, A. S. *et al.* NanoART synthesis, characterization, uptake, release and toxicology for human monocyte-macrophage drug delivery. *Nanomed.* **4,** 903–917 (2009).
13. Pirrone, V., Thakkar, N., Jacobson, J. M., Wigdahl, B. & Krebs, F. C. Combinatorial Approaches to the Prevention and Treatment of HIV-1 Infection. *Antimicrob. Agents Chemother.* **55,** 1831–1842 (2011).
14. Rohan, L. & Mallipeddi. Progress in antiretroviral drug delivery using nanotechnology. *Int. J. Nanomedicine* 533 (2010). doi:10.2147/IJN.S7681
15. das Neves, J., Amiji, M. M., Bahia, M. F. & Sarmento, B. Nanotechnology-based systems for the treatment and prevention of HIV/AIDS. *Adv. Drug Deliv. Rev.* **62,** 458–477 (2010).
16. Wong, H. L., Chattopadhyay, N., Wu, X. Y. & Bendayan, R. Nanotechnology applications for improved delivery of antiretroviral drugs to the brain. *Adv. Drug Deliv. Rev.* **62,** 503–517 (2010).
17. Nowacek, A. S. *et al.* Analyses of nanoformulated antiretroviral drug charge, size, shape and content for uptake, drug release and antiviral activities in human monocyte-derived macrophages. *J. Controlled Release* **150,** 204–211 (2011).
18. Huisman, M. T. *et al.* P-Glycoprotein Limits Oral Availability, Brain, and Fetal Penetration of Saquinavir Even with High Doses of Ritonavir. *Mol. Pharmacol.* **59,** 806–813 (2001).
19. Borroto-Esoda, K. *et al.* Baseline Genotype as a Predictor of Virological Failure to Emtricitabine or Stavudine in Combination with Didanosine and Efavirenz. *AIDS Res. Hum. Retroviruses* **23,** 988–995 (2007).
20. Bousquet, L., Pruvost, A., Guyot, A.-C., Farinotti, R. & Mabondzo, A. Combination of Tenofovir and Emtricitabine plus Efavirenz: In Vitro Modulation of ABC Transporter and Intracellular Drug Accumulation. *Antimicrob. Agents Chemother.* **53,** 896–902 (2009).
21. Lee, C. G. L. *et al.* HIV-1 Protease Inhibitors Are Substrates for the MDR1 Multidrug Transporter. *Biochemistry (Mosc.)* **37,** 3594–3601 (1998).
22. Bilati, U., Allémann, E. & Doelker, E. Development of a nanoprecipitation method intended for the entrapment of hydrophilic drugs into nanoparticles. *Eur. J. Pharm. Sci.* **24,** 67–75 (2005).
23. Bilati, U., Allémann, E. & Doelker, E. Sonication Parameters for the Preparation of Biodegradable Nanocapsulesof Controlled Size by the Double Emulsion Method: RESEARCH ARTICLE. *Pharm. Dev. Technol.* **8,** 1–9 (2003).

24. Galindo-Rodriguez, S., Allémann, E., Fessi, H. & Doelker, E. Physicochemical Parameters Associated with Nanoparticle Formation in the Salting-Out, Emulsification-Diffusion, and Nanoprecipitation Methods. *Pharm. Res.* **21,** 1428–1439 (2004).
25. Mudigonda, K. *et al.* HPLC quantification of the HIV-1 protease inhibitor saquinavir in brain and testis of mice. *Biomed. Chromatogr.* **20,** 1028–1032 (2006).
26. Owen, D. & Katz, D. A vaginal fluid simulant. *Contraception* **59,** 91–91–5 (1999).
27. Takeuchi, Y., McClure, M. O. & Pizzato, M. Identification of Gammaretroviruses Constitutively Released from Cell Lines Used for Human Immunodeficiency Virus Research. *J. Virol.* **82,** 12585–12588 (2008).
28. Derdeyn, C. A. *et al.* Sensitivity of human immunodeficiency virus type 1 to the fusion inhibitor T-20 is modulated by coreceptor specificity defined by the V3 loop of gp120. *J. Virol.* **74,** 8358–8367 (2000).
29. Platt, E. J., Wehrly, K., Kuhmann, S. E., Chesebro, B. & Kabat, D. Effects of CCR5 and CD4 Cell Surface Concentrations on Infections by Macrophagetropic Isolates of Human Immunodeficiency Virus Type 1. *J. Virol.* **72,** 2855–2864 (1998).
30. Wei, X. *et al.* Emergence of Resistant Human Immunodeficiency Virus Type 1 in Patients Receiving Fusion Inhibitor (T-20) Monotherapy. *Antimicrob. Agents Chemother.* **46,** 1896–1905 (2002).
31. Lusso, P. *et al.* Growth of macrophage-tropic and primary human immunodeficiency virus type 1 (HIV-1) isolates in a unique CD4+ T-cell clone (PM1): failure to downregulate CD4 and to interfere with cell-line-tropic HIV-1. *J. Virol.* **69,** 3712–3720 (1995).
32. Ham, A., Cost, M., Sassi, A., Dezzutti, C. & Rohan, L. Targeted Delivery of PSC-RANTES for HIV-1 Prevention using Biodegradable Nanoparticles. *Pharm. Res.* **26,** 502–511 (2009).
33. Herrera, C., Cranage, M., McGowan, I., Anton, P. & Shattock, R. J. Reverse Transcriptase Inhibitors as Potential Colorectal Microbicides. *Antimicrob. Agents Chemother.* **53,** 1797–1807 (2009).
34. Cummins, J. E. *et al.* Preclinical Testing of Candidate Topical Microbicides for Anti-Human Immunodeficiency Virus Type 1 Activity and Tissue Toxicity in a Human Cervical Explant Culture. *Antimicrob. Agents Chemother.* **51,** 1770–1779 (2007).
35. Rohan, L. C. *et al.* In Vitro and Ex Vivo Testing of Tenofovir Shows It Is Effective As an HIV-1 Microbicide. *PLoS ONE* **5,** e9310 (2010).
36. Abner, S. R. *et al.* A Human Colorectal Explant Culture to Evaluate Topical Microbicides for the Prevention of HIV Infection. *J. Infect. Dis.* **192,** 1545–1556 (2005).
37. Best, B. M. *et al.* Efavirenz concentrations in CSF exceed IC50 for wild-type HIV. *J. Antimicrob. Chemother.* **66,** 354–357 (2011).
38. Leo, A., Hansch, C. & Elkins, D. Partition coefficients and their uses. *Chem. Rev.* **71,** 525–616 (1971).
39. Lindenberg, M., Kopp, S. & Dressman, J. B. Classification of orally administered drugs on the World Health Organization Model list of Essential Medicines according to the biopharmaceutics classification system. *Eur. J. Pharm. Biopharm.* **58,** 265–278 (2004).
40. American Society for Testing and Materials. *Zeta Potential of Colloids in Water and Waste Water*. 4187–4182 (1985).
41. Woodrow, K. A. *et al.* Intravaginal gene silencing using biodegradable polymer nanoparticles densely loaded with small-interfering RNA. *Nat. Mater.* **8,** 526–533 (2009).
42. Jain, R. A. The manufacturing techniques of various drug loaded biodegradable poly(lactide-co-glycolide) (PLGA) devices. *Biomaterials* **21,** 2475–2490 (2000).
43. Destache, C. J. *et al.* Combination antiretroviral drugs in PLGA nanoparticle for HIV-1. *BMC Infect. Dis.* **9,** 198 (2009).
44. Mert, O. *et al.* A poly(ethylene glycol)-based surfactant for formulation of drug-loaded mucus penetrating particles. *J. Controlled Release* **157,** 455–460 (2012).
45. Lai, S. K. *et al.* Drug carrier nanoparticles that penetrate human chronic rhinosinusitis mucus. *Biomaterials* **32,** 6285–6290 (2011).
46. Feng, J. Y. *et al.* The triple combination of tenofovir, emtricitabine and efavirenz shows synergistic anti-HIV-1 activity in vitro: a mechanism of action study. *Retrovirology* **6,** 44 (2009).
47. Panyam, J. & Labhasetwar, V. Dynamics of Endocytosis and Exocytosis of Poly(D,L-Lactide-co-Glycolide) Nanoparticles in Vascular Smooth Muscle Cells. *Pharm. Res.* **20,** 212–220 (2003).
48. Panyam, J., Zhou, W.-Z., Prabha, S., Sahoo, S. K. & Labhasetwar, V. Rapid endo-lysosomal escape of poly(dl-lactide-co-glycolide) nanoparticles: implications for drug and gene delivery. *FASEB J.* **16,** 1217–1226 (2002).

49. Destache, C. J., Belgum, T., Goede, M., Shibata, A. & Belshan, M. A. Antiretroviral release from poly(dl-lactide-co-glycolide) nanoparticles in mice. *J. Antimicrob. Chemother.* **65,** 2183–2187 (2010).
50. Remmel, R. P., Kawle, S. P., Weller, D. & Fletcher, C. V. Simultaneous HPLC Assay for Quantification of Indinavir, Nelfinavir, Ritonavir, and Saquinavir in Human Plasma. *Clin. Chem.* **46,** 73–81 (2000).
51. Noble, S. & Faulds, D. Saquinavir. *Drugs* **52,** 93–112 (1996).
52. Flexner, C. Dual Protease Inhibitor Therapy in HIV-Infected Patients: Pharmacologic Rationale and Clinical Benefits. *Annu. Rev. Pharmacol. Toxicol.* **40,** 649–674 (2000).
53. Kuo, Y.-C. & Yu, H.-W. Expression of ornithine decarboxylase during the transport of saquinavir across the blood–brain barrier using composite polymeric nanocarriers under an electromagnetic field. *Colloids Surf. B Biointerfaces* **88,** 627–634 (2011).
54. Shah, L. K. & Amiji, M. M. Intracellular Delivery of Saquinavir in Biodegradable Polymeric Nanoparticles for HIV/AIDS. *Pharm. Res.* **23,** 2638–2645 (2006).
55. Chen, X.-Q. & Venkatesh, S. Miniature device for aqueous and non-aqueous solubility measurements during drug discovery. *Pharm. Res.* **21,** 1758–1761 (2004).
56. das Neves, J. *et al.* Polymeric Nanoparticles Affect the Intracellular Delivery, Antiretroviral Activity and Cytotoxicity of the Microbicide Drug Candidate Dapivirine. *Pharm. Res.* **29,** 1468–1484 (2012).

3 Drug-eluting fibers for HIV-1 inhibition and contraception.

Published as: Ball, C.*, Krogstad, E.*, Chaowanachan, T. & Woodrow, K. A. Drug-Eluting Fibers for HIV-1 Inhibition and Contraception. *PLoS ONE* **7,** e49792 (2012)

**Equally contributed to this work*

3.1 ABSTRACT

Multipurpose prevention technologies (MPTs) that simultaneously prevent sexually transmitted infections (STIs) and unintended pregnancy are a global health priority. Combining chemical and physical barriers offers the greatest potential to design effective MPTs, but integrating both functional modalities into a single device has been challenging. Here we show that drug-eluting fiber meshes designed for topical drug delivery can function as a combination chemical and physical barrier MPT. Using FDA-approved polymers, we fabricated nanofiber meshes with tunable fiber size and controlled degradation kinetics that facilitate simultaneous release of multiple agents against HIV-1, HSV-2, and sperm. We observed that drug-loaded meshes inhibited HIV-1 infection *in vitro* and physically obstructed sperm penetration. Furthermore, we report on a previously unknown activity of glycerol monolaurate (GML) to potently inhibit sperm motility and viability. The application of drug-eluting nanofibers for HIV-1 prevention and sperm inhibition may serve as an innovative platform technology for drug delivery to the lower female reproductive tract.

3.2 INTRODUCTION

HIV-1 infections and unintended pregnancies are inextricably linked by unprotected sex and represent a major health burden for women worldwide [1]. Access to MPTs combining safe, effective, and easily reversible options for contraception are essential for women who are also at risk for STIs including HIV-1. To date, no single product exists that women can use discreetly for simultaneous and effective prevention of STIs and pregnancy [2]. Women would also benefit from more options for chemical contraceptives that are nonhormonal [3,4]. In particular, an alternative to nonoxynol-9 (N-9) that is safe and non-toxic, does not alter the vaginal microflora, and does not enhance the risk for HIV-1 infection would have a major impact on women's sexual and reproductive health [5].

The materials chemistry and process of fabricating MPTs have a significant influence on their design and function. Existing MPTs are classified by their function as physical, chemical, or combined physical/chemical barriers to prevent STIs and unintended pregnancy [6,7]. Chemical barrier methods are the front-line approach being evaluated in clinical trials for multipurpose

protection, and include dosage forms such as gels, films, tablets, and intravaginal rings (IVRs) [8,9]. Gels containing tenofovir [10], UC781, dapivirine [11], and MIV-150 [12] are among the many anti-HIV-1 microbicides under development. Vaginal films have long existed for the prevention of pregnancy (Vaginal Contraceptive Film® by Apothecus) as well as the treatment of fungal and bacterial infections [9]. Recently, researchers have begun to formulate vaginal films and tablets that can provide quick release of antiviral compounds as an alternative dosage form to microbicide gels. For example, Akil et al. developed thin vaginal films that release 0.6 mg of dapivirine within 10 minutes following hydration [13]. IVRs, which are designed to provide sustained release of a combination of agents over several weeks or months, are the leading technologies being evaluated currently for multipurpose prevention [14,15]. However, the paucity of materials and the fabrication process for IVRs imposes constraints on their physical design (size, geometry, mechanical properties) and the pharmaceutical agents that are suitable for delivery [8]. Greater flexibility in the choice of polymers as well as the fabrication process could lead to innovative new dosage forms for a larger number of pharmaceutical agents.

Emerging technologies that integrate physical and chemical barriers provide the greatest potential for new MPT designs. To be effective, these technologies must address five fundamental design requirements: 1) deliver multiple drugs with differing physicochemical or pharmacokinetic properties from a single device, 2) provide extensive coverage of mucosal tissue, 3) be female-controlled and discreet, 4) deliver contraception that is fully reversible, and 5) be inexpensive so as to reach the most relevant populations. Based on these requirements, we have developed an innovative dosage form for vaginal drug delivery using drug-eluting nanofibers. Electrospinning is an elegant method to deliver combination drug therapies because polymers can be selected based on their drug compatibility as well as their degradation or dissolution rates [16]. In addition, controlling processing parameters (applied voltage, polymer flow rate, capillary-collector distance), nozzle configuration (single, multijet, coaxial), and choice of materials (non-degradable, biodegradable, water-soluble) allows greater versatility and flexibility to design topical prevention strategies [17].

To demonstrate the versatility of drug-eluting fibers for topical delivery to the vaginal mucosa in applications for multipurpose prevention, we generated nanofiber meshes that elute small molecule agents that target HIV-1, HSV-2, and sperm function. We demonstrated that these drug-eluting fibers deliver antiviral drugs with diverse physicochemical properties and mechanisms of action. Fibers loaded with antiretroviral drugs showed potent inhibition of HIV-1 infection *in vitro*. To address the need for contraception in a multipurpose prevention strategy, we screened multiple non-hormonal chemical contraceptive alternatives to N-9 and discovered

an unreported function of glycerol monolaurate (GML) to inhibit sperm motility and viability in a dose-dependent manner. We also showed that fiber meshes acted as a physical barrier to sperm penetration despite their porosity. The fiber meshes were readily electrospun in a geometry designed to provide physical coverage of both the vaginal epithelium and cervix. The functional combination offered by our drug-eluting nanofibers cannot be accomplished with any single technology currently in the development pipeline.

3.3 MATERIALS AND METHODS

3.3.1 Ethics statement

All animals were obtained and cared for in accordance with the University of Washington Institutional Animal Care and Use Committee (IACUC) guidelines, and animal studies were approved by the University of Washington IACUC. Human semen samples were obtained according to guidelines approved by the Institutional Review Board of the Human Subjects Division at the University of Washington. All subjects provided written, informed consent prior to participation, and the study protocol was approved by the University of Washington Institutional Review Board.

3.3.2 Polymer preparation

Polymers used for electrospinning included poly(L-lactide) with an inherent viscosity of 0.90–1.20 dL g^{-1} (MW ~117 kDa) (Lactel Absorbable Polymers), poly(ethylene oxide) with MW 100 kDa (Sigma-Aldrich), polycaprolactone of M_n 70-90 kDa (Sigma-Aldrich), and acid terminated poly(D,L-lactide) of M_w 18-24 kDa (Sigma Aldrich). Maraviroc was obtained from the NIH AIDS Research & Reference Reagent Program, Division of AIDS, NIAID, NIH. 3'-Azido-3'-deoxythymidine, methyl-β-cyclodextrin (M_n=1310), acyclovir, iron(II) D-gluconate, and L-ascorbic acid were purchased from Sigma-Aldrich. Glycerol monolaurate was purchased from MP Biomedicals, LLC. VFS was made according to methods described by Owen and Katz, *et al* [56]. Potassium hydroxide, calcium hydroxide, lactic acid, acetic acid, and glycerol were purchased from Fisher Scientific. Bovine serum albumin, urea, and glucose were obtained from Sigma-Aldrich. Sodium chloride was purchased from Mallinckrodt Chemicals. The pH for VFS was adjusted to 4.2 with HCl and filter sterilized.

3.3.3 Electrospinning

PLLA and PEO were dissolved at 5%, 10%, 15% (wt/vol) in mixtures of 1:1 or 3:1 (vol/vol) chloroform (EMD Chemicals) and 2,2,2-trifluoroethanol (Sigma-Aldrich). PCL was dissolved at 10% and 15% (wt/vol) in 2,2,2-trifluoroethanol. PDLLA and PLLA were dissolved at 15% (wt/vol)

in 1:1 chloroform and 2,2,2-trifluoroethanol. Drugs were mixed with polymers at 1 or 10% (wt/wt) prior to addition to solvent. Polymer solutions were loaded into glass gastight syringes (National Scientific) and set into a precision syringe pump (KD Scientific Inc.). Unless otherwise specified, fibers were produced with the following parameters. We dispensed 500 µL at a flow rate of 5 µL min^{-1} through a gauge 22 stainless steel dispensing needle (Integrated Dispensing Solutions, Inc.) that was clamped to +15 kV using a high voltage generator (Gamma High Voltage Research). The aluminum mandrel collector was machined at the University of Washington to have a diameter of 1.27 cm. The collector was placed 12 cm horizontally from the tip of the needle and set to 3,000 r.p.m. (linear rotational speed of 200 cm s^{-1} at the surface of the collector) with a 5.08 cm horizontal travel at a speed of 2.54 cm s^{-1}. A copper or graphite brush electrically grounded the mandrel. 3.4 µm 70:30 PLLA/PEO fibers were produced as above except polymers were dissolved at 25% (wt/vol) and spun at 100 µL min^{-1} at 1,200 rpm. 1.5 µm 70:30 PLLA/PEO fibers were produced as 3.4 µm fibers except a 20% (wt/vol) solution of polymer was used. PDLLA/PLLA fibers were produced as above except for the flow rate and mandrel speed, which were 100 µL min^{-1} and 1,200 rpm, respectively. PCL fibers were produced by dispensing 500 µL at a flow rate of 100 µL min^{-1} from a 25 G needle clamped to +12 kV voltage and set 8 cm from the collector, which was rotating at 1,200 rpm. Electrospun meshes were removed from the collector and lyophilized for at least 24 h before imaging or use in biological assays.

3.3.4 Material characterization

Polymer recovery was determined by dividing the mass of polymer removed from the mandrel by the theoretical mass of polymer and drug present in 500 µL of polymer solution. Meshes were sputtered with gold/palladium for 70 s and imaged with SEM (Sirion or JSM-7000F, JEOL Ltd.) at 500x and 5,000x magnification. Two scanning electron microscopes were used to complete imaging: a Sirion SEM at the University of Washington Nanotechnology Facility (funded by National Science Foundation), and a JSM-7000F SEM (JEOL Ltd.) at the Materials Science and Engineering Department at the University of Washington. Fiber size was determined in ImageJ (NIH) by measuring fibers that intersected a diagonal line drawn across each 5,000x micrograph to eliminate bias. At least 100 fibers from at least three separate micrographs were measured for each sample. Degradation in VFS was analyzed by placing 5 mg samples of mesh in 6 mL of VFS at 37°C for up to 15 days. Samples were removed at times up to 15 days, immersed gently in distilled water, inverted three times to remove salts, and lyophilized. The fibers were massed again, and percent mass loss was calculated as (original

mass – current mass) / (original mass) x 100%. Fiber mesh thickness was measured using calipers. Dog bone shaped samples were cut from collected meshes with a D1708-96-MET die (ODC Tooling and Molds) such that the long axis of the dog bone corresponded to the circumferential direction of the mandrel collector. Uniaxial tensile testing was performed with an Instron model 5543 instrument and model 2712-03 grippers (Instron). Samples were stretched at a rate of 10 mm/min until failure. Young's modulus was estimated by fitting stress-strain curves with a line for 0-15% of maximum stress.

3.3.5 Drug release and loading

Triplicate samples of mesh approximately 10 mg each containing AZT or MVC were placed into 6 mL glass vials, immersed in 6 mL of VFS, and incubated at 37°C on an orbital shaker at 200 r.p.m. At set time points (1h, 4h, 8h, 12h, 24h, 48h), 500 μL of buffer was removed and replaced with fresh VFS. A Shimadzu Prominence LC20AD UV-HPLC system equipped with a Phenomenex Luna C18 column (5 μm, 250x4.6 mm) and LCSolutions software were used to quantify drug levels in samples. Methods for MVC were based on those as described [57]. The mobile phase consisted of HPLC grade 0.01 M KH_2PO_4 buffer and acetonitrile (60:40, vol/vol) (EMD Chemicals) at isocratic flow rate of 1.0 mL min^{-1} for 10 min. Column oven temperature was 25ºC. Standards were made in VFS, with linearity established from 0.001 to 0.02 mg mL^{-1} with 20 μL injection volume. MVC was detected at 193 nm with a retention time of 3.1 to 4.1 min. AZT was detected using an isocratic mobile phase was composed of HPLC grade water with 0.045% trifluoroacetic acid and acetonitrile with 0.036% trifluoroacetic acid (72:28) at a flow rate of 1.0 mL min^{-1} for 15 min, with column oven temperature of 30ºC. AZT was detected at 265 nm at retention time of 4.4 min. Standards were prepared in water, with a linear range from 0.001 to 0.5 mg mL^{-1} with 10 μL injection volume. GML release from fiber meshes was detected using thin-layer chromatography (TLC). 10 mg pieces of either 30:70 PLLA/PEO or 70:30 PLLA/PEO with 10% (wt/wt) GML were added in triplicate to 6 mL of PBS at pH 4.2. Samples were incubated at 37°C, and 500 μL were removed at periodic intervals and replaced with fresh PBS (pH 4.2) for 48 h. 5 μL of release media (n=3) were added onto duplicate TLC plates. After drying, plates were baked at 100°C for 10 min, then allowed to cool to room temperature. Plates were then immersed in 0.025% (wt/vol) Coomassie blue (Fisher) in 20% (vol/vol) methanol for 10 s and allowed to dry for 1 h. Plates were then digitized using a scanner. Drug loading and stability was measured using fibers stored at room temperature (19-22°C) for at least five months. 10 mg pieces of fiber mesh were dissolved in 2.5 mL acetonitrile, centrifuged for 10 min at 10,000g, and added to 0.01 M KH_2PO_4 buffer or water at a 1:1 ratio for MVC or AZT fibers,

respectively. UV-HPLC was used to quantify amount of drug in samples as previously described. Encapsulation efficiency was calculated as the amount of drug in drug-loaded fibers relative to the amount of drug detected in dissolved blank fibers spiked at 1% (wt/wt) drug loading.

3.3.6 Mouse fiber coverage study

Two eight-week old female Balb/cByJ mice (Jackson Laboratories) were cycled with injections of medroxyprogesertone acetate (Greenstone LLC) four days prior to fiber insertion. Fiber meshes of dimensions 2 x 2 cm were folded around an applicator and inserted into the mouse vagina. The control mouse received blank 30:70 PLLA/PEO fibers, and the experimental mouse received 30:70 PLLA/PEO fibers electrospun with 1% (w/w) indocyanine green (Sigma-Aldrich). Mice were anesthetized during the procedure with isoflurane administered through nose cones. Mice were sacrificed after 30 minutes, and reproductive tracts were excised for imaging. Fiber meshes were removed after dissection and imaged with excised reproductive tracts. A Xenogen in vivo imaging system (IVIS) was used to measure fluorescence at 745/820 nm as a surrogate for fiber coverage.

3.3.7 HIV inhibition assay

TZM-bl cells and HIV-1 BaL isolate were obtained from the NIH AIDS Research and Reference Reagent Program, Division of AIDS, NIAID, NIH (http://www.aidsreagent.org/). TZM-bL cells, a derived HeLa cell line that expresses CD4, CCR5, and CXCR4 [58–61], were added to black 96-well plates (Corning, Corning, NY) with Dulbecco's Modified Eagle Medium (DMEM) (Gibco Life Technologies) with 10% fetal bovine serum (Hyclone), 1% 100X penicillin/streptomycin (Invitrogen), and 1% 200 mM L-glutamine (Invitrogen) with 50 μL/well at a density of 5,000 cells/well. Cells were incubated in 5% CO_2 and 37°C for 24 h prior to exposure to drugs or fibers. Fibers were sterilized by UV irradiation for 2 h (1 h per side). Treatments were added in 50 μL volumes. For the HIV-infectious inhibition assay, 100 μL of HIV-BaL (240 TCID/well) was added to wells 1 h after drug treatment. Media was removed from cells after 48 h post-treatment, and 100 μL of phosphate buffered saline (Gibco Life Technologies) and 100 μL of Bright-Glo Luciferase reagent (Promega) were added to wells. Infectious activity was quantified by measuring luminescence on a plate reader (Tecan). IC_{50} values of drug compounds were estimated using sigmoidal regression and bootstrapping in MATLAB version 7.11 (Mathworks).

3.3.8 Explant toxicity assay

Macaque ectocervical tissues (Tissue Banking and Distribution Program, University of Washington National Primate Research Center) were processed for polarized explant cultures in duplicate on the day of surgery as previously described [36–38]. Briefly, a circular tissue punch was inserted through the transwell membrane with the luminal side up. The edges around the explant were sealed with Matrigel^{TM} (BD Biosciences, San Jose, CA). A 0.6 mm diameter disc of either 30:70 PLLA/PEO, 70:30 PLLA/PEO, or 30:70 PLLA/PEO with 10% (wt/wt) GML fiber was placed on the apical side of the tissue with 200 μL of culture media (DMEM with 10% fetal bovine serum, 1% 100X penicillin/streptomycin, and 1% 200 mM L-glutamine). For controls, explants were untreated (culture media) or treated with a 0.4% dilution of nonoxynol-9 (N-9) gel. The explant cultures were maintained at 37°C in a 5% CO_2 atmosphere. After 18-24 h, the explants were washed and one of each duplicate was incubated in RPMI containing 250 μg/ml MTT [1-(4,5-dimethylthiazol- 2-yl)-3,5-diphenylformazan] for 4 h. The explants were removed and placed in 1 mL of methanol overnight to extract the formazan dye produced by live tissue. The next day, the explants were removed from methanol and placed on a marked paper towel to dry and be weighed. The color extracted in the methanol was read for optical density at 595 nm. The percent viability of the treated explants was determined by correcting the optical density (OD) with the weight of the corresponding explant. The other explant was frozen in an embedding medium (Tissue-Tek, Sakura Finetek USA Inc., CA) and processed for histology by cryosectioning and hematoxylin-eosin staining.

3.3.9 Sperm motility and viability assays

Sperm was obtained from two donors for sperm motility experiments. A third donor was recruited for sperm viability assays with glycerol monolaurate. Swim out sperm were obtained as described previously [62]. Briefly, we placed 0.5 mL aliquots of semen below 3 mL of Ham's F-10 media (Sigma-Aldrich) with 0.5% human serum albumin (Sigma-Aldrich) for 75 min in 5% CO_2 and 37°C. The aspirate, enriched for motile sperm, was centrifuged at 300 RCF for five min and resuspended in fresh Ham's F-10 to a concentration of 20 x 10^6 sperm mL^{-1}. The effect of drug dilutions on sperm motility were performed both in whole semen and in swimout sperm by adding 5 μL each of sperm and drugs to a slide and observing sperm motility with phase contrast either at 200x and 37°C (ECLIPSE Ti, Nikon), or by adding 200 μL of drug to 100 μL of semen and quantifying sperm motility with computer aided motility analysis for up to 7 min after the addition of drug. Multiple media only controls were run to ensure that any observed change in motility was minimally dependent upon time since ejaculation. Sperm viability was measured

by adding 20 μL of semen to 20 μL of Trypan blue (Sigma-Aldrich) and counting 100 live or dead sperm based on head staining after a 10 min incubation using 1000x brightfield microscopy.

3.3.10 Sperm migration assay

Millicell cell culture insert membranes (Millipore) with 3 μm pores were removed with forceps and replaced with square pieces of electrospun mesh. The mesh was attached to the inserts by applying firm pressure with a gloved finger. The thicknesses of cell culture insert membranes and electrospun meshes were measured using a micrometer. Modified and unmodified inserts were placed in a 12 well plate. Swimout sperm were diluted 1:10 in Ham's F-10 with no protein. 600 μL of Ham's F-10 was added to each of the twelve wells, and 400 μL of diluted sperm was added to each insert. Sperm were incubated for 2 h at 37 °C and 5% CO_2. The solutions from the inner and outer chambers of the wells were aspirated and used for counting to measure sperm concentration in media inside and outside of the inserts. Sperm were fixed by dipping membranes into ice cold ethanol and were then lyophilized for 24 h. Meshes were imaged using SEM with the same settings used to image blank meshes.

3.3.11 Statistical methods

Fiber diameters were plotted as geometric mean with 95% CI and reported in writing as geometric mean with standard deviation. As fiber diameters had lognormal distributions, they were transformed by taking the log of the diameters in nm prior to hypothesis testing. One-way ANOVA and Bonferroni t tests were used to compare the diameters of log-transformed fiber diameters. Drug release was reported as mean with standard deviation, and 6 d release values were compared by one-way ANOVA with Bonferroni t tests or compared to zero release with a one sample t test. Differences in amount of drug release were reported as mean difference with 95% confidence interval. Sperm viability in the presence of GML was analyzed using one-way ANOVA and a Bonferroni t test. The numbers of sperm counted in the transwell migration assay were reported as mean and standard deviation of log transformed data, except in the case where the number of sperm detected was zero. We used two-sided tests at a significance level of $\alpha=0.05$ for all hypothesis testing. Actual p values are reported unless $p < 0.0001$.

3.4 RESULTS

3.4.1 Electrospun fibers incorporate antiviral compounds with high drug loading.

We electrospun fibers from mixtures of hydrophilic polyethylene oxide (PEO) and hydrophobic poly-L-lactic acid (PLLA), two polymers with proven biocompatibility and FDA approval for use in medical implants [18,19]. We hypothesized that fibers with partially hydrophilic and partially hydrophobic composition would enable encapsulation of agents with high and low aqueous solubility, respectively. Previous studies with PLLA-PEO polymer blends found that blends act as a single material with averaged properties when mixed at a ratio up to 30:70 or 70:30 (wt/wt), but act as a composite of two materials with discrete properties when mixed at ratios approaching 50:50 (wt/wt) [20]. To fabricate homogeneous fibers with uniformly blended hydrophilicity/hydrophobicity, we electrospun 70:30 (wt/wt) PLLA/PEO and 30:70 (wt/wt) PLLA/PEO meshes. We also electrospun pure PLLA and pure PEO meshes. Polymer concentration in the electrospinning solution had a significant impact on the resulting fiber diameters between formulations with the same PLLA/PEO ratio and solvent choice, as assessed by ANOVA ($P < 0.0001$) (Fig. S1—See Appendix C for supplementary information). Electrospinning parameters were modified to yield fibers with reproducible size and high polymer recovery (Fig. S1-2), and two blends were identified for further study: 70:30 PLLA/PEO in 1:1 chloroform/2,2,2-trifluoroethanol and 30:70 PLLA/PEO in 3:1 chloroform/2,2,2-trifluoroethanol. These compositions produced fiber diameters of 200 - 700 nm and polymer recovery of >50% (Fig. S1-S2). The fibers were collected on a mandrel designed in the geometry of a tampon applicator (Figure 3-1) and resulted in fiber meshes in the shape of a hollow tube, which we were able to incorporate into a standard tampon applicator (Fig. S3). By controlling the axial deposition of the fibers near the apex of the collector, we could also form a thick barrier mesh (~2-3 mm thick) that is continuous with a thinner inner mesh (down to ~10 μm thick).

We selected several model compounds to demonstrate the versatility of electrospun fibers to deliver agents with differing solubility and mechanisms of action against either HIV-1 or HSV-2. We electrospun fibers containing either 1% (wt/wt) maraviroc (MVC), which inhibits CCR5-mediated HIV fusion, 1% (wt/wt) 3'-azido-3'-deoxythymidine (AZT), which inhibits viral reverse transcriptase, or 1% (wt/wt) acyclovir (acycloguanosine), which has antiviral activity against HSV-2. Collectively, these compounds vary in aqueous solubility (0.01–50 g L^{-1}) and span a wide range of log P values (-1 to 4). We assessed drug loading of MVC or AZT-loaded fiber meshes stored at room temperature (19-22°C) for at least five months by dissolving them in

acetonitrile and measuring drug content with HPLC. MVC and AZT were incorporated successfully into fibers at >95% drug encapsulation efficiency for both PLLA/PEO blend compositions. ARVs eluted from the polymer fibers were identical to the unformulated drugs as measured by UV-HPLC (Fig. S4), suggesting that the compounds are stable during electrospinning and during shelf storage for at least five months. Fiber meshes retained the same white color and soft, flexible texture over five months. While electrospinning did not compromise drug integrity, we found that drug incorporation into polymer fibers could influence fiber size, fiber alignment, and polymer recovery (Fig. S5-S8).

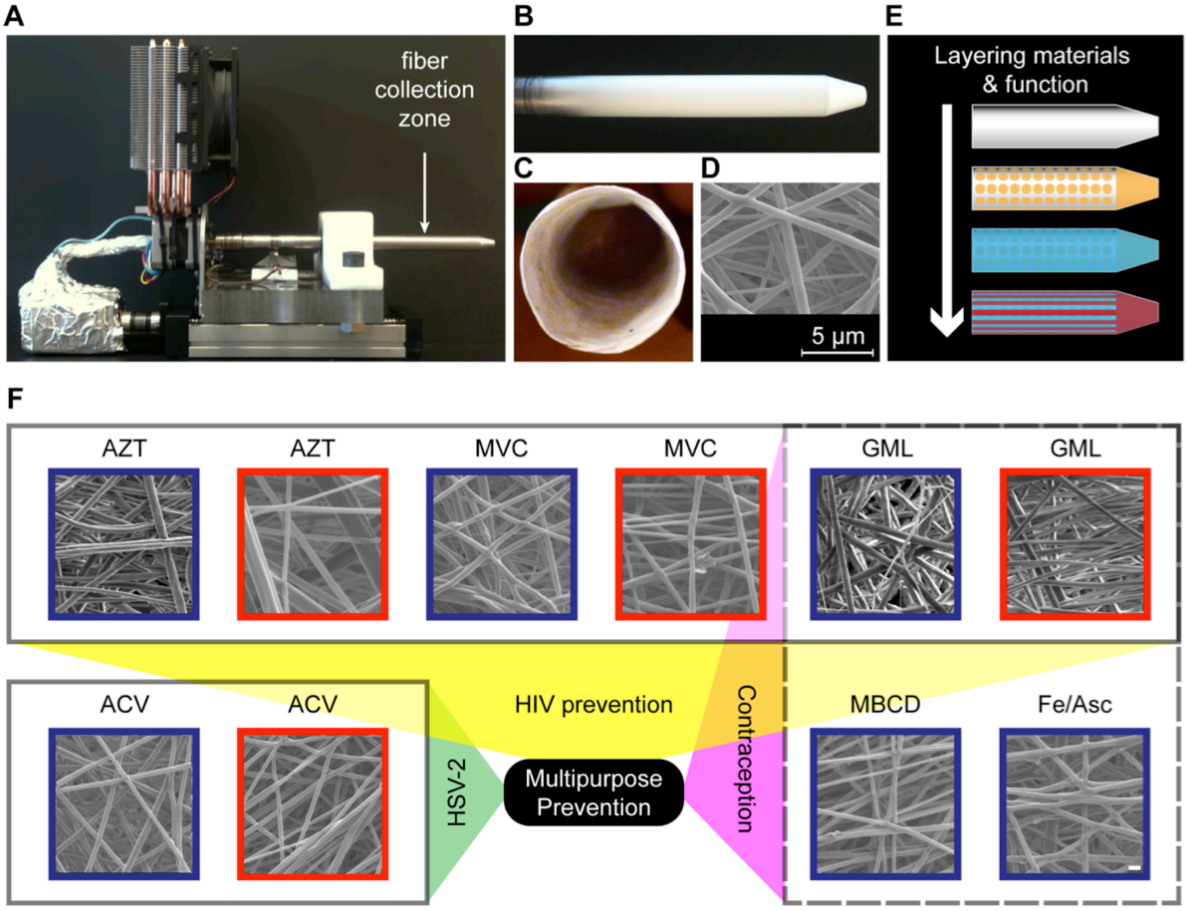

Figure 3-1. Electrospun fibers incorporate drugs for multipurpose prevention. (a) Two-axis mandrel electrospinning rig for fiber collection. (b) Controlled fiber deposition along a grounded aluminum collector produces a geometry that may be suitable for vaginal drug delivery. (c) Mesh abstracted from mandrel has a hollow interior. (d) Fiber meshes have porous microstructure. (e) Combining fiber meshes produces a multifunctional material. (f) Diverse agents with action against HIV, HSV-2, or sperm are incorporated into blends of PLLA and PEO. PLLA/PEO (30:70, blue) and PLLA/ PEO (70:30, red); AZT =1 wt% 39-azido-39-deoxythymidine, MVC =1 wt% maraviroc, ACV =1 wt% acycloguanosine, GML =10 wt% glycerol monolaurate, MBCD = 10 wt% methyl-b-cyclodextrin, Fe/Asc = 10 wt% iron (II) D-gluconate with 10 wt% ascorbic acid. Scale bar = 1 µm .

3.4.2 Drug-loaded fibers erode and release agents to potently inhibit HIV-1 activity in vitro.

Sustained drug release over weeks to months has potential for greater adherence whereas burst release of active agents may be desirable for pericoital prevention [2]. Since degradation of polymeric delivery systems can influence drug release properties, we fabricated fibers with varying degradation rates by modulating the hydrophilic and hydrophobic content of the fibers. We monitored fiber degradation in VFS over two weeks by recording mass loss and imaging with SEM (Figure 3-2). Fiber meshes with greater hydrophilic content showed the most pronounced change in individual fiber and overall mesh morphology (Figure 3-2). We observed that fibers decreased in diameter within hours to days, and then appeared to fuse into large fiber bundles. These observations were confirmed by measuring a 30% (95% CI = 25% to 35%, n = 117) reduction in 30:70 PLLA/PEO and a 32% (95% CI = 23% to 40%, n = 103) reduction in 70:30 PLLA/PEO fiber diameters after 3 days and over 30% mass loss of the meshes within one week. The percent mass loss corresponded with the percent PEO composition in the fibers (Figure 3-2). Pure PLLA fibers showed no mass loss after a one-hour incubation in VFS, whereas pure PEO fibers dissolved in less than 10 minutes upon contact with water.

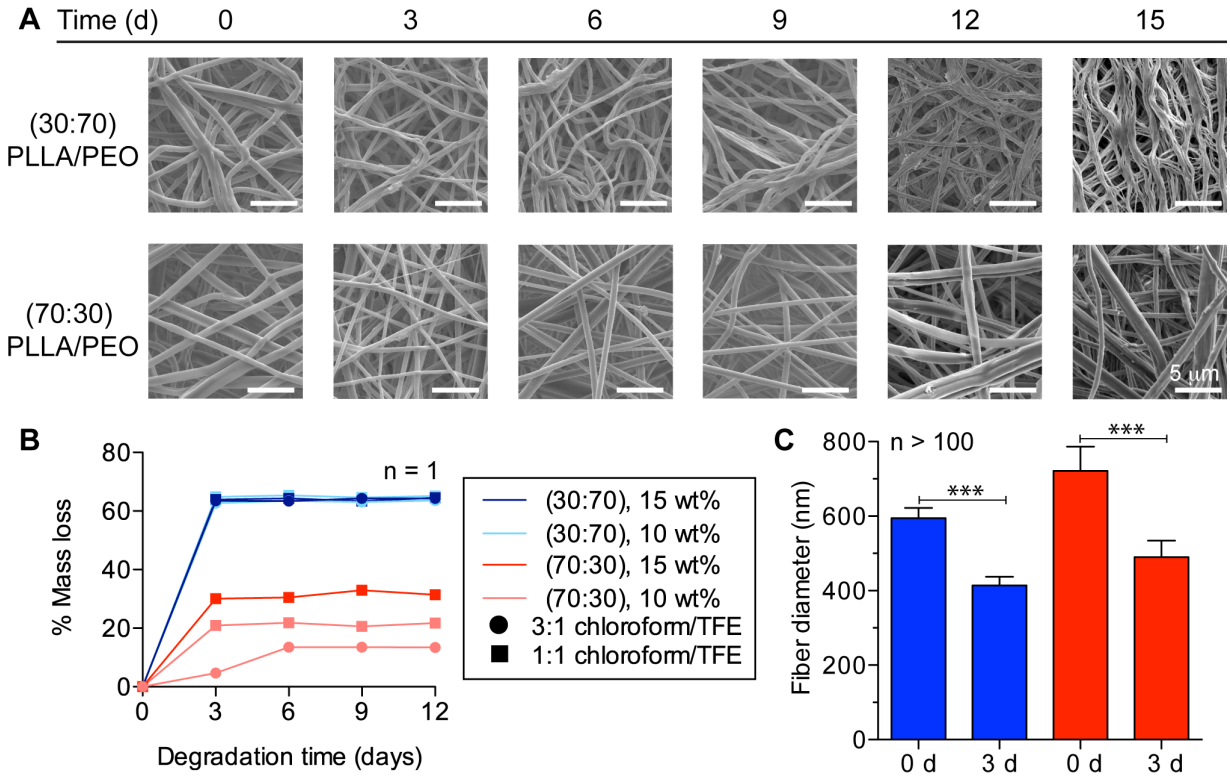

Figure 3-2. Fiber composition influences degradation properties. (a) SEM micrographs show that fiber and mesh morphology changes markedly over 15 d in VFS. (b) Mass loss of fibers over time is controlled by PEO content in fibers. (c) Fiber diameters, displayed as geometric mean with 95% confidence interval, and decrease significantly over three days of degradation in VFS (p,0.0001 for 30:70 and 70:30 PLLA/PEO fibers). 30:70 PLLA/PEO (blue) and 70:30 PLLA/PEO (red) for (b) and (c).

To investigate if drug release kinetics recapitulated polymer degradation kinetics, we monitored drug release from meshes incubated in VFS (Figure 3-3). We observed that AZT and MVC burst released from fibers within 1 h, but that the drug release profiles differed based on PLLA and PEO content of the fibers. For example, fibers with greater hydrophilic content (30:70 PLLA/PEO) released 2.1% more AZT (95% CI = 0.68% to 3.5%, n = 3) and 13% more MVC (95% CI = 6.8% to 20%, n = 3) over 6 d than corresponding meshes with greater hydrophobic content (70:30 PLLA/PEO). In 6 d, 70:30 PLLA/PEO fibers released 92 ± 0.75% of encapsulated AZT and 80 ± 3.9% of MVC into VFS (n = 3). The 30:70 PLLA/PEO fibers released 94 ± 0.48% of encapsulated AZT and 93 ± 0.98% of MVC into VFS (n = 3). We did not detect MVC release from pure PLLA fibers over 96 h in VFS. These results suggest that controlling polymer-drug interactions and the rate of polymer swelling and dissolution may alter the release kinetics of different active agents. Given the burst release of AZT and the aqueous solubility of indocyanine green (ICG) dye, we chose to electrospin ICG-loaded fibers to

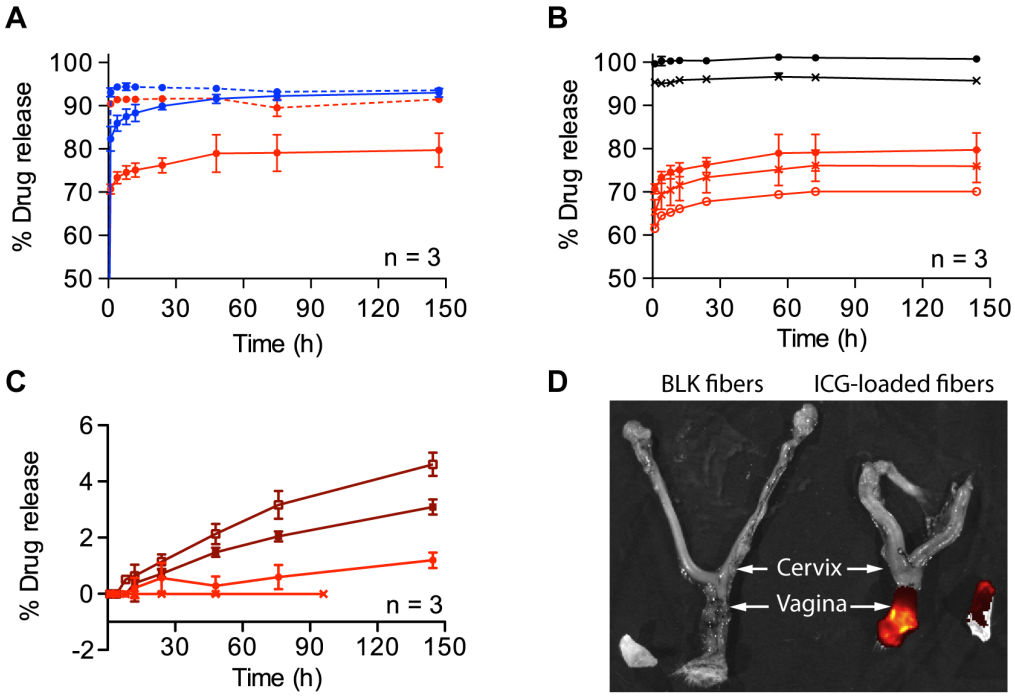

Figure 3-3. Fibers release active antiretroviral agents. (**a**) Cumulative drug release in VFS was measured for 30:70 PLLA/PEO (blue) and 70:30 PLLA/PEO (red). AZT (dashed line) and MVC (solid line) showed rapid burst release from blended fibers within 1 h. (**b**) Varying fiber diameter resulted in MVC burst release from PCL fibers (black) and 70:30 PLLA/PEO fibers (red). PCL meshes with two fiber diameters (• =370 nm and × =1.3 μm) and 70:30 PLLA/PEO fibers with three fiber diameters (• =560 nm, **o** = 1.5 μm, × = 3.4 μm) were tested. (**c**) Sustained release of MVC is achieved from PDLLA/PLLA blends and from 99:1 PLLA/PEO, but not from PLLA fibers. 50:50 PDLLA/PLLA (□), 25:75 PDLLA/PLLA (■), 99:1 PLLA/PEO (•), and 100% PLLA (×). (**d**) Insertion of fibers into mouse vagina and subsequent fluorescent imaging reveal release of dye within 30 minutes for ICG-loaded fibers (right) compared with blank fibers (left). Fiber meshes are shown next to excised reproductive tracts.

investigate the extent of fiber coverage and agent release in mice. After inserting 30:70 PLLA/PEO fibers loaded with 1% (wt/wt) ICG into mice, we observed that dye completely coated the vaginal tract after 30 minutes (Figure 3-3). This study provides initial evidence that fibers are able to sufficiently hydrate and release agents to coat the vaginal mucosa *in vivo*.

We tested multiple strategies to obtain sustained release of MVC from fibers by increasing fiber diameter, reducing hydrophilic polymer content, and modulating PLA crystallinity. MVC was chosen to establish proof of principle for controlled release because it was less hydrophilic than AZT. First, we tested the hypothesis that increasing fiber diameter would slow release of MVC from 70:30 PLLA/PEO fibers. We increased fiber diameters by raising the polymer concentration in 70:30 PLLA/PEO solutions (Fig. S9,10). Despite three- and six-fold increases in fiber diameter, all 70:30 PLLA/PEO fibers burst released MVC within one hour in VFS (Figure 3-3). Comparison of mean MVC release from variably sized 70:30 PLLA/PEO fibers with ANOVA showed that the fibers released significantly different amounts of MVC based on fiber size ($p = 0.0261$). The data suggested a trend for larger fiber diameters to release less MVC into VFS over six days, and 3.4 μm diameter fibers released 9.6% less MVC (95% CI = 1.17% to 18.1%, n = 3) than 560 nm fibers.

Our second strategy was to reduce hydrophilic polymer content by electrospinning fibers from a 99:1 PLLA/PEO blend containing 1% (wt/wt) MVC. The resulting fibers were smooth, regular, and similarly sized to 70:30 and 30:70 PLLA/PEO fibers (Fig. S10). When placed into VFS, the fibers showed no burst release of MVC. Rather, the fibers provided sustained release over six days, eluting an average of 1.19% of encapsulated MVC into VFS (95% CI = 0.51 to1.88 %, n = 3) (Figure 3-3).

Thirdly, we encapsulated 1% (wt/wt) MVC into fiber meshes made from polycaprolactone (PCL) or blends of poly(D,L)-lactic acid (PDLLA) and PLA to investigate the influence of polymer crystallinity on release rate. PCL is a bioabsorbable hydrophobic polymer with a long history of use in electrospinning [21]. PCL has a much lower melting temperature than PLLA, reflecting lower crystallinity and greater molecular flexibility in the polymer strands [22]. We electrospun PCL meshes containing 1% (wt/wt) MVC with two different fiber diameters: 371 nm and 1.3 μm (Fig. S10). Upon incubation in VFS, all PCL meshes burst released more than 95% of the encapsulated MVC within 1 hour (Figure 3-3). Larger PCL fibers released 5.04% less MVC over 6 days (95% CI = 3.92% to 6.17%, n = 3) than small PCL fibers.

We modulated the crystallinity of pure PLA fibers by blending PLLA with varying amounts of lower molecular weight poly(D,L-lactide) (PDLLA). PDLLA is chemically identical to PLLA, but displays key structural differences. In particular, PDLLA is amorphous, and allows for greater

penetration of water into PLA meshes [20]. We electrospun 25:75 and 50:50 PDLLA/PLLA blends containing 1% MVC. The resulting fibers showed regular morphology with similar fiber size (265 ± 145 nm and 190 ± 159 nm, respectively) to pure PLLA fibers (478 nm ± 287 nm) (Fig. S10). When placed into VFS, these PDLLA/PLLA meshes showed no burst release, and released MVC linearly over six days. The amount of encapsulated MVC released after six days was 3.09 ± 0.27% from 25:75 PDLLA/PLA fibers and 4.61 ± 0.41% from 50:50 PDLLA/PLLA fibers. 50:50 PDLLA/PLLA meshes released significantly more MVC than 25:75 PDLLA/PLLA meshes (P value = 0.0059, n = 3). Therefore, modulating the polymer crystallinity by blending PDLLA with PLLA provided small, but sustained, linear release of MVC from electrospun fibers.

We evaluated the activity and toxicity of our drug-loaded fibers in several relevant *in vitro* assays. MVC, AZT, and fibers were shown to be nontoxic to TZM-bL cells, and no difference between treated cells and media controls was found (Bonferroni post test, α = 0.05) (Fig. S11). We tested the ability of both the drug *eluates* released from 70:30 PLLA/PEO and 30:70 PLLA/PEO fibers and the drug-loaded fibers *themselves* to inhibit HIV-1 BaL infection in TZM-bL cells. First, we determined the specific antiviral activity of drug eluates released from the fibers to confirm that the absolute drug activity was not diminished by electrospinning. We measured an IC50 value of 0.90 nM and 2.3 nM for unformulated and eluted MVC, respectively. The IC50 of unformulated and eluted AZT was found to be 120 nM and 84 nM, respectively (Figure 3-4). The order of magnitude agreement between drug IC50 values before and after spinning suggests that the stabilities of MVC and AZT are maintained during electrospinning. Incubating TZM-bL cells with drug-loaded fiber discs significantly inhibited HIV-1 infection compared to blank fibers (P value < 0.0001) (Figure 3-4). The polymer composition of the mesh at this dosing did not impact their anti-HIV activity, and we saw equivalent viral inhibition for both drugs using the 30:70 and 70:30 PLLA/PEO meshes (Bonferroni post test, α = 0.05). Fiber toxicity was evaluated in an *ex vivo* tissue explant model using macaque cervical tissue. In contrast to tissue treated with N-9, we observed no reduction in tissue viability due to exposure to blank fibers or fibers loaded with 10% (wt/wt) GML as determined using an MTT assay and by histological examination of tissue morphology (Figure 3-4).

3.4.3 GML fibers are a chemical and physical barrier against sperm function.

To address the need for contraception in a multipurpose prevention strategy, we sought to identify non-hormonal chemical alternatives to N-9. We first evaluated the spermicidal capabilities of ferrous D-gluconate (FeGluc) and ascorbic acid (Asc) to corroborate findings from literature that the metal compound and ascorbic acid cause rapid spermiostasis due to lipid

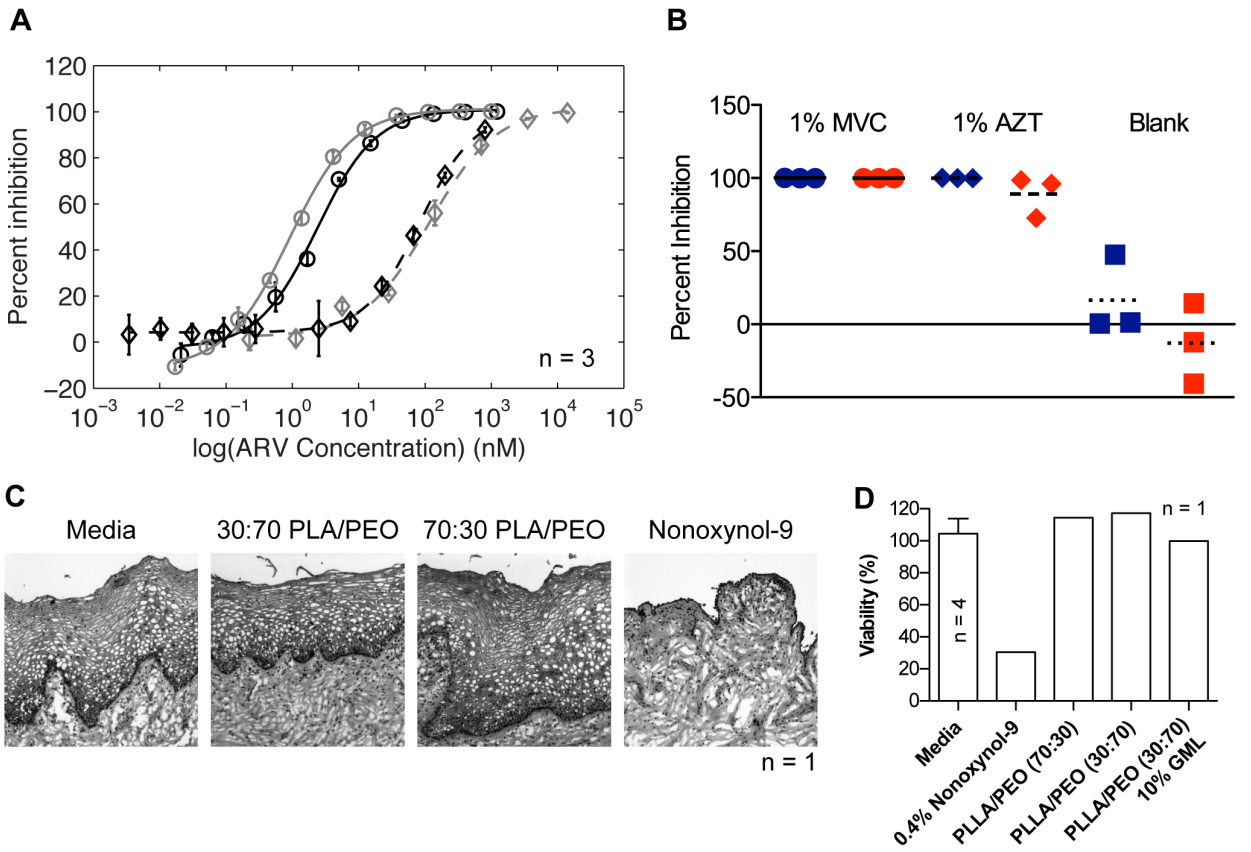

Figure 3-4. Fiber meshes inhibit HIV in vitro and are nontoxic to macaque cervical tissue explants. (a) Dose-response assay indicates that AZT and MVC released from fibers have similar potency to unformulated drugs (drug eluates, black and unformulated drug, gray). (b) Drug loaded fiber blends (30:70 PLLA/PEO (blue) and 70:30 PLLA/PEO (red)), but not blank fiber controls, show equivalent inhibition of HIV infection. (c) Histology indicates that 30:70 PLLA/PEO, 70:30 PLLA/PEO, and 30:70 PLLA/PEO fibers with 10% (wt/wt) GML are nontoxic to macaque cervical tissue explants compared to nonoxynol-9 control. (d) MTT assay confirms fibers, including those containing 10% (wt/wt) GML, are nontoxic to tissue explants. Note that for media controls n = 4, and for all other groups n = 1.

peroxidation of sperm [23]. We also evaluated methyl-β-cyclodextrin (MBCD), which we hypothesized might sequester cholesterol from semen and lead to premature sperm capacitation [24]. FeGluc and MBCD were readily incorporated into electrospun fibers (Figure 3-1, Fig. S5-6, 8), but these agents were ineffective at inhibiting sperm function as assayed by measuring motility of purified (swim-out) human sperm (Table S1).

Based on the amphiphilic properties of glycerol monolaurate (GML) and its reported function to interact with lipid bilayers [25], we were motivated to evaluate GML activity on sperm function. We hypothesized that GML could potentially interact with sperm plasma membranes to reduce sperm viability and motility. Using human swim-out sperm, GML inhibited sperm motility at concentrations of 0.05–0.5% (wt/vol) (Figure 3-5). At these concentrations, complete spermiostasis was measured in < 5 min (Video S2, 3). Reduction in motility was also observed

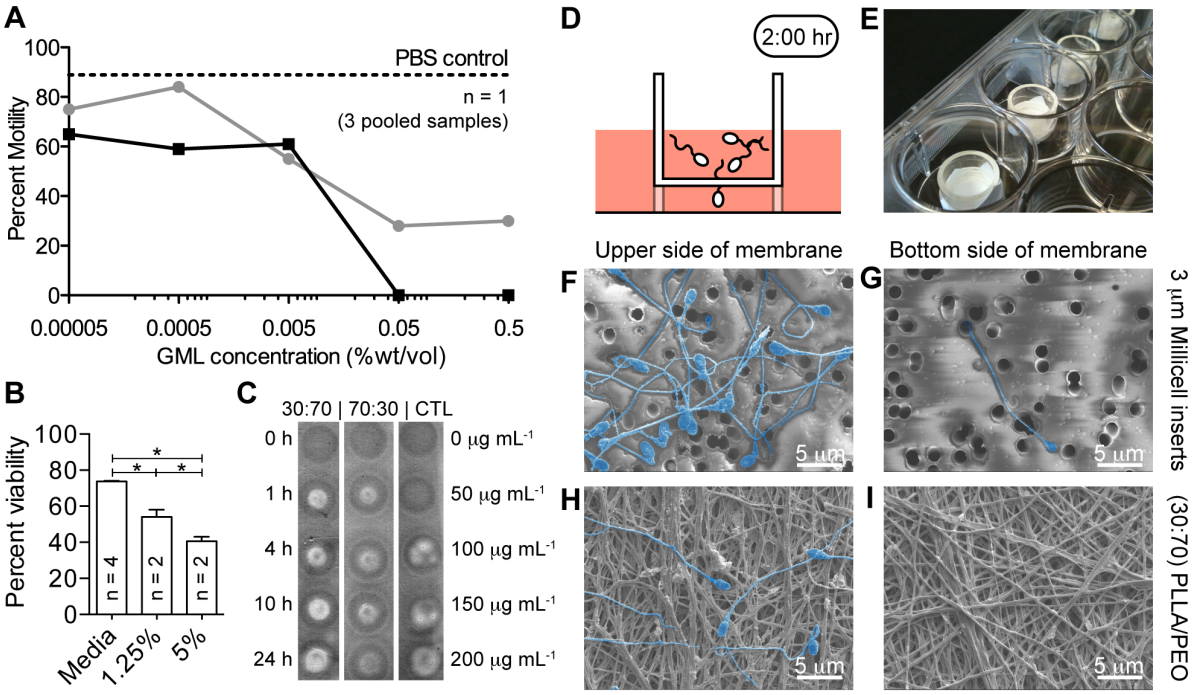

Figure 3-5. Fiber meshes are a physical and chemical barrier against sperm. (a) Motility of human swim-out sperm was completely inhibited within 5 min for 0.05 and 0.5% GML. Data show counts of motile and immotile sperm at 2 min (gray line) and 5 min (black line). Baseline sperm motility (,89%) was measured at the beginning and end of experiment using a PBS control (dotted line). (b) Sperm viability is reduced in whole semen incubated with GML compared with media control. (c) GML release from fiber meshes was qualitatively measured using TLC. (d, e) A transwell assay was used to test the physical barrier properties of the fiber meshes by replacing Millicell cell culture insert membranes (3 mm pore diameter) with a blank fiber mesh (n = 3). (f, g) SEM micrographs of the upper (f) and lower (g) side of Millicell control membrane. (h, i) SEM micrographs of upper (h) and lower side (i) of fiber mesh show that no sperm penetrate through the fiber mesh.

at concentrations down to 0.00005% (wt/vol) but did not result in complete spermiostasis during the measurement time (Table S1, and Video S1-S4). GML also reduced viability of human sperm in whole semen by 33.1% (95% CI = 24.0% to 42.2%, n = 2) when tested at a 5% (wt/vol) concentration and by 19.6% (95% CI = 10.7% to 28.9%, n = 2) (Figure 3-5). We also fabricated fibers loaded with 1% or 10% (wt/wt) GML using both PLLA/PEO blends. GML fibers were reproducibly electrospun to achieve polymer recoveries of >70% and fiber diameters between 600–800 nm (Fig. S5-S8). Fibers loaded with 10% (wt/wt) GML released ~100-200 μg mL^{-1} into VFS within 1 h, suggesting that 100% GML released from fibers within 1 hour of incubation with VFS (Figure 3-5).

In addition to encapsulating agents that chemically inhibited sperm function, the fibers served to physically block sperm penetration. We used a transwell assay to measure the ability of sperm to penetrate electrospun meshes in the absence of drugs. The thicknesses of the tissue insert controls and electrospun meshes used as barriers were 30 μm and 150 μm,

respectively. We found that motile sperm placed onto electrospun mesh were unable to swim through the fiber meshes despite the presence of numerous pores greater than 3 μm (Figure 3-5). In contrast, tissue culture insert controls with 3 μm diameter pores allowed sperm to penetrate into the bottom chamber. Approximately 58,000 sperm mL^{-1} (~1.7% of sperm) penetrated the commercial membranes in 2 h, whereas no sperm penetrated the fiber meshes (Table S2). SEM image analysis confirmed these results, as we observed sperm on the underside of the control membranes but not the electrospun fiber meshes (Figure 3-5). To assess the material strength of the electrospun meshes, we performed uniaxial tensile testing on samples of PCL containing 1% MVC that were spun at 5, 50, or 100 μL min^{-1} (n=2). We found that all materials had a Young's modulus between 25-120 MPa. In addition, materials were able to withstand at least 50% strain before failure. There was a statistically significant difference in Young's moduli between fibers spun at different flow rates, as determined by ANOVA ($P = 0.048$). A Bonferroni corrected t test was used to compare 5 μL min^{-1} and 50 μL min^{-1} fibers. It was found that fibers spun at a flow rate of 50 μL min^{-1} were on average 68 MPa stiffer than those spun at a flow rate of 5 μL min^{-1} (95% C.I = 2.8 to 130 MPa stiffer).

3.5 DISCUSSION

We have developed an innovative dosage form for intravaginal drug delivery using drug-eluting fibers fabricated by electrospinning. We show that electrospun fibers deliver agents that inhibit both HIV and sperm *in vitro* in addition to physically preventing sperm penetration. We also report on a novel function of GML to act as a spermicide and potential non-hormonal chemical contraceptive. This finding adds to the characteristics that make GML an attractive candidate for use in topical microbicides for multipurpose prevention [26]. Unlike existing vaginal drug delivery systems, polymer fibers may provide a single dosage form that is readily amenable to encapsulating an array of small molecule hydrophobic and hydrophilic compounds. The diversity and number of polymers that can be electrospun should enable a correspondingly large number of active agents to be encapsulated for sustained delivery [16]. Drug-eluting fibers formulated with a single agent can be assembled into a composite mesh to deliver drug combinations (Figure 3-1). Combined with the ability to control device geometry (Fig. S3), we expect that layered chemical function will enable delivery of specific drugs to defined regions within the lower female reproductive tract. The application of drug-eluting fibers for drug delivery to prevent HIV-1 and inhibit sperm function is unprecedented, and should have wide implications for the design of next generation multipurpose prevention technologies.

Topical delivery systems that combine potent and broadly active inhibitors have the greatest likelihood of protecting against the global diversity of STI and HIV variants that are transmitted sexually. The compounds that we incorporated into our fibers have different mechanisms of action against HIV and HSV-2. MVC prevents HIV entry by binding to CCR5 [27] and is already in clinical trials for use as a microbicide (MTN-013/IPM 026). While AZT is not currently a leading candidate for use in topical microbicides, its physicochemical properties are similar to those of tenofovir, which has been used in recent and ongoing clinical trials of microbicide gels [10]. GML, which we report has activity against sperm function, has also been shown to inhibit HIV infection *in vitro* and SIV infection of macaques *in vivo* by inhibiting the production of MIP-3α and other pro-inflammatory cytokines [26]. Finally, we also incorporated ACV into fibers, since HSV-2 infection is of great concern in its own right and in relation to risk of acquiring HIV and other STIs [28]. Together, these four compounds provide a strong proof of principle that electrospun fibers may be a useful platform for vaginal drug delivery and topical prevention of STIs.

For this work, we chose to electrospin fibers from mixtures of PEO and PLLA. We expected PEO to rapidly hydrate and dissolve in vaginal fluid and that PLLA would degrade slowly via hydrolysis at low pH into lactic acid [20], a natural component of vaginal fluid important for maintaining vaginal homeostasis [29]. We found that the magnitude of MVC release from PLLA/PEO blends was highly dependent upon the amount of PEO present. Over six days, 78% of encapsulated MVC was released from 70:30 PLLA/PEO fibers, compared with 93% of encapsulated MVC from 30:70 PLLA/PEO fibers. In contrast, approximately 90% of encapsulated AZT was released from both 70:30 and 30:70 PLLA/PEO fibers (Figure 3-3). This suggested that MVC could disperse evenly throughout both PEO and PLLA, while the majority of AZT partitioned into PEO. Small diameter hydrophilic fibers may be an improvement on current film devices that provide coitally dependent protection against STIs and pregnancy. Our data show that substantial amounts of hydrophilic and hydrophobic drugs can be delivered very quickly from nanometer diameter fibers. Meshes made from hydrophilic polymers have previously been found to dissolve and release encapsulated agents more rapidly than films cast from the same materials [30,31]. Yu et al. showed that 100% of encapsulated ferulic acid was released within 2 minutes from 250 nm polyvinylpyrrolidone fibers when dispersed with sodium dodecyl sulfate and sucralose, compared to 20 minutes from equivalent masses of thin films produced by casting. Furthermore, *in vitro* testing of ferulic acid permeation across the sublingual mucosa demonstrated a doubling of permeation rate for the fiber dosage form over the film dosage form [30]. Due to the high surface area-to-volume ratio of electrospun fiber

meshes, water may ingress more rapidly into hydrophilic electrospun materials than into cast films. Rapid hydration and a shorter diffusion distance offered by a nanofiber can create a very steep concentration gradient of encapsulated molecules, thus enhancing the rate of mass transport into mucosal tissues [31]. While we did not compare drug release from PLLA/PEO films to fibers, future studies should investigate how nanofibers can enhance the dissolution and mucosal delivery of ARVs.

The ability to hydrate rapidly upon insertion can aid in fast drug release and effective spreading of dissolved materials along the vagina. Material spreading can result in more complete coverage of the mucosal tissue that is vulnerable to infection by HIV and other pathogens [32]. We showed that insertion of indocyanine green loaded 30:70 PLLA/PEO fibers into the vagina of a mouse resulted in high levels of fluorescence throughout the vaginal tract (Figure 3-3). This suggests that fibers can sufficiently hydrate in small volumes of vaginal fluid and release encapsulated agents within 30 minutes *in vivo*. Hydrophilic polymer-based fiber meshes, including those made from PEO, may therefore provide a useful dosage form for pericoital prevention methods.

While rapid release of antivirals and contraceptives is desirable for pericoital prevention, sustained release of agents is desirable for providing extended periods of coverage that may increase user adherence. In contrast to PEO, PLLA is significantly hydrophobic, and fibers with high PLLA content more closely resemble solid depots like IVRs or drug-eluting diaphragms. We hypothesized that polymer fibers with a partially hydrophobic composition would enable encapsulation and sustained release of hydrophobic agents. While our results demonstrated that partially hydrophobic fibers could successfully incorporate MVC and GML (two hydrophobic agents), 70% and 30% PLLA content did not provide sustained release (Figure 3-3, Fig. S5-9), We evaluated multiple strategies for controlling the release of MVC from electrospun fibers by increasing fiber diameter, reducing hydrophilic polymer content, and modulating polymer crystallinity.

Our first strategy for sustaining release of MVC was to electrospin larger diameter fibers (Fig. S9-10). While Cui et al. showed that increasing PDLLA fiber diameter from 212 to 551 nm led to slower release of the highly water-soluble compound acetaminophen [33], we observed MVC release from 70:30 PLLA/PEO fiber meshes was not altered by increasing fiber diameter six fold from 560 nm to 3.4 μm. If the release of MVC from 70:30 PLLA/PEO fibers were diffusion controlled, an increase in diameter by a factor of six should have decreased release rates by a factor of approximately 36. While we did not observe significant slowing of drug

release, we did find that increasing fiber size resulted in a 9.64% (95% CI = 1.17% to 18.1%) reduction in the amount of drug released after 6 d (Figure 3-3).

We hypothesized that reducing the hydrophilic content in PLLA/PEO blends could mediate sustained release of MVC by reducing the amount of PEO at the surface of the fibers. Our release data from 70:30 and 30:70 PLLA/PEO fibers containing 1% (wt/wt) MVC showed that the extent of MVC release was related to PEO content. In fact, we did not detect any MVC release from 100% PLLA fibers in VFS. We electrospun 99:1 PLLA/PEO fibers to investigate if much smaller amounts of PEO could still allow for hydration of the mesh and release of MVC but prevent burst release. In fact, we observed that fibers composed of 99:1 PLLA/PEO gave linear release of 1.19 ± 0.28% of encapsulated MVC over six days. This amount of MVC corresponded to an average concentration of 360 ± 120 nM (n = 3) MVC, two orders of magnitude greater than MVC's IC50 *in vitro*. Nevertheless, much of the MVC remained trapped within the PLLA, highlighting that the PLLA/PEO blends that we tested are not ideal for sustained release applications for MVC. However, these results demonstrated proof of principle that controlling the relative amounts of polymers in blended fibers could modify not only the magnitude of release, but also the kinetics of release. The addition of porogens, acid catalysts, or glycolic acid groups in future formulations may enhance water penetration and polyester degradation, thereby improving the magnitude of drug release.

It is unlikely that the hydrophobic nature of PLLA alone was responsible for the lack of MVC release from PLLA. Forbes et al. documented release of MVC from a silicone based elastomer gel both into VFS and into the vaginal fluid of rhesus macaques, providing evidence that MVC can release from hydrophobic formulations [34]. Indeed, we found that MVC burst released from PCL meshes, which are also hydrophobic. We hypothesized that the semi-crystalline structure of PLLA is responsible for preventing MVC release from the hydrophobic portions of blended fibers by occluding water penetration. To test this hypothesis, we modulated the crystallinity of PLA fibers by blending PDLLA with PLLA and looked for sustained release of MVC in VFS over six days (Figure 3-3, Fig. S9-10). PDLLA is comprised of a racemic mixture of the D- and L-stereoisomers of lactic acid and has an amorphous microstructure that allows increased water entry and accelerated polymer degradation compared to PLLA [20]. We found that electrospinning 25:75 and 50:50 blends of PDLLA and PLLA allowed the ingress of water and the subsequent linear, sustained release of MVC over six days. 25:75 and 50:50 PDLLA/PLLA fibers had similar sizes; 25:75 fibers were around 20% larger than 50:50 fibers (Fig. S10). The rate of MVC release from PDLLA/PLLA fibers increased with the PDLLA content, but remained small. Cui et al. achieved sustained release of acetaminophen from electrospun PDLLA fibers

over six days and found that >70% of encapsulated drug could be released [33]. We found that 50:50 PDLLA/PLLA fibers only released 4.61 ± 0.41% of MVC into VFS over 6 d. Our results may differ from those of Cui et al. because of MVC's lower aqueous solubility, release media with lower pH (4.2 compared with 7.4), and different PLA isomer composition. Despite the low levels of drug release, our results provide proof of principle that electrospun fibers can sustain release of ARVs over multiple days. It is likely that encapsulating MVC in pure PDLLA would result in greater release of MVC due to reduced crystallinity and accelerated polymer degradation.

In addition to releasing ARVs, it is also critical that fibers are safe and effective in biological systems. We evaluated the antiviral activity of fibers loaded with either AZT or MVC using an *in vitro* TZM-bL assay. This model has previously been used to evaluate drug candidates for topical microbicides [11,35]. Both the drug eluates from *in vitro* fiber release studies and drug-loaded fibers themselves were found to potently inhibit HIV compared to blank fibers. The IC50 values of unformulated ARV versus eluted ARV were of a same order of magnitude (Figure 3-4). Our results suggest that fibers are able to release sufficient levels of drug in cDMEM to prevent HIV infection in TZM-bL cells over 48 hours, which is consistent with the release profiles obtained from *in vitro* release studies in VFS. Furthermore, these studies demonstrate that both drugs are in a bioavailable form after the electrospinning formulation process. The toxicity of fibers was measured with a macaque cervical explant model using histological examination and an MTT viability assay (Figure 3-4). A similar model has previously been used to evaluate the safety of microbicide candidates using human cervical explant tissue [36–38]. Tissue exposed to either 30:70 or 70:30 PLLA/PEO fibers was found to have similar epithelial layer integrity and cell viability compared with untreated control tissue, indicating the biological suitability of the polymer blends for additional studies in vaginal drug delivery.

Long-term shelf stability is another quality imperative to the design of effective dosage forms for multipurpose prevention. Ham *et al*. performed an extensive characterization of the long-term stability of pyrimidinedione vaginal film, measuring drug release, toxicity, and activity at specified time points over 12 months at both standard and elevated temperature and humidity [39]. We detected >95% of the initially-loaded AZT and MVC in fiber meshes stored at room temperature for at least five months and observed that fiber meshes retained similar appearance and texture over this period. While this data suggest that ARVs remain stable in PLLA/PEO fiber meshes under standard storage conditions, more comprehensive studies of drug stability are needed for the polymer-drug combinations chosen for future studies. We

expect that the solid dosage form of drug-loaded fibers will be advantageous for long-term stability compared with semi-solid dosage forms like vaginal gels.

There is a great need to develop multipurpose prevention strategies that provide contraception in addition to protecting against STIs including HIV. Topically applied non-hormonal chemical contraceptives for pericoital use would address an important gap in contraception needs for women. While N-9 is a highly effective spermicide, the same detergent properties responsible for immobilizing sperm are also known to promote vaginal inflammation and increase the risk of STI infection [5,40]. We first evaluated non-hormonal contraceptives described previously in the literature to be potent inhibitors of sperm function. We tested the function of FeGluc, Asc, and their mixture because these agents had been reported previously to potently inhibit sperm motility in solution and after elution from a vaginal ring [23,41]. At the highest concentration tested, FeGluc alone inhibited motility of ~37% of sperm within 2 minutes but did not result in complete spermiostasis (Supporting Table 1). Combining FeGluc with L-ascorbic acid (FeAsc) resulted in rapid spermiostasis in <30s. However, we observed equally rapid spermiostasis upon treatment with L-ascorbic acid alone. We conclude that the reported spermicidal effect of FeGluc when combined with L-ascorbic acid was likely due to the decrease in pH upon dissolution of L-ascorbic acid (pH ~2), since pure L-ascorbic acid was just as effective as its mixture with iron. Indeed, L-ascorbic acid at a pH of 5.5 had no effect on sperm motility (Supporting Table 1). MBCD was also evaluated as a non-hormonal chemical contraceptive but showed no effect on sperm function at the concentrations tested. In addition, due to the high amounts of free cholesterol present in whole semen, we estimate that the high concentration of MBCD required to induce sperm capacitation would exceed the concentration that causes inflammation [24,42].

We were motivated to evaluate GML's activity on sperm function based on its amphiphilic properties and its reported interaction with lipid bilayers [25]. GML, a glycerol ester of lauric acid that is used commonly as an emulsifier in foods and cosmetics, is regarded by the FDA as safe for topical use at doses up to 100 mg mL^{-1} [43]. Additionally, GML is inexpensive, possesses documented anti-inflammatory properties, and is antimicrobial for a number of vaginal pathogens [43,44]. We show for the first time that GML potently reduces sperm motility in a dose-dependent manner (EC_{50} ~ 0.005% wt/vol at 2 min) and significantly lowers sperm viability at concentrations equivalent to those used in recent microbicide studies with macaques (5% wt/vol) (Figure 3-5). Although its spermicidal mechanisms are as yet unknown, interference with signal transduction by incorporation into plasma membranes has been suggested as a mechanism for its antibacterial and anti-inflammatory properties [43,45,46] and may also be

involved in sperm inhibition. Future studies should perform an in-depth characterization of how GML causes spermiostasis. Our findings add to the list of properties that make GML an attractive candidate for use in topical microbicides for multipurpose prevention, including anti-inflammatory mediated prevention of SIV infection in macaques [26] and the capacity to prevent bacterial infections [47]. The low aqueous solubility of GML (50–100 μg mL^{-1} at pH 7) precluded our ability to evaluate the activity of higher concentrations of GML on human sperm in whole semen, but provided a strong rationale to formulate GML in polymer fibers [43]. A dosage form that enhances the bioavailability of GML could potentially enhance the spermicidal potency of the compound.

The potential of GML to act as a surfactant has raised controversy within the microbicide field over its safety as a topical product. Schlievert et al. provided extensive characterization of the safety of 5% GML in KY warming gel for daily use in macaques for up to 12 weeks (n=9) [43]. Using an MTT viability assay and histological examination of polarized cervical explants from macaques, we found that 30:70 PLLA/PEO fibers loaded with 10% (wt/wt) GML were nontoxic *ex vivo* and had similar epithelial layer integrity to untreated controls. Nonoxynol-9 has been found to increase the frequency of genital lesions, which, it is thought, subsequently increase the risk of HIV infection[5]. In contrast, GML actually stabilizes eukaryotic cell membranes and reduces production of IL-8, an inflammatory cytokine. Furthermore, GML does not negatively impact the growth of lactobacilli or the production of lactic acid *in vivo* [43]. In contrast, nonoxynol-9 irritates and removes vaginal and cervical epithelial cells Figure 3-4 and disrupts the normal vaginal flora [48,49]. While Moench et al. demonstrated that GML increased susceptibility to HSV-2 infection in mice, they acknowledged that the vaginal epithelium of medroxyprogesterone acetate treated mice is quite different from that of humans and nonhuman primates [50]. Depoprovera-treated murine vaginal lining is similar to endocervical columnar epithelium, which is much thinner and less robust than the non-keratinized stratified squamous epithelium of the ectocervix or vaginal wall in humans and non-human primates. Since HSV-2 infection may occur through the vulva, the vagina, or the cervix, the mouse model developed by Moench et al. may be too sensitive to draw conclusions about how GML may affect HSV-2 acquisition in humans or nonhuman primates. Despite the surfactant nature of GML, the compound has been shown to have several protective qualities, including the ability to neutralize the toxic effects of pathogenic gram-positive bacteria [25,51]. Recently, Li et al. provided preliminary evidence that GML is not only safe for chronic use in rhesus macaques, but actually prevents SIV mucosal transmission with repeated high dose challenge [26].

In addition to the chemical inhibition provided by GML, we also demonstrated that blank

fibers block sperm migration in a transwell assay (Figure 3-5, Supporting Table 2). Since the electrospun fibers used as a physical barrier were five times as thick as the tissue culture inserts, the tissue culture inserts cannot serve as a control to discern why the fiber meshes formed a functional barrier against sperm transport. Nevertheless, they do still provide a control to demonstrate that the sperm were motile and capable of traversing a membrane with 3 μm diameter pores. Relying upon a porous mesh to block sperm penetration differs from current barrier approaches, which rely on nonporous materials to block sperm entry into the cervix [52–54]. Our results showed that a porous, tortuous mesh fabricated by electrospinning could efficiently block sperm entry. This suggests that, if fabricated in the appropriate geometry and given the appropriate mechanical strength, electrospun fibers may serve as an effective barrier contraceptive. While the materials we presented are not yet suitable to be turned into a final barrier device, analysis of their mechanical properties does shed some light on potential product configurations. In particular, the Young's moduli of electrospun materials made from 70:30 PLLA/PEO fibers with 1% (wt/wt) MVC were around 50-100 MPa, and electrospun meshes withstood at least 50% extensional strain before failure (Fig. S12). For comparison, latex rubber condoms have a Young's modulus of approximately 2 MPa and can withstand inflation to volumes greater than 20 L [55]. Dapivirine films have a tensile modulus of 5.4 to 7.8 MPa [13]. Based on the mechanical properties of these electrospun materials, it is unlikely that they would be effective as a condom-like device, but they may be suitable as devices similar to vaginal sponges or diaphragms.

3.6 CONCLUSION

We have presented a versatile platform for topical drug delivery to the lower female reproductive tract. The electrospun fiber meshes were fabricated in geometries suitable for intravaginal drug delivery, and we showed that our fibers incorporate agents with differing aqueous solubility and mechanisms of action against HIV-1, HSV-2, or sperm. Layering or co-electrospinning drug-loaded fibers may create composite materials that are multifunctional by virtue of simultaneous delivery of multiple agents with different mechanisms of action. In particular, fibers incorporating inhibitors of viral reverse transcriptase and CCR5 binding prevented HIV infection *in vitro*. We also screened non-hormonal chemical contraceptive alternatives to N-9 and identified a novel function of GML to inhibit sperm motility and reduce sperm viability. In addition to chemically inhibiting sperm function, fibers also physically inhibit sperm penetration by creating a tortuous path that sperm cannot navigate. This system is

expected to provide enhanced coverage of the mucosal tissue and vaginal rugae by covering both the vaginal wall and the cervix, supported by the extent of coverage demonstrated when fiber meshes were applied to mice. We envision that the fiber meshes could be inserted simply with a tampon applicator, rendering it discreet, female-controlled, and wholly reversible. Further research will be conducted to investigate the mechanical properties of the fibers and explore other methods to modulate drug release. The functional combination offered by our drug-eluting fibers cannot be accomplished with any single technology currently in the development pipeline. To our knowledge, this research represents the first application of electrospinning to vaginal drug delivery. We envision other applications for drug-eluting fibers along with prevention technology, including mucosal vaccine delivery, STI treatment, rectal microbicides, and other reproductive health applications.

3.7 ACKNOWLEDGEMENTS

We thank J. Amory, C.H. Muller and the University of Washington Male Fertility Laboratory for technical assistance with the sperm function assays and critical discussions of the manuscript. Collection of human semen samples from volunteers was performed at the University of Washington Male Fertility Laboratory. We also thank F. Hladik and R. Astronomo for assistance with the cervical tissue explant models. We thank A. Chen for technical assistance with tensile testing of electrospun materials.

3.8 REFERENCES

1. Glasier A, Gülmezoglu AM, Schmid GP, Moreno CG, Van Look PF (2006) Sexual and reproductive health: a matter of life and death. The Lancet 368: 1595–1607. doi:10.1016/S0140-6736(06)69478-6.
2. CAMI Multipurpose Prevention Technologies for Reproductive Health: 2011 Symposium (2012) pp. 1–24.
3. Blish C, Baeten J (2011) Hormonal Contraception and HIV-1 Transmission. American Journal of Reproductive Immunology 65: 302–307.
4. Baeten JM, Lavreys L, Overbaugh J (2007) The Influence of Hormonal Contraceptive Use on HIV-1 Transmission and Disease Progression. Clinical Infectious Diseases 45: 360–369. doi:10.1086/519432.
5. Van Damme L, Ramjee G, Alary M, Vuylsteke B, Chandeying V, et al. (2002) Effectiveness of COL-1492, a nonoxynol-9 vaginal gel, on HIV-1 transmission in female sex workers: a randomised controlled trial. The Lancet 360: 971–977. doi:10.1016/S0140-6736(02)11079-8.
6. Friend DR, Doncel GF (2010) Combining prevention of HIV-1, other sexually transmitted infections and unintended pregnancies: Development of dual-protection technologies. Antiviral Research 88, Supplement: S47–S54. doi:10.1016/j.antiviral.2010.09.005.
7. Minnis A, Padain N (2005) Effectiveness of female controlled barrier methods in preventing sexually transmitted infections and HIV: current evidence and future research directions. Sexually transmitted infections 81: 193–200.

8. Malcolm RK, Edwards K-L, Kiser P, Romano J, Smith TJ (2010) Advances in microbicide vaginal rings. Antiviral Research 88, Supplement: S30–S39. doi:10.1016/j.antiviral.2010.09.003.
9. Garg S, Goldman D, Krumme M, Rohan LC, Smoot S, et al. (2010) Advances in development, scale-up and manufacturing of microbicide gels, films, and tablets. Antiviral Research 88: S19–S29. doi:10.1016/j.antiviral.2010.09.010.
10. Karim Q, Karim SSA, Frohlich, JA, Grobler, AC, Baxter, C, et al. (2010) Effectiveness and Safety of Tenofovir Gel, an Antiretroviral Microbicide, for the Prevention of HIV Infection in Women. Science 329: 1168.
11. Herrera C, Cranage M, McGowan I, Anton P, Shattock RJ (2009) Reverse Transcriptase Inhibitors as Potential Colorectal Microbicides. Antimicrobial Agents and Chemotherapy 53: 1797–1807. doi:10.1128/AAC.01096-08.
12. Singer R, Derby N, Rodriguez A, Kizima L, Kenney J, et al. (2011) The Nonnucleoside Reverse Transcriptase Inhibitor MIV-150 in Carrageenan Gel Prevents Rectal Transmission of Simian/Human Immunodeficiency Virus Infection in Macaques. Journal of Virology 85: 5504–5512. doi:10.1128/JVI.02422-10.
13. Akil A, Parniak M, Dezzutti C, Moncla B, Cost M, et al. (2011) Development and characterization of a vaginal film containing dapivirine, a non-nucleoside reverse transcriptase inhibitor (NNRTI), for prevention of HIV-1 sexual transmission. Drug Delivery and Translational Research 1: 209–222. doi:10.1007/s13346-011-0022-6.
14. Malcolm K, Woolfson D, Russell J, Andrews C (2003) In vitro release of nonoxynol-9 from silicone matrix intravaginal rings. Journal of Controlled Release 91: 355–364. doi:10.1016/S0168-3659(03)00260-8.
15. Malcolm RK (2005) Long-term, controlled release of the HIV microbicide TMC120 from silicone elastomer vaginal rings. Journal of Antimicrobial Chemotherapy 56: 954–956. doi:10.1093/jac/dki326.
16. Szentivanyi A, Chakradeo T, Zernetsch H, Glasmacher B (2011) Electrospun cellular microenvironments: Understanding controlled release and scaffold structure. Advanced Drug Delivery Reviews 63: 209–220. doi:10.1016/j.addr.2010.12.002.
17. Teo W-E, Inai R, Ramakrishna S (2011) Technological advances in electrospinning of nanofibers. Science and Technology of Advanced Materials 12: 013002. doi:10.1088/1468-6996/12/1/013002.
18. Ratner B, Hoffman A, Schoen F, Lemons J (1996) Biomaterials science : an introduction to materials in medicine. San Diego: Academic Press. 297-308 p.
19. Anderson JM, Shive MS (1997) Biodegradation and biocompatibility of PLA and PLGA microspheres. Advanced Drug Delivery Reviews 28: 5–24. doi:10.1016/S0169-409X(97)00048-3.
20. Auras RA, Lim L-T, Selke SEM, Tsuji H (2010) Poly(Lactic Acid): Synthesis, Structures, Properties, Processing, and Applications. John Wiley & Sons. 356-357 p.
21. Teo W-E, He W, Ramakrishna S (2006) Electrospun scaffold tailored for tissue-specific extracellular matrix. Biotechnology Journal 1: 918–929. doi:10.1002/biot.200600044.
22. Yohe ST, Colson YL, Grinstaff MW (2012) Superhydrophobic Materials for Tunable Drug Release: Using Displacement of Air To Control Delivery Rates. Journal of the American Chemical Society 134: 2016–2019. doi:10.1021/ja211148a.
23. Saxena B, Singh M, Gospin R, Chu C, Ledger W (2004) Efficacy of nonhormonal vaginal contraceptives from a hydrogel delivery system. Contraception 70: 213–9.
24. Zidovetzki R, Levitan I (2007) Use of cyclodextrins to manipulate plasma membrane cholesterol content: evidence, misconceptions and control strategies. Biochimica et biophysica acta 1768: 1311–24.
25. Peterson ML, Schlievert PM (2006) Glycerol Monolaurate Inhibits the Effects of Gram-Positive Select Agents on Eukaryotic Cells. Biochemistry 45: 2387–2397. doi:10.1021/bi051992u.
26. Li Q, Estes J, Schlievert P, Duan L, Brosnahan A, et al. (2009) Glycerol monolaurate prevents mucosal SIV transmission. Nature 458: 1034.
27. Dorr P, Westby M, Dobbs S, Griffin P, Irvine B, et al. (2005) Maraviroc (UK-427,857), a Potent, Orally Bioavailable, and Selective Small-Molecule Inhibitor of Chemokine Receptor CCR5 with Broad-Spectrum Anti-Human Immunodeficiency Virus Type 1 Activity. Antimicrob Agents Chemother 49: 4721–4732. doi:10.1128/AAC.49.11.4721-4732.2005.

28. Wald A, Link K (2002) Risk of Human Immunodeficiency Virus Infection in Herpes Simplex Virus Type 2–Seropositive Persons: A Meta-analysis. The Journal of Infectious Diseases 185: 45–52. doi:10.1086/338231.
29. Graver MA, Wade JJ (2011) The role of acidification in the inhibition of Neisseria gonorrhoeae by vaginal lactobacilli during anaerobic growth. Annals of Clinical Microbiology and Antimicrobials 10: 8. doi:10.1186/1476-0711-10-8.
30. Yu D-G, Yang J-M, Branford-White C, Lu P, Zhang L, et al. (2010) Third generation solid dispersions of ferulic acid in electrospun composite nanofibers. International Journal of Pharmaceutics 400: 158–164. doi:10.1016/j.ijpharm.2010.08.010.
31. Yu D-G, Branford-White C, White K, Li X-L, Zhu L-M (2010) Dissolution Improvement of Electrospun Nanofiber-Based Solid Dispersions for Acetaminophen. AAPS PharmSciTech 11: 809–817. doi:10.1208/s12249-010-9438-4.
32. Kieweg SL, Katz DF (2006) Squeezing Flows of Vaginal Gel Formulations Relevant to Microbicide Drug Delivery. Journal of Biomechanical Engineering 128: 540. doi:10.1115/1.2206198.
33. Cui W, Li X, Zhu X, Yu G, Zhou S, et al. (2006) Investigation of Drug Release and Matrix Degradation of Electrospun Poly(dl-lactide) Fibers with Paracetanol Inoculation. Biomacromolecules 7: 1623–1629. doi:10.1021/bm060057z.
34. Forbes CJ, Lowry D, Geer L, Veazey RS, Shattock RJ, et al. (2011) Non-aqueous silicone elastomer gels as a vaginal microbicide delivery system for the HIV-1 entry inhibitor maraviroc. Journal of Controlled Release 156: 161–169. doi:10.1016/j.jconrel.2011.08.006.
35. Ham A, Cost M, Sassi A, Dezzutti C, Rohan L (2009) Targeted Delivery of PSC-RANTES for HIV-1 Prevention using Biodegradable Nanoparticles. Pharmaceutical Research 26: 502–511. doi:10.1007/s11095-008-9765-2.
36. Abner SR, Guenthner PC, Guarner J, Hancock KA, Cummins JE, et al. (2005) A Human Colorectal Explant Culture to Evaluate Topical Microbicides for the Prevention of HIV Infection. J Infect Dis 192: 1545–1556. doi:10.1086/462424.
37. Rohan LC, Moncla BJ, Kunjara Na Ayudhya RP, Cost M, Huang Y, et al. (2010) In Vitro and Ex Vivo Testing of Tenofovir Shows It Is Effective As an HIV-1 Microbicide. PLoS ONE 5: e9310. doi:10.1371/journal.pone.0009310.
38. Cummins JE, Guarner J, Flowers L, Guenthner PC, Bartlett J, et al. (2007) Preclinical Testing of Candidate Topical Microbicides for Anti-Human Immunodeficiency Virus Type 1 Activity and Tissue Toxicity in a Human Cervical Explant Culture. Antimicrob Agents Chemother 51: 1770–1779. doi:10.1128/AAC.01129-06.
39. Ham AS, Rohan LC, Boczar A, Yang L, W. Buckheit K, et al. (2012) Vaginal Film Drug Delivery of the Pyrimidinedione IQP-0528 for the Prevention of HIV Infection. Pharmaceutical Research 29: 1897–1907. doi:10.1007/s11095-012-0715-7.
40. Fichorova RN, Tucker LD, Anderson DJ (2001) The Molecular Basis of Nonoxynol-9-Induced Vaginal Inflammation and Its Possible Relevance to Human Immunodeficiency Virus Type 1 Transmission. Journal of Infectious Diseases 184: 418 –428. doi:10.1086/322047.
41. Han YA, Singh M, Saxena BB (2007) Development of vaginal rings for sustained release of nonhormonal contraceptives and anti-HIV agents. Contraception 76: 132–138. doi:10.1016/j.contraception.2007.04.006.
42. Boulmedarat L, Bochot A, Lesieur S, Fattal E (2005) Evaluation of buccal methyl-β-cyclodextrin toxicity on human oral epithelial cell culture model. Journal of Pharmaceutical Sciences 94: 1300–1309. doi:10.1002/jps.20350.
43. Schlievert P, Strandberg K, Brosnahan A, Haase A, Pambuccian S, et al. (2008) Glycerol monolaurate does not alter rhesus macaque (Macaca mulatta) vaginal lactobacilli and is safe for chronic use. Antimicrobial Agents and Chemotherapy 52: 4448–4454.
44. Lin Y-C, Schlievert PM, Anderson MJ, Fair CL, Schaefers MM, et al. (2009) Glycerol Monolaurate and Dodecylglycerol Effects on Staphylococcus aureus and Toxic Shock Syndrome Toxin-1 In Vitro and In Vivo. PLoS ONE 4: e7499. doi:10.1371/journal.pone.0007499.
45. Vetter SM, Schlievert PM (2005) Glycerol Monolaurate Inhibits Virulence Factor Production in Bacillus anthracis. Antimicrob Agents Chemother 49: 1302–1305. doi:10.1128/AAC.49.4.1302-1305.2005.

46. Projan SJ, Brown-Skrobot S, Schlievert PM, Vandenesch F, Novick RP (1994) Glycerol Monolaurate Inhibits the Production of Beta-Lactamase, Toxic Shock Toxin-1, and Other Staphylococcal Exoproteins by Interfering with Signal Transduction. J Bacteriol 176: 4204–4209.
47. Strandberg KL, Peterson ML, Lin Y-C, Pack MC, Chase DJ, et al. (2009) Glycerol Monolaurate Inhibits Candida and Gardnerella vaginalis In Vitro and In Vivo but Not Lactobacillus. Antimicrobial Agents and Chemotherapy 54: 597–601. doi:10.1128/AAC.01151-09.
48. Watts DH, Rabe L, Krohn MA, Aura J, Hillier SL (1999) The Effects of Three Nonoxynol-9 Preparations on Vaginal Flora and Epithelium. J Infect Dis 180: 426–437. doi:10.1086/314881.
49. Patton DL, Kiddera GG, Sweeneya YC, Rabeb LK, Hillier SL (1999) Effects of multiple applications of benzalkonium chloride and nonoxynol 9 on the vaginal epithelium in the pigtailed macaque (Macaca nemestrina). American Journal of Obstetrics and Gynecology 180: 1080–1087. doi:10.1016/S0002-9378(99)70598-3.
50. Moench TR, Mumper RJ, Hoen TE, Sun M, Cone RA (2010) Microbicide excipients can greatly increase susceptibility to genital herpes transmission in the mouse. BMC Infectious Diseases 10: 331. doi:10.1186/1471-2334-10-331.
51. Schlievert PM, Deringer JR, Kim MH, Projan SJ, Novick RP (1992) Effect of glycerol monolaurate on bacterial growth and toxin production. Antimicrob Agents Chemother 36: 626–631. doi:10.1128/AAC.36.3.626.
52. Major I, Lowry D, Malcolm K, Woolfson D, Cohen J, et al. (2010) Development of a microbicide-releasing diaphragm as an HIV prevention strategy. Conference proceedings : . Annual International Conference of the IEEE Engineering in Medicine and Biology Society IEEE Engineering in Medicine and Biology Society Conference 2010: 1089–92.
53. Ballagh SA, Brache V, Mauck C, Callahan MM, Cochon L, et al. (2008) A phase I study of the functional performance, safety and acceptability of the BufferGel® Duet (TM). Contraception 77: 130–137.
54. Schwartz JL, Ballagh SA, Creinin MD, Rountree RW, Kilbourne-Brook M, et al. (2008) SILCS diaphragm: postcoital testing of a new single-size contraceptive device. Contraception 78: 237–244. doi:10.1016/j.contraception.2008.04.118.
55. Free MJ, Srisamang V, Vail J, Mercer D, Kotz R, et al. (1996) Latex rubber condoms: predicting and extending shelf life. Contraception 53: 221–229.
56. Owen D, Katz D (1999) A vaginal fluid simulant. Contraception 59: 91–5.
57. Notari S, Tommasi C, Nicastri E, Bellagamba R, Tempestilli M, et al. (2009) Simultaneous determination of maraviroc and raltegravir in human plasma by HPLC-UV. IUBMB Life 61: 470–470–475.
58. Takeuchi Y, McClure MO, Pizzato M (2008) Identification of Gammaretroviruses Constitutively Released from Cell Lines Used for Human Immunodeficiency Virus Research. J Virol 82: 12585–12588. doi:10.1128/JVI.01726-08.
59. Derdeyn CA, Decker JM, Sfakianos JN, Wu X, O'Brien WA, et al. (2000) Sensitivity of human immunodeficiency virus type 1 to the fusion inhibitor T-20 is modulated by coreceptor specificity defined by the V3 loop of gp120. J Virol 74: 8358–8367.
60. Platt EJ, Wehrly K, Kuhmann SE, Chesebro B, Kabat D (1998) Effects of CCR5 and CD4 Cell Surface Concentrations on Infections by Macrophagetropic Isolates of Human Immunodeficiency Virus Type 1. J Virol 72: 2855–2864.
61. Wei X, Decker JM, Liu H, Zhang Z, Arani RB, et al. (2002) Emergence of Resistant Human Immunodeficiency Virus Type 1 in Patients Receiving Fusion Inhibitor (T-20) Monotherapy. Antimicrobial Agents and Chemotherapy 46: 1896–1905. doi:10.1128/AAC.46.6.1896-1905.2002.
62. World Health Organization (2010) WHO laboratory manual for the examination and processing of human semen. Geneva: World Health Organization.

4 Manufacturing scale-up of electrospun poly(vinyl alcohol) fibers containing tenofovir for vaginal drug delivery.

Published as: E. Krogstad and K.A. Woodrow, Manufacturing scale-up of electrospun poly(vinyl alcohol) fibers containing tenofovir for vaginal drug delivery. *Int J Pharm* **475**, 282–291 (2014).

4.1 ABSTRACT

Electrospun fibers containing antiretroviral drugs have recently been investigated as a new dosage form for topical microbicides against HIV-1. However, little work has been done to evaluate the scalability of the fiber platform for pharmaceutical production of medical fabrics. Scalability and cost-effectiveness are essential criteria in developing fibers as a practical platform for use as a microbicide and for translation to clinical use. To address this critical gap in the development of fiber-based vaginal dosage forms, we assessed the scale-up potential of drug-eluting fibers delivering tenofovir (TFV), a nucleotide reverse transcriptase inhibitor and lead compound for topical HIV-1 chemoprophylaxis. Here we describe the process of free-surface electrospinning to scale up production of TFV fibers, and evaluate key attributes of the finished products such as fiber morphology, drug crystallinity, and drug loading and release kinetics. Poly(vinyl alcohol) (PVA) containing up to 60 wt% TFV was successfully electrospun into fibers using a nozzle-free manufacturing-scale electrospinning instrument. Actual TFV loading in fibers increased with increasing weight percent TFV in solution, and encapsulation efficiency was improved by maintaining TFV solubility and preventing drug sedimentation during batch processing. These results define important solution and processing parameters for scale-up production of TFV drug-eluting fibers by wire electrospinning, which may have significant implications for pharmaceutical manufacturing of fiber-based medical fabrics for clinical use.

4.2 INTRODUCTION

Women under the age of 24 years have three- to six-fold higher rates of HIV-1 infection than men in the same age category in some parts of sub-Saharan Africa[1,2]. Given the lack of an effective HIV-1 vaccine and no available options for effective female-initiated prevention, there is a need for a microbicide against HIV-1 that women can use discreetly to protect themselves from infection. Products such as vaginal rings, films, and gels are being investigated as potential dosage forms for the delivery of antiretroviral agents for the prevention of HIV-1. Pericoital dosage forms are preferred by some women, but challenges such as inadequate retention, low drug loading, and the lack of sustained release capabilities have limited their effectiveness. For

example, challenges associated with low user adherence to daily gel use in some populations have been cited as a concern in the recent VOICE clinical trial[3]. Vaginal films are an alternative pericoital dosage form to gels and can be advantageous because of their compact size, ease of insertion without an applicator, and limited leakage or messiness[4,5]. However, some vaginal films exhibit relatively long dissolution times[6], and the small dosing volume combined with the low drug loadings of <~1%[7–9] may limit the effectiveness of vaginal films unless used with exceptionally potent drugs. As such, more options are needed for female-initiated protection against HIV-1 that are culturally acceptable, shelf-stable, effective, and inexpensive.

Electrospun fibers are a solid dosage form with versatility in terms of the diversity of polymers and antiviral agents that can be formulated, and they have recently been explored as a platform for vaginal drug delivery[10,11]. Fibers can be formed into multiple geometries (sheets, tubes, coatings), and conceptual dosage forms have been identified for vaginal application of fibers that are similar to vaginal films or cervical barrier devices [12]. One criteria of an ideal microbicide platform is its ability to be scaled up inexpensively, which is of particular importance for low resource settings where HIV-1 is most prevalent. Methods for scaling up the electrospinning process have already been developed and are currently being used to produce products for filtration and purification[13]. On the laboratory scale, small volumes of polymer solution are typically electrospun using a single needle electrode, syringe pump, voltage generator, and metal collector (Figure 4-1). Formats used for electrospinning scale-up include multi-nozzle, centrifuge-based, and free surface, and they have been reported to increase productivity from 0.1-1 g/h (single needle electrode) to up to 6.5 kg/h (multi-nozzle)[14,15]. The two lead technologies for the scale-up of electrospinning are multi-nozzle and free-surface electrospinning. Multi-nozzle systems contain between 2-100,000 nozzles in various configurations that can electrospin simultaneously[16]. While these systems have produced the highest reported production yield to date (6.5 kg/h), drawbacks of multi-nozzle systems include electric field shieling between nozzles and nozzle clogging[17]. Free surface electrospinning allows for self-optimization of the distance between liquid jets, with jets emerging spontaneously out of a charged polymer liquid surface. While free-surface electrospinning systems currently available have lower production rates (0.5 kg/h)[15], the ability to electrospin at higher voltages allows for the realization of a wider material space for fiber production[16].

In this work, we aimed to directly compare physical properties of drug-loaded fibers produced using needle-based electrospinning versus free-surface electrospinning. The NS-1WS500U (Elmarco, Inc.) is the only commercially available production-scale electrospinning instrument that uses similar technology to existing manufacturing instruments for free-surface

electrospinning, which is important for process transferability. The instrument employs free surface electrospinning, in which a high voltage is applied across either a wire or a rotating metal drum electrode. For the wire electrode used in this work, a moving carriage deposits polymer solution onto the wire. The polymer coating undergoes a Plateau-Rayleigh instability, resulting in the formation of many charged droplets on the wire[14]. Numerous electrospinning jets emerge simultaneously from these droplets, producing a large sheet of fibers collected on a negatively charged parallel electrode. Such a system can process much larger volumes of solution than single needle electrode systems and has been reported to produce ~200 g of fibers/h, with potential for even greater productivity by combining multiple units in series[13].

Evaluating the scale-up potential is the first step in evaluating cost-effectiveness of the fiber platform, and essential to determining its practicality as a microbicide platform and translation to clinical use. The electrospinning industry in the US has been fueled by demand for electrospun products for applications including air and water filtration, construction, and energy[16], with the

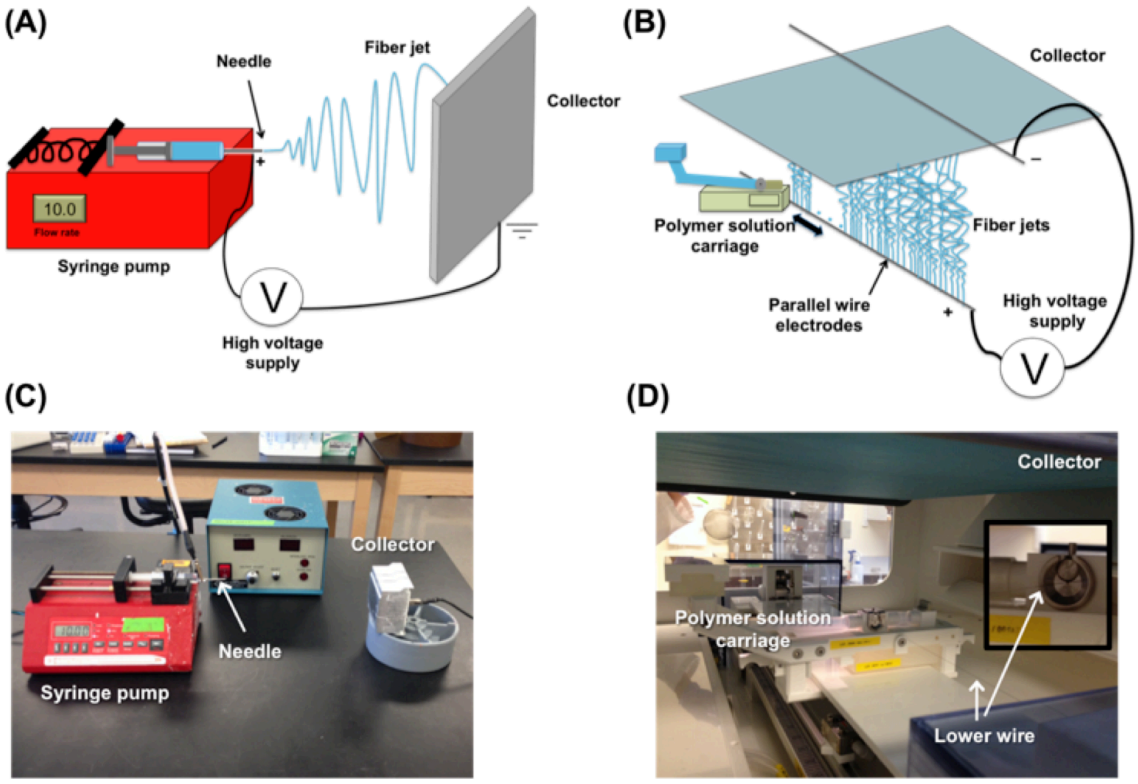

Figure 4-1. Electrospinning instrumentation for needle and wire electrode instruments. Schematic (A) and photograph (C) of laboratory scale electrospinning in which a single fiber jet is electrospun from a needle/syringe pump. Schematic (B) and photograph (D) of scale-up free surface electrospinning, where numerous fiber jets are spontaneously produced from charged polymer droplets deposited on a wire electrode. A magnified inset view of the lower wire electrode is shown in (D).

market demand for fiber products expected to reach $2.2 billion USD by 2020[15]. At least 11 corporations offer equipment for the large-scale manufacturing of electrospun nanofibers[18], and over 18 companies supply electrospun fiber products[13]. Given the existing current market for electrospun fibers for various applications, there is great potential for realizing inexpensive manufacturing of drug-loaded fibers such as those proposed in this work. Assuming a fiber dose similar to that of a vaginal film of ~300-400 mg, around 10-20 million doses/year could be produced that would be estimated to cost $0.003-0.60 USD per dose, not including APIs[16]. These estimated production rates and costs would be expected to be feasible for conducting microbicide clinical trials. However, it will be important to consider many additional factors that may affect this estimated productivity, including addition of APIs, excipients, and capital investments required to begin production.

In this report, we hypothesize that electrospun PVA fibers may be a good candidate for a quick-dissolving pericoital microbicide. The amorphous domains of partially hydrolyzed PVA allow for swelling and dissolution in water, and the large surface area of electrospun fibers may further promote fast dissolution and drug release. PVA has documented biocompatibility, being one of the primary components of the commercially available Vaginal Contraceptive Film (Apothecus). Tenofovir (TFV), a nucleotide reverse transcriptase inhibitor, has been widely investigated for HIV-1 prevention. CAPRISA 004 was the first clinical trial in which a microbicide was shown to protect against HIV-1 acquisition, with a 39% overall reduction in HIV acquisition for women in the 1% TFV vaginal gel arm, and 54% reduction for women with high gel adherence[19]. TFV has also been shown to be effective when administered orally for pre-exposure prophylaxis in three clinical trials (iPrEx, Partners PrEP, TDF2)[20–22]. Given its extensive use in antiretroviral-based prevention methods, we have selected TFV to load into PVA fibers.

Here we present our work evaluating PVA fibers as a platform for vaginal drug delivery and their potential to be scaled up for mass production. We directly compare fiber morphology, drug loading, release kinetics, and crystallinity of TFV-loaded fiber meshes electrospun using a laboratory scale needle instrument or a manufacturing scale wire instrument. Using only water as a solvent, we encapsulated up to 60 wt% TFV (wt drug/wt fiber) into electrospun fibers without compromising fiber integrity or productivity on both needle and wire instruments. Additionally, we show the ability to electrospin solid dispersions of TFV. Surprisingly, we found that electrospun fibers containing solid dispersions of drug, even when highly crystalline, may not in fact alter release kinetics under sink conditions compared to electrospun fibers containing fully solubilized drug. Where limited solubility has previously precluded the use of some

extremely hydrophobic drugs as microbicides, these results suggest that high crystallinity may not significantly impact release kinetics for electrospun fibers containing TFV. This is the first report to our knowledge of TFV fiber scale-up on a free-surface production scale electrospinning unit with direct transferability to the manufacturing scale.

4.1 MATERIALS AND METHODS

4.2.1 Solution preparation and characterization

PVA solutions were prepared by heating a proprietary blend of PVA in water (previously optimized for electrospinning on the NS-1WS500U) at 80°C until the polymer was completely dissolved. TFV (a gift from CONRAD) was added to polymer solutions at 0, 5, 10, 20, 40, 60, and 80 wt% TFV theoretical drug loading (defined as mass drug/mass fiber). Drug precipitate was observed in all pH-unadjusted (pH 3) TFV solutions. Given that TFV has a pKa of 4.1[23], we hypothesized that by increasing the pH, we could increase drug solubility in the polymer solutions. The pH of each of the TFV-containing solutions was adjusted from pH ~3.3 to a final pH of 7.0 using 10 M sodium hydroxide. A bench top conductivity meter (Thermo Scientific Orion Star A212), pH meter (Thermo Scientific Orion Star A111), and surface tensiometer (Kibron AquaPi) were used to measure solution parameters in duplicate for both pH 3 and pH 7 solutions. Solution viscosity was measured using an ARG2 rheometer (TA Instruments) fitted with cone and plate geometry (1°58'48" cone angle, 40 mm diameter). A frequency sweep test was performed with a constant strain of 0.04 and ramping up angular frequency from 1-628.3 rad/s at 10 points/decade.

4.2.2 Electrospinning parameter optimization

We established electrospinning parameters for PVA solutions containing 0, 5, 10, 20, 40, and 60 wt% TFV. For small-scale electrospinning, we used a needle instrument apparatus in our lab consisting of a 30 kV voltage generator (Gamma High Voltage Research, Inc.), syringe pump (KD Scientific, Inc.), and flat metal block as a grounded collector. Parameters that were varied included flow rate (10-100 µL/min), voltage (15-20 kV), and distance to collector (9-21 cm). Observations of the formation of fiber meshes on the collector, the presence of a Taylor cone, and dripping solution were recorded for each set of parameters. One fiber mesh from 500 µL of polymer solution was electrospun for each pH 3 and pH 7 solution using the optimal electrospinning parameters (i.e., the fastest flow rate possible for which no dripping was observed). Because of our interest in comparing the properties of fibers electrospun using a large-scale instrument and with our small-scale laboratory system, we also electrospun these

solutions into nanofiber meshes using a Nanospider™ (NS) 1WS500U large-scale production instrument (Elmarco, Inc., Czech Republic). NS-1WS500U (wire instrument) parameters were optimized by increasing the voltage until fiber strands were visible. Orifice size, carriage speed, and distance to collector were also adjusted to result in fiber production. We scaled up our production by electrospinning fiber meshes from ~20 mL of solution for each of the TFV solutions. The 10 wt% and 60 wt% TFV meshes were chosen to move forward with for fiber mesh characterizations to represent low and high drug loading.

4.2.3 Physical characterization of fiber mesh

Fiber diameter and morphology for each mesh was characterized using scanning electron microscopy (SEM). Meshes were sputtered with gold/palladium for 70 s and imaged with SEM (JSM-7000F, JEOL Ltd.) with 5,000x magnification, 5-10 kV, and 10 mm working distance. Fiber size was determined using ImageJ (NIH) by measuring fibers that intersected a diagonal line drawn across each 5,000x micrograph, with n=45 fibers measured for each sample. Mass productivity was characterized by massing the amount of fibers recovered for a given volume (500 µL for small scale) or run time (30 min for large scale). Mesh thickness was measured using calipers, with n=3 measurements in random locations on the fiber mesh.

4.2.4 Drug loading and release

We evaluated actual drug loading and encapsulation efficiency by dissolving ~5-6 mg pieces of electrospun mesh in 20-40 mL citrate buffer (25 mM, pH 4.3) or phosphate buffered saline (PBS, pH 7.4). These conditions were chosen to simulate normal vaginal pH (~4-6) and the pH of semen (~7-8). Drug loading was calculated as mass of drug / total mass of fiber. Encapsulation efficiency was calculated as the actual amount of drug loaded in fibers / theoretical amount of drug in fiber, accounting for the mass of sodium hydroxide used to pH-adjust solutions. Drug content was measured for triplicate mesh samples using high performance liquid chromatography (HPLC). Release kinetics were monitored at two pH values relevant to vaginal drug delivery. Citrate buffer (25 mM, pH 4.3) or PBS (150 mM, pH 7.4) were added to fiber samples to establish sink conditions (i.e., sufficient volume to be below the solubility limit of TFV), and 200 µL samples were taken at 5 min, 1h, 4h, and 24h. Drug content in release media was evaluated using HPLC methods. A Shimadzu Prominence LC20AD HPLC system and LC Solutions software was used to quantify TFV content. A Luna C18 column with 5 µm particle size and 250x4.6 mm dimensions (Phenomenex, Torrance, CA) was used for analysis, run isocratically at a flow rate of 1.0 mL/min. The mobile phase consisted of a mixture of 0.045% trifluoroacetic acid (TFA) in HPLC grade water and 0.036% TFA in HPLC grade

acetonitrile at a 72:28 ratio (v/v). TFV was detected at 259 nm with a retention time of 2.3 min. Standard solutions of TFV were prepared at 200 µg/mL in citrate buffer (25 mM, pH 4.3) or PBS and diluted to generate the calibration curves. Analysis methods were validated with standard solutions and spiked samples to ensure no interference from blank polymer fibers. Linearity was established from 1 µg/mL to 200 µg/mL in citrate buffer using a 20 µL injection volume. A separate standard curve was created for TFV in PBS for release studies conducted in PBS, with linearity from 0.5 µg/mL to 200 µg/mL.

4.2.5 Dissolution

We performed dissolution studies in sink conditions in parallel with release studies in both PBS and citrate buffer. Dissolution was monitored visually at 5 min, 1 h, 4 h, 8 h, and 24 h by rating using a qualitative scale from 0-4, with 0 being fibers completely undissolved and 4 being fibers fully dissolved. Ratings were assigned as follows: 0 = fiber mesh intact; 1= fibers wet out; 2= fiber mesh broken into large pieces; 3= fiber mesh broken into small pieces (less than a pinhead in size); 4= fiber mesh fully dissolved (no mesh visible by eye).

4.2.6 Differential scanning calorimetry

The amount of TFV in crystalline versus amorphous state was measured using differential scanning calorimetry (DSC). Samples were prepared by massing 6-7 mg of fibers and firmly packing fibers together before placing in aluminum pans. Pans were punctured with a needle to allow volatiles to escape prior to measurements. Temperature was ramped from 25-350°C at 10°C/min with 0.20 s/pt sampling interval under 50 mL/min nitrogen gas purge using a Q20 Differential Scanning Calorimeter (TA Instruments). TA Universal Analysis software (TA Instruments) was used to analyze data. Melting endotherms were integrated using sigmoidal tangential integration. The heat of fusion for TFV was determined by integrating the endothermic peak corresponding to the melting temperature of TFV at 283°C. Relative drug crystallinity was calculated as the heat of fusion of TFV in fibers (ΔH_f) relative to the heat of fusion of TFV powder (ΔH_f^0), corrected for mass fraction of TFV in the sample (w_{drug}) determined from actual drug loading measurements (Equation 1).

$$Relative\ drug\ crystallinity = \frac{\Delta H_f}{w_{drug} * \Delta H_f^0} \times 100 \qquad \text{(Equation 1)}$$

Normalized polymer crystallinity was calculated using Equation 2, with ΔH_f being the area of the melting endotherm for PVA at 193°C, ΔH_f^0 as the heat of fusion for 100% crystalline PVA (ΔH_f^0 = 138.6 J/g)[24], and $w_{polymer}$ being the mass fraction of polymer in the sample.

$$Normalized\ polymer\ crystallinity = \frac{\Delta H_f}{w_{polymer} * \Delta H_f^0} \times 100 \qquad \text{(Equation 2)}$$

4.2.7 X-ray Diffraction

Diffractograms for ground TFV powder, blank PVA fibers, and 60 wt% TFV fibers (pH 3 and pH 7) were obtained using a Bruker F8 Focus Powder X-ray Diffractometer. Nickel-filtered CuKα radiation was used in the 2θ range of 5–32° at 40 kV and 40 mA. SEM, DSC, and XRD were performed at the Materials Science and Engineering Department at the University of Washington.

4.2.8 Stability Studies

Drug release kinetics, drug and polymer crystallinity, and fiber morphology of four fiber formulations stored under varying temperature and humidity conditions were compared. Samples of fibers spun on the wire electrode instrument were stored under laboratory conditions for 12 months and compared to samples placed in an accelerated temperature/humidity chamber for an additional 30 days. Laboratory conditions refer to samples that were stored under vacuum desiccation for 6 months, heat-sealed in a plastic bag, and stored for an additional 7 months at room temperature and humidity. Accelerated conditions refer to samples stored under laboratory conditions for 12 months and then stored under high heat (40°C) and relative humidity (75% R.H.) for 30 days. We used a custom-built humidity chamber that consisted of a closed box containing a vial with saturated sodium chloride solution to establish 75% R.H. [25], and placed the chamber in an incubator to maintain 40°C. Release studies were performed in 25 mM citrate buffer as previously described. Fiber morphology and drug/polymer crystallinity were characterized using SEM and DSC, respectively, as previously described. SEM for stability studies was performed using a Sirion SEM (FEI) at the Molecular and Nanotechnology User Facility at the University of Washington, a member of the NSF National Nanotechnology Infrastructure Network (NNIN).

4.2.9 Statistics

Data are displayed as mean ± standard deviation unless otherwise indicated. Student's t-tests (two-tailed with unequal variance) were performed to assess differences between encapsulation efficiency between the needle wire instruments, with statistical significance defined as $p<0.05$. Supplementary information (figures and tables) is located in Appendix C.

4.3 RESULTS AND DISCUSSION

4.3.1 Electrospinning parameter optimization

Using both a custom-built, small-scale laboratory system (needle electrode) and a commercial production electrospinning instrument (wire electrode), we successfully fabricated PVA fibers containing up to 60 wt% TFV. All electrospinning solutions were transferrable between the needle and wire instruments, and did not require changes to any solution properties such as conductivity, viscosity, surface tension, or pH to fabricate fibers from either platform (Table 4-1). PVA solutions containing TFV had measured pH values of 3.3-5.3, conductivity of 0.075-0.201 mS/cm, surface tension of 62.5-67.0 mN/m, and viscosity of 0.45-2.52 Pa*s. Viscosity increased by approximately 5-fold for the 60 wt% TFV (pH 3) solution relative to the other solutions, and was likely due to large amount of undissolved drug present in the solution at acidic pH. While it has previously been established that viscosity increases with the volume fraction of solids in solution[26], this change in viscosity was still within the range of values for productive electrospinning.

Table 4-1. Electrospinning solution properties for PVA solutions containing 0, 10, or 60 wt% TFV

	pH	Volume of NaOH added (mL) [b]	Conductivity (mS/cm)	Surface Tension (mN/m)	Viscosity (Pa*s) [c]
0% TFV, pH 5	5.31 ± 0.01	--	0.075 ± 0.000	62.9 ± 0.4	0.458 ± 0.014
0% TFV, pH 7	6.95 ± 0.00	0.004	0.111 ± 0.000	67.0 ± 1.1	0.486 ± 0.013
10% TFV, pH 3	3.33 ± 0.01	--	0.201 ± 0.001	62.5 ± 0.8	0.454 ± 0.006
10% TFV, pH 7	6.89 ± 0.02	0.200	2.230 ± 0.006	63.4 ± 0.3	0.701 ± 0.360
60% TFV, pH 3	3.32 ± 0.01	--	0.175 ± 0.002	67.0 ± 5.0	2.515 ± 0.226
60% TFV, pH 7	6.94 ± 0.01	2.940	14.94 ± 0.099	62.3 ± 0.1	0.457 ± 0.008

[a]Values represent average of duplicate measurements ± standard deviation.
[b]Volume of NaOH refers to amount of 10 M NaOH necessary to adjust ~40 mL batch of polymer solution to pH ~7.
[c]Viscosity is reported at an angular frequency of 10 rad/s.

Increasing the solution pH above the pKa of TFV enhanced drug solubility and resulted in homogenous rather than colloidal solid suspensions. However, both types of solutions showed similar surface tension and viscosity. As expected, addition of sodium hydroxide to increase pH resulted in higher solution conductivity (Table 4-1). For example, TFV solutions of 10 wt% and 60 wt% adjusted to pH 7 resulted in a 11-fold and 85-fold increase in solution conductivity compared to similar solutions at pH 3. The homogenous and colloidal solid suspensions were equally electrospinnable from the nozzle and wire electrodes, which allowed us to investigate the impact from electrospinning solid dispersions on the finished fibers (discussed below).

Optimized parameters for electrospinning TFV-loaded PVA fibers on both the needle and wire instruments are given in Supplementary Table 1. Because the needle and wire

electrospinning systems use different electrospinning processes, it is difficult to directly correlate parameters used for each system. In the needle system, the polymer solution is mechanically forced through a needle by a syringe pump at a controlled flow rate and deposited onto a grounded metal surface. In contrast, a moving carriage is used in the free-surface system to deposit droplets of polymer solution onto a wire electrode, and fibers are pulled upward toward a parallel negatively charged wire electrode.

While this needle system produces fibers from only one Taylor cone, hundreds of Taylor cones can be simultaneously produced using the wire electrode system[14]. As expected, mass productivity greatly increased for fibers electrospun on the wire compared with the needle instrument, with 2.9-7.6 g/h produced using the wire electrode (for a single wire with length of 25 cm), and 0.04-0.14 g/h for a single needle electrode. We also observed increasing productivity with increasing drug loading, particularly for the needle instrument. This trend is likely due to the increased mass of drug in solution for electrospinning, which is not accounted for in the mass productivity calculation.

4.3.2 Physical properties of fibers electrospun using needle versus wire instruments

We observed that the needle and wire electrodes produced materials with similar mesh and fiber properties (Table 4-2). Fiber mesh thickness was approximately 50-220 μm and fiber diameter was approximately 200-300 nm. Fiber diameter decreased with increasing drug loading for both the needle and wire instruments, except for formulations used to fabricate 60 wt% TFV (pH 7) fibers. The wire instrument also produced fibers with slightly smaller diameters compared with the needle instrument. We attribute these differences to greater solution conductivity with increasing drug loading, and greater overall electric field strength for the wire

Table 4-2. Physical properties of electrospun meshes on needle v. wire instruments

	Fiber Diameter[a] (nm)		**Thickness[b] (mm)**		**Mass Productivity[c] (g/h)**	
	Needle	Wire	Needle	Wire	Needle	Wire
0% TFV, pH 5	301 ± 84	265 ± 68	0.07 ± 0.01	0.08 ± 0.01	0.043	5.54
0% TFV, pH 7	296 ± 87	243 ± 69	0.09 ± 0.00	0.12 ± 0.01	0.058	6.94
10% TFV, pH 3	205 ± 34	176 ± 55	0.14 ± 0.01	0.10 ± 0.01	0.067	5.56
10% TFV, pH 7	188 ± 44	155 ± 59	0.17 ± 0.02	0.05 ± 0.02	0.060	2.89
60% TFV, pH 3	184 ± 44	141 ± 65	0.22 ± 0.01	0.18 ± 0.01	0.135	7.64
60% TFV, pH 7	320 ± 70	242 ± 81	0.11 ± 0.03	0.05 ± 0.01	0.093	5.53

[a]Fiber diameter represents average ± standard deviation (n=45 fibers).
[b]Thickness values represent average of triplicate measurements ± standard deviation.
[c]Mass productivity is defined as mass of final mesh divided by time to electrospin for 500 uL volume (needle) or 30 min run time (wire), with n=1. Wire length=25 cm; Wire diameter=0.2 mm.

compared to needle electrode ($5.4x10^5$ V/m and $1.6\text{-}2.2x10^5$ V/m, respectively).

The fiber meshes were generally white in color, soft, and flexible, with the exception of meshes of the 60 wt% TFV (pH 7) fibers, which displayed variable delamination and brittleness after storage on vacuum. That is, we observed that these fiber meshes contained separate layers that peeled apart or became stiff upon storage. Meshes with a similarly high TFV loading but fabricated without sodium hydroxide did not exhibit delamination or brittleness. Therefore, we expect that these physical properties are not due to high drug content but are a result of base catalyzed hydrolysis of the acetyl groups on the PVA polymer, which result in hydroxyls that can participate in interchain hydrogen bonding. Further studies are needed to quantify the actual mechanical changes in fibers resulting from pH adjustment and storage conditions.

Electrospinning solid dispersions of TFV resulted in fibers with visible solid deposits that we attribute to TFV drug crystals. SEM images of fibers electrospun on the needle and wire instrument show that the finished fibers have a generally smooth and cylindrical morphology (Figure 4-2). Of particular note, the 60 wt% TFV formulations that were pH-adjusted with base (pH 7) produced fibers with fused morphology and diameters that were 100-130 nm larger than

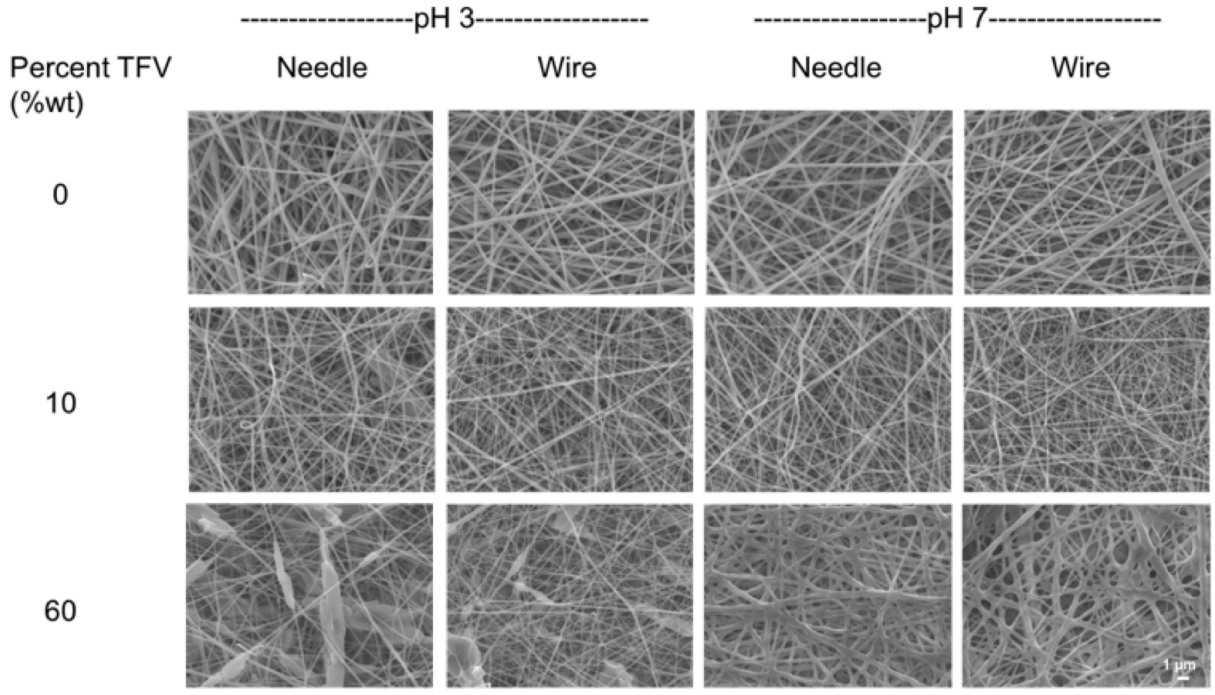

Figure 4-2. Fiber morphology is consistent between needle and wire electrospinning for fibers containing up to 60 wt% TFV. SEM images of PVA fibers containing 0, 10, or 60 wt% TFV from needle instrument (laboratory scale) and wire instrument (manufacturing scale). Images of both unadjusted (pH 3) and pH 7 fibers are displayed. Scale bar = 1 µm.

fibers formulated from pH-unadjusted solutions (pH 3). This observation was similar on both the needle wire instruments. The larger diameter may be caused by sodium hydroxide used to adjust pH mediating increased inter- and intra-chain hydrogen bonding, resulting in decreased chain flexibility during electrospinning. Taken together, these results indicate that physical properties of TFV fabrics based on PVA are consistent between fibers electrospun using laboratory scale needle-based electrospinning and manufacturing scale wire electrode electrospinning.

4.3.3 Drug loading is consistent between needle and wire electrospinning

Encapsulation efficiency, drug loading, and drug crystallinity were compared between meshes with 10 wt% and 60 wt% TFV drug loading to understand the influence of drug content on the electrospinning process and resulting materials. We found that actual drug loading and encapsulation efficiency of TFV was comparable between needle and wire electrospinning. Actual TFV loading was found to increase with increasing TFV content in solution (Table 4-3). As expected, encapsulation efficiency was improved from ~75-80% to nearly 100% when solution pH was adjusted to maintain TFV solubility compared with electrospinning solid dispersions of TFV (Figure 4-3). The only significant difference observed between actual drug loading and encapsulation efficiency values for needle versus wire electrospinning was for the 60 wt% TFV (pH 3) fibers, in which the fibers produced with the wire instrument had a ~10% decrease in absolute actual drug loading compared with the fibers produced with the needle instrument. We attribute this difference to the settling of drug precipitate in the carriage tube during electrospinning with the wire instrument, leading to a lower actual drug encapsulation. This problem may be overcome by more uniformly micronizing the drug prior to electrospinning or by actively mixing the polymer solution in the reservoir during electrospinning.

Table 4-3. Actual drug loading and crystallinity of fibers electrospun from needle or wire electrodes.

	Actual Drug Loading[a] (wt%)		**Relative drug crystallinity[b] (%)**	
	Needle	Wire	Needle	Wire
0% TFV, pH 5	0	0	nd	nd
0% TFV, pH 7	0	0	nd	nd
10% TFV, pH 3	7.5	7.3	nd	nd
10% TFV, pH 7	9.4	9.4	nd	nd
60% TFV, pH 3	59.2	49.7	96.1	96.3
60% TFV, pH 7	52.4	51.9	nd	2.0

[a]Actual drug loading represents average measured by dissolving meshes in citrate buffer (n=3).
[b]Relative drug crystallinity was calculated from differential scanning calorimetry (DSC) thermograms and is reported as percentage of crystalline TFV in fibers relative to the heat of fusion of TFV drug in powder form, correcting for mass fraction of drug in sample. Nd=not detected.

Interestingly, fibers were able to incorporate a remarkably high drug loading of up to 60% of TFV by mass. We also attempted to electrospin a PVA solution containing 80% TFV (pH adjusted to 7) on the wire instrument, but no fiber formation was observed. Therefore, we expect the upper limit of drug loading to be between 60-80 wt% TFV in this fiber formulation using the wire instrument. Antiretroviral-containing vaginal films in development have been reported to have drug loadings of 0.04 - 1.4% (w/w)[7–9]. Thus, the nanofiber platform appears to offer potential for much higher drug loadings than can be obtained with published film formulations.

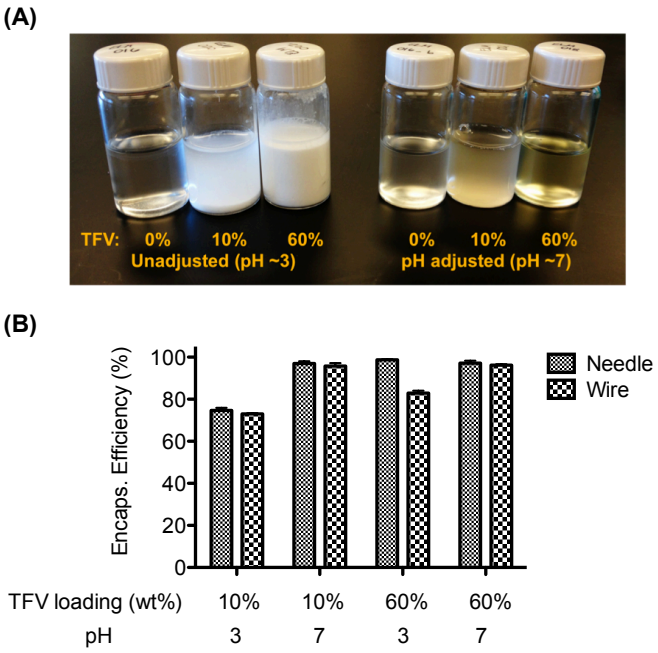

Figure 4-3. Electrospinning solid suspensions of TFV results in reduced encapsulation efficiency. (A) The solubility of TFV in polymer solutions is visibly improved by using sodium hydroxide to raise solution pH. (B) The increased solubility of TFV in solution translates to an increased encapsulation efficiency of TFV in PVA nanofibers, measured by analyzing drug content in dissolved fibers with HPLC.

Achieving high drug loading is advantageous in that it allows for drugs with a wider range of potency to be delivered in addition to minimizing the mass of final product that must be administered. For example, to deliver a 40 mg dose of TFV that is consistent with what was used in the CAPRISA 004 trial[19], a fiber mesh ranging from 67-400 mg would need to be administered for 60 wt% and 10 wt% loaded fibers, respectively. While vaginal films in development have been dosed at comparable masses of 90-400 mg [7,9,27], to achieve an equivalent dose of 40 mg of TFV at the currently published drug loading of ~1.4% (w/w) would necessitate a vaginal film mass of ~3,000 mg.

4.3.4 Drug and polymer crystallinity

Relative drug crystallinity was found to be similar for fibers electrospun from the wire compared to the needle electrode (Figure 4-4, Table 4-3). The DSC thermograph we obtained for TFV is consistent with previously observed results[28] that shows a broad peak near 100°C indicative of release of water from monohydrate form of TFV, recrystallization of drug at 210°C, melting at approximately 280°C, and exothermic degradation above 300°C. For 60 wt% TFV fibers (pH 3) electrospun using both the needle and wire electrode, a large melting endotherm was observed near 290°C that correlates to a 96% relative drug crystallinity. In contrast, for 60 wt% TFV fibers (pH 7), this peak was absent and indicated that only a small amount of loaded TFV (0-2%) is in the crystalline form relative to TFV drug powder. A small second peak was observed near ~270°C for this sample only that we attribute to an alternate drug crystal packing conformation. The high relative drug crystallinity in 60 wt% TFV (pH 3) samples is expected because of the presence of solid dispersions of TFV drug in pH-unadjusted (pH 3) solutions and resulting fibers, as confirmed by SEM micrographs. Upon increasing the solution pH to 7, TFV was completely solubilized and resulted in homogenous electrospinning solutions. No peaks were detected for 10% TFV solutions (either pH 3 or pH 7). Results from DSC were consistent with XRD data on the same samples, indicating that a greater amount of crystalline TFV is present in 60 wt% TFV fibers that contain solid dispersions (pH 3) compared to 60 wt% TFV fibers (pH 7) (Supplementary Fig. 1).

The melting temperature of the PVA polymer was found to be 193°C and is evident in all fiber samples, except for 60 wt% TFV (pH 7) samples, which had no peaks near this temperature. TFV-containing fiber samples resulted in a 4-8°C decrease in the polymer melting temperature relative to pure PVA powder or blank PVA fibers, likely due to drug molecules disrupting the hydrogen bonding between PVA chains (Supplementary Table 2). Similar additive-induced melting temperature depression has been observed previously and attributed to disruption of the crystal structure [29–31]. Blank PVA fibers and PVA powder had similar nominal values of polymer crystallinity of approximately 29%. There was minimal change in polymer crystallinity for 10% TFV fibers samples compared to blank PVA fibers. In contrast, normalized polymer crystallinity was reduced to ~22% for fibers with 60 wt% TFV loading (pH 3). No Tm peak was detected for PVA in the 60 wt% TFV (pH 7) samples. Since this peak was absent for only the 60 wt% TFV (pH 7) fibers, we expect that the high volume of sodium hydroxide needed to pH-adjust these solutions influenced the final polymer crystal structure and also affected the bulk physical properties of these fibers. Overall, there is a trend for decreasing PVA crystallinity with increasing TFV loading. In addition, these results suggest that both polymer and drug

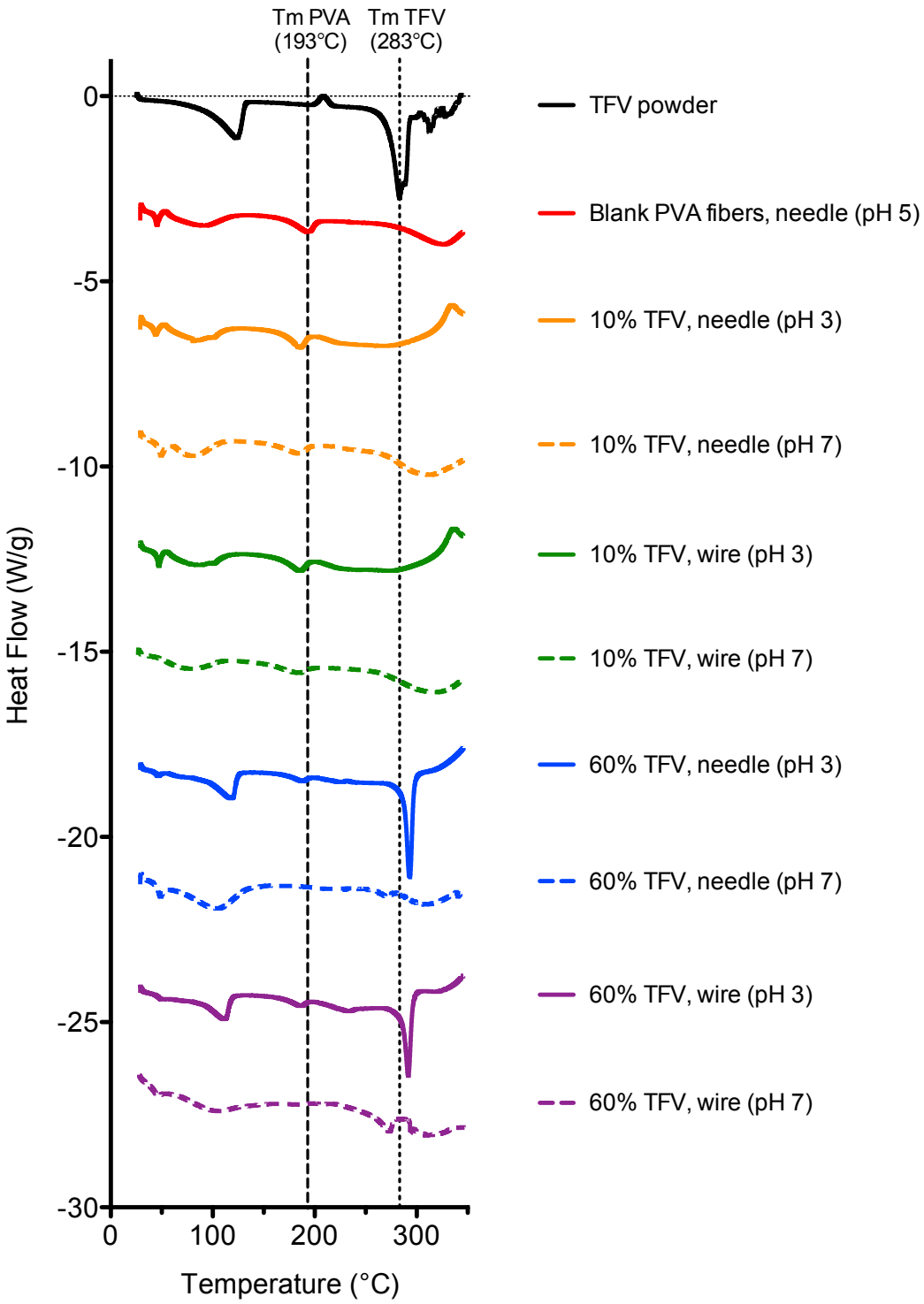

Figure 4-4. Increasing TFV solubility prior to electrospinning reduces the final crystalline drug content in fiber meshes. Representative DSC thermograms of TFV-containing fibers and controls (TFV drug standard and blank PVA fibers) are displayed here. While a large peak indicative of crystalline drug is present for unadjusted 60 wt% TFV fibers, fibers made from pH-adjusted 60 wt% TFV solutions do not have this peak. Vertical lines indicate the melting temperatures of PVA (193°C) and TFV (283°C) standards.

crystallinity in fibers is similar for needle and wire electrospinning systems, and that solid dispersions of drug result in increased drug crystallinity in the final fibers.

4.3.5 Quick fiber dissolution and burst release of TFV from electrospun meshes

Burst release of >95% TFV from fibers was observed within 5 min for nearly all formulations under sink conditions in both PBS (pH 7.4) and citrate buffer (pH 4.3) (Figure 4-5). Release kinetics were consistent between the small scale needle instrument and large scale wire instrument. While reduced drug crystallinity has previously been associated with faster release[32,33], we observed only a small impact of TFV crystallinity on the release rate. Burst release occurred for all fiber formulations regardless of their crystallinity, with a slightly prolonged release of about 85% of total contents within 5 min for needle-based 60 wt% TFV fibers (pH 3). We hypothesize that the electrospinning process constrained the size of crystals

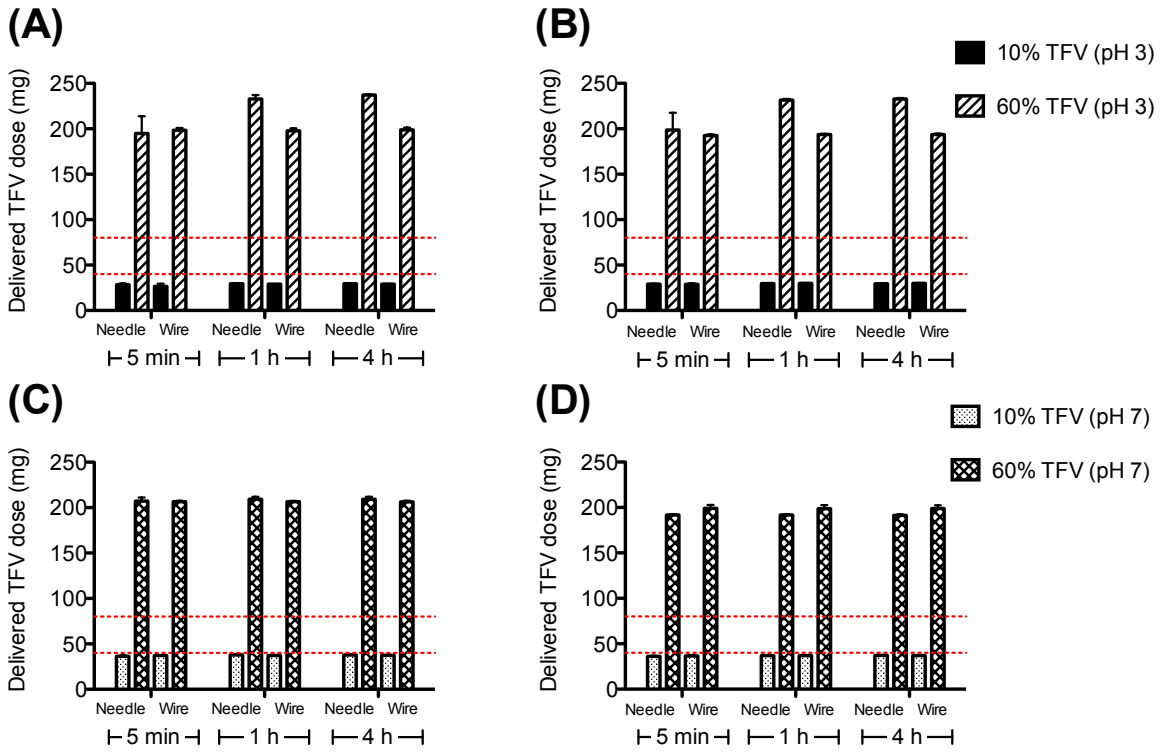

Figure 4-5. Burst release of TFV within 5 min at pH 4.3 and 7.4 is similar for meshes electrospun using both needle and wire instruments. Graphs display cumulative release of TFV in pH 4.3 citrate buffer (A, C) or pH 7.4 PBS (B, D) for fibers spun on needle versus wire instruments. Release from fibers incorporating solid dispersions of TFV (solution unadjusted at pH 3) are displayed in (A) and (B), and release from fibers from solutions adjusted to pH 7 are shown in (C) and (D). The y axis shows delivered dose TFV per 400 mg fiber mesh, with red lines indicating the recommended range for daily vaginal application (40-80 mg). 100% release corresponds to ~40 mg delivered dose for 10% TFV fibers and ~240 mg delivered dose for 60 wt% TFV fibers.

that were incorporated into final fiber meshes to a threshold below which differences in crystalline state have an indistinguishable impact on release rate.

All TFV-containing fibers were qualitatively observed to dissolve completely within 1 h in both PBS and citrate buffer, with most samples dissolving in 5 min or less (Supplementary Table 3). Notably, drug-containing fibers dissolved more quickly than blank fibers in citrate buffer (pH 4.3), possibly due to the more intact polymer crystalline structure present within blank fibers. Because of the quick fiber dissolution and the hydrophilic nature of both PVA and TFV, monophasic burst release was expected from these polymeric fibers. Such a release profile may be beneficial for pericoital microbicides in which it is desirable to have having high concentrations of drug that is immediately bioavailable (i.e., drug that is dissolved and able to be taken up by cells, as opposed to locked in solid dispersions). These studies were performed under sink conditions to better understand the material properties of the nanofiber delivery system. Further release and dissolution studies evaluating drug release kinetics and fiber dissolution in low volumes of fluid will be important to better understand translation of these systems for intravaginal drug delivery.

4.3.6 Stability Studies

We found that the actual drug content did not change for fiber samples stored under both laboratory and accelerated storage conditions (Supplementary Fig. 2). Additionally, the storage conditions tested did not affect release kinetics for PVA fibers containing 10 and 60 wt% TFV for both unadjusted and pH-adjusted fibers, with all fiber formulations releasing >95% of total drug content within 1 h.

Storage conditions had little effect on polymer melting temperature, polymer crystallinity, or TFV crystallinity for fiber samples stored under laboratory or accelerated conditions, except for 60 wt% TFV (pH 7) fibers (Figure 4-6). For this sample, we observed a large peak near ~160°C for the 13 mo. room temp/humidity condition only, suggesting a change in polymer crystallinity. Relative drug crystallinity for 60 wt% TFV (pH 7) fiber samples corresponding to the peak at 293°C remained at <2% of the total TFV content, despite differing storage conditions (Supplementary Table 4). A second peak around ~270°C observed only for the 60 wt% TFV (pH 7) fiber samples increased in size upon long-term storage, corresponding to an increase in relative drug crystallinity of 18% (freshly electrospun) to 35% (both laboratory and accelerated conditions). The increase in crystallinity in this sample did not result in a change in drug release kinetics, supporting our hypothesis that electrospun fibers may constrain crystal size below a

threshold where changes in crystallinity do not significantly impact drug release.

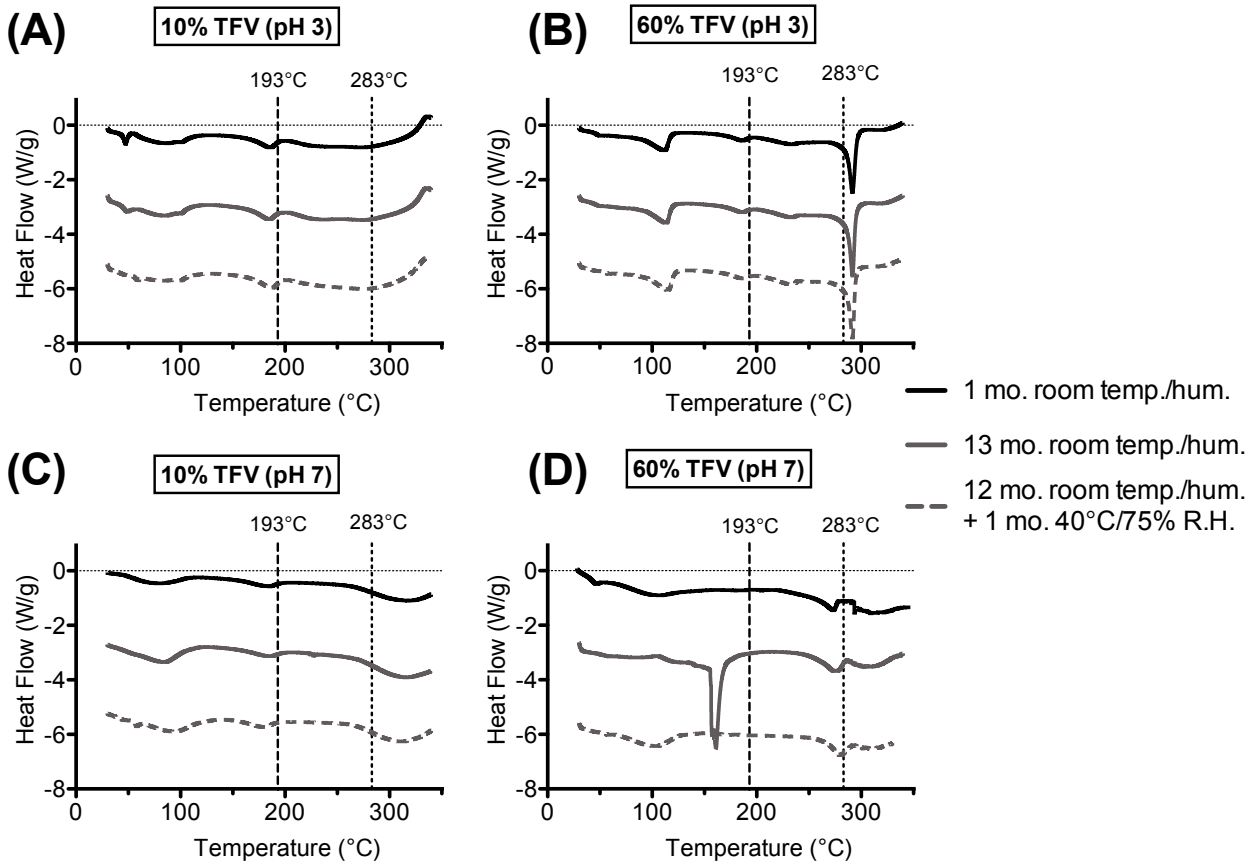

Figure 4-6. Drug and polymer crystallinity are minimally impacted by storage conditions. DSC thermograms indicate minimal effect of storage condition on polymer or drug crystallinity, with the exception of fibers containing 60 wt% TFV (pH 7). Conditions include original electrospun fibers (<1 month storage at room temperature and humidity), fibers stored for 13 months under laboratory conditions (room temperature and humidity), and samples stored for 12 months under laboratory conditions and an additional 30 days at 40°C / 75% R.H.

Morphology of fiber meshes remained similar for fibers stored under laboratory conditions compared with fibers stored at accelerated temperature and humidity (Supplementary Fig. 3). Fiber diameter increased for both storage conditions compared with freshly electrospun meshes, but this change did not impact drug release kinetics. We also observed an increase in fusing of 60 wt% TFV (pH 7) meshes for both storage conditions compared to the freshly electrospun mesh.

The minimal changes we observed in crystallinity, drug loading, release, and morphological properties of TFV-PVA fiber meshes suggest that they are stable over 12 months under laboratory conditions and for at least 30 days at high humidity and temperature. The accelerated

condition of this study may be limited in that 75% R.H. may not have been maintained throughout the entire period due to water absorption by the PVA fibers. Future studies will need to accommodate water absorption by the fibers to maintain constant humidity.

4.4 CONCLUSION

In this work, we established parameters for electrospinning PVA solutions containing 0-60 wt% TFV into fibers. We successfully transferred materials used to electrospin TFV-PVA fibers from a laboratory scale system to a production scale system, demonstrating that both systems can be used to produce fibers with similar morphologies, drug loading, and release kinetics. Additionally, we found that while solid dispersions of TFV can be successfully electrospun into fibers at loadings of up to 60 wt% by mass, fibers containing fully solubilized TFV had enhanced encapsulation into fibers and reduced drug crystallinity. Degree of crystallinity was not found to impact release rate under sink conditions for these formulations. However, high drug crystallinity affect biodistribution by reducing drug solubility, in addition to influencing the mechanical properties and uniformity of fiber meshes.

Physical characterization of fiber meshes including mechanical testing of fibers, evaluating the transition into "gel-like" material in low volumes of fluid, and post-dissolution studies to assess osmolarity, pH, and rheology of hydrated fibers will be critical for moving a microbicide formulation forward[4]. These characterizations have not been performed for these TFV-PVA formulations, as the focus of this work was to evaluate the potential for scale-up of drug-loaded fibers from a laboratory scale to a manufacturing scale. Future work will investigate properties such as pH, osmolarity, and rheology of electrospun fibers post-dissolution in physiologically relevant conditions.

Overall, given the comparability of needle and wire electrospinning instruments in terms of fiber morphology, drug loading, encapsulation efficiency, and release kinetics, these results support the potential for scale-up of TFV-loaded fibers. The transferability of electrospun fibers to manufacturing scale justifies continued investigation of fibers for use as topical microbicides.

4.5 ACKNOWLEDGEMENTS

The research was supported by a grant from the Bill and Melinda Gates Foundation (OPP1067729) and the National Institutes of Health (AI09864801) to KAW. EK was supported by a NSF graduate research fellowship. Assistance with solution property characterization and XRD was provided by Rick Edmark and Christina Nhan. We thank Rick Edmark and Shih-Feng Chou for critical discussions and review of the manuscript.

4.6 REFERENCES

1. Gengiah, T. N. & Abdool Karim, Q. Implementing microbicides in low-income countries. *Best Pract. Res. Clin. Obstet. Gynaecol.* **26,** 495–501 (2012).
2. Glynn, J. R. *et al.* Why do young women have a much higher prevalence of HIV than young men? A study in Kisumu, Kenya and Ndola, Zambia. *AIDS Lond. Engl.* **15 Suppl 4,** S51–60 (2001).
3. Microbicide Trials Network. *Daily HIV Prevention Approaches Didn't Work for African Women in the VOICE Study*. (2013). at <http://www.mtnstopshiv.org/node/4877>
4. Garg, S. *et al.* Advances in development, scale-up and manufacturing of microbicide gels, films, and tablets. *Antiviral Res.* **88,** S19–S29 (2010).
5. Nel, A. M., Mitchnick, L. B., Risha, P., Muungo, L. T. M. & Norick, P. M. Acceptability of Vaginal Film, Soft-Gel Capsule, and Tablet as Potential Microbicide Delivery Methods Among African Women. *J. Womens Health* **20,** 1207–1214 (2011).
6. CAMI Multipurpose Prevention Technologies for Reproductive Health: 2011 Think Tank. in 1–34 (2011).
7. Akil, A. *et al.* Development and characterization of a vaginal film containing dapivirine, a non-nucleoside reverse transcriptase inhibitor (NNRTI), for prevention of HIV-1 sexual transmission. *Drug Deliv. Transl. Res.* **1,** 209–222 (2011).
8. Sassi, A. B. *et al.* Formulation Development of Retrocyclin 1 Analog RC-101 as an Anti-HIV Vaginal Microbicide Product. *Antimicrob. Agents Chemother.* **55,** 2282–2289 (2011).
9. Ham, A. S. *et al.* Vaginal Film Drug Delivery of the Pyrimidinedione IQP-0528 for the Prevention of HIV Infection. *Pharm. Res.* **29,** 1897–1907 (2012).
10. Huang, C. *et al.* Electrospun cellulose acetate phthalate fibers for semen induced anti-HIV vaginal drug delivery. *Biomaterials* **33,** 962–969 (2012).
11. Ball, C., Krogstad, E., Chaowanachan, T. & Woodrow, K. A. Drug-Eluting Fibers for HIV-1 Inhibition and Contraception. *PLoS ONE* **7,** e49792 (2012).
12. Blakney, A. K., Ball, C., Krogstad, E. A. & Woodrow, K. A. Electrospun fibers for vaginal anti-HIV drug delivery. *Antiviral Res.* **100, Supplement,** S9–S16 (2013).
13. Persano, L., Camposeo, A., Tekmen, C. & Pisignano, D. Industrial Upscaling of Electrospinning and Applications of Polymer Nanofibers: A Review. *Macromol. Mater. Eng.* **298,** 504–520 (2013).
14. Forward, K. M. & Rutledge, G. C. Free surface electrospinning from a wire electrode. *Chem. Eng. J.* **183,** 492–503 (2012).
15. Luo, C. J., Stoyanov, S. D., Stride, E., Pelan, E. & Edirisinghe, M. Electrospinning versus fibre production methods: from specifics to technological convergence. *Chem. Soc. Rev.* **41,** 4708 (2012).
16. Cameron Ball & Kim A. Woodrow. in *Drug delivery and development of anti-HIV microbicides* (eds. José das Neves & Bruno Sarmento) 459–508 (Pan Stanford Publishing Pte. Ltd., 2014).
17. Zhou, F.-L., Gong, R.-H. & Porat, I. Mass production of nanofibre assemblies by electrostatic spinning. *Polym. Int.* **58,** 331–342 (2009).
18. Teo, W.-E., Inai, R. & Ramakrishna, S. Technological advances in electrospinning of nanofibers. *Sci. Technol. Adv. Mater.* **12,** 013002 (2011).
19. Karim, Q. *et al.* Effectiveness and Safety of Tenofovir Gel, an Antiretroviral Microbicide, for the Prevention of HIV Infection in Women. *Science* **329,** 1168 (2010).
20. Grant, R. M. *et al.* Preexposure Chemoprophylaxis for HIV Prevention in Men Who Have Sex with Men. *N. Engl. J. Med.* **363,** 2587–2599 (2010).
21. Baeten, J. M. *et al.* Antiretroviral Prophylaxis for HIV Prevention in Heterosexual Men and Women. *N. Engl. J. Med.* **367,** 399–410 (2012).
22. Thigpen, M. C. *et al.* Antiretroviral Preexposure Prophylaxis for Heterosexual HIV Transmission in Botswana. *N. Engl. J. Med.* **367,** 423–434 (2012).
23. Costa, A. P., Xu, X. & Burgess, D. J. Freeze-Anneal-Thaw Cycling of Unilamellar Liposomes: Effect on Encapsulation Efficiency. *Pharm. Res.* 1–7 (2013). doi:10.1007/s11095-013-1135-z
24. Peppas, N. A. & Merrill, E. W. Differential scanning calorimetry of crystallized PVA hydrogels. *J. Appl. Polym. Sci.* **20,** 1457–1465 (1976).
25. Greenspan, L. Humidity fixed points of binary saturated aqueous solutions. *J Res. Natl. Bur. Stand.* **81A,** 81–89 (1977).
26. Jeffrey, D. J. & Acrivos, A. The rheological properties of suspensions of rigid particles. *AIChE J.* **22,** 417–432 (1976).

27. Dobaria, N., Badhan, A. & Mashru, R. A Novel Itraconazole Bioadhesive Film for Vaginal Delivery: Design, Optimization, and Physicodynamic Characterization. *AAPS PharmSciTech* **10,** 951–959 (2009).
28. Johnson, T. J., Gupta, K. M., Fabian, J., Albright, T. H. & Kiser, P. F. Segmented polyurethane intravaginal rings for the sustained combined delivery of antiretroviral agents dapivirine and tenofovir. *Eur. J. Pharm. Sci.* **39,** 203–212 (2010).
29. Craig, D. Q. . The mechanisms of drug release from solid dispersions in water-soluble polymers. *Int. J. Pharm.* **231,** 131–144 (2002).
30. Guirguis, O. W. Thermal and structural studies of poly (vinyl alcohol) and hydroxypropyl cellulose blends. *Nat. Sci.* **04,** 57–67 (2012).
31. Ago, M., Okajima, K., Jakes, J. E., Park, S. & Rojas, O. J. Lignin-Based Electrospun Nanofibers Reinforced with Cellulose Nanocrystals. *Biomacromolecules* **13,** 918–926 (2012).
32. Verreck, G., Chun, I., Peeters, J., Rosenblatt, J. & Brewster, M. E. Preparation and Characterization of Nanofibers Containing Amorphous Drug Dispersions Generated by Electrostatic Spinning. *Pharm. Res.* **20,** 810–817 (2003).
33. Yu, D.-G., Branford-White, C., White, K., Li, X.-L. & Zhu, L.-M. Dissolution Improvement of Electrospun Nanofiber-Based Solid Dispersions for Acetaminophen. *AAPS PharmSciTech* **11,** 809–817 (2010).

5 Nanoparticle-releasing Nanofiber Composites for Enhanced *In Vivo* Vaginal Retention

Emily Krogstad, Renuka Ramanathan, Christina Nhan, Anna Blakney, Shijie Cao, Jake Kraft, Rodney Ho, and Kim A. Woodrow *(Manuscript in preparation)*

5.1 ABSTRACT

Current approaches for intravaginal administration of nanoparticles *in vivo* result in poor retention and extensive loss of the administered dose. To overcome these challenges, we developed a nanoparticle-releasing nanofiber composite designed specifically for intravaginal delivery, and evaluated its ability to improve nanoparticle retention in a murine model. We individually tailored two components of this drug delivery system for optimal interaction with mucus, designing mucoadhesive fibers for better retention in the vaginal tract, and using PEGylated nanoparticles that will diffuse quickly through mucus and deliver their payload into tissue. We hypothesized that this novel dual-functioning (mucoadhesive/mucus–penetrating) composite material would provide enhanced retention of nanoparticles in the vaginal mucosa compared to existing approaches for intravaginal delivery. Fluorescent polymeric nanoparticles were successfully electrospun into nanofiber composites from two different mucoadhesive polymers, poly(vinyl alcohol) (PVA) or poly(vinylpyrrolidone) (PVP). Equivalent doses of fluorescent nanoparticles were vaginally administered to mice in either 25 μL water (aqueous suspension) or ~3 mg PVA or PVP fiber composites, and fluorescent content quantified in cervicovaginal mucus, vaginal tissue, and uterine horns at 24h. This study was repeated to assess long-term retention for PVA fiber composites out to 7d, as well as for etravirine-loaded nanoparticle composites to investigate the pharmacokinetics of this system. We found that our composite materials provided approximately 30-fold greater retention of nanoparticles in the reproductive tract at 24 hours compared to an equivalent dose delivered in an aqueous suspension. Remarkably, the long-term retention study demonstrated that after a single administration of PVA fiber composites, a mean of 39% of the total nanoparticle dose was recovered after three days with 6.2% detected in the vaginal tissue. Here we show that fiber composites significantly increase retention of both nanoparticles and drug in the reproductive tract of mice compared to aqueous suspensions, demonstrating the capabilities of this new delivery platform to sustain nanoparticle retention out to at least three days after a single administration. This is the first report to our knowledge of nanoparticle-releasing fibers for vaginal drug delivery, as well as the first study of a single delivery system that combines two components uniquely engineered for complementary interactions with mucus.

5.2 INTRODUCTION

HIV-1 disproportionately impacts women in sub-Saharan Africa, with infection rates two to seven times higher among young women and adolescent girls than in their male counterparts[1,2]. With few options available that women can use to protect themselves against infection, new methods for prevention are urgently needed, including more effective topical microbicides. Exciting developments have recently been made in engineering nanoparticles to overcome physiological barriers for intravaginal administration. Nanoparticles have been designed to rapidly diffuse through the cervicovaginal mucus barrier by PEGylating the nanoparticle surface to impart a net neutral surface charge[3,4]. The variable pH of the vaginal environment has been considered in the design of pH-responsive Eudragit nanoparticles[5] and hyaluronidase-responsive nanoparticles[6] that can release drug in response to changes in pH or enzyme concentration due to the presence of semen. Nanoparticles have also been demonstrated to improve drug delivery to vaginal tissue *in vivo* relative to free drug in suspension. A 5-fold increase in drug concentration in vaginal tissue was observed for nanoparticles relative to free drug in suspension in mice[7], and greater protection against HSV-2 has been documented *in vivo* for nanoparticles even when administered at 10-fold lower concentration than free drug[3]. These developments may have application in creating more effective products for the prevention and treatment of STIs, including microbicides for female-initiated HIV prevention.

Current methods for intravaginal administration of nanoparticles are limited by extensive leakage of the administered dose and poor retention. *In vivo* studies to date have used aqueous suspensions (water or PBS) to intravaginally administer nanoparticles in mice[3,4,7,8]. Extensive leakage has been documented *in vivo* for aqueous suspensions, with over 50-70% of the administered nanoparticle (NP) dose leaking out within 30 minutes, and <1-2% of the total nanoparticle dose retained at 24 hours[7,8]. Such administration methods also often require the need to maintain mice in an inverted position for 1-10 minutes to reduce leakage[7,8], and practical translation of such methods to clinical use is unlikely. Gel-based dosage forms used once-daily or pericoitally have also been associated with poor adherence in clinical trials[9,10]. External leakage and messiness from liquid or gel dosage forms have been cited as reasons for poor adherence[11]. Given the combination of extensive leakage observed with liquids in preclinical studies and poor adherence with gels in clinical studies, new dosage forms are needed for the intravaginal administration of nanoparticles that can increase dose retention in the reproductive tract and provide a more practical method for administration.

Nanofibers have previously been investigated as a platform for vaginal drug delivery[12–19]. Proof-of-concept of the application of electrospun fibers to vaginal drug delivery has previously been demonstrated, showing that fibers can deliver active antiretroviral drugs and contraceptive agents with diverse properties[12,13]. Further work has shown that electrospun nanofibers can incorporate a remarkably high drug content, up to 60% by mass[16], and that fiber polymer ratios and core-shell structure can be tuned to control drug release kinetics[17,18]. Nanofibers offer many other advantages for vaginal drug delivery, including flexibility in processing parameters (polymer/solvent selection, controllable fiber diameter, thickness), nearly unlimited material space for electrospinning, ability to encapsulate diverse agents, and multiple conceptual geometries for practical administration[14,20,21]. Electrospun fibers containing antiretroviral drugs[20,22] or microparticles[23] have also been fabricated using free-surface electrospinning, a technique often used for production scale instrument. Scalability is an important consideration in evaluating new dosage forms for feasibility as vaginal drug delivery products, particularly for HIV microbicides.

We hypothesized that because nanofibers are a solid dosage form and offer a high surface area-to-volume ratio for quick dissolution, they would provide enhanced retention and quick release of nanoparticles in the vaginal tract. Nanoparticle/nanofiber composites have previously been investigated as a strategy for sustaining drug or protein release[24–27], but have not yet been studied for their capabilities to sustain *nanoparticle* release separately from drug or protein release, nor investigated for vaginal drug delivery applications. In this work, we aim to study the release and biodistribution of *nanoparticles* from composite fibers after intravaginal administration. We also compare the pharmacokinetics of drug after delivery in nanoparticles from nanofiber composites compared to aqueous suspensions.

We designed nanoparticle-releasing nanofiber composites for increased nanoparticle retention in the reproductive tract, individually tailoring each component for optimal interaction with mucus. For the fiber component, we selected two mucoadhesive polymers, poly(vinyl alcohol) (PVA) and poly(vinyl pyrrolidone) (PVP), aimed to increase retention in the vaginal tract through association with the mucosa. Both polymers are hydrophilic and expected to dissolve quickly to release nanoparticles, but PVP is slightly more mucoadhesive than PVA[28–31], providing an interesting comparison to study how mucoadhesivity affects NP delivery. Building on recent work published on mucus-penetrating particles[3], we used a similar strategy to synthesize PEGylated PLGA nanoparticles designed to rapidly penetrate cervicovaginal mucus and deliver the drug payload to vaginal tissue.

We directly compared the retention of fluorescent nanoparticles in the reproductive tract of mice after intravaginal administration in either composite PVA or PVP fibers or aqueous suspensions. The pharmacokinetics of the antiretroviral drug etravirine (ETR) was also compared over seven days for ETR-loaded nanoparticles delivered from either composite fibers or aqueous suspensions. ETR, a non-nucleoside reverse transcriptase inhibitor (NNRTI), was selected for its high potency, excellent resistance profile, and good penetration into the cervicovaginal compartment[32–34]. Here we show that fiber composites dramatically enhance both nanoparticle and drug retention in the reproductive tract relative to aqueous suspensions and sustain nanoparticle release out to three days after a single administration.

5.3 MATERIALS AND METHODS

5.3.1 Ethics statement

Animal studies were approved by the Institutional Animal Care and Use Committee (IACUC) at the University of Washington (Protocol # 4260-01). All animals were obtained and cared for in accordance with the IACUC guidelines.

5.3.2 Materials

PLGA (50:50 L:G, ester-terminated, inherent viscosity = 0.55-0.75 dL/g in HFIP) was purchased from Lactel Absorbable Polymers. Rhodamine-B, Pluronic® F-127, agar, and poly(vinyl pyrrolidone) (PVP) (Mw~1.3 MDa) were purchased from Sigma-Aldrich. Poly(vinyl alcohol (PVA) (Mw~105 kDa, P1180) was purchased from Spectrum Chemical. Other reagents used include acetone (Fisher), ethanol (Decon Laboratories, Inc.), dimethyl sulfoxide (DMSO) (BDH Solvents), sodium chloride (EMD Millipore), and PBS (1X, Mediattech, Inc.). All solvents used for HPLC were of HPLC grade, including water (Fisher), acetonitrile (ACN) (Fisher), and ammonium acetate (Sigma-Aldrich). Etravirine was given as a generous gift from Dr. Ian Suydam at Seattle University (Seattle, WA).

5.3.3 Nanoparticle synthesis

PLGA nanoparticles were synthesized using a nanoprecipitation technique based on modifying previously described methods[35] for passive PEGylation with Pluronic® F-127[3]. PLGA was dissolved in acetone at 20 mg/mL and added to 0.1% (w/v) Pluronic® F-127 at a 1:11 (v/v) ratio with a syringe pump at a flow rate of 1 mL/min. Acetone was evaporated from the aqueous phase over 4-6 h in a fume hood. Particles were then washed by centrifugation at 10,000g x 20 min and resuspended in water using alternating vortexing and water bath sonication as needed.

Aliquots of NP suspension were lyophilized and analyzed for fluorescence or drug content. Remaining suspensions were stored at 4°C until further use.

For fluorescent nanoparticles, we first synthesized a rhodamine-B-PLGA conjugate using methods described by Costantino *et al*[36]. We determined the conjugation efficiency to be 15.7% (loading of 0.169% (w/w) rhodamine B:PLGA) by dissolving polymer conjugate and measuring fluorescence. Rhodamine-B-PLGA conjugate was dissolved in acetone and NP formed as described above. To synthesize drug-loaded NP, we dissolved ETR at 10% (w/w ETR/PLGA) theoretical loading to the PLGA/acetone solution. ETR-NP were synthesized as described above, except that the NP suspension was filtered after evaporation using 2 micron syringe filter to remove any drug precipitate before washing. Characterization of ETR-NP in terms of size, zeta potential, PDI, drug loading, and encapsulation efficiency is described in the supplementary results (Supplementary Table S1).

5.3.4 Composite electrospinning

Nanoparticle/nanofiber composites were fabricated using the "direct addition" method that has been most commonly used to create composites[26,37–39]. Preformed nanoparticles concentrated in suspension were directly added to either PVA or PVP polymer solution prior to electrospinning, mixed well, and electrospun into composite materials. Polymer solutions for electrospinning were prepared by dissolving PVA at 22% (w/v) in water and heating gently for 1-2h, and by dissolving PVP at 24% (w/v) in ethanol. Solutions were placed on a slowly rotating rotisserie apparatus overnight to ensure complete dissolution. Composite materials were fabricated by adding equivalent volumes of freshly synthesized NP (resuspended in water at 34.4-37.5 mg/mL) to PVA or PVP polymer solutions. Solutions were slowly rotated for 20-30 minutes prior to electrospinning. The electrospinning set-up consisted of a high voltage power supply (Gamma High Voltage Research) and syringe pump (New Era Pump Systems, Inc.). Polymer solution was loaded into a plastic 6 mL syringe (ThermoScientific) with 18G needle (2 inches long) and a rubber stopper (size 10) to focus the electric field. Fibers were collected onto brown waxed paper on a house-made rotating mandrel collector (diameter = 5 inches, speed = 1725 rpm, electrically grounded with a graphite brush) to provide consistent fiber mesh thickness. Electrospinning parameters were optimized independently for each polymer to result in a stable Taylor cone with minimal polymer dripping. PVA composite fibers containing PLGA-NP were electrospun at 22.5 kV, 10 cm collector distance, and 10 µL/min flow rate. PVP composite fibers containing PLGA-NP were electrospun at 21 kV, 15 cm collector distance, and 25 µL/min flow rate. All composites were electrospun using a total of ~3.5 mL of polymer

solution per mesh. Electrospun composites were stored under vacuum desiccation until further use.

5.3.5 Transmission electron microscopy

Freshly synthesized blank PLGA NP and ETR-PLGA NP were dried on TEM sample grids and imaged using transmission electron microscopy (TEM) with a FEI 200 kV Tecnai G^2 TEM at the University of Washington Nanotechnology Facility.

5.3.6 Scanning electron microscopy

Composite fibers were imaged using scanning electron microscopy (SEM) with a Sirion SEM at the University of Washington Nanotechnology Facility. Samples were placed on carbon tape and sputtered for 70s with gold/palladium. Images were taken at 5.0 kV, 5 mm working distance, and spot size of 3 at 500x, 5000x, and 20000x magnification from random locations on the sample. Fiber diameter was measured as previously described[13]. Briefly, ImageJ (National Institutes of Health) was used to measure the diameter of at least n=45 fibers per sample.

5.3.7 Confocal microscopy

Fiber samples were collected onto glass slides for 10-15 seconds during composite electrospinning and imaged using a Zeiss 510 META confocal microscope at the Keck Microscopy Facility at the University of Washington. Contrast and gain were adjusted uniformly across an image for optimal imaging of Rho-NP using Fiji/ImageJ[40].

5.3.8 Composite dissolution in vitro

We placed fiber samples on agar hydrogels to visually observe wetting and dissolution time based on previously described methods[15]. Circular punches of PVA or PVP fibers were obtained using a metal die punch to obtain samples with constant area and basis weight (mean of 20 mm diameter, 4.32 mg, 13.8 g/m^2 basis weight). Black agar hydrogels were prepared by dissolving agar in water 1.5% (w/v) and adding several drops of India ink to provide sufficient black color contrast to the white fibers. Fiber samples were gently placed on agar hydrogels, and fiber wetting and dissolution was assessed over 2 hours by video recording using an iPhone4 (Apple).

5.3.9 In vitro *nanoparticle release from composites*

For *in vitro* release experiments, 4 mg of PVA or PVP composite fibers were placed in 2 mL of deionized water (n=3 per fiber type). At various time points (1.5 min, 10 min, 20 min, 30 min, 1h, 2h, 6h, 24h, and 72h), 100 µL of release media was removed and volume replaced. Release

samples were dissolved in 500 µL DMSO and fluorescence content determined using a TECAN infinite M200PRO fluorescent plate reader (Tecan Austria GmbH) with wavelength set to 570/620 nm Ex/Em.

5.3.10 Nanoparticle integrity post-release

In parallel with *in vitro* release experiment, dynamic light scattering was used to measure the size and colloidal properties of released nanoparticles from samples taken at at 10 min, 60 min, and 24h during the *in vitro* release study. Samples were diluted in 10 mM NaCl and size, zeta, and PDI were measured using a Zetasizer Nano ZS90 (Malvern Instruments).

5.3.11 Actual loading of Rho-NP composites and ETR-NP composites

To determine the actual loading of nanoparticles within Rho-NP composite fibers, 3 mg fiber samples (n=3) were dissolved in 100 µL H20 for 45 min. 500 µL DMSO was then added, samples were dissolved an additional 1 hour, and fluorescence measured using a fluorescent plate reader as described above. Fluorescent content in aqueous NP suspensions was measured by adding 75 µL water to 25 µL aqueous suspension of Rho-NP (n=3), and then adding 500 µL DMSO and measuring fluorescence as for the fibers. The concentration of aqueous suspension used for *in vivo* studies was adjusted to match the fluorescent signal from composite fiber dose to ensure dose equivalency.

Actual drug loading of ETR-NP was measured by dissolving samples (n=3) of lyophilized NP in DMSO and determining drug content with HPLC methods. Samples of ETR-NP composites were dissolved as described above and analyzed using HPLC to determine drug content. PLGA-NP content in drug-loaded composites calculated directly from the actual drug loading of ETR-NP. Equivalent doses of ETR-NP were delivered for fibers and aqueous suspensions for *in vivo* studies.

5.3.12 Animals

Female C57/Bl6 mice (The Jackson Laboratory, Bar Harbor, ME) 8-9 weeks old were cycled three days prior to intravaginal administration by subcutaneously injecting with 2 mg medroxyprogesertone acetate (Greenstone LLC). Medroxyprogesterone acetate has been shown to induce a diestrus-like state in mice, resulting in a thinned vaginal epithelium layer, thicker mucus barrier, and reduced variability from mouse-to-mouse based on time of cycle[3,7,41].

5.3.13 In vivo *methods*

Animals were abdominally taped prior to administration to prevent self-grooming. Mice were anaesthetized with isoflurane during abdominal taping and intravaginal administrations.

Equivalent doses of NP were administered intravaginally in either aqueous suspensions (25 µL) or 2.8-3.5 mg composite fibers. Composite fibers were cut in the form of circular discs using metal punches (punch size = 16-18 mm). Fibers were then rolled up and folded to fit into modified 10-100 µL positive displacement pipette tips (Rainin), which functioned similarly to tampon applicators for administering fibers in mice. Immediately after intravaginal administration, mice were allowed to recover in the resting prone position. No vaginal pre-treatments, mucus alteration or removal, or inverting mice to prevent leakage were used for these studies. After administration, mice were individually caged to prevent cross-grooming between mice and given *ad libitum* access to food and water.

Mice were sacrificed at specified time points by cervical dislocation (Rho-NP studies) or cardiac exsanguination under isoflurane overdose for terminal blood collection (ETR-NP studies). Immediately after death, one of two washing methods was used to separate mucus-associated NP and undissolved fibers from vaginal tissue: (1) placing vaginal tissue in washing buffer (5 mL PBS) or (2) cervicovaginal lavage (4 x 50 µL water). Necropsy was performed and specified organs removed, including draining lymph nodes (iliac and inguinal), reproductive tract (cut above cervix to separate uterine horns from vaginal tract), rectum, and liver. Organs were massed and stored at -80°C until processing.

5.3.14 Washing methods for removing mucus-associated NP and undissolved fibers

The most common method for doing removing vaginal mucus is by cervicovaginal lavage, where the vagina is washed 2-4 separate times by repeatedly pipetting with 50 µL of water or PBS[3,7,8,42]. We initially tried this method for PVA and PVP fibers, but found that while this method worked for PVA, it did not completely remove undissolved PVP fibers (Supplementary Fig. S4). PVP was so mucoadhesive that it was still visibly stuck to vaginal tissue, even after the lavage. Instead, we developed a more stringent washing method intended to remove any undissolved fibers. After dissection of the reproductive tract, the vaginal tract was separated from the uterine horns and cut open longitudinally up to the cervix. Vaginal tissues were then placed in a wash buffer containing 5 mL PBS and agitated at 37°C on an orbital shaker for 30 min. Wash buffer and vaginal tissue (post-wash) and were analyzed separately for NP content.

Studies were performed to compare the ability of the wash buffer vs. the lavage method to remove undissolved fibers for Rho-NP (PVA and PVP) (Figure 5-4, Supplementary Figure S4), and for ETR-NP (PVA only) (Supplementary Figure S5). For PVA fibers, both the wash buffer and the lavage method worked to remove undissolved fibers, and amounts of NP detected in the wash buffer and lavage were similar. For PVP fibers, neither the wash buffer nor the lavage

method worked to fully remove undissolved fibers.

We used the wash buffer method for all Rho-NP composite studies, and have discussed resulting limitations resulting from undissolved PVP fibers sticking to tissue. We used the lavage method for ETR-NP composite PK studies, since only PVA fibers were carried forward into PK study and the lavage method worked to fully remove any undissolved PVA fibers. The lavage method allowed for more direct comparisons of results to be made to previous studies that used the same method[7,8].

5.3.15 Fluorescent nanoparticle in vivo studies

For the 24h Rho-NP study (Figure 5-4), four groups were compared: untreated/blank fiber control, Rho-NP in aqueous suspension, Rho-NP in PVA composite fibers, and Rho-NP in PVP composite fibers, with n=7 mice per group (n=5 for blank control). Equivalent doses of Rho-NP (~298 μg) were administered intravaginally to mice in either aqueous suspensions (25 μL water) or 2.8 mg composite fibers. Untreated mice received no treatment (abdominal taping only). Blank fibers were PVA composites with a similar loading of blank PLGA NP as Rho-PVA composites. Mice were sacrificed at 24h by cervical dislocation, and draining lymph nodes (iliac and inguinal) and reproductive tracts excised. Whole reproductive tracts were imaged using Xenogen IVIS® Spectrum imaging system before washing, and then opened vaginal tracts were imaged again after the wash method. Mucus-associated NP and undissolved fibers were removed by cutting open vaginal tract up to the cervix and placing tissue in wash buffer (5 mL PBS) for 30 minutes. Lymph nodes, vaginal tract (post-wash), and uterine horns were weighed and stored at -80°C until analysis. Xenogen images were taken at 570/620 nm ex/em and a 30s exposure time. Images were analyzed using Living Image® 4.0 Software (Caliper Life Sciences, Inc.).

Wash buffer (5 mL PBS) samples were frozen at -80°C and lyophilized for at least 48h. Lyophilized buffer was dissolved in 600 μL 1:5 H2O:DMSO for 1-2h to dissolve NP. Wash buffer samples were then centrifuged at 10,000g for 10 min. The supernatant was analyzed for fluorescent content using a TECAN plate reader at 570/620 nm. Vaginal tracts and uterine horns were thawed and minced with scissors in 500 μL DMSO/organ. Tissues were homogenized using a Precellys 24-Dual bead homogenizer (Bertin Technologies). One mixed zirconium oxide bead kit (Bertin Technologies) was used per tissue, containing ~650 mg 1.4 mm beads and six 2.8 mm beads. Precellys settings were 6,500rpm x 20s x 3 cycles, with a 30s pause in between each cycle. Two homogenization runs completed with these settings to ensure full homogenization, with a 10 minute incubation at 4°C in between runs to allow for

cooling. Samples were centrifuged at 5,000 rpm for 15 min. Supernatant was analyzed for fluorescent content in triplicate for each sample using a TECAN plate reader as described above and compared to a standard curve of Rho-NP prepared in blank organ homogenate. Linearity was established from 0.5 µg to 298 µg (0.2-100% total Rho-NP dose).

The same methods were used for the 7d Rho-NP study (Figure 5-5) to evaluate NP retention from PVA composite fibers over a longer time. Two groups were compared at each of four time points (2d, 3d, 5d, and 7d): untreated control (n=1) and Rho-NP in PVA composites (n=3). Equivalent doses of Rho-NP (~368 µg NP in 25 µL water or 3.5 mg composite fibers) were administered for the long-term retention study.

5.3.16 Black paper leakage study

In parallel with the 24h Rho-NP study, we measured external leakage (Figure 5-3) based on methods previously described by Cu *et al*[8]. Immediately after intravaginal administration of equivalent doses of Rho-NP in either composite fibers or aqueous suspensions, mice (n=4 per group) were placed in plastic beakers lined with circles cut from black paper (Artagain® 400 Series, Strathmore) and allowed to recover normally for 1h. Leakage of Rho-NP on black paper circles was measured using Xenogen imaging to detect fluorescent content. Fluorescent signal was quantified by drawing an ROI defined around each black paper circle and quantifying maximum radiance.

5.3.17 ETR nanoparticle in vivo *studies*

Two groups were compared for this study: aqueous suspensions versus composite PVA fibers containing equivalent doses of ETR-NP (~446 µg ETR-NP containing 11.42 µg ETR/dose), with n=5 mice per group per time point. Doses were administered intravaginally to mice in either aqueous suspensions (25 µL H20) or in 2.8 mg PVA composite fibers. At various time points (1h, 6h, 12h, 24h, 2d, 3d, 5d-fibers only, 7d-fibers only), mice were sacrificed by cardiac exsanguination under isoflurane overdose. At least 500 µL of blood per mouse was collected in K_2EDTA-coated tubes (BD Microtainer®). Blood samples were centrifuged at 1,300g for 10 min and plasma separated. Cervicovaginal lavage was performed immediately after death (4 x 50 µL H20), and organs excised for drug content analysis (draining lymph nodes, vaginal tract, uterine horns, rectum, liver). All samples were massed and kept at -80°C until analysis.

Lavage samples were thawed and 800 µL DMSO added to dissolve NP. After rotating for 4 h, samples were centrifuged at 13,000g for 10 min. Supernatant was diluted if necessary to be within the linear range for quantification and analyzed for ETR content using HPLC methods

described below. Plasma samples were thawed and 25 µL of plasma was added to 50 µL ACN to precipitate protein content, followed by a 30 min on a plate shaker. Plasma was centrifuged at 5000g x 10 min, and supernatant analyzed for ETR content using LC-MS/MS methods. Vaginal tissue (post-lavage), uterine horns, rectum were homogenized in 500 µL ACN/organ using Precellys bead homogenizer as described above. Livers were homogenized in 1 mL ACN/organ using a probe homogenizer (Tissue Tearor, Biospec Products, Inc.) and centrifuged at 4700 rpm for 5 min at 4°C. Supernatant from homogenized organs was filtered through a 0.22 µL syringe filter and analyzed for ETR content using LC-MS/MS methods.

5.3.18 HPLC

HPLC methods were used to quantify ETR content for drug loading measurements of NP and composites, *in vitro* release experiments for ETR-NP, lavage samples from PK study, and for pilot PK studies. A Prominence LC20AD (Shimadzu) HPLC system was used that was fitted with a photodiode array detector and Phenomenex Kinetex C18 column (250x4.6 mm, 5 µm particle size). Mobile phase was 65% ACN:35% ammonium acetate buffer (10 mM) at a flow rate of 1 mL/min under isocratic conditions. The column oven was set to 30°C. ETR was detected at 309 nm at a retention time of 6.3 min. Linearity was established from 0.024 – 100 µg/mL using a 10 µL injection volume (standard curve in DMSO). Blank samples containing homogenized organs from untreated mice were run in parallel with mice from treatment groups to ensure there was no background interference, as well as standards and spiked samples in blank tissue homogenate (Supplementary Fig S6).

5.3.19 LC-MS/MS

Mass spectrometry methods were used to quantify ETR content in all organs for the PK study except the lavage, including vaginal tissue, uterine horns, rectum, liver, and plasma.

Sample Prep. Etravirine-$^{13}C_6$ was used as an internal standard. All samples were vialed at a volume of 50 µL and spiked with 5 µL of a 10 ng mL^{-1} solution of the internal standard mix (50 pg per sample). A standard curve ranging from 0.01-100 ng mL^{-1} was prepared in ACN and run before and after unknown sample sets.

Mass Spectrometry. ETR concentration in tissue was analyzed using LC-MS/MS method on a Waters Xevo TQ-S couple with an I-Class Acquity UPLC (Waters Corporation, Milford, MA, USA). All analytes were acquired in electrospray positive mode and used the following parameters: capillary voltage of 3 kV, source temperature of 150 °C, cone gas flow of 150 L hr^{-1}, desolvation gas flow of 1000 L hr^{-1}, and collision gas flow of 0.15 mL min^{-1}. The spectrometer was analyzing during minutes 2-7 of each run. The drug and internal standard were analyzed at

the following m/z transitions: 435.22 to 162.98 (ETR) and 441.20 to 162.98 (ETR-$^{13}C_6$). All species were analyzed as a cone voltage of 50 kV and collision energy of 28 V (full list of parameters can be found at Blakney *et al*., publication in process).

Liquid Chromatography. A Chromolith Performance RP-18e 100-3mm column was used for analysis, with a gradient method of 10 mM formic acid in H_2O (Mobile Phase A) and 10 mM formic acid in 80:20 ACN:MeOH (Mobile Phase B). The gradient consists of 98% A + 2% B for 1 minute, transitioning to 100% B by 6 minutes and holding for an additional 1 minute, and then transitioning back to 98% A + 2% B over 1.5 minutes (see Supplementary Table S2), with a flow rate of 0.5 mL min^{-1} and an injection volume of 20 µL.

5.3.20 PK parameter analysis

Pharmacokinetic parameters were analyzed using noncompartmental analysis with sparse sampling using Phoenix WinNonlin software (Version 6.4). The terminal elimination rate constant (λ_z) was estimated from the data by the software (see Supplementary Fig. S7, S8), and terminal half-life ($t_{1/2z}$) calculated as 0.693 / λ_z. The ratio of AUC values shown in Table 5-3 was calculated as AUC_{fib} / AUC_{sus} = $AUC_{1.35\text{-}72.29h,\ fibers}$ / $AUC_{1.35\text{-}72.29h,\ suspension}$. Differences in AUC and C_{max} were assessed using two-tailed, Student's *t*-test, assuming equal variance (GraphPad Version 6.0f).

5.3.21 Statistical Methods

Data is presented as mean +/- standard deviation unless otherwise indicated, with statistical significance defined as $p<0.05$. Statistics were calculated using Prism 6.0 (GraphPad Software, Inc.). For Rho-NP studies where there were multiple groups, one-way ANOVA with Bonferroni correction for multiple comparisons was used to compare all groups. For ETR studies, an unpaired t-test (equal variance assumed) was used to compare two groups within the same time point. Grubb's test for determining outliers was used to remove outliers prior to PK analysis (alpha = 0.01).

5.4 RESULTS AND DISCUSSION

5.4.1 Nanoparticle/nanofiber composite fabrication

We optimized nanoparticle/nanofiber composite materials for the following design constraints: (1) nanoparticle diameter of ~200-500 nm, (2) neutral nanoparticle zeta potential (+/- 10 mV), (3) quick fiber dissolution (<30 min), (4) fast release of nanoparticles from fiber composites, and (5) released nanoparticles retained similar size and surface charge.

Nanoparticles with a diameter of 200-500 nm and neutral surface charge have previously been shown to be optimal for mucus-penetration[43]. Since we aimed to deliver intact nanoparticles to tissue as opposed to sustaining drug release, quick fiber dissolution and nanoparticle release was important.

We synthesized rhodamine-conjugated PLGA nanoparticles (Rho-NP) and etravirine-PLGA nanoparticles (ETR-NP) using a nanoprecipitation technique. Actual loading of nanoparticles in Rho-NP composites and ETR-NP composites was measured to ensure dose equivalency between composites and aq. susp for *in vivo* studies. Actual loading of nanoparticles within fibers (wt NP / wt composite fiber) was found to be 10.6% for Rho-NP/PVA composites, 9.7% for Rho-NP/PVP composites, and 15.9% for ETR-NP/PVA composites. NP loading was higher for drug-loaded composites to ensure detectable drug concentrations for PK studies while keeping fiber dose consistent with fluorescent studies. Additional data on characterization of ETR-NP is found in Supplementary Table S1 (see Appendix E for supplemental information).

TEM micrographs showed that nanoparticles were spherical and smooth, and SEM micrographs showed that both PVA and PVP composite fibers had smooth, cylindrical morphology (Figure 5-1). Uniform morphology is ideal for predictable dissolution and drug release kinetics. Composite fiber diameter and nanoparticle diameter were both around 200-300 nm, with PVA fibers having a mean diameter of 248 ± 88 nm, PVP fibers of 297 ± 125 nm, and PLGA nanoparticles of 172 ± 19 nm (Figure 5-1). Nanoparticle size in the range of 200-500 nm has been found to be optimal for mucus penetration[43], meaning that Rho-NP are near the desirable size range to diffuse quickly through mucus. Matching the fiber diameter to the nanoparticle diameter may facilitate quick dissolution and release of nanoparticles by reducing the thickness of the fiber polymer coating that must dissolve before nanoparticles can be released.

We used confocal fluorescent imaging to probe the sub-structure of the composite fibers since nanoparticles could not be visualized within fibers using SEM. Punctate fluorescent particles were visible within fibers for both PVA and PVP and were uniformly distributed within the fibers (Figure 5-1). Fiber density was higher in SEM images compared with confocal images due to differences in imaging techniques. A full-thickness fiber mesh was imaged for SEM, versus a thin single fiber layer collected onto glass slides for confocal imaging. Some images showed fluorescence within fibers, although the fluorescence signal was low relative to that of NP. We expect that the amount of free rhodamine within fibers was small relative to PLGA-conjugated rhodamine due to the multiple wash steps during rhodamine-PLGA conjugation and nanoparticle synthesis, and that the ratio of free vs. conjugated rhodamine was consistent

among all groups tested for *in vivo* studies. These results demonstrate that nanoparticle/nanofiber composites were successfully electrospun from both PVA and PVP solutions with similar mean diameter and nanoparticle uniformity, and that this method is suitable for fabricating composite materials.

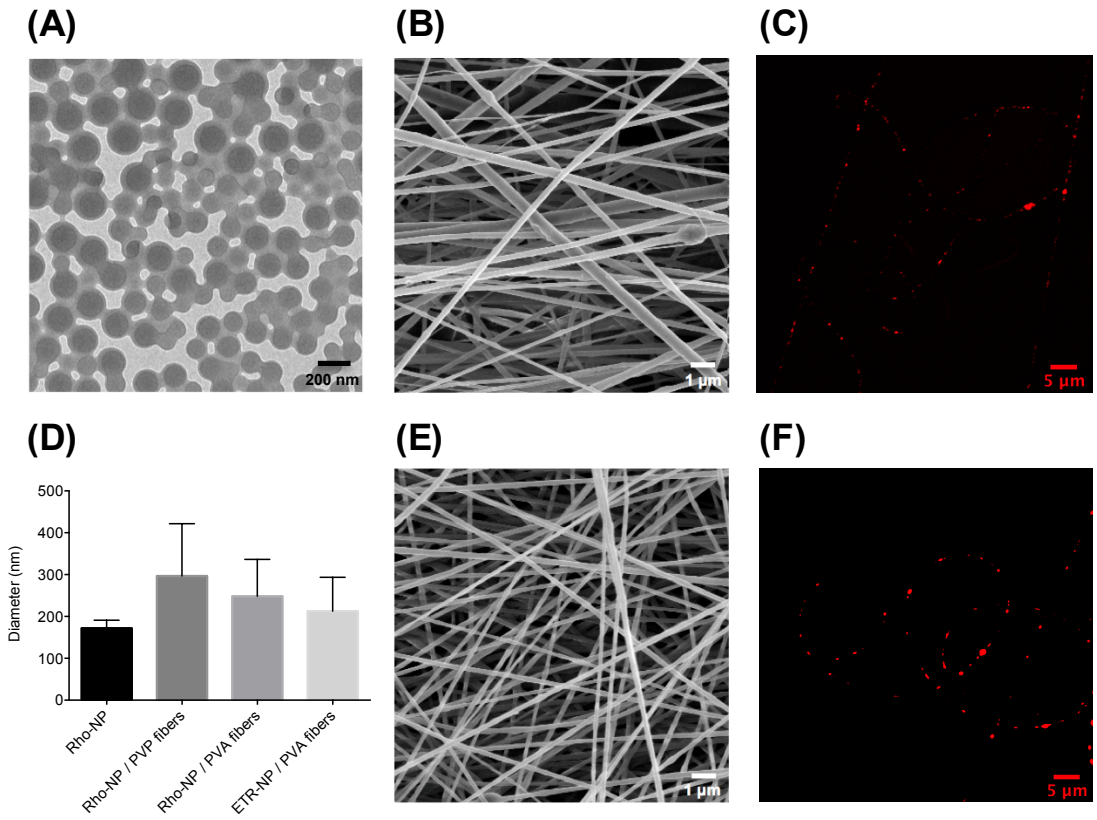

Figure 5-1. Fiber composites successfully formed with similar nanoparticle and nanofiber diameter. (A) TEM micrograph of blank PLGA nanoparticles. (B, E) SEM micrographs of PVP (B) or PVA (E) composite fibers containing rhodamine-PLGA nanoparticles. (D) Diameter (mean +/- S.D.) of rhodamine-NP, Rho-NP / PVP composite fibers, Rho-NP / PVA composite fibers, and ETR-NP / PVA composite fibers. NP diameter measured using DLS; fiber diameter measured from SEM images. (C, F) Confocal imaging of rhodamine-PLGA np electrospun within PVP composite fibers (C) or PVA composite fibers (F).

5.4.2 Considerations in using the direct addition method for composite fabrication for nanoparticle delivery

This "direct addition" method of forming nanoparticle/nanofiber composites in which preformed particles are added directly to a polymer solution and then electrospun has been frequently used in literature[26,37–39]. While this strategy has worked to successfully electrospin composites for sustained *drug* release, it has limitations for sustaining *nanoparticle* release. Most significantly, the solvent for electrospinning fiber polymer must be compatible with the

nanoparticle system. Otherwise, the nanoparticle may swell, release drug into fiber polymer solution, or dissolve prematurely during electrospinning.

Using this work as an example, a volatile solvent such as 100% ethanol (EtOH) was most suitable for electrospinning PVP. However, the polymer used for nanoparticles (PLGA) swelled in EtOH. This swelling may cause premature drug release from nanoparticles into fibers during electrospinning, or may result in nanoparticle aggregation that clogs the needle. For our PVP fiber system, we aimed to find the lowest amount of EtOH necessary as an electrospinning co-solvent that would still produce consistent fibers as opposed to films. We tested a range of EtOH:H2O ratios, and found the lowest concentration for stable electrospinning was 50:50 EtOH:H2O (anything with higher water content produced films instead of fibers). We then measured the drug release kinetics of ETR from ETR-NP in this solvent system, and found it to be minimal (~3% of total drug content released in 24h, see Supplementary Fig S1). We also chose to limit the theoretical NP loading within fibers to <15% (w/w) for PVP to prevent issues with needle clogging. Water was used as both the electrospinning solvent and nanoparticle resuspension media, so this was not a problem for PVA composites containing PLGA nanoparticles. For future work using the direct addition method to form composites, solvent compatibility with nanoparticle system, nanofiber polymer, and encapsulated drug need to be carefully considered. Higher nanoparticle loading in fiber composites may be achieved by exploring alternate methods for composite fabrication, such as aerosolization of spray-dried or lyophilized particles.

5.4.3 Fiber composites dissolve quickly in vitro *to release intact nanoparticles*

A key design constraint for nanoparticle-releasing nanofiber composites is that the fibers must wet out rapidly to release nanoparticles. We observed that both PVA and PVP composite fibers rapidly wet out within 30s on black agar hydrogels (Figure 5-2). PVP composites wet out immediately upon contact (<1s), whereas PVA composites took slightly longer to wet out (within 30s). Interestingly, PVP fiber meshes did not change in area as they wet, but PVA fiber meshes reduced by about 50% in total area within 30s. This difference may be to PVA fibers initially being mechanically stretched during electrospinning onto a rotating collector, and subsequently relaxing when in contact with water. Additionally, the hydroxyl and acetyl groups present on partially hydrolyzed PVA polymer chains can form hydrogen bonds with water, potentially causing rearrangement and shrinkage of the fiber chains as they realign toward the most energetically favorable state in water.

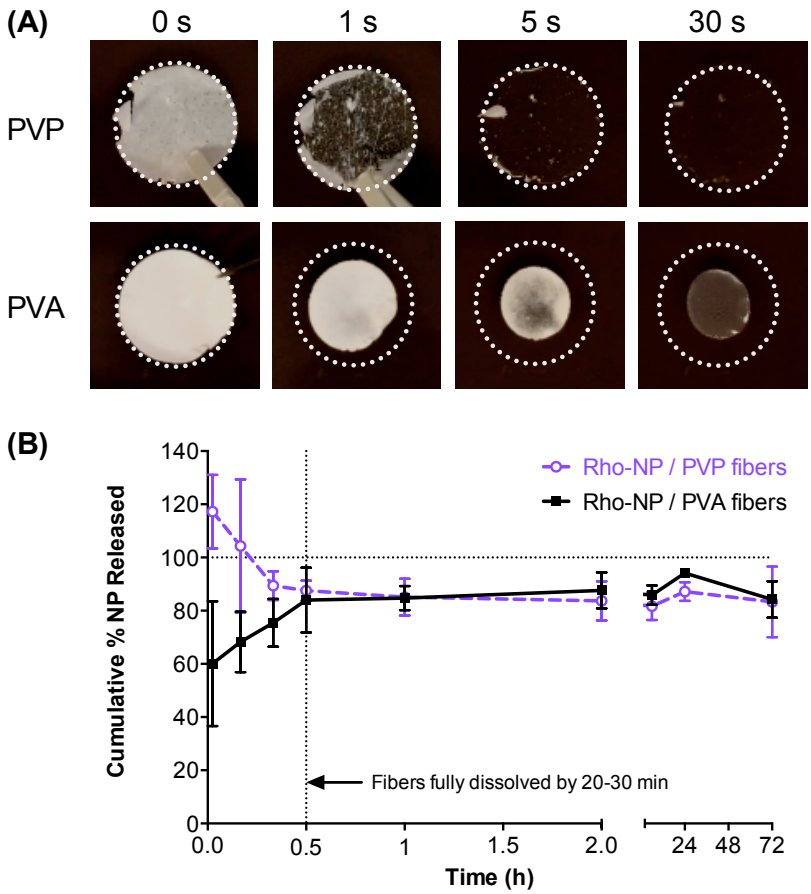

Figure 5-2. Fiber composites dissolve quickly *in vitro* to release nanoparticles. (A) Composite fiber dissolution on black agar hydrogels used to simulate low fluid volume conditions. White dotted circle represents original area of fiber mesh. (B) Cumulative rhodamine-NP release from composite fibers under *in vitro* sink conditions (4 mg composite fibers in 2 mL water). Dotted line at 0.5 h indicates time when both PVA and PVP fibers had fully dissolved.

Even though the time to wet out is different for PVA and PVP composite fibers, both fibers were observed to dissolve within 30 minutes under *in vitro* sink conditions in water. PVA and PVP composites both resulted in burst release to give >85% cumulative nanoparticle release in less than 30 min (Figure 5-2). The burst release kinetics of nanoparticles is consistent with our hypothesis for quickly dissolving, hydrophilic polymers. At early time points (< 30 min), nanoparticle release from PVP fibers was measured to be >100%. This is attributable to PVP fibers initially breaking into very small pieces that were inadvertently included during sampling at early time points, leading to an inaccurately high estimation pre-complete fiber dissolution. For PVA fibers, nanoparticles took slightly longer to dissolve out of hydrated gel/fiber network as it continued to wet and dissolve over 30 minutes. This study is significant in that it demonstrates that particles are able to diffuse out of the polymer network *in vitro*.

However, a significant limitation of the *in vitro* release study is that *in vivo* release occurs under much different conditions. In the vaginal lumen, the fibers would dissolve in a low fluid volume comprised of highly viscous mucus and hydrated polymer gel (3 mg fibers/~50-100 µL mucus), instead of *in vitro* sink conditions of excess water (4 mg fibers/2 mL H20). Composite fiber dissolution and nanoparticle release are expected to be much slower *in vivo*, even for hydrophilic polymers like PVA and PVP. Mun *et al* have studied nanoparticle trafficking in dilute polymer solutions *in vitro*, and attributed differences in diffusion to varying degrees of interaction with the nanoparticle surface and polymer solution[44]. Although actual *in vivo* conditions would likely be concentrated polymer gels rather than dilute polymer solutions, we hypothesize that the PEGylated nanoparticles used in this work would diffuse faster in PVP solutions than PVA solutions due to differences in hydrogen bonding. Since PVP and PEG both act as proton acceptors, they are expected to have minimal interactions compared to PVA, which can act as a proton donor and form hydrogen bonds with PEG. Nonetheless, the *in vitro* dissolution and release studies confirm that PVA and PVP composites meet the design constraints of fast fiber dissolution and quick nanoparticle release.

5.4.4 Nanoparticle properties are retained after in vitro release from composite fibers

Nanoparticles recovered from the composite release studies were found to have similar physical and colloidal properties to the original nanoparticles used to make the composites (Table 5-1). It is important that the nanoparticles maintain a size and surface charge amenable to diffusing through mucus after release from fibers so that they can traffic through mucus towards the vaginal tissue target. Overall, this data is the first to our knowledge that demonstrates that nanoparticles can retain their physical properties after release from composite fibers.

Along with changes in fiber dissolution kinetics, nanoparticle properties may also differ under actual *in vivo* conditions in the presence of mucus and hydrated polymer gel. The fiber polymer may interact with the nanoparticle directly to slow or speed its diffusion, but may also alter the properties of mucus itself. Recent work has shown that the presence of a PVA coating

Table 5-1. Physical properties of nanoparticles before and after release from composite fibers.

Sample	Z-avg size (nm)	PDI	Zeta potential (mV)
Rho-NP (original)	171.9 ± 19.1	0.089 ± 0.011	-5.64 ± 0.80
Rho-NP, released from PVP composites	204.9 ± 39.0	0.247 ± 0.060	-5.56 ± 1.49
Rho-NP, released from PVA composites	294.9 ± 9.3	0.078 ± 0.027	-0.58 ± 0.06

[a]Data presented as mean ± S.D with n=4 for each sample (n=2 for Rho-NP-PVA composites).
[b]Measured using dynamic light scattering in 10 mM NaCl solution (pH = 5.7)

on nanoparticles results in slower diffusion through human cervicovaginal mucus, and that Pluronic® F-127-coated nanoparticles also have reduced diffusion when in solutions containing PVA[45]. Thus, the PVA present from fibers may interact with the Pluronic® F-127 coating on nanoparticles and reduce their mucus-penetrating potential. On the other hand, the fiber polymer may induce changes in the overall mucus structure, making it either more or less of a barrier to nanoparticle trafficking. Pretreatment of human cervicovaginal mucus with 1% Pluronic® F-127 has been shown to enhance diffusion of conventional polystyrene nanoparticles, likely due to changes in the diffusive properties of the mucus network itself[46]. Others have shown that the presence of polymer can have dramatic effects on the mucus structure by altering water content, pore size, or packing of mucin fibers[47,48]. Nanoparticle diffusion through mucus may potentially be enhanced due to the fiber polymer favorably changing the structure of the mucus. For example, since PVP is hygroscopic, it may be expected to absorb water from the mucus, resulting in the reduction of mucus pore size and aggregation of mucin fibers such that it is no longer a barrier. The complex interactions between fiber polymer, mucus, and nanoparticles are challenging to recapitulate *in vitro* and point to the need for *in vivo* models for evaluation.

5.4.5 Negligible external leakage in vivo *from composite fibers within 1h*

After comparing the amount of external leakage of Rho-NP within one hour of intravaginal administration, we found that composite fibers resulted in significantly less leakage than aqueous suspensions (Figure 5-3). All mice receiving PVA and PVP composite fibers were found to have no detectable leakage above control mice that received blank composite fibers, whereas significant external leakage was visible for all mice that received aqueous suspensions of Rho-NP (Figure 5-3). These findings are consistent with previous reports for intravaginal administration of NP in aqueous suspensions *in vivo* that report that more than half of the total NP dose is unaccounted for within 30 minutes of administration[7,8]. Cu *et al* measured that ~3-13% of total NP dose had leaked externally within 30 min, but also report total NP dose recoveries of 30-49% at 30 minutes, suggesting that an even higher fraction of the dose leaked externally within this time[8]. Das Neves *et al* reported that ~70% of the total NP dose was unaccounted for within 30 minutes of administration, which they attributed to external leakage[7]. These data support the hypothesis that composite fibers provide enhanced retention of NP in the reproductive tract compared to aqueous suspensions currently used for *in vivo* intravaginal administration of NP.

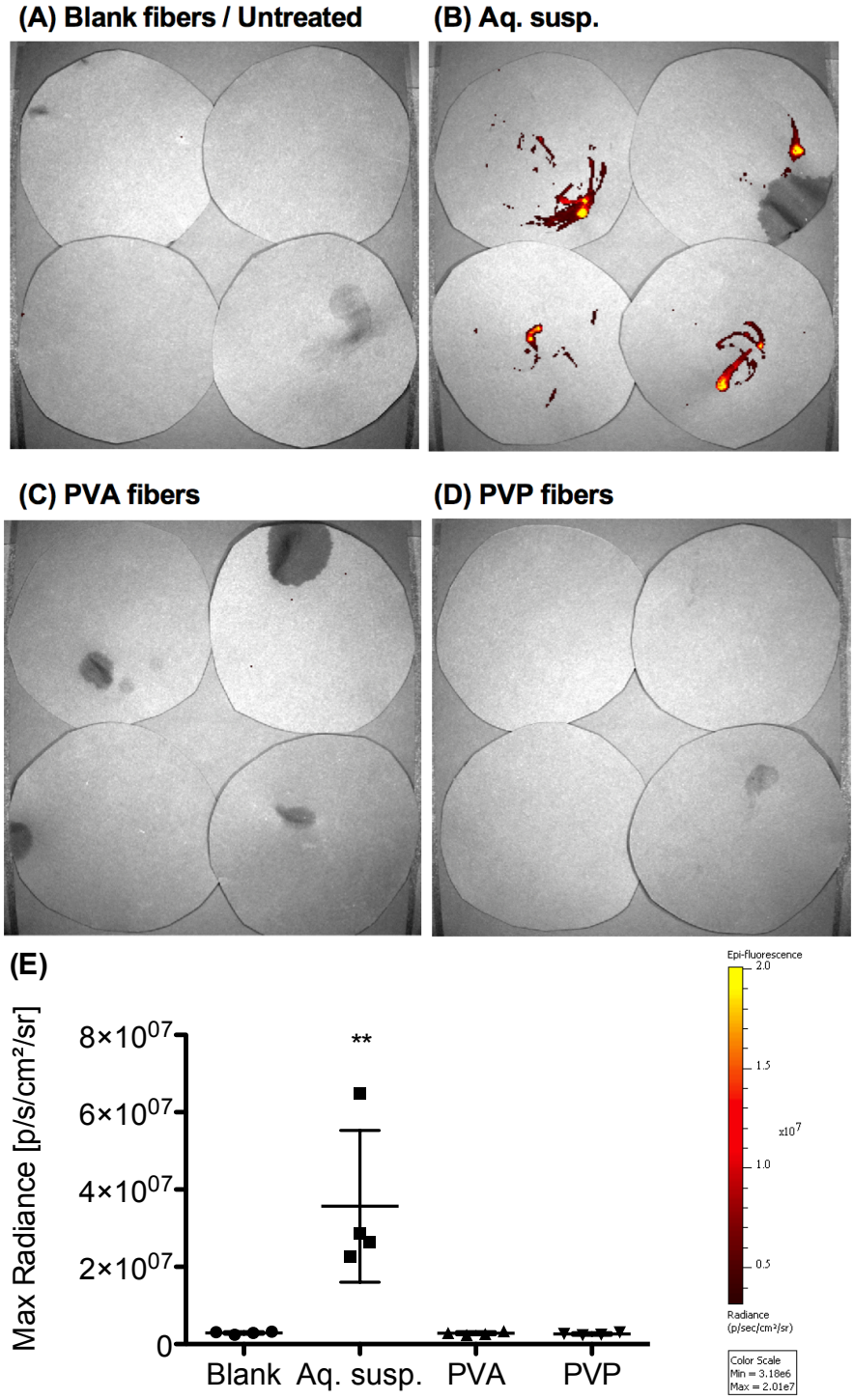

Figure 5-3. Significantly less external leakage of nanoparticles is observed for PVA and PVP composite fibers compared to aqueous suspensions. (A-D) Xenogen imaging of black paper circles used to measured external leakage for 1 h immediately after administration, with n=4 mice per group. In (A), the top two circles represent mice receiving blank PVA composite fibers, and the bottom two circles represent untreated mice. All images were set to the same scale of minimum and maximum radiance. (E) Maximum radiance quantified from Xenogen images in (A-D).

5.4.6 *Enhanced* in vivo *nanoparticle dose retention for composite fibers at 24h*

To test our hypothesis that composite fibers significantly enhance dose retention relative to aqueous suspensions, we intravaginally administered equivalent doses of Rho-NP in aqueous suspension or composite fibers to mice and measured fluorescent content in the reproductive tract at 24h. We found that Rho-NP were significantly better retained in the reproductive tract at 24h for both PVA and PVP composite fibers relative to aqueous suspensions (Figure 5-4).

Xenogen imaging of whole reproductive tracts prior to washing shows greater fluorescence for all mice that received PVA and PVP composite fibers compared to mice that received aqueous suspensions at 24h (Figure 5-4). Total percent dose recovery was calculated by summing total Rho-NP content in wash buffer, homogenized vaginal tissue, and homogenized

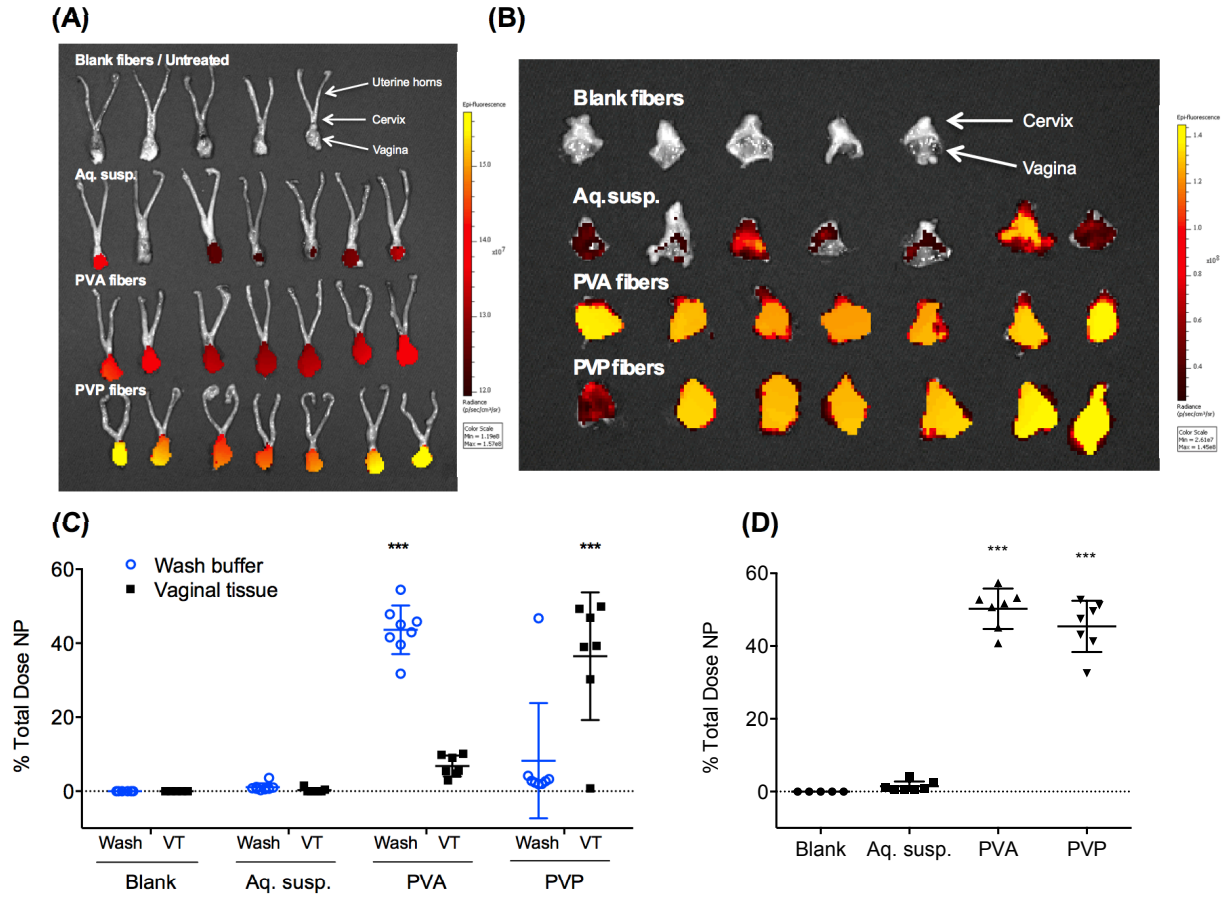

Figure 5-4. Fiber composites result in increased nanoparticle dose retention in the reproductive tract and trafficking to vaginal tissue at 24h. (A) Whole reproductive tracts imaged after dissection at 24 h, pre-wash. (B) Opened vaginal tissue imaged after wash (tissues placed in 5 mL PBS for 30 minutes). (C) Dose recovery of fluorescent nanoparticles at 24h in wash buffer (open circles) or homogenized vaginal tissue, post-wash (squares). (D) Total dose recovery is the sum of dose recovered at 24h in wash buffer, vaginal tissue (post-wash), and uterine horns. *** $p<0.0001$ relative to all other groups (one-way ANOVA comparing all four groups within same tissue type).

uterine horns. A mean of only 1.4% of initially administered Rho-NP dose was recovered for mice receiving aqueous suspensions, while almost half the dose was retained for both PVA (50.3%) and PVP fibers (45.4%) (Table 5-2). This 32- to 35-fold increase in total *nanoparticle* dose retention at 24h is very significant in context of previous work on the intravaginal administration of nanoparticles. Other *in vivo* studies using aqueous suspensions that have measured NP dose retention based on initial dose have shown 0.6-2% total NP dose recovery at 24h, and report extensive NP external leakage as a major limitation[7,8]. These results demonstrate that composite fibers can dramatically increase local retention of NP over a much longer time period than existing methods for nanoparticle delivery, providing a more flexible platform for sustained nanoparticle delivery and the potential for greatly enhanced local NP concentration.

Table 5-2. Fluorescent nanoparticle recovery in the reproductive tract at 24h.

	Wash Buffer (% Total Dose NP)	**Vaginal Tissue** (% Total Dose NP)	**Uterine Horns** (% Total Dose NP)	**Total Dose Recovery**[a] (% Total Dose NP)
Aq. susp.	1.1 ± 1.1	0.3 ± 0.6	N.D.	1.4 ± 1.3
PVA fibers	43.6 ± 6.6	6.8 ± 2.8	0.4 ± 1.0	50.3 ± 5.5
PVP fibers	8.2 ± 15.6	36.5 ± 17.2	N.D.	45.4 ± 7.0

Data shown is mean ± S.D. of n=7 mice per group.
[a]Total dose recovery is the sum of the total dose of nanoparticles administered recovered in the wash buffer, vaginal tissue (post-wash), and uterine horns.
N.D. = not detected (signal below blank/untreated control)

5.4.7 Nanoparticle association with vaginal tissue at 24h

For many agents of interest in intravaginal delivery, including ARVs that act intracellularly like tenofovir and etravirine, the vaginal tissue is the ultimate target for drug action. The ideal dosage form would not only be able to provide high dose retention in the reproductive tract, but also release nanoparticles that can diffuse through cervicovaginal mucus into the vaginal epithelium. Therefore, we sought to compare the amount of NP associated with the vaginal tissue for each dosage form. We aimed to separate the amount of nanoparticles associated with the lumenal mucus (or still remaining in undissolved fibers) from nanoparticles that had trafficked into vaginal tissue using a wash procedure. After washing vaginal tissues in 5 mL PBS for 30 minutes, the opened vaginal tracts were imaged again using Xenogen, and the fluorescent NP content in the wash buffer versus homogenized vaginal tissue post-wash was measured (Figure 5-4).

We found that NP association with vaginal tissue was higher for both composite fibers (PVA and PVP) compared with aqueous suspension (Table 5-2). Xenogen imaging of opened vaginal tracts after the wash procedure showed greater fluorescence dispersed uniformly in the vaginal tract for both PVA and PVP fibers compared to the limited, non-uniform coverage observed for aqueous suspensions (Figure 5-4). We found that that a mean of 1.1% of the total dose of Rho-NP were recovered in the wash buffer for aqueous suspensions, versus 43.6% for PVA fibers and 8.2% for PVP fibers. In the vaginal tissue, 0.3% of the total dose was recovered for aqueous suspensions, versus 6.8% for PVA fibers and 36.5% for PVP fibers. These results show that in addition to enhancing total NP dose retention in the reproductive tract by >30-fold, composite fibers also significantly increase NP delivery to vaginal tissue by 22-fold or higher at 24h.

We tested two fiber materials with varying mucoadhesivities to study the effect of fiber mucoadhesivity on NP retention and trafficking. We found that PVA fibers resulted in greater NP association with the lumenal mucus (wash buffer), while PVP fibers result in greater NP association with the vaginal tissue. This is consistent with the higher degree of mucoadhesivity for PVP compared to PVA. However, there is an important observation regarding the wash method for PVP fibers only. The wash method worked well for separating undissolved PVA fibers from vaginal tissue, with all undissolved PVA fibers separating completely from the tissue during the wash (visible as a large fiber piece in the buffer). Conversely, the washing method did not work for PVP: small pieces of undissolved PVP fibers were still visibly stuck to the tissue after the wash.

This limitation is important for interpreting the data in Figure 5-4 in terms of differentiating between NP associated with the lumenal mucus/undissolved fibers versus the vaginal tissue. For PVP only, the amount of NP that are associated with the vaginal tissue was confounded by the presence of small pieces undissolved fibers stuck to the vaginal tissue. In other words, for PVP fibers, the 37% total NP dose associated with the vaginal tissue not only includes NP that have left fibers and trafficked into vaginal tissue, but also includes NP trapped within undissolved fibers. In contrast, for PVA fibers, the 7% of total NP dose associated with the vaginal tissue represents only the portion of total NP dose that has left fibers and trafficked into vaginal tissue. Continued method development would be needed to separate undissolved PVP fibers from the vaginal tract in order to make any claims concerning *in vivo nanoparticle release* from PVP fibers. However, claims about *total dose retention* in the reproductive tract are still valid for both PVA and PVP fibers. Given this limitation, we chose to move forward with PVA fibers only for future work. It is not necessarily that PVA fibers are better than PVP fibers for

intravaginal delivery, but that with the current methods, we are able to differentiate where nanoparticles are trafficking with more confidence for PVA than PVP.

5.4.8 Long-term nanoparticle retention and in vivo release kinetics for PVA fiber composites

Given that nanoparticle retention was >50% of the total dose at 24h for PVA composite fibers, we next evaluated how long nanoparticles were retained in the vaginal tract after a single administration. We intravaginally administered Rho-NP in composite PVA fibers and measured fluorescent content as described previously at 2d, 3d, 5d, and 7d after administration. We found that nanoparticles were retained in the reproductive tract and vaginal tissue at detectable levels out to 3 days for composite PVA composite fibers, visible by Xenogen fluorescent imaging (Figure 5-5). At 72h after administration, a mean of 38.5% of the total NP dose was retained in the reproductive tract overall, and 6.0% of the total NP dose was associated with the vaginal tissue (Figure 5-5). The total NP dose recovery decreased slightly from a mean of 47.0% of the total NP dose at 48h to 38.5% at 72h, and then dropped off to below detection (<0.2%) after 5d. These NP release kinetics are consistent with the hypothesis that in low fluid volume conditions *in vivo*, the fiber polymer wets and dissolves slowly to sustain release of nanoparticles. After release from fibers, some nanoparticles diffuse through the lumenal mucus into the adherent mucus and/or vaginal tissue, while some nanoparticles are lost externally due to mucus turnover. This study is significant in that it is the first to our knowledge showing capability for sustained released of *nanoparticles* for intravaginal delivery out to three days by using a fiber dosage form.

Interestingly, we found that both PVA and PVP fibers dissolved more slowly *in vivo* than we predicted based on results from *in vitro* fiber dissolution and NP release experiments. We observed during necropsy that undissolved fibers were still visibly present in the vaginal tract of mice at 24h for both PVA and PVP composites. Even at 72h, we observed that some animals still had a much smaller but visible portion of undissolved PVA fibers inside the vaginal tract. As discussed previously, this is likely due to the low fluid volume conditions and presence of viscous mucus that slowed the *in vivo* dissolution of fibers. Additionally, a relatively large dose of composite fibers was administered to mice (~3 mg), which took up ~25-50% of the mouse vaginal tract by volume. A dosing study was performed in which doses of 1, 3, and 5 mg fibers were administered to mice, and the 3 mg dose was chosen to maximize detectability but still allow for fiber dissolution (Supplementary Fig S2). Even though both PVA and PVP are hydrophilic polymers, their wetting and dissolution requires a sufficient volume of water. The NP release kinetics could potentially modulated by using different polymers and/or excipients for the

fiber material, altering NP:fiber loading, or changing the total dose of composites administered. In future studies, the *in vivo* release rate may also be controlled by using more hydrophobic polymers for the fiber material to sustain release out to even longer times, or using excipients to increase water uptake in fibers to provide faster NP release.

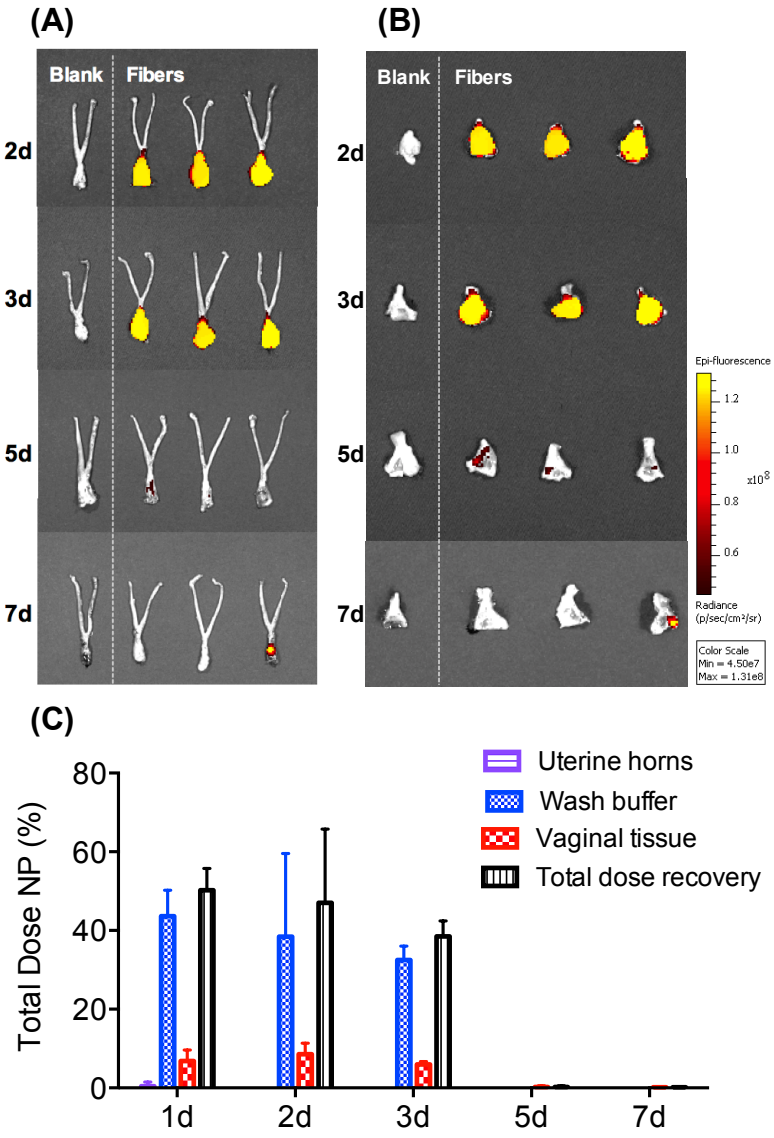

Figure 5-5. Nanoparticles are retained in the reproductive tract out to three days after a single PVA composite fiber administration. (A) Whole reproductive tracts, pre-wash. (B) Opened vaginal tissues post-wash, cut open to the cervix. Minimum and maximum radiance were set to the same values for all Xenogen images taken in (A) and (B). (C) Dose recovery of fluorescent nanoparticles at 1d, 2d, 3d, 5d, and 7d, measured by tissue homogenization methods, plotted as mean +/- S.D. For each time point, n=3 animals received PVA composite fibers and n=1 untreated mouse was used as a control (1d time point from Fig. 4, different study with same methods, but n=7 mice per group).

5.4.9 Pharmacokinetics of ETR after intravaginal delivery in fibers vs. suspensions

Pharmacokinetic parameters were calculated for mice receiving aqueous suspensions (sampled from 1h to 72h) and for mice receiving composite fibers (sampled from 1h to 7d), with n=5 mice for each condition tested. Cmax is defined as the maximum observed concentration, Tmax is the time at which Cmax occurred, AUC is the area under the concentration-time curve, and $t_{1/2}$ as the terminal elimination half-life (estimated from the terminal phase of the log-linear concentration-time curve).

5.4.10 Cervicovaginal lavage PK

Drug release kinetics in the cervicovaginal lavage were also remarkably different for aqueous suspensions compared to composite fibers. Aqueous suspensions provided an initial burst release of drug at early time points, shown by the high Cmax, short Tmax, and shorter terminal half-life relative to composite fibers for most organs, including the lavage (Table 5-3). For mice that received aqueous suspensions, Cmax occurred at around 1h, with a mean 9.72 µg ETR /mL detected in the lavage (17.0% total ETR dose administered). The drug concentration fell rapidly, down to a mean of 0.67 µg ETR /mL (1.2% total dose) by 24h. For PVA composite fibers, Cmax also occurred around 1h, with a mean of 47.5 µg ETR /mL detected in the lavage (83.7% total ETR dose). However, for fibers, the drug concentration

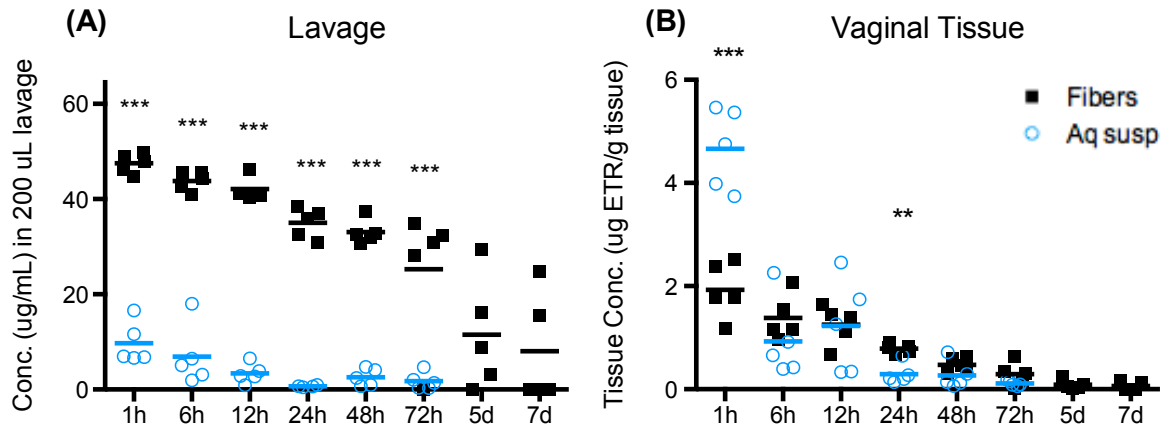

Figure 5-6. PVA composite fibers result enhanced ETR retention over 7 days in the cervicovaginal lavage and vaginal tissue relative to aqueous suspensions. (A) ETR content in 200 µL cervicovaginal lavage, including any undissolved fibers present (analyzed by HPLC). (B) ETR content in homogenized vaginal tissue, post-lavage (analyzed by LC-MS/MS). **p<0.01, **p<0.001. n=5 mice per group at each time point out to 72h, with fiber group only extended to 5d and 7d. Statistical outliers were identified with Grubb's test (alpha = 0.01) and were not included for PK analysis or displayed in this figure.

decreased much more slowly in the lavage out through 72h compared to aqueous suspensions. At 72h, there was still 33.1 µg ETR/mL (44.0% total dose) was detected in the lavage, which is quite similar to the 38.5% total dose of Rho-NP recovered in the lavage for the PVA composite fibers (Figure 5-5).

Table 5-3. Effect of nanoparticle dosage platform on pharmacokinetic parameters of ETR following intravaginal administration using noncompartmental analysis.

Biological sample	ETR formulation	$t_{1/2z}$ (h)[a]	T_{max} (h)	C_{max} (µg/g)[b] Mean *(± SEM)*	*P*	$AUC_{1.35\text{-}72.29h}$ (hr*µg/g)[c] Mean *(± SEM)*	*P*	AUC_{fib}/AUC_{sus}
Vaginal lavage	Suspension	36.41	1.35	9.72 *(1.96)*	<0.0001	202.11 *(29.01)*	<0.0001	12.53
	Fibers	62.09	1.35	47.51 *(0.94)*		2,531.69 *(85.63)*		
Vaginal tissue	Suspension	21.08	1.35	4.66 *(0.35)*	0.0002	44.29 *(5.42)*	0.1419	1.23
	Fibers	33.13	1.35	1.93 *(0.24)*		54.29 *(2.88)*		
Liver	Suspension	17.09	1.35	0.028 *(0.005)*	0.1247	0.266 *(0.027)*	0.0005	1.81
	Fibers	44.87	6.47	0.018 *(0.003)*		0.481 *(0.027)*		
Rectum	Suspension	NA	1.35	0.049 *(0.020)*	0.5213	0.625 *(0.105)*	0.0238	2.29
	Fibers	25.69	24.38	0.033 *(0.013)*		1.431 *(0.270)*		
Uterine horns	Suspension	NA	1.35	0.041 *(0.015)*	>0.9999	0.654 *(0.109)*	0.0258	2.02
	Fibers	25.99	12.52	0.041 *(0.017)*		1.322 *(0.219)*		
Plasma	Suspension	7.58	1.35	0.0038 *(0.0006)*	0.0170	0.0255 *(0.0024)*	0.0003	1.75
	Fibers	22.11	1.35	0.0019 *(0.0002)*		0.0446 *(0.0021)*		

[a] Calculated using data from 0-3 days for suspension (upon which values reached baseline) and 0-7 days for fibers
[b] µg/mL for vaginal lavage and plasma
[c] hr•µg/mL for vaginal lavage and plasma
NA, not available.

At 5d or longer, the drug concentration in the lavage for PVA fibers became more variable, but declined overall to a mean of 8.1 µg ETR/mL (14.3% total dose) at 7d. The terminal half-life values for the two NP dosage platforms show the differences in drug release kinetics, with aqueous suspensions having an ETR terminal half-life of 36.4h in the cervicovaginal lavage, versus 62.0h for the PVA fibers (Table 5-3). The differences in release kinetics in the lavage are likely due to the high degree of external leakage at early time points for aqueous suspensions, compared to the enhanced retention, slow hydration, dissolution, and subsequent release of NP

provided by fibers. At 5-7d, we observed some mice that received PVA fibers had a small, hardened chunk of polymer and/or mucus near the vaginal opening, while other mice had no visible sign of undissolved fibers. Since there were still undissolved fibers present at 5-7d, it suggests that the total mass of fibers administered (2.8 mg) was relatively high compared to the volume of fluid available for dissolution. Perhaps using a smaller dose (mass of fibers) in future studies would allow for a higher fluid:solid mass ratio and provide quicker *in vivo* fiber dissolution and increased release and diffusion of NP into vaginal tissue.

One limitation of the study design is that neither the lavage nor the wash method was able to differentiate between NP/drug trapped within undissolved fibers, and NP/drug that was released from fibers into the mucus. Both undissolved fibers and cervicovaginal mucus were "counted" as part of the lavage. It is possible that much of the ETR dose detected in the lavage was actually still within undissolved PVA fibers. Still, the results demonstrate that the hypothesis tested was true: composite fibers did indeed result in much less leakage and greater retention of ETR in the reproductive tract than aqueous suspensions did. Given the extremely high drug concentrations detected in lavage for the PVA composite fibers, the current platform may be suitable for agents that act as entry inhibitors to HIV-1 like maraviroc, griffithsin, or cyanovirin-N. High concentrations of entry inhibitors are desirable in the vaginal lumen to prevent virus from trafficking further into vaginal tissue and entering cells. Further studies will investigate how to optimize the composite fiber delivery system for increased diffusion of NP into vaginal tissue, the target for drugs that have intracellular mechanisms of action like ETR or other NNRTIs.

Although ETR has not been evaluated in clinical studies as a vaginally applied product, comparisons can be made from oral dosing studies. The DIVA-2 study evaluated ETR concentrations in cervicovaginal fluid (CVF) after oral dosing of ETR in HIV-1-infected women, and found good penetration of ETR into the CVF at concentrations of 0.857 μg/mL[33]. In comparison, the PVA fiber group provided ~10-fold higher ETR concentration in lavage at 7 d after a single dose. Overall, the dramatically enhanced ETR retention in the vaginal lumen and increased terminal half-life for composite fibers demonstrates the potential of fibers to increase retention and sustain drug release relative to aqueous suspensions. The data suggests that a fiber platform could provide sustained release of both NP and drug *in vivo*. Since nanofibers are also able to deliver drug in a burst release manner[15,16], the fiber platform may be able to meet design criteria for new microbicide technologies designed for both "on-demand" / pericoital use and sustained protection[49].

5.4.11 Vaginal tissue PK

We found that PVA composite fibers resulted in slightly increased ETR bioavailability to vaginal tissue from 1-72h, with relative bioavailability ($AUC_{fiber}/AUC_{suspension}$) of 1.23 (Table 5-3). The overall drug delivery to vaginal tissue as a function of percent total dose delivered is low relative to the cervicovaginal lavage for both platforms ($Cmax_{aq.\ susp.}$ = 1.90% total dose ETR, $Cmax_{fibers}$= 0.94% total dose ETR). Similar to the cervicovaginal lavage release kinetics, aqueous suspensions resulted in a high Cmax at early time (4.66 µg ETR/g at 1h), but tissue levels dropped quickly, down to 0.094 µg ETR/g at 24h. This compares to PVA composite fibers, which provided a lower initial drug concentration, but more constant, sustained ETR delivery to vaginal tissue out to 72h. For PVA fibers, Cmax occurred at 1h (1.93 µg ETR/g) and decreased slowly to 0.078 µg ETR/g at 72h. Vaginal tissue concentrations were approximately two-fold higher for fibers than suspensions from 24h-72h (Figure 5-6). The prolonged release kinetics is also captured by the longer terminal half-life value for fibers (33.1h) relative to aqueous suspensions (22.1h) (Table 5-3). This data is significant in that the vaginal tissue is where etravirine would be expected to actively inhibit HIV-1 reverse transcriptase.

However, the two-fold enhancement in ETR content in vaginal tissue provided by fibers is much lower than anticipated based on fluorescent NP experiments. We described previously in this manuscript that the Rho-NP content in vaginal tissue at 24h was approximately 20-fold higher for fibers relative to suspensions (Figure 5-4, Table 5-2). An important difference to highlight is that for this PK study, we tracked the movement of *drug* as opposed to *fluorescent nanoparticles.* Since the fluorescent NP studies and PK studies are tracking two different components (drug vs. nanoparticle), differences are expected. One likely explanation for the differences in vaginal tissue content between these studies is that the ETR burst released from the NP in the lumen while the NP were still diffusing out of the fibers and through the mucus. The NP may have eventually trafficked to the vaginal tissue, but released nearly all of their drug contents in the lumen before getting to their target. The physicochemical properties of ETR may also contribute to drug partitioning into mucus instead of tissue. Protein binding is a significant factor in mucosal drug delivery[50], and since ETR is 99.9-99.8% protein-bound in plasma[51], its penetration into vaginal tissue may also be limited by protein binding in vaginal fluid. Therefore, testing other ARVs with different physicochemical properties in this system would be useful to understand drug properties contribute to differences in drug tissue concentrations and elimination kinetics for the composite fiber system.

To test the hypothesis that ETR burst released before reaching vaginal tissue, we measured the *in vitro* release from ETR-NP under sink conditions and found that >95% of drug had

released within 2 h (Supplementary Fig. S3). As discussed already, the low volume conditions for *in vivo* release are not likely to be recapitulated by sink conditions established for the *in vitro* release experiment. However, burst release of ETR in the lumen would account for the observed high concentrations of drug in the lavage relative to the vaginal tissue. For future studies, this nanoparticle formulation may be further optimized to limit burst release. Along with optimizing NP for sustained release, NP should ideally be optimized for trafficking through the vaginal epithelium in addition to mucus. While PEGylated PLGA NP have been shown to diffuse quickly through mucus[3,43], there is limited knowledge on the transport mechanisms of these NP in the vaginal tissue. PEGylation of the nanoparticle surface has been demonstrated to result in decreased cell uptake and reduce efficiency of endosomal escape[52]. Thus, there is need for development of new strategies to create NP that can cross the vaginal epithelial barrier and be taken up intracellularly by target cells for HIV-1.

Another possibility is that the fluorescent NP studies were confounded by the presence of free rhodamine along with nanoparticle-conjugated rhodamine, resulting in artificially high values for the total dose of nanoparticles associated with vaginal tissue. Rhodamine was conjugated to PLGA via an ester bond and can be dissociated by hydrolysis by water or enzymes present in vaginal fluid. As mentioned previously, the rhodamine-PLGA conjugate was washed several times during the conjugation reaction and nanoparticle synthesis, so we expect the amount of free rhodamine to be small relative to conjugated rhodamine for the initial nanoparticles administered. Even if a large proportion of rhodamine did hydrolyze *in vivo*, we expect this amount to be consistent between both the aqueous suspension and fiber groups. Thus, this explanation still would not account for the large differences (>22-fold) in Rho-NP retention at 24h between composite fiber and aqueous suspension groups. We plan to directly measure the amount of free rhodamine versus nanoparticle-conjugated rhodamine *in vitro* using various buffers to test this explanation in future studies.

Vaginal tissue concentrations of ETR observed in this study are lower than those reported for some other studies for intravaginal administration of nanoparticles in mice, but still relevant in the context of establishing protective drug concentration for HIV-1 prevention. Das Neves *et al* studied biodistribution and pharmacokinetics of dapivirine (DPV), an NNRTI with similar physicochemical properties to ETR[7]. They detected a mean of ~3 μg ETR/g in the vaginal tissue at 24h after administration of DPV-NP (dosed at 5 μg DPV/mouse). In contrast, we observed a mean of 0.29 μg ETR/g for aqueous suspensions at 24h, and 0.79 μg ETR/g for PVA fibers (dosed at 11.5 μg ETR/mouse). Disparities may be due to differences in drug loading and release kinetics of nanoparticle formulations, as well as variations in administration methods

(das Neves *et al* positioned mice in an inverted position for 1 min after administration to reduce leakage). Cu *et al* did not directly measure drug content, but reported that nanoparticle content in vaginal tissue had decreased to near background levels by 24h[8]. Even though we observed low drug concentrations in vaginal tissue, the amount of drug present is still relevant in terms of being in range for protective action against HIV-1. The mean vaginal tissue concentrations detected for the PVA fiber group at 72 h was 293 ng/g, nearly 150-fold higher than the *in vitro* IC_{50} for ETR of ~2 ng/mL[33]. Dapivirine vaginal ring studies in humans reported vaginal tissue concentrations in the range of 0.3 to 3.5 μg/g[53], similar to the range of ETR detected for the PVA fiber group between 1-72h for this study of 0.3-1.9 μg/g. Overall, the PK data for vaginal tissue showed that composite PVA fibers improved ETR delivery to vaginal tissue by about two-fold relative to aqueous suspensions out three days after a single application.

5.4.12 Secondary organs PK

We found that systemic exposure to ETR was very low for both delivery platforms (Figure 5-7). Maximum ETR concentrations in the uterine horns, rectum or liver were approximately two orders of magnitude lower (50-fold to 70-fold less) than maximum concentration in the vaginal tissue (Table 5-3). Maximum ETR concentrations in the plasma were even lower, about three orders of magnitude (1000-fold to 1200-fold less) than the Cmax in vaginal tissue for both delivery platforms. These concentrations represent than 0.02% of the total ETR dose administered for the uterine horns and rectum, and less than 0.25% of the total dose for liver. This data is consistent with previous reports for intravaginal delivery of antiviral drug-loaded NP showing low systemic exposure[7], corroborating the rationale for local vaginal drug delivery to provide high concentrations of drug in target tissue while limiting systemic exposure and corresponding side effects.

For the secondary organs located anatomically closest to the vaginal tract, the rectum and uterine horns, we observed unique patterns in ETR drug exposure for aqueous suspensions compared to composite fibers (Figure 5-7). For aqueous suspensions, all secondary organs resulted in Cmax occurring at the earliest time point (1h) and decreasing rapidly to the last time point (72h) (Table 5-3), consistent with release kinetics observed for lavage and vaginal tissue. For PVA fibers, we observed a delay in Cmax, with the uterine horns and rectum reaching Cmax at 12h and 24h, respectively. Fibers also show a long terminal elimination half-life of 25-26h for both the uterine horns and rectum. The delay in Cmax for composite fibers is consistent with visual observations of slow fiber degradation over the course of days and hypothesis that fibers would take a longer time to hydrate, dissolve, and release NP. The $AUC_{1\text{-}72h}$ was about

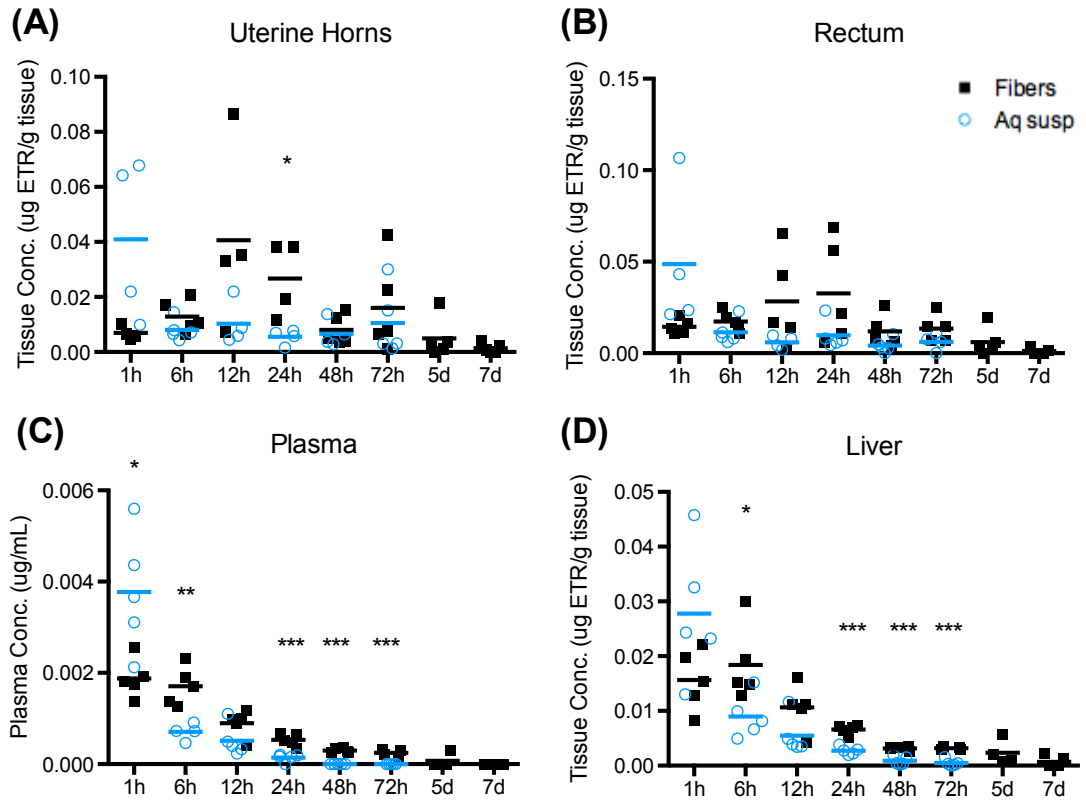

Figure 5-7. Low systemic drug exposure observed for both delivery platforms, with sustained release observed for the PVA composite fibers. (A)-(D) ETR content detected by LC-MS/MS in homogenized tissues. *p<0.05, **p<0.01, **p<0.001. n=5 mice per group at each time point out to 72h, with fiber group only extended to 5d and 7d. Statistical outliers were identified with Grubb's test (alpha = 0.01) and were not included for PK analysis or displayed in this figure.

two-fold higher for fibers than aqueous suspensions for both uterine horns and rectum, showing significantly higher overall drug exposure to tissue for fibers (Table 5-3). Though low relative to vaginal tissue AUC values, this data also supports the claim that the fiber platform is more suitable for sustained release of drug over the course of days, compared to the burst release over minutes or hours seen for the aqueous suspension group.

The drug concentrations measured in liver and plasma follow similar patterns for both total drug exposure and release kinetics, with overall low concentrations detected, but significantly higher drug concentrations for fibers than aqueous suspensions from 24h – 72h (Figure 5-7). The terminal elimination half-life in liver was longer for the PVA fiber group compared to the suspension, at 44.8h compared to 17.6h (Table 5-3). Following a similar pattern, the terminal elimination half-life in plasma was longer for PVA fibers, at 22.1h, compared to 7.6h for suspensions. These release kinetics observed in the liver and plasma for PVA fiber composites

parallel the two-fold increase in vagina tissue ETR concentrations seen for fibers (Figure 5-6). Again, this data supports the claim that composite fibers can provide sustained release of ETR over the course of three days.

5.5 CONCLUSIONS

In this work, we explored electrospun fibers as a novel intravaginal delivery platform for nanoparticles. We demonstrate the ability of composite fibers to release intact nanoparticles with maintained size and surface properties. Significantly, composite fibers were shown to enhance retention of NP and drug in the reproductive tract and sustain release of both NP and drug *in vivo* out to at least 3 days. This work demonstrates the capability of fibers as a sustained release platform *in vivo* and has potential applications in clinical use as a long-acting microbicide. It is the first report to our knowledge evaluating the *in vivo* retention of an intravaginal dosage form for NP delivery other than aqueous suspensions. This work is also significant in that two components within a single delivery platform were engineered independently for optimal interactions with cervicovaginal mucus. Such a system may have applications to other target sites for mucosal delivery including pulmonary, nasal, and buccal delivery.

From the pharmacokinetic study, we observed extremely high drug concentrations retained in the cervicovaginal lavage out to 7 days and a two-fold increase in ETR concentration in vaginal tissue from 24-72h for PVA composite fibers relative to aqueous suspensions. While there are still many variables left to explore for optimizing drug delivery to vaginal tissue from composite fibers, this work clearly demonstrates that composite fibers substantially improve both nanoparticle and drug retention in the reproductive tract. Composite fibers offer a new platform for the intravaginal administration of nanoparticles that is both solid-state and practical to administer.

5.6 ACKNOWLEDGEMENTS

We acknowledge J. Park for discussions on *in vivo* experimental design, particularly with the black paper leakage study. We also acknowledge L. Chan for insightful discussions on the pharmacokinetic study design. We thank S. Golan-Paz for her assistance with TEM and *in vitro* ETR-NP release studies, and K. Thoreson and L. Habernicht for their assistance with *in vivo* studies. We thank the Ian Suydam Laboratory at Seattle University for the gift of etravirine, and the Suzie Pun Laboratory at the University of Washington for use of the Xenogen imaging

system. We also acknowledge several technology user facilities at the University of Washington: the Molecular Analysis Facility (SEM, TEM), Keck Microscopy Center (confocal microscopy), and Mass Spectroscopy Center (LC-MS/MS). This work was funded by grants from the National Institutes of Health (NIAID and DAIDS): Microbicide Innovation Program VI (AI 094412), and Preclinical Innovation Program (AI 112002). The National Science Foundation provided Graduate Research Fellowships to EK and AB. The SURP Space Grant Program 6 (ecG1 A68796) provided funding for CN.

5.7 REFERENCES

1. UNAIDS. *The Gap Report*. 127 (2014). at <http://www.unaids.org/sites/default/files/media_asset/UNAIDS_Gap_report_en.pdf>
2. UNAIDS & The African Union. *Empower young women and adolescent girls: fast-tracking the end of the AIDS epidemic in Africa*. 5, 8 (Joint United Nations Programme on HIV/AIDS (UNAIDS), 2015). at <http://www.unaids.org/sites/default/files/media_asset/JC2746_en.pdf>
3. Ensign, L. M. *et al.* Mucus-Penetrating Nanoparticles for Vaginal Drug Delivery Protect Against Herpes Simplex Virus. *Sci. Transl. Med.* **4,** 138ra79–138ra79 (2012).
4. Yang, M. *et al.* Vaginal Delivery of Paclitaxel via Nanoparticles with Non-Mucoadhesive Surfaces Suppresses Cervical Tumor Growth. *Adv. Healthc. Mater.* **3,** 1044–1052 (2014).
5. Yoo, J.-W., Giri, N. & Lee, C. H. pH-sensitive Eudragit nanoparticles for mucosal drug delivery. *Int. J. Pharm.* **403,** 262–267 (2011).
6. Agrahari, V. *et al.* Hyaluronidase-Sensitive Nanoparticle Templates for Triggered Release of HIV/AIDS Microbicide In Vitro. *AAPS J.* **16,** 181–193 (2014).
7. das Neves, J. *et al.* Biodistribution and Pharmacokinetics of Dapivirine-Loaded Nanoparticles after Vaginal Delivery in Mice. *Pharm. Res.* **31,** 1834–1845 (2014).
8. Cu, Y., Booth, C. J. & Saltzman, W. M. In vivo distribution of surface-modified PLGA nanoparticles following intravaginal delivery. *J. Controlled Release* **156,** 258–264 (2011).
9. Marrazzo, J. *et al.* Pre-exposure prophylaxis for HIV in women: daily oral tenofovir, oral tenofovir/emtricitabine, or vaginal tenofovir gel in the VOICE Study (MTN 003). (2013).
10. Rees, H. FACTS 001 Phase III Trial of Pericoital Tenofovir 1% Gel for HIV Prevention in Women. (2015).
11. van der Straten, A. *et al.* Women's Experiences with Oral and Vaginal Pre-Exposure Prophylaxis: The VOICE-C Qualitative Study in Johannesburg, South Africa. *PLoS ONE* **9,** e89118 (2014).
12. Huang, C. *et al.* Stimuli-responsive electrospun fibers and their applications. *Chem. Soc. Rev.* **40,** 2417 (2011).
13. Ball, C., Krogstad, E., Chaowanachan, T. & Woodrow, K. A. Drug-Eluting Fibers for HIV-1 Inhibition and Contraception. *PLoS ONE* **7,** e49792 (2012).
14. Blakney, A. K., Ball, C., Krogstad, E. A. & Woodrow, K. A. Electrospun fibers for vaginal anti-HIV drug delivery. *Antiviral Res.* **100, Supplement,** S9–S16 (2013).
15. Ball, C. & Woodrow, K. A. Electrospun Solid Dispersions of Maraviroc for Rapid Intravaginal Preexposure Prophylaxis of HIV. *Antimicrob. Agents Chemother.* **58,** 4855–4865 (2014).
16. Krogstad, E. A. & Woodrow, K. A. Manufacturing scale-up of electrospun poly(vinyl alcohol) fibers containing tenofovir for vaginal drug delivery. *Int. J. Pharm.* **475,** 282–291 (2014).
17. Carson, D., Jiang, Y. & Woodrow, K. A. Tunable Release of Multiclass Anti-HIV Drugs that are Water-Soluble and Loaded at High Drug Content in Polyester Blended Electrospun Fibers. *Pharm. Res.* (2015). doi:10.1007/s11095-015-1769-0
18. Chou, S.-F., Carson, D. & Woodrow, K. A. Current strategies for sustaining drug release from electrospun nanofibers. *J. Controlled Release* (2015). doi:10.1016/j.jconrel.2015.09.008
19. Brako, F., Raimi-Abraham, B., Mahalingam, S., Craig, D. Q. M. & Edirisinghe, M. Making nanofibres of mucoadhesive polymer blends for vaginal therapies. *Eur. Polym. J.* **70,** 186–196 (2015).

20. Krogstad, E. A., Rathbone, M. J. & Woodrow, K. A. in *Focal Controlled Drug Delivery* (eds. Domb, A. J. & Khan, W.) 607–651 (Springer US, 2014). at <http://link.springer.com/chapter/10.1007/978-1-4614-9434-8_27>
21. Cameron Ball & Kim A. Woodrow. in *Drug delivery and development of anti-HIV microbicides* (eds. José das Neves & Bruno Sarmento) 459–508 (Pan Stanford Publishing Pte. Ltd., 2014).
22. Blakney, A. K., Krogstad, E. A., Jiang, Y. H. & Woodrow, K. A. Delivery of multipurpose prevention drug combinations from electrospun nanofibers using composite microarchitectures. *Int. J. Nanomedicine* **9,** 2967–2978 (2014).
23. Brettmann, B. K. *et al.* Free Surface Electrospinning of Fibers Containing Microparticles. *Langmuir* **28,** 9714–9721 (2012).
24. Qiu, K. *et al.* Doxorubicin-loaded electrospun poly(L-lactic acid)/mesoporous silica nanoparticles composite nanofibers for potential postsurgical cancer treatment. *J. Mater. Chem. B* (2013). doi:10.1039/C3TB20636J
25. Zomer Volpato, F. *et al.* Preservation of FGF-2 bioactivity using heparin-based nanoparticles, and their delivery from electrospun chitosan fibers. *Acta Biomater.* **8,** 1551–1559 (2012).
26. Wang, Y. *et al.* Electrospun composite nanofibers containing nanoparticles for the programmable release of dual drugs. *Polym. J.* **43,** 478–483 (2011).
27. Song, B., Wu, C. & Chang, J. Controllable delivery of hydrophilic and hydrophobic drugs from electrospun poly(lactic-co-glycolic acid)/mesoporous silica nanoparticles composite mats. *J. Biomed. Mater. Res. B Appl. Biomater.* **100B,** 2178–2186 (2012).
28. Solomonidou, D., Cremer, K., Krumme, M. & Kreuter, J. Effect of carbomer concentration and degree of neutralization on the mucoadhesive properties of polymer films. *J. Biomater. Sci. Polym. Ed.* **12,** 1191–1205 (2001).
29. Salamat-Miller, N., Chittchang, M. & Johnston, T. P. The use of mucoadhesive polymers in buccal drug delivery. *Adv. Drug Deliv. Rev.* **57,** 1666–1691 (2005).
30. de Araújo Pereira, R. R. & Bruschi, M. L. Vaginal mucoadhesive drug delivery systems. *Drug Dev. Ind. Pharm.* **38,** 643–652 (2012).
31. Asane, G. S. *et al.* Polymers for Mucoadhesive Drug Delivery System: A Current Status. *Drug Dev. Ind. Pharm.* **34,** 1246–1266 (2008).
32. Schöller-Gyüre, D. M., Kakuda, T. N., Raoof, A., Smedt, G. D. & Hoetelmans, R. M. W. Clinical Pharmacokinetics and Pharmacodynamics of Etravirine. *Clin. Pharmacokinet.* **48,** 561–574 (2012).
33. Clavel, C. *et al.* Etravirine Concentrations in the Cervicovaginal Compartment in HIV-1-Infected Women Receiving Etravirine-Containing Antiretroviral Therapy: DIVA 02 Study. *Antimicrob. Agents Chemother.* **56,** 4018–4020 (2012).
34. Patterson, K., Jennings, S., Falcon, R., Mrus, J. & Kashuba, A. Darunavir, Ritonavir, and Etravirine Pharmacokinetics in the Cervicovaginal Fluid and Blood Plasma of HIV-Infected Women. *Antimicrob. Agents Chemother.* **55,** 1120–1122 (2011).
35. Chaowanachan, T., Krogstad, E., Ball, C. & Woodrow, K. A. Drug Synergy of Tenofovir and Nanoparticle-Based Antiretrovirals for HIV Prophylaxis. *PLoS ONE* **8,** e61416 (2013).
36. Costantino, L. *et al.* Peptide-derivatized biodegradable nanoparticles able to cross the blood–brain barrier. *J. Controlled Release* **108,** 84–96 (2005).
37. Beck-Broichsitter, M. *et al.* Novel 'Nano in Nano' Composites for Sustained Drug Delivery: Biodegradable Nanoparticles Encapsulated into Nanofiber Non-Wovens. *Macromol. Biosci.* **10,** 1527–1535 (2010).
38. Chen, M. *et al.* Chitosan/siRNA Nanoparticles Encapsulated in PLGA Nanofibers for siRNA Delivery. *ACS Nano* **6,** 4835–4844 (2012).
39. Xie, Z. *et al.* Dual growth factor releasing multi-functional nanofibers for wound healing. *Acta Biomater.* **9,** 9351–9359 (2013).
40. Schindelin, J. *et al.* Fiji: an open-source platform for biological-image analysis. *Nat. Methods* **9,** 676–682 (2012).
41. Moench, T. R., Mumper, R. J., Hoen, T. E., Sun, M. & Cone, R. A. Microbicide excipients can greatly increase susceptibility to genital herpes transmission in the mouse. *BMC Infect. Dis.* **10,** 331 (2010).
42. Woodrow, K. A. *et al.* Intravaginal gene silencing using biodegradable polymer nanoparticles densely loaded with small-interfering RNA. *Nat. Mater.* **8,** 526–533 (2009).
43. Lai, S. K., Wang, Y.-Y. & Hanes, J. Mucus-penetrating nanoparticles for drug and gene delivery to mucosal tissues. *Adv. Drug Deliv. Rev.* **61,** 158–171 (2009).

44. Mun, E. A. *et al.* On the Role of Specific Interactions in the Diffusion of Nanoparticles in Aqueous Polymer Solutions. *Langmuir* **30,** 308–317 (2014).
45. Yang, M. *et al.* Nanoparticle penetration of human cervicovaginal mucus: The effect of polyvinyl alcohol. *J. Controlled Release* **192,** 202–208 (2014).
46. Ensign, L. M. *et al.* Pretreatment of Human Cervicovaginal Mucus with Pluronic F127 Enhances Nanoparticle Penetration without Compromising Mucus Barrier Properties to Herpes Simplex Virus. *Biomacromolecules* **15,** 4403–4409 (2014).
47. Willits, R. K. & Saltzman, W. M. Synthetic polymers alter the structure of cervical mucus. *Biomaterials* **22,** 445–452 (2001).
48. Willits, R. K. & Mark Saltzman, W. The effect of synthetic polymers on the migration of monocytes through human cervical mucus. *Biomaterials* **25,** 4563–4571 (2004).
49. CAMI Health. *MPT Product Prioritization and Gap Analysis: 2014 Summary*. (Initiative for Multipurpose Prevention Technologies (IMPT), 2014). at <http://www.cami-health.org/documents/MPTProductPrioritizationGapAnalysis2014Sum.pdf>
50. Cottrell, M. L., Srinivas, N. & Kashuba, A. D. Pharmacokinetics of antiretrovirals in mucosal tissue. *Expert Opin. Drug Metab. Toxicol.* **11,** 893–905 (2015).
51. Liedtke, M. & Rathbun. The next generation: etravirine in the treatment of HIV-1 infection in adults refractory to other antiretrovirals. *Virus Adapt. Treat.* 91 (2010). doi:10.2147/VAAT.S6413
52. Suk, J. S., Xu, Q., Kim, N., Hanes, J. & Ensign, L. M. PEGylation as a strategy for improving nanoparticle-based drug and gene delivery. *Adv. Drug Deliv. Rev.* (2015). doi:10.1016/j.addr.2015.09.012
53. Adams, J. L. & Kashuba, A. D. M. Formulation, pharmacokinetics and pharmacodynamics of topical microbicides. *Best Pract. Res. Clin. Obstet. Gynaecol.* (2012). doi:10.1016/j.bpobgyn.2012.01.004

6 Summary and Future Perspectives.

6.1 OVERALL SUMMARY AND CONCLUSIONS

In this dissertation, nanomaterial platforms for drug delivery including nanoparticles and electrospun nanofibers were investigated for the context of vaginal drug delivery. This work was especially motivated by the high global burden of HIV-1, particularly in low-resource settings like sub-Saharan Africa, and the lack of female-initiated prevention methods for HIV-1. We loaded antiretroviral drugs in nanoparticles and nanofibers and evaluated their ability to retain drug activity against HIV-1 *in vitro* and sustain release of drug for longer-acting protection. We then studied the potential of electrospun fibers for multipurpose prevention of HIV-1, HSV-2, and unintended pregnancy, as well as the scalability of this platform using a production-scale instrument. Finally, we combined the nanoparticle and electrospun fiber platforms into composite materials and investigated their potential as a novel dosage form for increasing vaginal retention of nanoparticles using *in vivo* murine models.

In Chapter 2, we synthesized and characterized antiretroviral drug-loaded nanoparticles for their physicochemical properties, drug loading, toxicity and ability to prevent HIV-1 infection *in vitro* relative to free drug. We found that the nanoparticle platform can enhance drug activity against HIV-1 by up to 50-fold for efavirenz nanoparticles, demonstrating that nanoparticles can improve ARV delivery to cells. Toxicity to TZM-bl cells and macaque cervical explant tissue was found to be low, suggesting good biocompatibility of the PLGA nanoparticle system for topical vaginal application. Importantly, we applied the TZM-bL cell reporter assay to determine the added benefit of using nanoparticles to delivery drug as opposed to free drug, and also to evaluate synergism obtained by delivering ARV nanoparticles in combination with tenofovir. While this work was applied specifically for efavirenz or saquinavir-loaded PLGA nanoparticles, we expect the methods to be translatable for evaluating other candidate drugs or carrier systems as next-generation microbicides.

In Chapter 3, we investigated electrospun fibers as a vaginal drug delivery platform for simultaneous STI prevention and contraception. We fabricated electrospun fibers containing antiretroviral drugs with action against HIV-1 and HSV-2, as well as chemical inhibitors of sperm motility. Proof-of-concept was demonstrated for fibers as a multipurpose prevention technology, as fibers were shown to load and release ARVs that potently inhibited HIV-1 *in vitro* in addition to acting as a physical and chemical barrier to sperm. Significantly, we also showed by modulating polymer type and content in fibers, both burst and sustained drug release kinetics

were achieved. This work is relevant for the field of multipurpose prevention technology in that it introduces a new platform for intravaginal administration that meets many key design criteria for new products. We showed that electrospun fibers are incredibly versatile with regard to the types of polymers/agents that can be incorporated, can provide both burst and sustained release (significant for both pericoital and sustained dosing frequency), and can act as a physical barrier to sperm (new potential contraceptive method).

In Chapter 4, we evaluated the manufacturing scale-up potential of drug-loaded electrospun fibers. We electrospun tenofovir-containing PVA fibers on a small-scale needle rig system (commonly used in laboratories) and a production-scale free surface electrospinning instrument. We characterized the properties of fibers produced using each system and found that fiber diameter, actual drug loading, encapsulation efficiency, and burst release kinetics were similar for fibers produced on both the small-scale and production-scale instruments. These results demonstrate that tenofovir-containing PVA fibers are scalable to the production scale, and results may be translatable for other types of drug-loaded fibers. This is an important finding for the microbicide field in that scalability and cost-effectiveness are necessary for evaluating new dosage platforms. Surprisingly, we found that at least 60% TFV (drug:fiber mass) could be incorporated into fibers, meaning there was more drug by mass than fiber itself within the fiber meshes. This is remarkably high relative to similar solid state dosage forms, vaginal films, which only have reported drug loadings of up to 1.3% (w/w). This means that fibers may be able to provide the same amount of drug as similar dosage forms using a much smaller dose (>45x less by mass) or deliver drugs with reduced potency, which may expand the types of vaginal products achievable for the fiber platform.

In Chapter 5, we addressed a major gap in the microbicide field by investigating a new platform for the delivery of nanoparticles: nanoparticle-releasing nanofiber composites. There have been many advances made in engineering nanoparticles to overcome physiologic barriers to vaginal drug delivery, but the field currently lacks a practical method for administering nanoparticles. In this work, we directly compared the vaginal retention of nanoparticles delivered in aqueous suspensions versus composite nanofibers in mice. We found that fibers enhance the retention of nanoparticles in the reproductive tract at 24h by over 30-fold relative to aqueous suspensions. Further, we found that fibers can sustain significant amounts of nanoparticle retention in the reproductive tract (and vaginal tissue) out to three days, compared to <1% of total dose remaining for aqueous suspensions at 24h. Importantly, we learned that composite fibers behave very differently *in vivo* that predicted by *in vitro* experiments under sink conditions, likely due to much lower fluid volumes *in vitro* and interactions with cervicovaginal mucus.

Overall, we found that both nanoparticles and nanofibers have high potential for enhancing vaginal drug delivery, with many impacts for the microbicide field as a whole. Nanoparticles were found to be able to load high amounts of antiretroviral drugs and enhance efficacy against HIV-1 *in vitro* compared to free drug alone. Nanofibers were demonstrated to be able to load many agents relevant to vaginal drug delivery at remarkably high levels (up to 60% by mass), provide both quick and sustained drug release, release active drug with action against HIV-1, and act as a physical and chemical barrier to sperm. Both particle and fiber platforms demonstrated good biocompatibility, showing maintained vaginal epithelial integrity when tested *ex vivo* tissue explants and comparable cytotoxicity to media controls in a human cervical cancer cell line. Fibers were shown to be scalable to the manufacturing level, an important criterion for developing cost-effective microbicides and advancing studies to human clinical trials. Finally, nanoparticle/nanofiber composites were found to dramatically enhance retention in the reproductive tract of mice and delivery to vaginal tissue, characterizing a new platform for vaginal administration of nanoparticles that is both solid-state and practical to administer.

Many aspects of this work were novel: (1) the first demonstration of using electrospun fibers as a platform for multipurpose prevention of HIV-1 and contraception; (2) the first *in vivo* studies testing electrospun fibers for intravaginal administration; (3) the first studies exploring glycerol monolaurate for its ability to inhibit sperm motility; (4) the first investigation of using electrospun nanofibers to deliver intact *nanoparticles* (as opposed to drug/protein); (5) the first platform containing two components uniquely tailored for optimal interactions with mucus (mucus-penetrating and muco-adherent components); (6) the first *in vivo* studies of vaginally administered nanoparticle/nanofiber composites.

Several limitations were discovered while completing this work. In Ch. 2, we found that nanoparticle loading was limited to ~7 wt% and that encapsulation efficiency was limited to around 50% for this particular system. It is also unclear if these nanoparticles can provide significant sustained release beyond 24h. Release may be limited by either drug solubility in PLGA or the nanoscale dimensions that provide fast diffusion. In Ch. 3 and 4, further work is needed to optimize the uniformity of fiber thickness when electrospinning on the manufacturing scale. Additionally, more in-depth toxicity and safety studies should evaluate how vaginal tissue responds to the presence of nanofibers, including characterizing changes in inflammation, pH, cell populations, and the vaginal microbiome. Finally, in Ch. 5, we were unable to differentiate between drug that was still entrapped in nanoparticles versus released drug for our *in vivo* pharmacokinetic study. Future studies are needed to explore alternate methods for fabricating composite materials and for independently tracking free drug vs. nanoparticle-associated drug.

6.2 FUTURE DIRECTIONS

There is much left to be explored for all of the nanomaterial platforms studied in this dissertation. For nanoparticles, exciting developments have been made in engineering nanoparticles to diffuse rapidly through mucus[1,2], but work is still needed to design nanoparticles for increased transport through the vaginal epithelium and enhanced cellular uptake. Future challenges for the fiber platform include further characterizing *in vivo* dissolution and effects on mucus barrier properties, as well as determining the appropriate dosing for pericoital and sustained use products. Moving forward, since user adherence has been a major challenge in many vaginal microbicide clinical trials[3,4], it will also be important to obtain feedback from potential end-users on their preferences for product attributes in a fiber-based platform. For the nanoparticle/nanofiber composite platform in particular, several studies are described below that would be informative for the continued investigation of fibers as a vaginal delivery platform.

6.2.1 Nanofiber composites for the release of other types of nanocarriers.

Composite fibers could be studied for their ability to release other types of delivery vehicles beside PLGA-ETR nanoparticles. Drug and protein release, but not nanocarrier release, has been evaluated for electrospun fiber composite materials. Our PLGA nanoparticles described in Ch. 5 likely resulted in burst release of ETR. Studies could be done to test the potential of this system for nanoparticle that shows sustained release of drug over 5-7 days *in vitro*, matching the *in vivo* elimination rate of the PVA fibers that we observed in Ch. 5. Other studies could investigate using composites to deliver nanoparticles that are engineered to specifically penetrate the vaginal epithelial barrier. Finally, other types of carriers including liposomes, mesoporous silica nanoparticles, and dendrimers could be electrospun into fibers and characterized for their nanoparticle:fiber loading potential, nanoparticle release kinetics, physicochemical properties after release.

6.2.2 Identifying a method for removal of undissolved PVP fibers from vaginal tissue.

Continued methods development could be done to find an appropriate method to fully remove undissolved PVP fibers from vaginal tissue. PVP fibers could not be removed from vaginal tissue using either the wash buffer or lavage method described in Ch. 5 due to their high degree of mucoadhesivity, confounding our ability to make claims regarding nanoparticle trafficking into vaginal tissue. To more fully dissolve mucus and PVP fibers, various wash buffers that contain different concentrations of enzymes, mucus thinning agents, or PVP solvents could be tested for their ability to dissolve cervicovaginal mucus from excised

reproductive tracts of mice. Alcain blue staining could also be used to probe for the presence of mucus as described previously[5]. In parallel, complete removal of undissolved fibers could be determined by using fluorescently conjugated PVP fibers, and fluorescence microscopy and homogenization techniques described in Ch. 5 to detect fibers remaining after the wash procedure. After a method is identified to remove PVP fibers from tissue, PVP fibers could be added as comparison group for the long-term retention (Rho-NP) study and pharmacokinetic study presented in Ch. 5 and compared to results for PVA composite fibers and aqueous suspensions.

6.2.3 Alternate methods for fabricating nanoparticle/nanofiber composites.

Fourth, challenges related to finding a solvent that is compatible with all composite components may be overcome by exploring alternate methods for composite fabrication. The optimal composite fabrication strategy would result in high nanoparticle:nanofiber loading and uniformity across a large area of fiber mesh. Alternate methods for fabrication may allow for different spatial presentation of nanoparticles on fiber structures (i.e., on the outside of fibers versus the inside) that could improve nanoparticle release kinetics from fibers and allow for higher nanoparticle loadings to be achieved. There are few reports of methods for fabricating composites other than the "direct addition" method. Ionescu *et al* electrospun a second "sacrificial" fiber polymer containing nanoparticles that was dissolved away to leave nanoparticles trapped within a primary fiber polymer[6]. However, this method still requires considering solvent compatibility with all components and is unlikely to be feasible for hydrophilic fiber polymers.

Two other strategies for composite fabrication could be explored: nanoparticle aerosolization and nanoparticle "rubbing". Aerosolization of nanoparticles has previously been investigated for administering dry nanoparticles in powdered form for pulmonary applications[7,8]. Nanofibers have been extensively investigated for use as air filters because of their high efficiency at trapping fine particles on the order of 10-500 nm[9,10]. By simultaneously applying these concepts, fibers could be used as a filter to trap aerosolized nanoparticles as a method for fabricating nanoparticle/nanofiber composites. Second, composites could be created by "rubbing" dry nanoparticles onto nanofiber mats. "Rubbing" has been described for creating uniform monolayers of particles on a rubber substrates[11], but has not yet been described as a method for fabricating composites using electrospun composites. Future studies could test a "rubbing" method as a means of distributing large amounts of nanoparticles uniformly across a fiber surface. This work would provide valuable data on two new methods for fabricating

nanoparticle/nanofiber composites in terms of highest achievable nanoparticle:nanofiber loading and nanoparticle uniformity across the fiber mesh, two key parameters in the development of a new vehicle for vaginal application of nanoparticles.

6.2.4 Effects of fiber composites on cervicovaginal mucus properties and nanoparticle diffusion.

Studying the effects of fiber composites on the barrier properties of cervicovaginal mucus and nanoparticle diffusion would be valuable for better predicting how composites will behave *in vivo*. It has been shown previously that presence of polymer can affect the physical properties of cervicovaginal mucus by causing mucin fiber aggregation[12] or result in changes in nanoparticle diffusion through polymer/mucus[13,14]. It will be important to evaluate how high polymer concentrations on the order of those provided by composite fibers affect the properties of cervicovaginal mucus. *In vitro* studies could be performed to study the effects of high concentrations of polymer addition on mucus network, including imaging of the mucin network to probe for physical changes. Further studies could also measure how nanoparticle diffusion is altered in combination mucus/polymer gels by developing new tracking techniques that are better suited for viscous polymer solutions containing biological components.

6.2.5 Effect of modifying nanoparticle/nanofiber composite parameters on *in vivo* fiber dissolution and nanoparticle release in the vaginal tract.

Fifth, electrospun fibers are a newly investigated dosage form for vaginal drug delivery, with the first reports of *in vitro* testing for vaginal application occurring only within the last three years[15,16]. As such, there is limited data on how fibers behave *in vivo* after intravaginal administration. To our knowledge, the only reports are those presented in Ch. 3[16] and Ch. 5. There is therefore much left to explore with regard to the *in vivo* behavior of the fiber platform for vaginal drug delivery. The vaginal mucosa is dynamic, with an overall low volume of fluid for dissolution, highly viscous mucus, variable pH, and high degree of mucus turnover[17]. Since it is difficult to recapitulate all of these conditions for *in vitro* dissolution or release studies, there is need for further investigation using *in vivo* models to understand how varying parameters of the fiber platform affect its dissolution in the vaginal tract.

Building on work presented in Ch. 5 on nanoparticle-releasing nanofiber composites for vaginal drug delivery, another idea is to explore in more depth how modifying various parameters of the fiber platform affect *in vivo* dissolution. The effect of modifying the following

four parameters on *in vivo* fiber dissolution time could be studied: (1) fiber dose administered, (2) polymer type, (3) use of dissolution-enhancing excipients, (4) geometry of fiber for insertion. This work may help identify key attributes of composite fiber meshes that significantly impact *in vivo* dissolution time in the mouse vaginal tract. In addition, it would provide valuable data on how these parameters also influence nanoparticle delivery from composite fibers and retention in vaginal tissue over time. This understanding would be greatly impactful for continued development of the nanofiber platform for vaginal drug delivery applications, including HIV microbicides, STI prevention and treatment, and contraception, as well as for drug delivery to other mucosal sites.

6.3 LIST OF CONTRIBUTIONS FROM THIS WORK

Peer-reviewed publications

1. **Krogstad E** *et al***,** Nanoparticle-releasing nanofiber composites for enhanced *in vivo* vaginal retention (manuscript in preparation).

2. **Krogstad E**, Woodrow KA (2014) Manufacturing scale-up of electrospun poly(vinyl alcohol) fibers containing tenofovir for vaginal drug delivery. Int J Pharm 475: 282–291.

3. Blakney A, **Krogstad E**, Jiang YH, Woodrow KA (2014) Delivery of multipurpose prevention drug combinations from electrospun nanofibers using composite microarchitectures. Int J Nanomedicine 9: 2967–2978.

4. Blakney A, Ball C, **Krogstad E**, Woodrow KA (2013) Electrospun fibers for vaginal anti-HIV drug delivery. Antiviral Res 100, Supplement: S9–S16.

5. Chaowanachan T, **Krogstad E**, Ball C, Woodrow KA (2013) Drug Synergy of Tenofovir and Nanoparticle-Based Antiretrovirals for HIV Prophylaxis. Plos One 8: e61416.

6. Ball C*, **Krogstad E***, Chaowanachan T, Woodrow KA (2012) Drug-Eluting Fibers for HIV-1 Inhibition and Contraception. Plos One 7: e49792 (*equally contributed to this work).

Book chapter

1. **Krogstad E**, Rathbone MJ, Woodrow KA (2014) Vaginal Drug Delivery. In: Domb AJ, Khan W, editors. Focal Controlled Drug Delivery. Advances in Delivery Science and Technology. Springer US. pp. 607–651.

Patent

1. KA Woodrow, C Ball, AK Blakney, **E Krogstad**, H Nie. “Vaginal Matrices: Nanofibers for Contraception and Prevention of HIV Infection.” US Patent Application filed November 6, 2013, University of Washington.

Presentations at national conferences

1. Nanoparticle-releasing nanofiber composites for enhanced *in vivo* vaginal retention, **E Krogstad***, R Ramanathan, C Nhan, K Thoreson, and KA Woodrow, presented Biomedical Engineering Society Annual Meeting, Tampa, FL, 2015, oral presentation.

2. Levonorgestrel and tenofovir composite fibers for dual prevention of HIV-1 and pregnancy, AK Blakney, **E Krogstad**, and KA Woodrow, presented at Biomedical Engineering Society Annual Meeting, Seattle, WA, 2013.

3. Developing nanoparticle-based combination ARVs as an effective strategy for HIV prevention, E Do, **E Krogstad**, D Bright, IT Suydam, and KA Woodrow, presented at Biomedical Engineering Society Annual Meeting, Seattle, WA, 2013.

4. Manufacturing scale-up potential of electrospun poly(vinyl alcohol) fibers containing tenofovir for vaginal drug delivery, **E Krogstad*** and KA Woodrow, presented at Controlled Release Society Annual Meeting and Exposition, Honolulu, HI, 2013.

5. Drug eluting fibers for STI inhibition and contraception, C Ball, **E Krogstad**, and KA Woodrow, presented at Biomedical Engineering Society Annual Meeting, Atlanta, GA, 2012, oral presentation.

6. Drug synergy of tenofovir and nanoparticle-based antiretroviral drugs for prophylaxis, T Chaowanachan, **E Krogstad***, C Ball, and KA Woodrow, presented at Biomedical Engineering Society Annual Meeting, Atlanta, GA, 2012.

7. Evaluating drug synergy of tenofovir and nanoparticle-based antiretroviral microbicides, T Chaowanachan, **E Krogstad**, C Ball, J Phan and KA Woodrow, presented at International Microbicides Conference, Sydney, NSW, AU, 2012.

8. Drug-eluting nanofibers for multipurpose prevention of sexually transmitted infections and unintended pregnancy, C Ball, **E Krogstad** and KA Woodrow, presented at International Microbicides Conference, Sydney, NSW, AU, 2012, oral presentation.

9. Nanomaterials for combination chemo-prophylaxis against sexual HIV transmission, **E Krogstad***, T Chaowanachan, C Ball, J Phan, and KA Woodrow, presented at Conference on Retroviral and Opportunistic Infections, Seattle, WA, 2012.

10. Vaginal matrices for dual prevention of HIV and unintended pregnancy, C Ball, **E Krogstad***, KA Woodrow, presented at CAMI Multipurpose Prevention Technologies Symposium, Washington, D.C., 2011, invited.

**Presenting author*

6.4 REFERENCES

1. Lai, S. K., Wang, Y.-Y. & Hanes, J. Mucus-penetrating nanoparticles for drug and gene delivery to mucosal tissues. *Adv. Drug Deliv. Rev.* **61,** 158–171 (2009).
2. Ensign, L. M. *et al.* Mucus-Penetrating Nanoparticles for Vaginal Drug Delivery Protect Against Herpes Simplex Virus. *Sci. Transl. Med.* **4,** 138ra79–138ra79 (2012).
3. Marrazzo, J. *et al.* Pre-exposure prophylaxis for HIV in women: daily oral tenofovir, oral tenofovir/emtricitabine, or vaginal tenofovir gel in the VOICE Study (MTN 003). (2013).
4. Rees, H. FACTS 001 Phase III Trial of Pericoital Tenofovir 1% Gel for HIV Prevention in Women. (2015).
5. Neves, J. das *et al.* Biodistribution and Pharmacokinetics of Dapivirine-Loaded Nanoparticles after Vaginal Delivery in Mice. *Pharm. Res.* **31,** 1834–1845 (2014).
6. Ionescu, L. C., Lee, G. C., Sennett, B. J., Burdick, J. A. & Mauck, R. L. An anisotropic nanofiber/microsphere composite with controlled release of biomolecules for fibrous tissue engineering. *Biomaterials* **31,** 4113–4120 (2010).
7. Sham, J. O.-H., Zhang, Y., Finlay, W. H., Roa, W. H. & Löbenberg, R. Formulation and characterization of spray-dried powders containing nanoparticles for aerosol delivery to the lung. *Int. J. Pharm.* **269,** 457–467 (2004).
8. Rubin, B. K. & Williams, R. W. Emerging aerosol drug delivery strategies: From bench to clinic. *Adv. Drug Deliv. Rev.* **75,** 141–148 (2014).
9. Wang, N., Mao, X., Zhang, S., Yu, J. & Ding, B. in *Electrospun Nanofibers for Energy and Environmental Applications* (eds. Ding, B. & Yu, J.) 299–323 (Springer Berlin Heidelberg, 2014). at <http://link.springer.com/10.1007/978-3-642-54160-5_12>
10. Podgórski, A., Bałazy, A. & Gradoń, L. Application of nanofibers to improve the filtration efficiency of the most penetrating aerosol particles in fibrous filters. *Chem. Eng. Sci.* **61,** 6804–6815 (2006).
11. Park, C. *et al.* Quick, Large-Area Assembly of a Single-Crystal Monolayer of Spherical Particles by Unidirectional Rubbing. *Adv. Mater.* **26,** 4633–4638 (2014).
12. Willits, R. K. & Saltzman, W. M. Synthetic polymers alter the structure of cervical mucus. *Biomaterials* **22,** 445–452 (2001).
13. Ensign, L. M. *et al.* Pretreatment of Human Cervicovaginal Mucus with Pluronic F127 Enhances Nanoparticle Penetration without Compromising Mucus Barrier Properties to Herpes Simplex Virus. *Biomacromolecules* **15,** 4403–4409 (2014).
14. Mun, E. A. *et al.* On the Role of Specific Interactions in the Diffusion of Nanoparticles in Aqueous Polymer Solutions. *Langmuir* **30,** 308–317 (2014).
15. Huang, C. *et al.* Electrospun cellulose acetate phthalate fibers for semen induced anti-HIV vaginal drug delivery. *Biomaterials* **33,** 962–969 (2012).
16. Ball, C., Krogstad, E., Chaowanachan, T. & Woodrow, K. A. Drug-Eluting Fibers for HIV-1 Inhibition and Contraception. *PLoS ONE* **7,** e49792 (2012).
17. Krogstad, E. A., Rathbone, M. J. & Woodrow, K. A. in *Focal Controlled Drug Delivery* (eds. Domb, A. J. & Khan, W.) 607–651 (Springer US, 2014). at <http://link.springer.com/chapter/10.1007/978-1-4614-9434-8_27>

APPENDIX A. Properties of Selected Antiretroviral Drugs

Drug	MW (g/mol)	BCS Class	Solubility	pKa	logP	Half-life (h)	Mechanism of action*
Dapivirine	329.4	II	<10 ug/mL	5.27	5.27	72-73 (plasma) 15-17 (vaginal fluid)	NNRTI
Efavirenz	315.7	II	<10 ug/mL	10.2	3.68	40-50	NNRTI
Etravirine	435.3	IV	<10 ug/mL	3.5	5.2	30-40	NNRTI
Maraviroc	513.7	III	~1 mg/mL	3.3, 7.9	4.37	14-18	EI
Raltegravir	482.5	II	<1 mg/mL	~1.25	1.06	9	II
Saquinavir mesylate	670.86 (free base)	I	2.22 mg/mL (aq) ~73 ug/mL (pH 6.5)	7.0 or 5.5	2.73	7-12	PI
Tenofovir	287.2	III	13.4 mg/mL	4.1	-1.1	17 / 150 (plasma / intracellular)	NtRTI
Tenofovir disoproxil fumarate	635.5	III	13.4 mg/mL	3.75	1.25	17 / 150 (plasma / intracellular)	NtRTI

*NRTI= nucleoside reverse transcriptase inhibitor, NtRTI=nucleotide reverse transcriptase inhibitor, NNRTI=non-nucleoside reverse transcriptase inhibitor, II=integrase inhibitor, PI=protease inhibitor, EI =entry inhibitor

References:

1. Date, A. A. & Destache, C. J. A review of nanotechnological approaches for the prophylaxis of HIV/AIDS. *Biomaterials* **34,** 6202–6228 (2013).
2. Sharma, P. & Garg, S. Pure drug and polymer based nanotechnologies for the improved solubility, stability, bioavailability and targeting of anti-HIV drugs. *Adv. Drug Deliv. Rev.* **62,** 491–502 (2010).
3. Piliero, P. Pharmacokinetic Properties of Nucleoside/Nucleotide Reverse... : JAIDS Journal of Acquired Immune Deficiency Syndromes. *J. Acquir. Immune Defic. Syndr.* **37,** S2–S12 (2004).
4. Kasim, N. A. *et al.* Molecular Properties of WHO Essential Drugs and Provisional Biopharmaceutical Classification. *Mol. Pharm.* **1,** 85–96 (2004).
5. Costa, A. P., Xu, X. & Burgess, D. J. Freeze-Anneal-Thaw Cycling of Unilamellar Liposomes: Effect on Encapsulation Efficiency. *Pharm. Res.* 1–7 doi:10.1007/s11095-013-1135-z
6. Gallant, J. E. & Deresinski, S. Tenofovir Disoproxil Fumarate. *Clin. Infect. Dis.* **37,** 944–950 (2003).
7. Taylor, S. *et al.* Antiretroviral drug concentrations in semen of HIV-infected men: differential penetration of indinavir, ritonavir and saquinavir. *J. Antimicrob. Chemother.* **48,** 351–354 (2001).
8. Nel, A. M., Smythe, S. C., Habibi, S., Kaptur, P. E. & Romano, J. W. Pharmacokinetics of 2 Dapivirine Vaginal Microbicide Gels and Their Safety Vs. Hydroxyethyl Cellulose-Based Universal Placebo Gel. *JAIDS J. Acquir. Immune Defic. Syndr.* **55,** 161–169 (2010).
9. De Clercq, E. Antiviral drugs in current clinical use. *J. Clin. Virol.* **30,** 115–133 (2004).

APPENDIX B. Antiretroviral Drug Structures

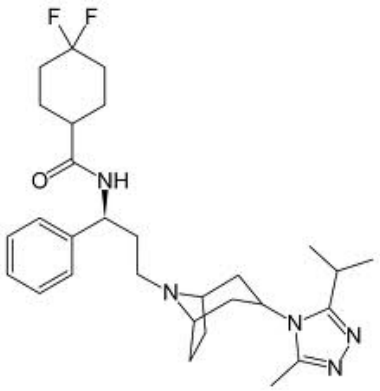

Maraviroc

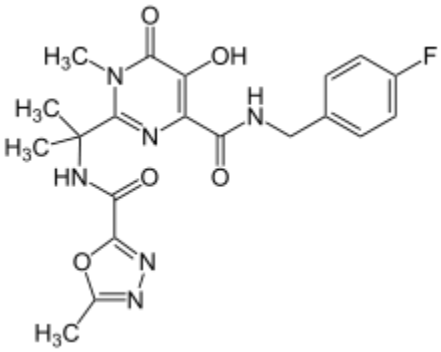

Raltegravir

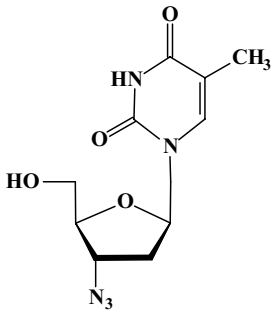

Zidovudine

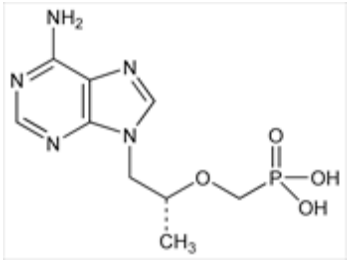

Tenofovir (GS1278)

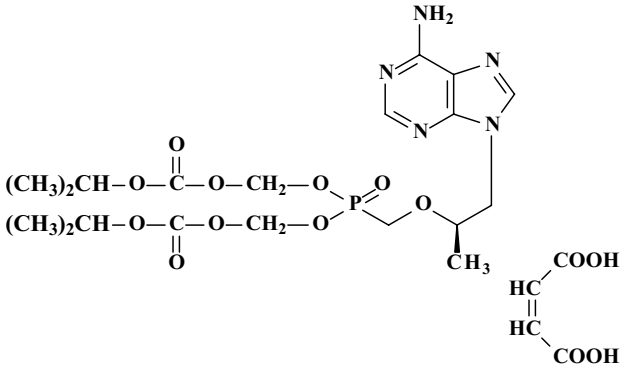

Tenofovir disoproxil fumarate

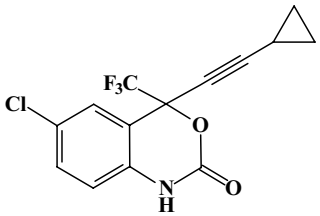

Efavirenz

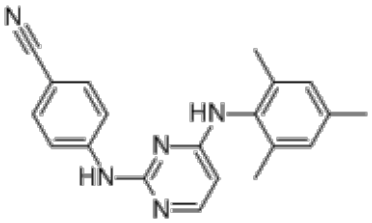

Dapivirine

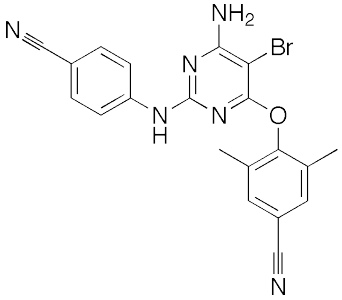

Etravirine

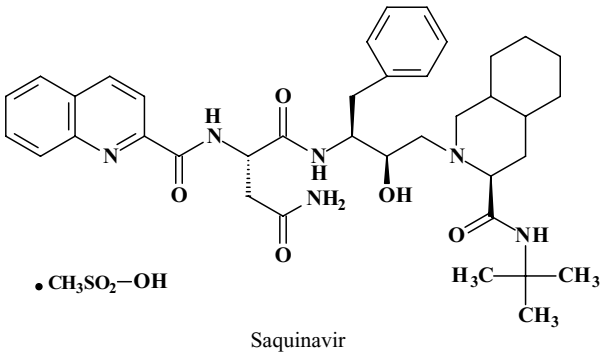

Saquinavir

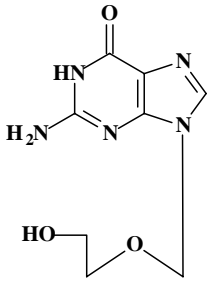

Acyclovir

APPENDIX C. Supplementary Information for Chapter 3

Available electronically in online publication:
Ball, C., Krogstad, E., Chaowanachan, T. & Woodrow, K. A. Drug-Eluting Fibers for HIV-1 Inhibition and Contraception. *PLoS ONE* 7, e49792 (2012)

Supporting figures

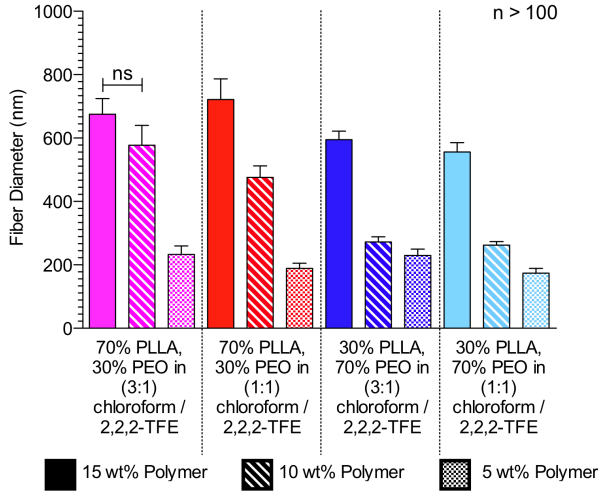

Fig. S1—Fiber diameters depend upon polymer viscosity, composition, and solvent. Geometric mean fiber diameters with 95% confidence intervals are shown for 70:30 PLLA/PEO fibers (red) and 30:70 PLLA/PEO fibers (blue) made from polymers dissolved in either 1:1 or 3:1 (vol/vol) chloroform/2,2,2-trifluoroethanol). Geometric mean fiber diameter was found to vary significantly between all groups based on the concentration of polymer in the electrospinning solution (solid = 15% wt/vol, dashed = 10% wt/vol, dots = 5% wt/vol) ($P < 0.0001$), except as indicated.

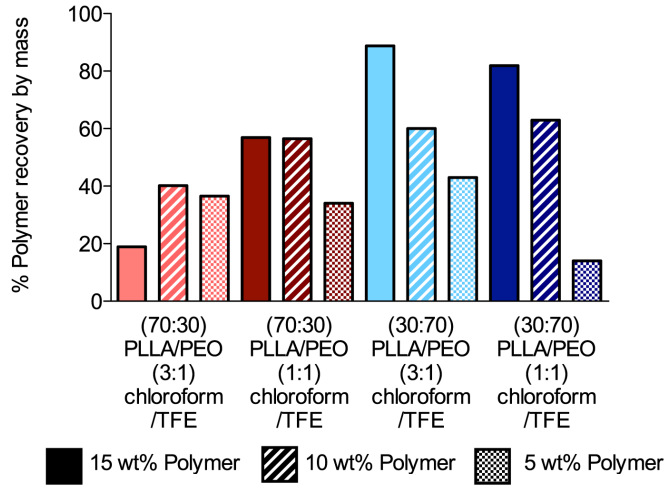

Fig. S2—Material efficiency was positively correlated with % wt/vol of polymer in solution for most polymer blends. Here we define material efficiency as the percent polymer recovered from the mandrel by mass. For 30:70 PLLA/PEO blends, material efficiency increased with the % wt/vol of polymer in solution. Material efficiency is important for cost effectiveness. Based on these results, we chose the 15% (wt/vol) 70:30 PLLA/PEO in 1:1 chloroform/TFE and 15% wt/vol 30:70 PLLA/PEO in 3:1 chloroform/TFE as the base formulations for all further work with drug encapsulation.

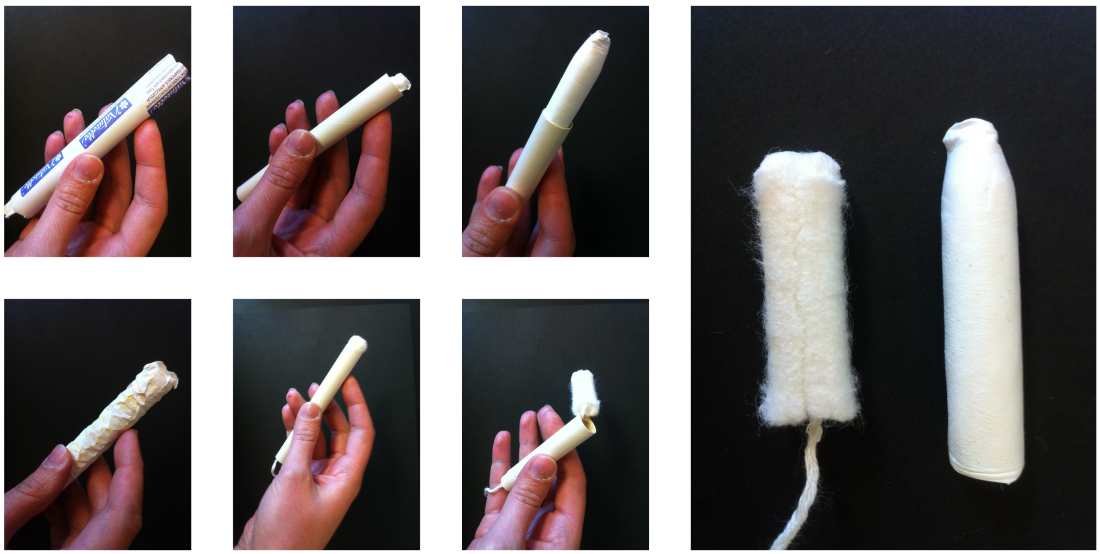

Fig. S3—Electrospun fibers can be made sufficiently thick to be easily pushed out of a tampon applicator. The mesh device can be loaded into standard packaging (top and bottom images on the left), and resembles a tampon once opened (2nd to left, top – mesh, bottom – tampon). The device is delivered by pushing the inner cardboard tube through the outer cardboard tube of the applicator, revealing the fiber mesh, which would then hydrate and release active agents (3rd to left, top – mesh, bottom – tampon). A side-by-side comparison of a tampon and the tubular mesh reveals comparable geometry (right).

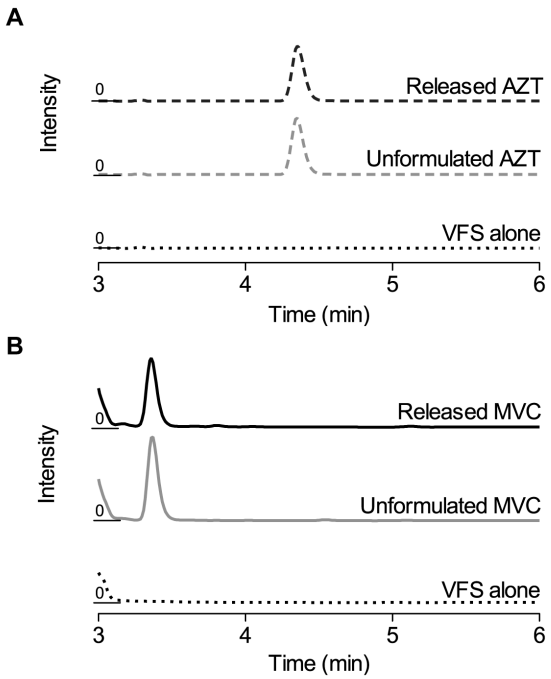

Fig. S4—Electrospinning does not alter drug retention time with HPLC. (**a**) Representative chromatogram for AZT. (**b**) Representative chromatogram for MVC. Peak shapes and retention times do not change for unformulated drugs (gray lines) compared with drugs released from fibers (black lines).

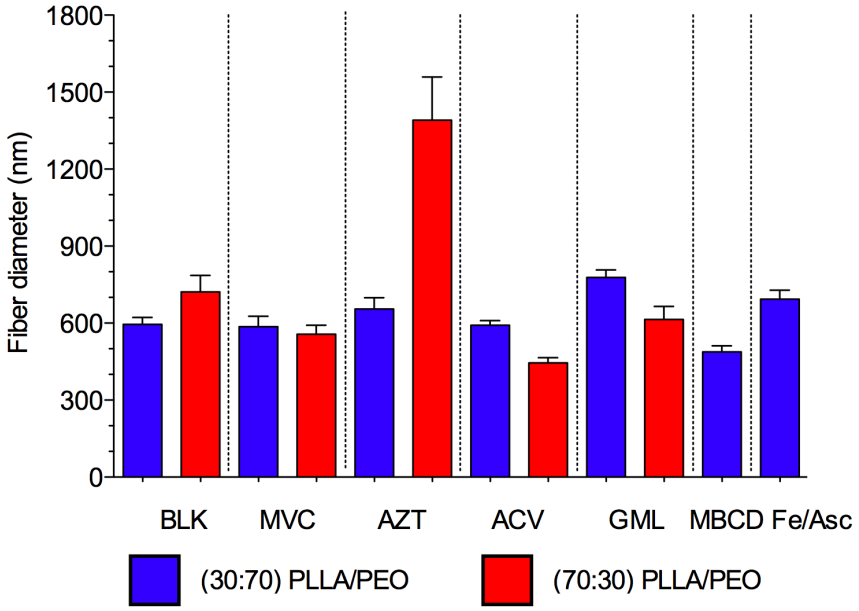

Fig. S5— Drug incorporation into 30:70 and 70:30 PLLA/PEO electrospun fibers can alter fiber diameter distributions. Geometric mean fiber diameters with 95% confidence intervals are shown for 70:30 PLLA/PEO fibers (red) and 30:70 PLLA/PEO fibers (blue) incorporating MVC, AZT, ACV, GML, MBCD, or Fe/Asc compared to blank fibers.

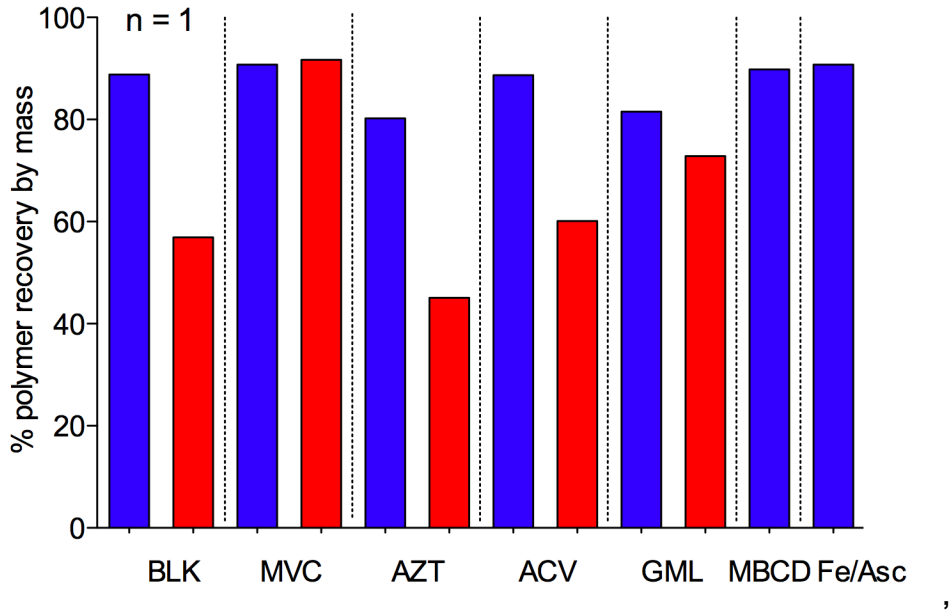

Fig. S6—Agent incorporation into fibers influences material efficiency. Incorporating drugs into 30:70 and 70:30 PLLA/PEO blends (blue and red, respectively) affected polymer recovery. Interestingly, MVC dramatically increased material efficiency for 70:30 PLLA/PEO fibers.

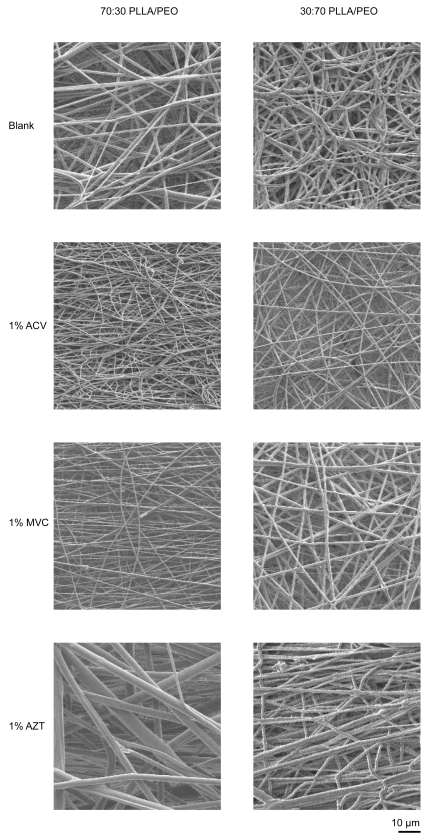

Fig. S7—Fiber morphology and alignment for antiviral compounds ACV, MVC, and AZT. Increased alignment of 70:30 PLLA/PEO fibers is apparent in 1% MVC samples. Increased alignment of 30:70 PLLA/PEO fibers is apparent in 1% AZT samples. Differences in fiber diameter, previously shown in Fig. S5, are also apparent.

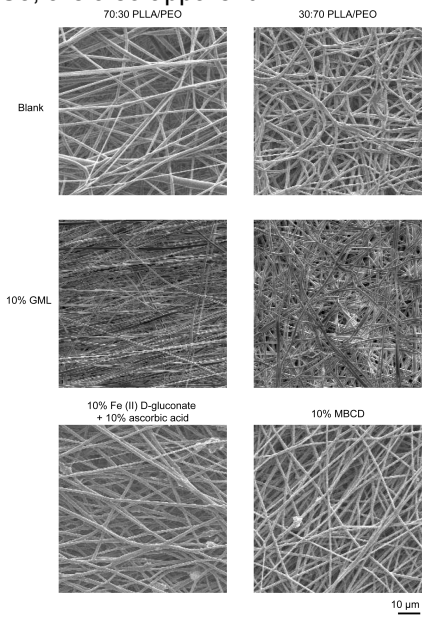

Fig. S8—Fiber morphology and alignment for contraceptive compounds GML, Fe/Asc, and MBCD. Increased alignment of 70:30 PLLA/PEO fibers is apparent in 10% GML samples. Increased alignment of 30:70 PLLA/PEO fibers is apparent in 10% MBCD samples. Differences in fiber diameter, previously shown in Supporting Fig. S5, are also apparent.

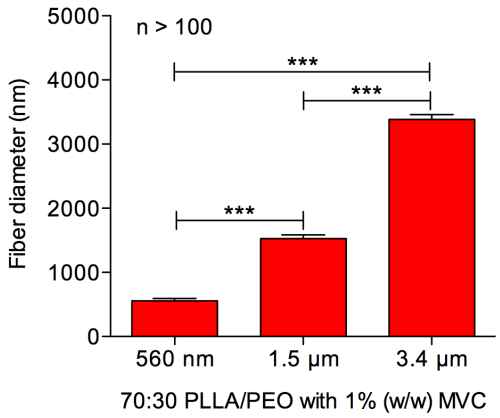

Fig. S9—Fiber diameters of 70:30 PLLA/PEO with 1% (w/w) MVC. Geometric mean fiber diameters with 95% confidence intervals are displayed for 70:30 PLLA/PEO fibers with 1% (w/w) MVC made by varying polymer concentration and electrospinning parameters. Geometric mean fiber diameters of all three mesh types are significantly different from each other ($p<0.0001$). These fibers correspond to cumulative release curves displayed in Fig. 3b.

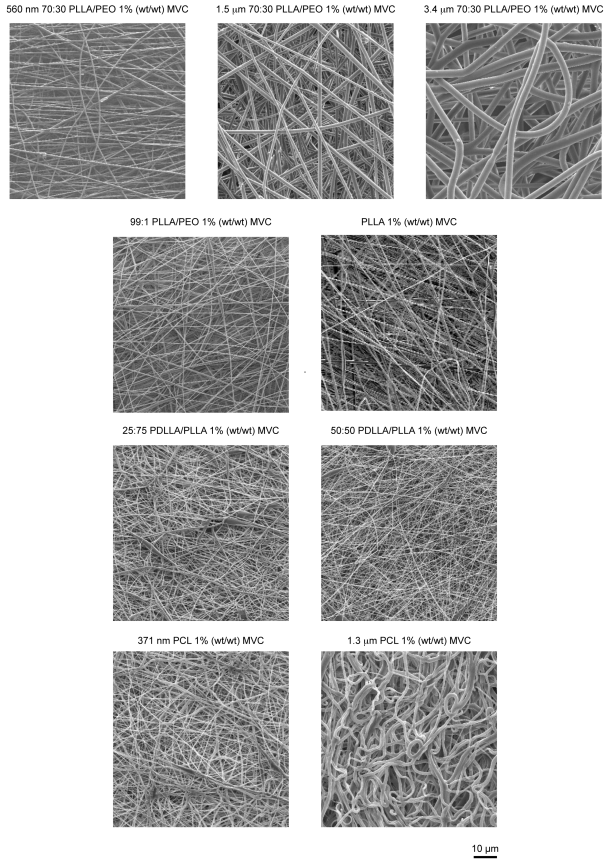

Fig. S10—Morphology of additional polymeric fibers incorporating 1% (wt/wt) MVC. Scanning electron micrographs of fibers made from different polymers incorporating 1% (wt/wt) MVC are shown, including 70:30 PLLA/PEO of three fiber diameters (560 nm, 1.5 µm, and 3.4 µm), 99:1 PLLA/PEO, PLLA, 25:75 PDLLA/PLLA, 50:50 PDLLA/PLLA, and PCL of two fiber diameters (371 nm and 1.3 µm). These fibers correspond to cumulative release curves displayed in Fig. 3.

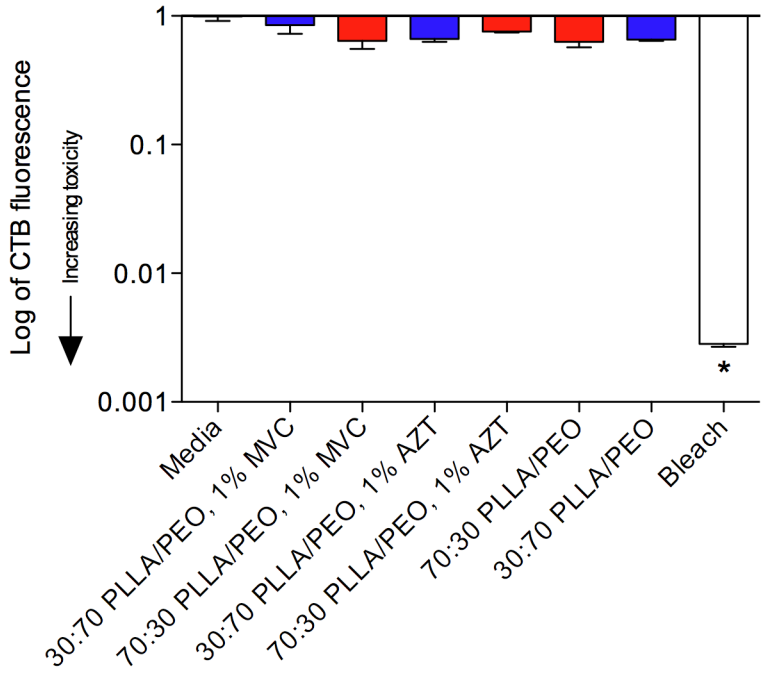

Fig. S11—Fibers are not cytotoxic to TZM-bl cells. Cytotoxicity was tested using the CellTiter-BlueTM cell viability assay by culturing TZM-bL cells with disks of blank and drug-loaded meshes (n = 3) for 48h. Fluorescence signals for each condition are plotted as log-transformed values. Media-only treated cells and fiber-treated cells show significantly less cytotoxicity than bleach-treated cells ($p<0.05$).

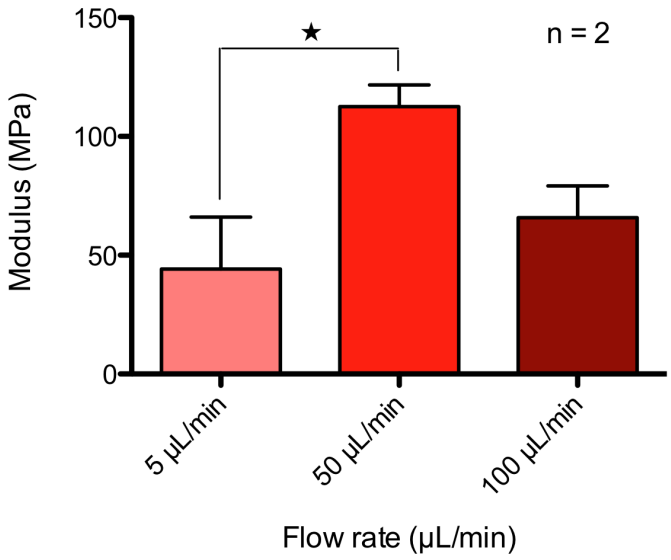

Fig. S12—Flow rate influences modulus of PCL fibers incorporating 1% (w/w) MVC. Moduli of PCL fiber meshes made from electrospinning at varying flow rates (5, 50, and 100 µL/min) were measured. The modulus of PCL fibers electospun at a flow rate of 50 µl/min is significantly different than the modulus of PCL fibers electrospun at 5 µL/min ($p<0.05$).

Supporting Tables

Table S1—GML inhibits sperm motility in swimout sperm at 0.05 and 0.5% (wt/vol).

Solution	Concentration (wt/vol)	Percent Motility at 2 min	Complete Inhibition within 5 min
PBS	1x	89	No
Nonoxynol-9	0.4%	0	Yes (< 30 s)
Glycerol Monolaurate	0.5% (pH 7)	30	Yes (< 4 min)
	0.05%	28	Yes (< 5 min)
	0.005%	55	No
	0.0005%	84	No
	0.00005%	75	No
Fe(II) D-gluconate	5%	52	No
L-ascorbic acid	5% (pH 2)	0	Yes (< 30 s)
	0.5% (pH 4)	21	No
Fe(II) D-gluconate + L-ascorbic acid	5% / 5%	0	Yes (< 30 s)
	0.5% / 0.5% (pH 4)	12	No
	0.05% / 0.05% (pH 5.5)	85	No
Methyl-β-cylcodextrin	5%	94	No

We tested the contraceptive agents for their ability to inhibit sperm motility in a dose response motility experiment. Equal amounts of drug solution and human swimout sperm were combined on a glass slide. Changes in sperm motility over 2–5 min were recorded using a microscope and video recording system. Time point controls with PBS were performed to ensure drug effects on motility were independent of sperm incubation time. PBS percent motility at 2 min reflects average over all PBS control measurements, with range from 72%–100%.

Table S2—Electrospun fibers effectively block sperm migration in a transwell assay.

	30:70 PLLA/PEO fibers	Control membranes
Upper chamber	$10^{6.05 \pm 0.036}$ sperm mL^{-1}	$10^{6.52 \pm 0.25}$ sperm mL^{-1}
Bottom chamber	0 sperm mL^{-1}	$10^{4.76 \pm 0.405}$ sperm mL^{-1}

We tested the ability of electrospun fiber mats to block sperm migration in a transwell assay. 30:70 PLLA/PEO fibers without drug were used to replace existing membranes in transwell cups. Motile sperm collected by swimout into media were added to the upper chamber (inside of the cup) and allowed to attempt to enter the bottom chamber for 2 hours. Sperm were then counted in both chambers to assess if sperm could penetrate the meshes.

Supporting videos
Videos show sperm motility at 5 min after addition of GML, PBS, or Nonoxynol 9. See published version online for links.

Video S1—Sperm in PBS. 10 uL of PBS were added to 10 uL of swimout sperm and then a glass coverslip was added to the sample while imaging at 100x magnification. The edges of the coverslip were sealed with clear nail polish to prevent streaming. Shown in this video are the PBS-treated sperm after 5 minutes of imaging. The sperm are clearly still motile.

Video S2—Sperm in nonoxynol-9. 10 uL of 0.4% wt/vol nonoxynol-9 were added to 10 uL of swimout sperm and then a glass coverslip was added to the sample while imaging at 100x magnification. The edges of the coverslip were sealed with clear nail polish to prevent streaming. Shown in this video are the nonoxynol-9-treated sperm after 5 minutes of imaging. The sperm are clearly completely immotile. Loss of motility was instant following addition of nonoxynol-9.

Video S3—Sperm in 0.5% wt/vol GML. 10 uL of 0.5% wt/vol GML were added to 10 uL of swimout sperm and then a glass coverslip was added to the sample while imaging at 100x magnification. The edges of the coverslip were sealed with clear nail polish to prevent streaming. Shown in this video are the GML-treated sperm after 5 minutes of imaging. The sperm are clearly immotile. Loss of motility was complete in under 4 minutes.

Video S4—Sperm in 0.05% wt/vol GML. 10 uL of 0.05% wt/vol GML were added to 10 uL of swimout sperm and then a glass coverslip was added to the sample while imaging at 100x magnification. The edges of the coverslip were sealed with clear nail polish to prevent streaming. Shown in this video are the GML-treated sperm after 5 minutes of imaging. The sperm are clearly immotile. Loss of motility was complete in under 5 minutes.

APPENDIX D. Supplementary Information for Chapter 4

Available electronically in online publication:
E. Krogstad and K.A. Woodrow, Manufacturing scale-up of electrospun poly(vinyl alcohol) fibers containing tenofovir for vaginal drug delivery. *Int J Pharm* **475**, 282–291 (2014).

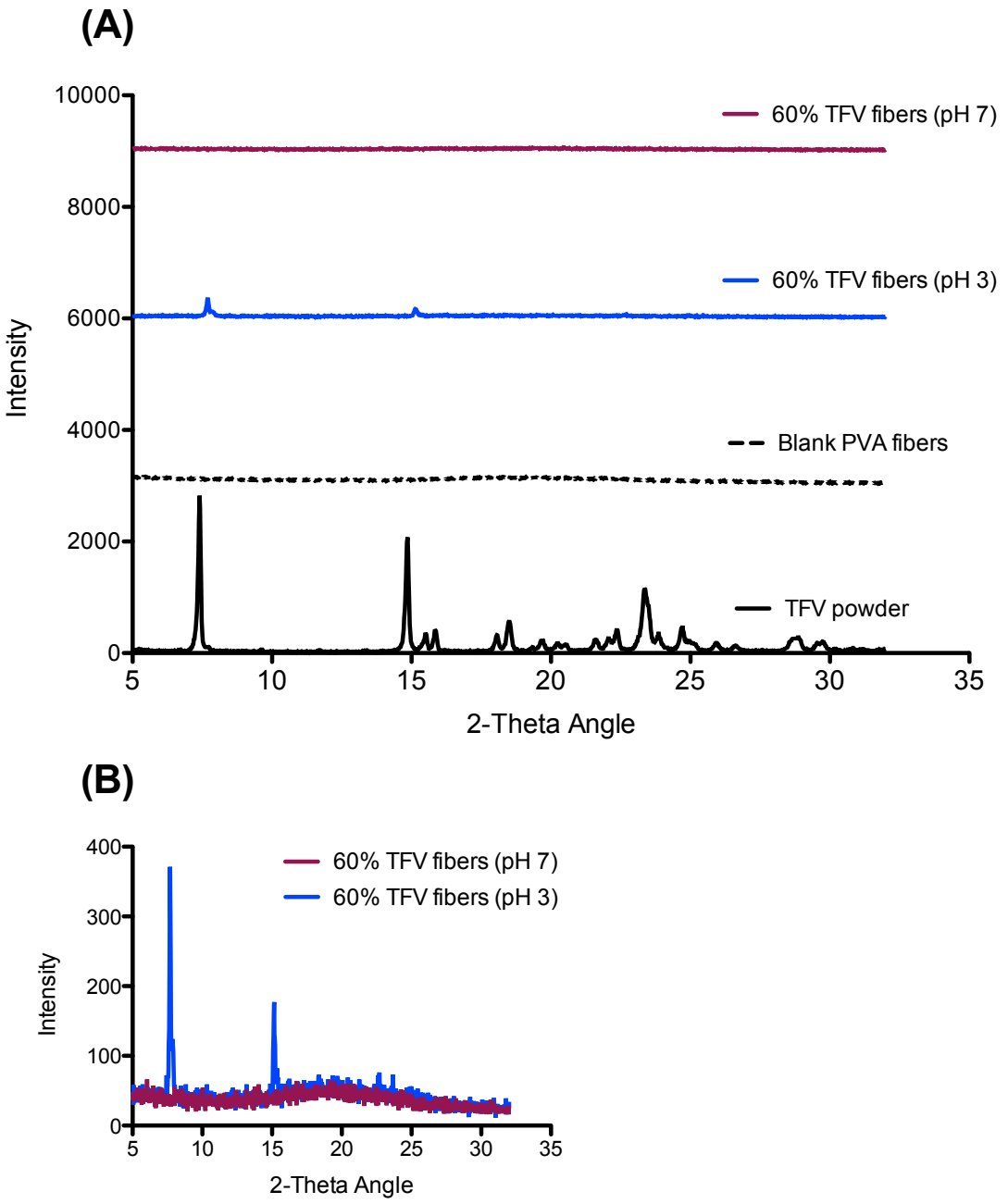

Supplementary Figure 1. X-ray diffraction (XRD) analysis of ground TFV powder and TFV fibers. XRD confirms presence of crystalline TFV drug in 60% TFV fibers (pH 3), but not in 60% TFV fibers (pH 7). (A) Comparison of blank fibers, TFV powder, and 60% TFV fibers (pH 3 and pH 7). (B) Inset view of 60% TFV fibers (pH 3) and 60%TFV fibers (pH 7). Fiber meshes used for this analysis were electrospun using the wire instrument.

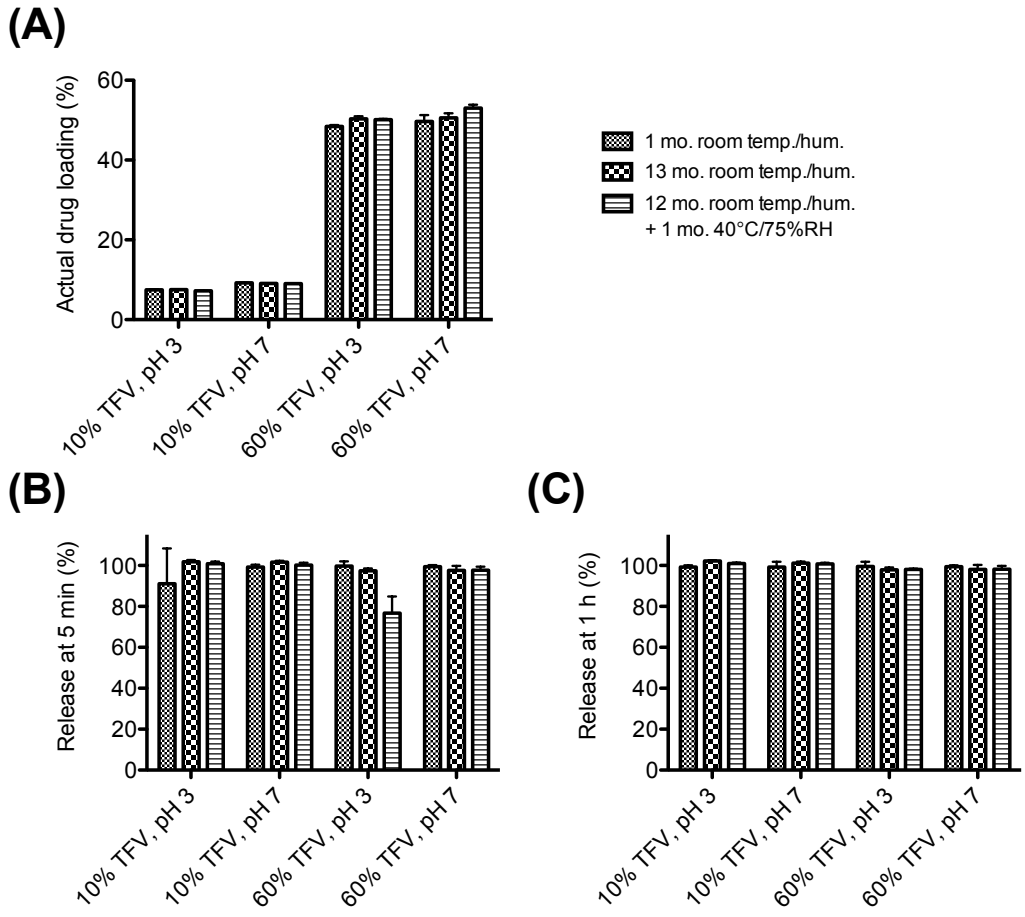

Supplementary Figure 2. Drug loading and release kinetics are unchanged for fibers stored under laboratory and accelerated conditions. Fiber samples were stored under laboratory conditions (room temperature and humidity) for 1 month, laboratory conditions for 13 months, or accelerated conditions (laboratory conditions for 12 months and an additional 30 days at 40°C/ 75%RH). Drug loading (A) and release (B, C) were measured in 25 mM citrate buffer, with n=3 for each sample. Cumulative release is displayed at 5 min (B) and 1 h (C).

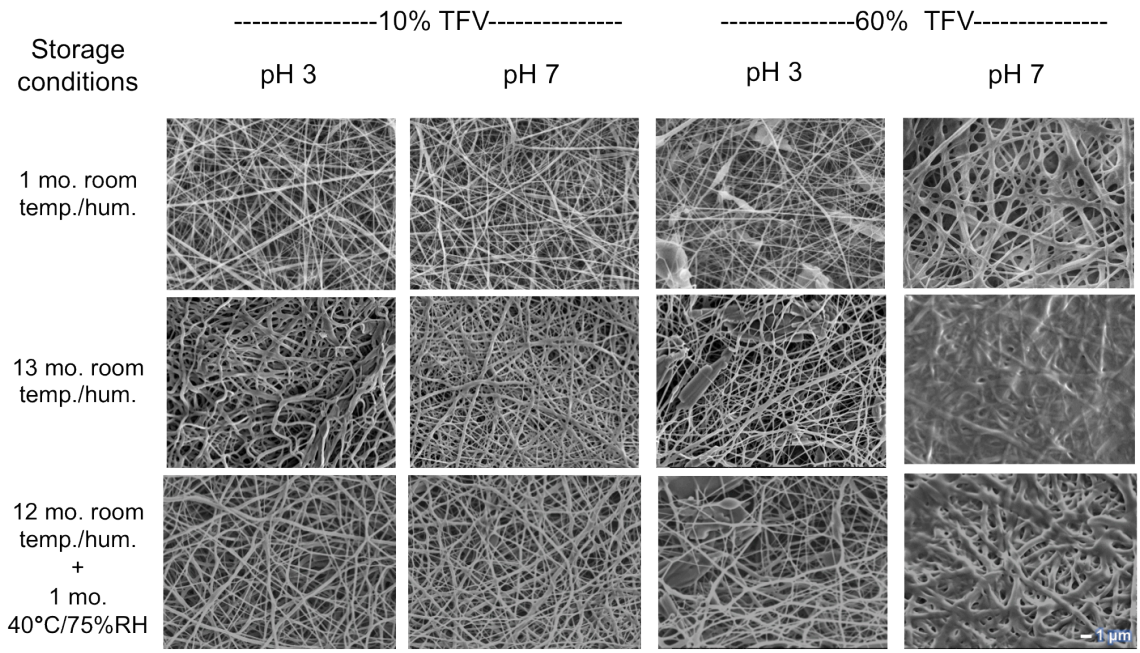

Supplementary Figure 3. SEM of fibers stored under varying conditions. Scale bar = 1 micron.

Supplementary Table 1. Electrospinning parameters for needle v. wire instruments

Parameter	Needle	Wire
Scale	Laboratory	Manufacturing
Voltage	20 kV	-26 kV / + 60 kV
Distance to collector	9-12 cm	16 cm
Volumetric productivity	Flow rate: 10-100 µL/min	Volume processed: 0.5-0.7 mL/min
Electrode	21 G needle	Wire (length=25 cm, diameter=0.2 mm) 0.7 mm diameter orifice
Collector	Metal block	Parallel wires
Substrate	Waxed paper	Spunbond polypropylene
Amount spun	500 µL	30 min run time (~15-20 mL)

Supplementary Table 2: Polymer crystallinity in PVA/TFV fibers.

Electrode	Sample	Tm (°C)	Enthalpy (J/g)	Normalized polymer crystallinity (%)
--	PVA powder	193.3	39.6	28.6
Needle	0% TFV, pH 5	193.1	42.1	30.4
	10% TFV, pH 3	186.6	38.0	29.6
	10% TFV, pH 7	186.0	35.6	28.9
	60% TFV, pH 3	189.2	12.6	21.7
	60% TFV, pH 7	nd	nd	nd
Wire	0% TFV, pH 5	193.0	40.2	29.0
	10% TFV, pH 3	186.4	37.0	28.9
	10% TFV, pH 7	185.3	32.0	25.9
	60% TFV, pH 3	187.4	16.3	22.8
	60% TFV, pH 7	nd	nd	nd

Normalized polymer crystallinity has been corrected by actual mass fraction of polymer in sample and normalized to literature enthalpy value for 100% crystalline PVA (138.6 J/g, Peppas and Merrill 1976). nd = not detected.

Supplementary Table 3: Fiber mesh dissolution in PBS and citrate buffer.

		Dissolution Rating (avg, n=3)					
		PBS (pH 7.4)			Citrate buffer (pH 4.3)		
Electrode	Sample	5 min	1 h	24 h	5 min	1 h	24 h
Needle	0% TFV (pH 5)	2.0	4	4	1.0	1.0	1.7
	10% TFV (pH 3)	3.7	4	4	3.3	4	4
	10% TFV (pH 7)	3.0	4	4	3.0	4	4
	60% TFV (pH 3)	2.7	4	4	2.0	4	4
	60% TFV (pH 7)	3.7	4	4	2.0	3.0	3.0
Wire	10% TFV (pH 3)	4	4	4	3.0	4	4
	10% TFV (pH 7)	4	4	4	3.0	4	4
	60% TFV (pH 3)	4	4	4	4	4	4
	60% TFV (pH 7)	4	4	4	3.7	4	4

Qualitative dissolution rating: 0= not wet out, fiber mesh intact 1= wet out; 2= broken into large pieces; 3= broken into small pieces (less than a pinhead in size); 4=fully dissolved (no mesh visible to naked eye).

Supplementary Table 4: Polymer and drug crystallinity in fibers stored under varying conditions.

Formulation	Storage Conditions[a]	Tm, PVA (°C)	Normalized Polymer Crystallinity[b] (%)	Tm, TFV (°C)	Relative Drug Crystallinity[c] (%)
10% TFV (pH 3)	1 mo. Lab	186.4	28.9	nd	nd
	13 mo. Lab	185.6	30.2	nd	nd
	12 mo. Lab + 1 mo. Accel.	188.2	32.6	nd	nd
10% TFV (pH 7)	1 mo. Lab	185.3	25.9	nd	nd
	13 mo. Lab	185.6	25.7	nd	nd
	12 mo. Lab + 1 mo. Accel.	180.7	22.9	nd	nd
60% TFV (pH 3)	1 mo. Lab	187.4	22.8	291.9	96.3
	13 mo. Lab	187.1	20.8	291.7	95.5
	12 mo. Lab + 1 mo. Accel.	187.7	23.3	291.7	91.0
60% TFV (pH 7)	1 mo. Lab	nd	nd	293.5[d]	2.0
	13 mo. Lab	nd	nd	nd[d]	nd
	12 mo. Lab + 1 mo. Accel.	192.1	0.8	nd[d]	nd

[a]Storage conditions indicate fiber samples stored under laboratory conditions (room temperature and humidity) for 1 month, laboratory conditions for 13 months, or accelerated conditions (laboratory conditions for 12 months and an additional 30 days at 40°C/ 75%R.H.).
[b]Normalized polymer crystallinity has been corrected by actual mass fraction of polymer in sample and normalized to literature enthalpy value for 100% crystalline PVA (138.6 J/g, Peppas and Merrill 1976). nd = not detected.
[c]Relative drug crystallinity was calculated from differential scanning calorimetry (DSC) thermograms and is reported as percentage of crystalline TFV in fibers relative to the heat of fusion of TFV drug in powder form, correcting for mass fraction of drug in sample.
[d]For 60% TFV (pH 7) samples only, a second peak was detected near 275°C for all three storage conditions tested.

APPENDIX E. Supplementary Information for Chapter 5

Table S1: ETR-PLGA nanoparticle characterization

Formulation Number	*n*	Size, Z-avg (nm)	PDI	Zeta Potential (mV)	Actual Drug Loading (%)	EE (%)
87, 88	2	176.0	0.074	-5.19	3.29	36.2
89, 90	2	178.2	0.091	-4.03	3.17	34.9
91, 92, 93	3	173.5	0.069	-5.13	2.56	28.1
Average:		175.9 ± 2.4	0.078 ± 0.012	-4.78 ± 0.65	3.01 ± 0.39	33.1 ± 4.4

All data represent mean +/- standard deviation.
Theoretical ETR Loading (w/w ETR:PLGA) = 10%; same synthesis conditions for all replicates above.
Zeta potential measured in 10 mM NaCl (pH unadjusted, ~5.7).
%EE is calculated from actual ETR drug loading (%EE= actual DL / theoretical DL*100).
NP Formulation 91, 92, 93 (combined) used for PK study.

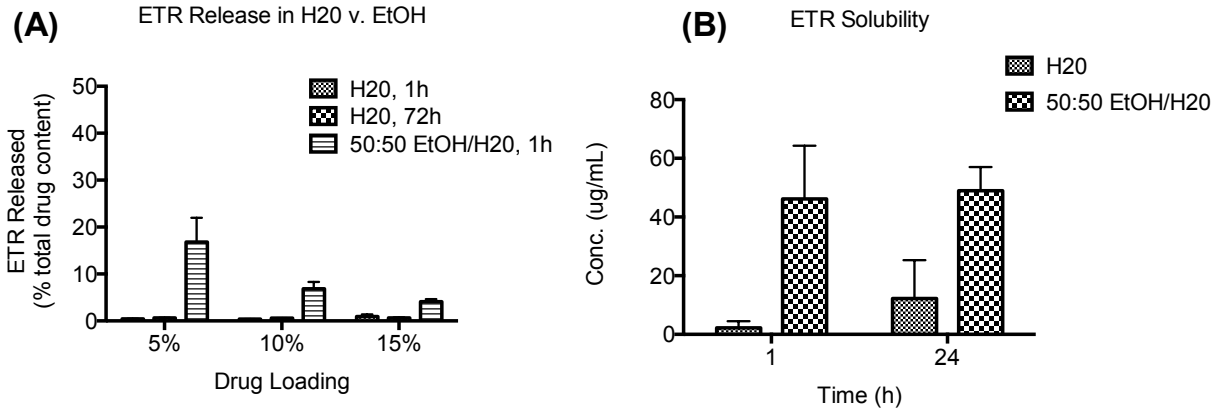

Buffer	Solubility Limit (1h)	Total ETR Released in 4 mL solution (1h)	% Total ETR in free form
H2O	~5 ug/mL	20 ug	0.3%
50/50 EtOH/ H2O	~50 ug/mL	200 ug	3.1%

Fig S1. Predicted release of ETR during electrospinning in 50:50 EtOH:H20. (A) ETR release in from nanoparticles with varying theoretical loadings (5%, 10%, 15%) in H20 vs. 50:50 EtOH/H2O. H2O is the electrospinning solvent for PVA composites, and 50:50 EtOH/H2O is the electrospinning solvent for PVP composites. (B) ETR solubility in H20 vs. 50:50 EtOH/H2O at 1h and 24h when added to solution in excess. The table shows predicted release of ETR from ETR-NP during electrospinning of PVP composites, assuming 15% theoretical ETR loading.

For these conditions, a negligible amount of ETR would be expected to release from ETR-NP during. This data would be important to obtain for any drug / solvent pair using the direct addition method for composite fabrication to understand how much drug is in NP-associated form versus free form.

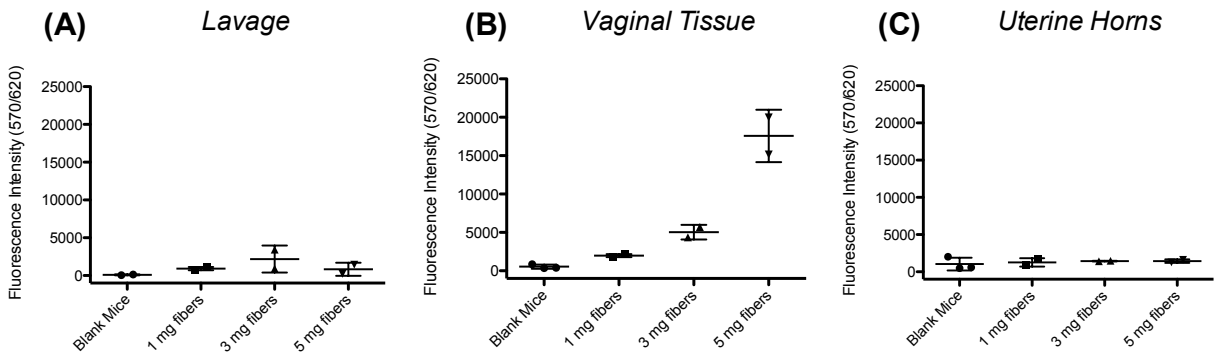

Fig S2. Pilot dosing study of 1, 3, 5 mg composite Rhod-NP / PVP fibers in mice. We dosed Rhod-NP / PVP composite fibers at 1 mg, 3 mg, or 5 mg doses, with n=2 mice per group. Tissue homogenization results at 24h after administration for (A) lavage (4x50 uL), (B) vaginal tissue (after lavage), and (C) uterine horns (tissues homogenized in 500 uL DMSO), with y-axis in showing raw fluorescent intensity at 570/620 nm. Blank mice (n=3) received blank PVP fibers only (n=1 at 1 mg, 3 mg, and 5 mg). We visually observed that undissolved fibers were still present at 24h for both the 3 mg and 5 mg dose, but less so for 3 mg dose. We also observed that undissolved PVP fibers were more associated with the vaginal tissue than the cervicovaginal lavage.

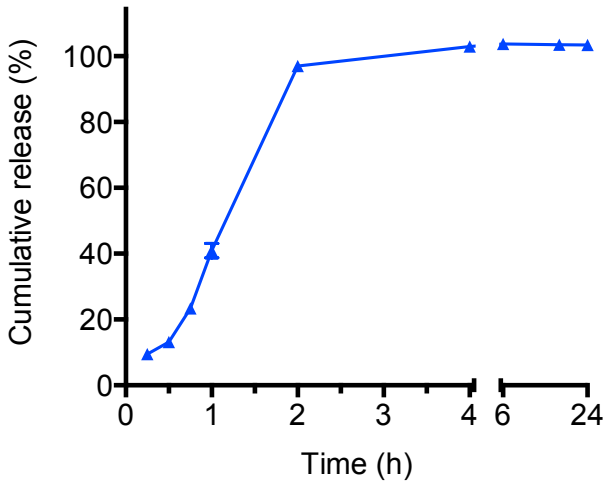

Fig S3. *In vitro* release of ETR from PLGA-NP under sink conditions. We placed 3.9 mg of ETR-NP in 50 mL of 2% solutol/PBS buffer to maintain sink conditions (n=2). Samples (1 mL) were taken at various times and volume replaced. Samples were centrifuged at 14,000g x 10 min and supernatant analyzed for drug content using HPLC. We observed burst release kinetics of >95% of drug contents within 2 hours, which is similar to what das Neves *et al* observed (release of ~80% of drug contents within 2-4h under sink conditions for their dapivirine-PCL nanoparticle. See Das Neves *et al,* 2014 in manuscript reference list).

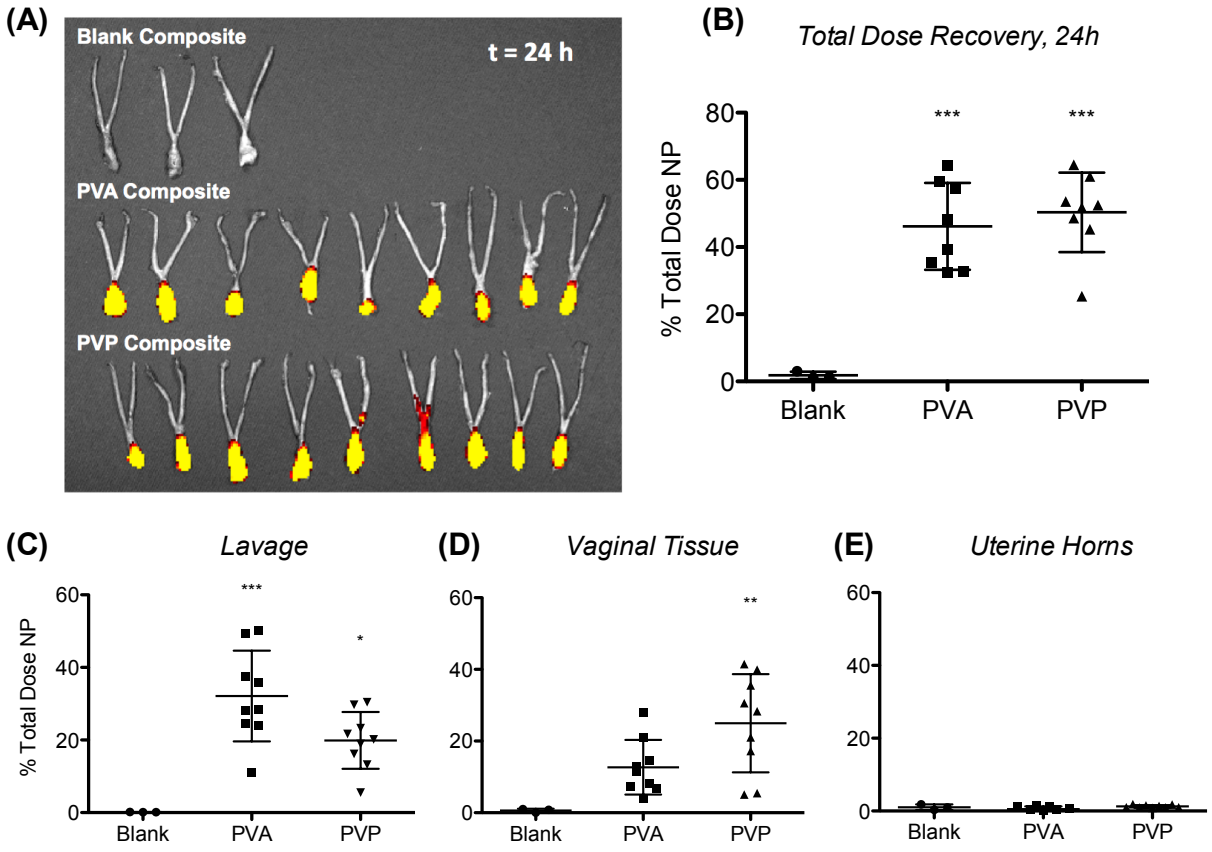

Fig S4: Lavage method for removing mucus-associated Rho-NP and undissolved PVA and PVP composite fibers (n=9 per group). (A) Xenogen imaging of whole reproductive tracts after cervicovaginal lavage. (B) Total Rho-NP dose recovery from tissue homogenization (sum of Rho-NP content in lavage, vaginal tissue, and uterine horns). (C-E) Tissue homogenization results for individual compartments: lavage (C), vaginal tissue (post-lavage) (D), and uterine horns (E).

We visually observed during the lavage method that PVP fibers were still associated with vaginal tissue (small pieces came out in all four lavages). The lavage method for PVA was more consistent: undissolved PVA fibers came out in one viscous chunk/plug. Both lavage and wash buffer method worked well to remove undissolved PVA fibers. Results from the lavage method show consistency with wash buffer method for total dose recovery (~50% total dose recovered for both PVA and PVP, for both lavage and wash buffer methods). The lavage method showed slightly increased PVA nanoparticle association with vaginal tissue (12-13%) at 24h relative to sink method (~7-8%).

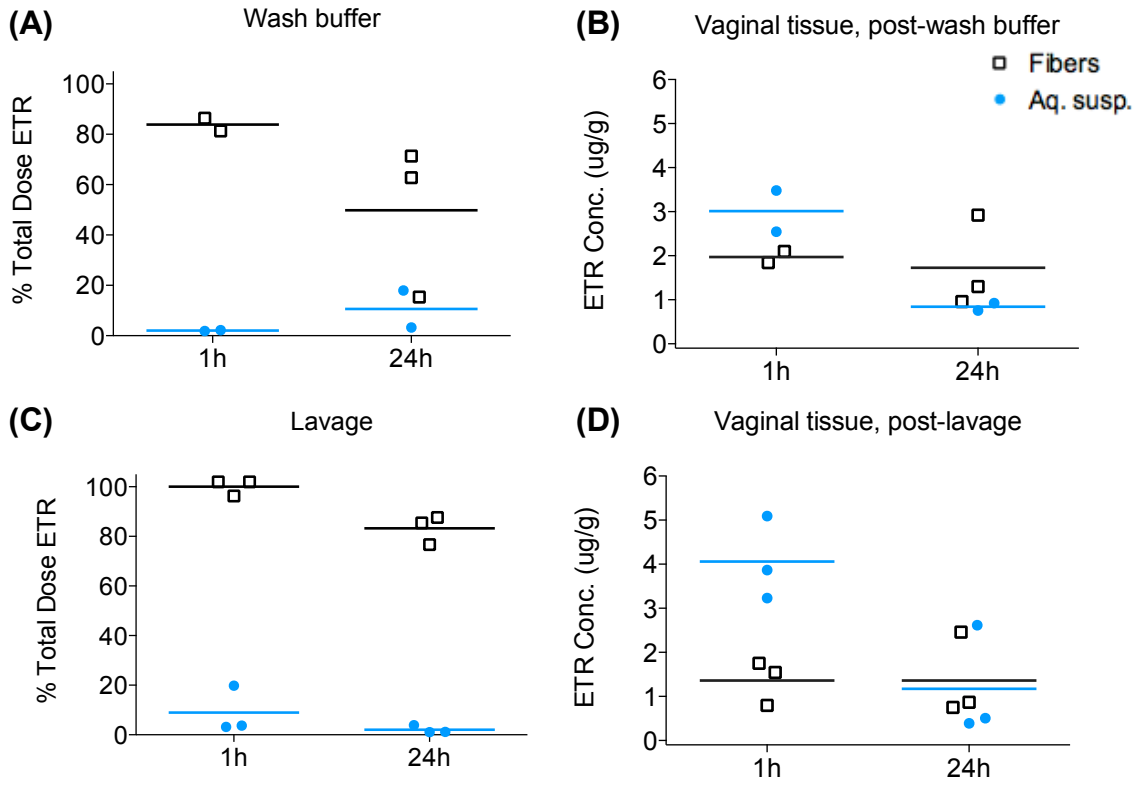

Wash buffer Method	**1h**		**24h**	
	Fibers	*Aq susp*	*Fibers*	*Aq susp*
Wash buffer (% total dose)	83.88	2.05	49.84	10.62
Vaginal tissue (ug ETR/g tissue)	1.97	3.01	1.73	0.84

Lavage Method	**1h**		**24h**	
	Fibers	*Aq susp*	*Fibers*	*Aq susp*
Lavage (% total dose)	100.06	8.94	83.25	2.07
Vaginal tissue (ug ETR/g tissue)	1.36	4.06	1.36	1.17

Fig S5: Lavage and wash buffer method comparison for ETR-NP / PVA composite fibers. We ran two pilot studies (n=2 or 3 mice per group, depending on study) to compare the lavage and wash buffer methods for removing undissolved ETR-NP / PVA composite fibers from the vaginal tract. (A) and (B) show results for wash buffer and vaginal tissue (post-wash) for ETR Pilot Study #1 (wash buffer method). (C) and (D) show results for lavage and vaginal tissue (post-lavage) for ETR Pilot Study #2 (lavage method). Equivalent doses of ETR (14.72 ug ETR / mouse) in 2.8-3.4 mg composite fibers or 25 uL H2O for aqueous suspensions for both Pilot #1 and Pilot #2. Mean values for each group are shown in the tables below as a function of % total ETR dose and ug ETR / g tissue.

Similar trends wereseen for both methods, with about two-fold higher vaginal tissue concentrations for PVA fibers than for aqueous suspensions at 24h. The lavage method was chosen for scaled-up pharmacokinetic study due to higher overall dose recovery and to allow for more comparisons to previous reports in literature that have used the lavage method

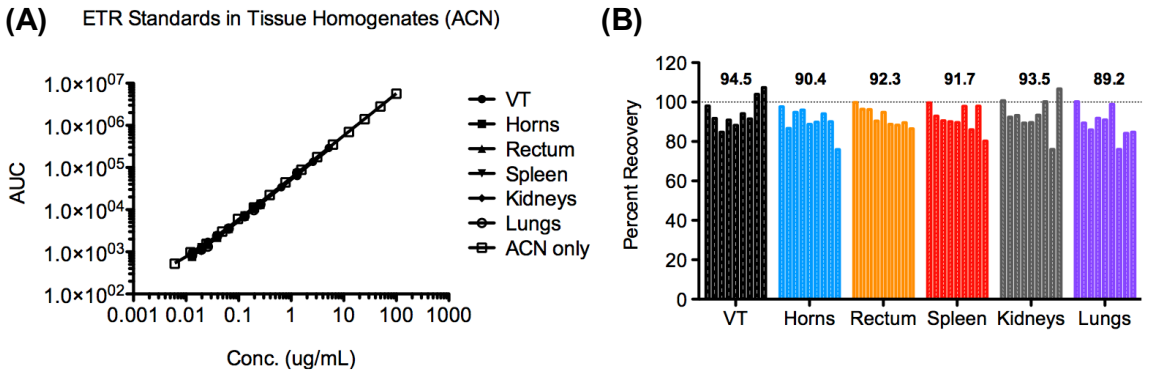

	VT	Horns	Rectum	Spleen	Kidneys	Lungs	ACN only
Straight line							
Best-fit values							
YIntercept	331.0	93.18	115.1	127.5	225.6	111.2	196.3
Slope	51689	54106	54642	53964	52572	52927	56984
Std. Error							
YIntercept	33.93	37.72	22.60	45.03	71.66	53.68	14.04
Slope	993.0	1320	791.0	1576	2508	1879	685.7
95% Confidence Intervals							
YIntercept	250.7 to 411.2	3.970 to 182.4	61.64 to 168.5	20.95 to 234.0	56.14 to 395.1	-15.74 to 238.2	165.9 to 226.6
Slope	49340 to 54037	50985 to 57228	52772 to 56513	50237 to 57691	46642 to 58503	48485 to 57370	55503 to 58465
Goodness of Fit							
Degrees of Freedom	7	7	7	7	7	7	13
R square (weighted)	0.9974	0.9959	0.9985	0.9941	0.9843	0.9913	0.9981
Weighted Sum of Squares (1/(X*X))	4.325e+007	5.368e+007	1.928e+007	7.651e+007	1.937e+008	1.087e+008	7.335e+007
Sy.x	2486	2769	1659	3306	5261	3941	2375
Number of points							
Analyzed	9	9	9	9	9	9	15

Fig S6: Standards and spiked controls of ETR-NP in blank tissue homogenates from untreated mice (HPLC). (A) Standard curves created by spiking 10 uL of ETR-NP standard into 90 uL of supernatant from blank tissue homogenate over a range of concentrations for vaginal tissue (VT), uterine horns (horns), rectum, spleen, kidneys, lungs, and acetonitrile (ACN) only. Linear regression of standard curves for each organ is shown in the table. (B) Percent ETR recovery for organs from untreated mice spiked with a known concentration of ETR prior to homogenization. There was minimal background interference on HPLC for all organs analyzed here.

Supplementary Table S2. Gradient method for LC-MS/MS detection of etravirine.

Time	% A	% B
0	98	2
1	98	2
6	0	100
7	0	100
7.1	98	2
8.5	98	2

	Suspension	Fibers
Plasma	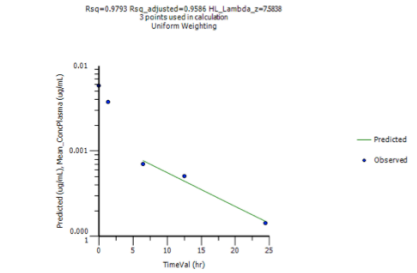	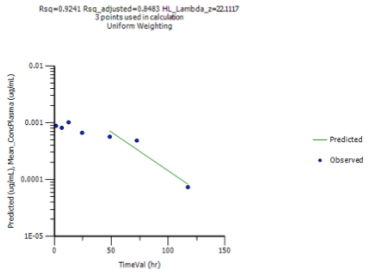
Vaginal lavage	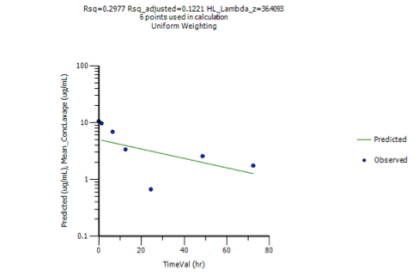	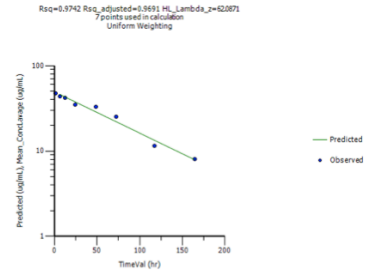
Vagina	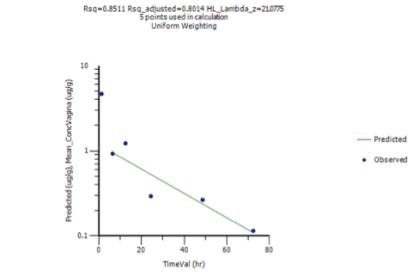	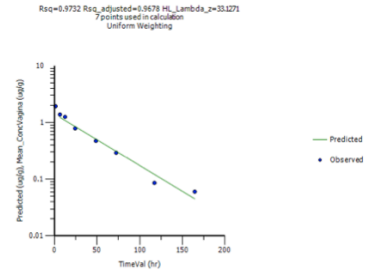

Supplementary Fig S7. Terminal elimination half-life estimation by Phoenix WinNonlin for PK parameters for plasma, vaginal lavage, and vaginal tissue. Aqueous suspension is shown on the left side, composite fibers are shown on the right side.

Liver	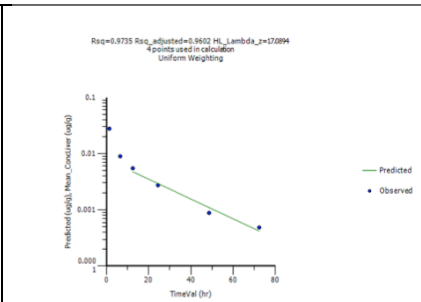	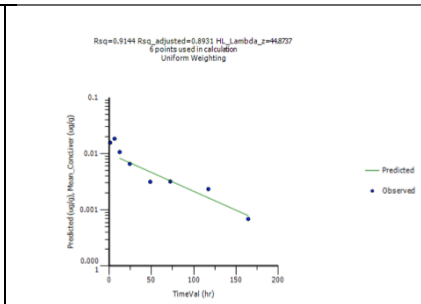
Rectum	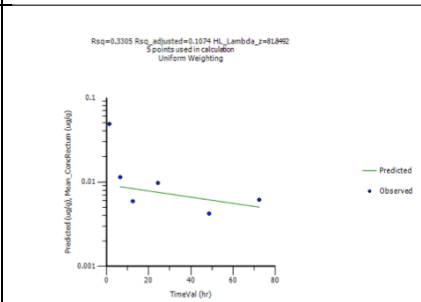	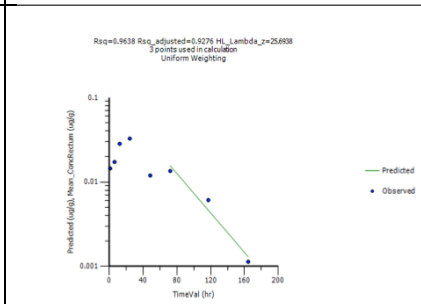
Uterine horn	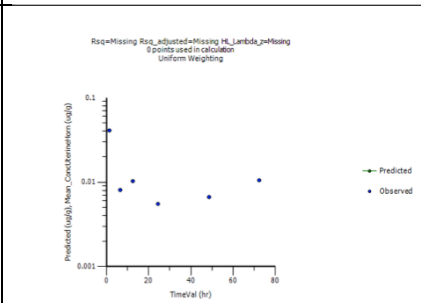	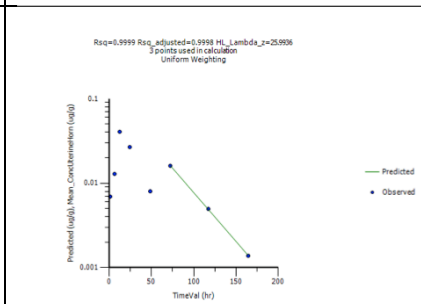

Supplementary Fig S8. Terminal elimination half-life estimation by Phoenix WinNonlin for PK parameters for liver, rectum, and uterine horns. Aqueous suspension is shown on the left side, composite fibers are shown on the right side.

APPENDIX F. Literature comparison: intracellular drug levels after in vitro delivery of ARV nanoparticles

Particles	Coating	Drug	Cell Type	Time Scale	Conditions	Results	Source
PLGA (single emulsion) 260 nm	PVA (aqueous phase); PEO/PPO (Poloxamer-127) Zeta: -11 mV	efavirenz, lopinavir, ritonavir	Human PBMCs	28 d	Media ½ exchanged every 2-3 days	**Free drugs:** eliminated in 48h **ARV-np:** >0.9 ug/mL for 28 d	Destache 2009
PLGA (single emulsion) 80 nm	PEO/PPO, (Poloxamer 127) Zeta: -23 mV	efavirenz, raltegravir	HeLa cells (human cervical epithelial cell line)	14 d	Media ½ exchanged every 2-3 days; all media removed on day of analysis	**Free drugs:** not tested **ARV-np**: EFV >150 ng/10^5 cells for 14 d; RAL below LOD after 6 d	Date 2012
PLGA (high pressure homogenization) 138 nm	PEO/PPO, Poloxomer 407 (Pluoronic F127) Zeta: -13 mV	efavirenz, lopinavir, ritonavir	H9 (human T cell line)	7 d	Treatment added at 1 d (post-infection); cells washed after 24h and then cultured 7 d	**Free drugs**: RTV at 0.2 ug/10^6 cells after 7 d, others below LOD **ARV-np:** EFV, LPV, and RTV detected in all subcellular fractions after 7 d, with most drug in membrane (12-15 ug/10^6 cells)	Shibata 2013
PCL (solvent displacement / nanoprecipitation) 190 nm	(1) PEO / PPO Poloxamer 338 NF (Pluronic® F 108 NF) Zeta: -29 mV (2) SLS (sodium lauryl sulfate) Zeta: -58 mV (3) CTAB (cetyl trimethylammonium bromide) Zeta: +48 mV	dapivirine	VK2/E6E7 (human vaginal epithelial cells) HeLa TZM-bL cells J774A.1 (mice Mo/Mac) DC-100 dendritic cells (from human umbilical cord blood) human PBMCs	6 h	Treatment added to cells, cells washed 2x with PBS and lysed (protein content measured) Free DPV delivered in DMSO	**Free drugs:** lower conc. at 6 h than ARV-np **ARV-np:** ARV np had higher intracellular drug levels for most cell types relative to free drug, particularly for phagocytic cells Negative zeta potential of PEO particles indicates only partial coverage with surface coating	das Neves 2012
Wet-milled "nanoART" (nano-sized drug crystals) 310 nm	5 surfactants tested: (1) P188 (2) PVA and SDS (3) P188 and SDS (4) P188 and mPEG2000DSPE (5) P188, mPEG2000DSPE, and DOTAP Zeta: -42 to + 23 mV	indinavir, ritonavir, atazanavir, and efavirenz	Human MDM (monocyte-derived macrophages)	15 d	Treatment added to cells, cultured 8h, then complete media change and monitored 15 d	**Free drug**s: no apparent free drug controls **ARV-np:** Formulations (20 total) scored based on cell uptake, retention, media release, activity Higher intracellular drug conc. correlated to higher protection against HIV (0.92) for EFV and ATV (regardless of media drug concentration)	Nowacek 2011

References:
1. Destache, C. J. *et al. BMC Infect. Dis.* **9,** 198 (2009). 2. Date, A. A. *et al. Antiviral Res.* **96,** 430–436 (2012). 3.Shibata, A. *et al. AIDS Res. Hum. Retroviruses* (2013). doi:10.1089/aid.2012.0301 4. Das Neves, J. *et al.. Pharm. Res.* **29,** 1468–1484 (2012). 5. Nowacek, A. S. *et al. J. Controlled Release* **150,** 204–211 (2011).

APPENDIX G. Literature review on nanoparticle/nanofiber composites for medical applications

Agent Encapsulated* (in NP or NF)	Nanoparticle (NP) material	Nanofiber (NF) material	Key results	Application	Citation
Small molecule dyes or drugs					
Coumarin-6 (hydrophobic dye)	PLGA	PVA, crosslinked-PVA, or PEO	-Slightly slowed release of drug over 24h in crosslinked PVA fibers compared to PVA fibers, PEO fibers or NP alone	Drug delivery, biomedical applications	Beck-Broichsitter *et al* (2010)
Rhodamine B Naproxen	Chitosan	PCL	-NP/NF composites reduced burst release of drugs over 3d	Drug delivery, tissue engineering	Wang *et al* (2011)
Simvastatin (hydrophobic small molecule drug) in NF	Bioactive glass-NP	PCL	-Sustained release of simvastatin over 7d -Bioactive glass NP modulate fiber degradation rate, drug release	Bone regeneration	Kouhi *et al* (2013)
Doxorubicin (DOX)	Mesoporous silica	PLLA	-Sustained release and high loading of DOX*, in vitro* antitumor efficacy	Cancer treatment	Qiu *et al* (2013)
DOX	Nano-hydroxyapatite (rod form)	PLGA	-Sustained release of DOX over 30d (dramatically reduced burst from fibers only) -*In vitro* antitumor activity in KB cells	Cancer treatment	F Zheng *et al* (2013)
DOX and indomethacin (IMC)	Mesoporous silica / iron-oleate (core-shell NP design)	PCL / gelatin	-Sustained release of DOX over 6d -Fast release of IMC	General drug delivery (wound healing, surgical implants)	Hou *et al* (2013)
Stimuli-responsive drug release (pH, heat, or enzyme)					
Garlic extract	Mesoporous silica	Nylon-6	-"Molecular gate design" of NP for stimuli-responsive release of garlic extract from NP -Release triggered by pH change from 2-7 or presence of enzyme	Antimicrobial, antioxidative, antiatherosclerotic properties	Acosta *et al* (2014)
Doxycycline hyclate	Chitosan	PNN, PNIPAAm, and chitosan	-pH-responsive (pH 2-7) and heat-responsive (25-37C) drug release over 7 days from NF -Release slowed by incorporating drug in NP/NF composites	Controlled release; hydrophilic drug delivery	Huang *et al* (2014)
DOX and sodium bicarbonate (NP), Ibuprofen (IBU) (in NF only)	Mesoporous silica	PLLA	-pH-sensitive release from NP due to addition of sodium bicarbonate - Release slowed by incorporating drug in NP/NF composites	In vivo liver tumor model (mice) showed prolonged survival by 1.5x	Yuan *et al* (2015)
Proteins and growth factors					
Bovine serum albumin (BSA)	Calcium alginate microspheres	PLLA	-Emulsion electrospinning -Prolonged release, lower burst from NP/NF composites than bare NP	Drug delivery, tissue engineering	Qi *et al* (2006)
BSA Epidermal growth factor (EGF)	PLGA or PU; coated with PVA	PU	-NP/NF composites successfully formed	Tissue engineering	Dong *et al* (2009)
Fibroblast growth factor (FGF-2)	Heparin	Chitosan	-Zero-order release of FGF-2 from NP/NP composites and maintained activity for 30d	Tissue engineering; wound healing	Zomer-Volpato *et al* (2012)
Growth factors (VEGF in NF, and PDGF-BB in NP)	PLGA	Chitosan / PEO	-Sustained release of PDGF-BB over 7 d -Accelerated wound healing and better *in vivo* (rat)	Wound healing	Xie *et al* (2013)

Agent Encapsulated (in NP or NF)	Nanoparticle (NP) material	Nanofiber (NF) material	Key results	Application	Citation
Metallic nanoparticles					
DOX Au-NP	Au-NP	Chitosan/PVA, crosslinked	-Controllable release (20-65% cumulative release over 48h by varying fiber crosslinking time	Drug delivery, biomedical applications	Yan E *et al* (2013)
Silver ions (from Ag-NP)	Ag-NP	Chitosan	-Controllable loading of Ag-NP -In vitro antibacterial effects enhanced	Topical antibiotic treatment; wound care	Lee *et al* (2014)
Other					
siRNA	Chitosan	PLGA	-Controlled siRNA release over 30d (pH-dependent) -50% gene silencing activity up to 10d *in vitro*	siRNA transfection	Chen *et al* (2012)
Biphasic calcium phosphate (BCP)	BCP-NP	PVA / Gelatin	-Improved mechanical properties -Improved osteoblast penetration *in vivo*	Bone regeneration and tissue engineering	Ba Linh *et al* (2013)

Table Footnotes:
This table is not a complete list of all nanoparticle/nanofiber composite work published in literature, only representative. It has been focused on applications of composites to the field of drug delivery for biomedical applications, and represents a literature search performed on October 23, 2015 concentrating on work published in the last five years (2010-2015). References: in order of appearance [1–16]

*Agent is encapsulated in nanoparticles unless otherwise stated

Abbreviations:
Ag = silver
Au = gold
DOX = doxorubicin
NF = nanofibers
NP = nanoparticles
PCL = poly(ε-caprolactone)
PEO = poly(ethylene oxide)
PLGA = poly(lactic-*co*-glycolic) acid
PNIPAAm = poly(N-isopropylacrylamide)
PNN = poly(NIPAAm-co-N-methylolacrylamide)
PU = poly(urethane)
PVA = poly(vinyl alcohol)

References

1. Beck-Broichsitter, M. *et al.* Novel 'Nano in Nano' Composites for Sustained Drug Delivery: Biodegradable Nanoparticles Encapsulated into Nanofiber Non-Wovens. *Macromol. Biosci.* **10,** 1527–1535 (2010).
2. Wang, Y. *et al.* Electrospun composite nanofibers containing nanoparticles for the programmable release of dual drugs. *Polym. J.* **43,** 478–483 (2011).
3. Kouhi, M., Morshed, M., Varshosaz, J. & Fathi, M. H. Poly (ε-caprolactone) incorporated bioactive glass nanoparticles and simvastatin nanocomposite nanofibers: Preparation, characterization and in vitro drug release for bone regeneration applications. *Chem. Eng. J.* **228,** 1057–1065 (2013).
4. Zheng, F., Wang, S., Shen, M., Zhu, M. & Shi, X. Antitumor efficacy of doxorubicin-loaded electrospun nano-hydroxyapatite–poly(lactic-co-glycolic acid) composite nanofibers. *Polym Chem* **4,** 933–941 (2013).
5. Hou, Z. *et al.* Electrospun Upconversion Composite Fibers as Dual Drugs Delivery System with Individual Release Properties. *Langmuir* **29,** 9473–9482 (2013).
6. Acosta, C. *et al.* Polymer Composites Containing Gated Mesoporous Materials for On-Command Controlled Release. *ACS Appl. Mater. Interfaces* **6,** 6453–6460 (2014).
7. Huang, C.-H. *et al.* Preparation of a thermo- and pH-sensitive nanofibrous scaffold with embedded chitosan-based nanoparticles and its evaluation as a drug carrier. *Cellulose* **21,** 2497–2509 (2014).
8. Yuan, Z. *et al.* Synergistic mediation of tumor signaling pathways in hepatocellular carcinoma therapy via dual-drug-loaded pH-responsive electrospun fibrous scaffolds. *J Mater Chem B* **3,** 3436–3446 (2015).
9. Qi, Hu, P., Xu, J. & Wang. Encapsulation of Drug Reservoirs in Fibers by Emulsion Electrospinning: Morphology Characterization and Preliminary Release Assessment. *Biomacromolecules* **7,** 2327–2330 (2006).
10. Dong, B., Smith, M. E. & Wnek, G. E. Encapsulation of Multiple Biological Compounds Within a Single Electrospun Fiber. *Small* **5,** 1508–1512 (2009).

11. Zomer Volpato, F. *et al.* Preservation of FGF-2 bioactivity using heparin-based nanoparticles, and their delivery from electrospun chitosan fibers. *Acta Biomater.* **8,** 1551–1559 (2012).
12. Xie, Z. *et al.* Dual growth factor releasing multi-functional nanofibers for wound healing. *Acta Biomater.* **9,** 9351–9359 (2013).
13. Yan, E. *et al.* Electrospun polyvinyl alcohol/chitosan composite nanofibers involving Au nanoparticles and their in vitro release properties. *Mater. Sci. Eng. C* **33,** 461–465 (2013).
14. Lee, S. J. *et al.* Electrospun chitosan nanofibers with controlled levels of silver nanoparticles. Preparation, characterization and antibacterial activity. *Carbohydr. Polym.* **111,** 530–537 (2014).
15. Chen, M. *et al.* Chitosan/siRNA Nanoparticles Encapsulated in PLGA Nanofibers for siRNA Delivery. *ACS Nano* **6,** 4835–4844 (2012).
16. Ba Linh, N. T., Lee, K.-H. & Lee, B.-T. Functional nanofiber mat of polyvinyl alcohol/gelatin containing nanoparticles of biphasic calcium phosphate for bone regeneration in rat calvaria defects. *J. Biomed. Mater. Res. A* **101A,** 2412–2423 (2013).